Compatibilization and Characterization of Bio-Based and Bio-Degradable Poly (Lactic Acid) Blends and Composites

Thesis submitted in partial fulfillment of the requirements
for the award of the degree of

DOCTOR OF PHILOSOPHY

by

ASHISH KUMAR
(Roll No. 716053)

Supervisor:

Dr. T. VENKATAPPA RAO

DEPARTMENT OF PHYSICS
NATIONAL INSTITUTE OF TECHNOLOGY
WARANGAL-506 004 (T.S.), INDIA
APRIL, 2019

Dedicated To

My Parents

and

All My Teachers

National Institute of Technology, Warangal

Department of Physics

Certificate

This is to certify that the thesis entitled **"Compatibilization and Characterization of Bio-based and Bio-degradable Poly (lactic acid) Blends and Composites"**, is being submitted by **Mr. Ashish Kumar** (Roll No. 716053) to the Department of Physics, **National Institute of Technology, Warangal, India,** is a record of bonafide research work carried out by him under my supervision and it has not been submitted elsewhere for the award of any degree.

Date:

Place: Department of Physics
NIT Warangal

(Dr. T. Venkatappa Rao)

Thesis Supervisor
Associate Professor

NATIONAL INSTITUTE OF TECHNOLOGY WARANGAL-506004, INDIA

DEPARTMENT OF PHYSICS

Approval

The thesis entitled **"Compatibilization and Characterization of Bio-based and Bio-degradable Poly (lactic acid) Blends and Composites"** by **Mr. Ashish Kumar (Roll No. 716053)** is approved for the degree of Doctor of Philosophy.

Examiner **Thesis Supervisor**

Chairman, DSC

Date:

Declaration

This is to certify that the work presented in the thesis entitled **"Compatibilization and Characterization of Bio-based and Bio-degradable Poly (lactic acid) Blends and Composites"** is a bonafied work done by me under the supervision of **Dr. T. Venkatappa Rao**, Associate Professor, Department of Physics, National Institute of Technology, Warangal and was not submitted elsewhere for the award of any degree.

I declare that this written submission represents my ideas in my own words and where others ideas or words have been included, I have adequately cited and referenced the original sources. I also declare that I have adhered to all the principles of academic honesty and integrity and have not misrepresented or fabricated or falsified any idea / data / fact / source in my submission. I understand that any violation of the above will be a cause for disciplinary action by the Institute and can also evoke penal action from the sources which have thus not been properly cited or from whom proper permission has not been taken when needed.

Date: **(Ashish Kumar)**

Place: Department of Physics **Roll No.: 716053**
NIT Warangal

Abstract

The bio-based and biodegradable poly (lactic acid) (PLA) is a commercially available synthetic biopolymer. It is being exploited to develop green plastic which can replace the currently existing petrochemical based non-degradable plastic in the near future. The major drawbacks of PLA such as poor toughness, brittleness, low heat resistance and high cost hamper its growth in the development of commercial green plastic. Hence, the prime objective of the thesis is to circumvent these drawbacks of PLA. The polymers and fillers such as poly (ethylene-co-glycidyl methacrylate (PEGM), lignin (LG) and hexagonal boron nitride (HBN) particles, bamboo powder (BP) respectively are employed to develop PLA based blends and composites. The compatibility between the PLA matrix and dispersed phase or filler is a key parameter to tailor the mechanical and thermal properties of the PLA in the resulting blends and composites. The melt blending method is opted to prepare all reported PLA blends and composites. Further, to improve the compatibility between the PLA matrix and dispersed phases the various compatibilizers have been used. In some cases, the fillers are physically modified with an electron beam (E-beam) prior to blending with PLA to enhance their compatibility. The effect of blending of reinforcement on the hydrolytic degradation of PLA is also studied and reported in the thesis. The blending of PLA with PEGM at weight ratio 80:20 (PLA:PEGM) significantly improves the elongation at break from 5.76 % to 157.40%, tensile toughness from 2.70 MJ/m^3 to 36.82 MJ/m^3 and notched impact strength from 2.65 kJ/m^2 to 5.91 kJ/m^2. The PLA/PEGM blend is compatibilized with in-situ formed PLA-g-PEGM graft copolymers explained with possible reaction mechanism. These properties are further enhanced with the incorporation of HBN particles at low concentrations i.e. 1 phr (part per hundred) such that elongation at break 166.50 %, tensile toughness 37.73 MJ/m^3 and notched impact strength 8.89 kJ/m^2. Further, heat deflection temperature (HDT) is also improved from 52.60 °C to 54.50 °C. The blending of PEGM with PLA and further incorporation of HBN particles restrict the hydrolytic degradation of PLA. So, to achieve the good impact strength and fast hydrolytic degradation the samples of prepared blend-composites were irradiated to E-beam. Moreover, in the view of cost reduction of PLA and complete biodegradation, the fully bio-based PLA/lignin blends and PLA/bamboo powder composites are prepared. The commercial lignin and bamboo powder are second most inexhaustible and low-cost fillers which are used as an additive to reduce the cost of PLA. The PLA/lignin blends and PLA/bamboo powder composites are compatibilized with the simple green physical approach in which the fillers were physically modified with E-beam irradiation prior to melt blending. The modification of the bio-fillers with E-beam irradiation

at low radiation doses is an inexpensive technique and can be done at a large scale. The PLA/LG-5% 30 kGy and PLA/LG-20% 30 kGy blends having 5 wt% and 20 wt% E-beam irradiated lignin respectively and TAIC is compatibilized with PLA-TAIC-Lignin crosslinked structures formed during melt blending. The formation of PLA-TAIC-Lignin crosslinked structures during melt blending is explained with proposed possible reaction mechanism. The PLA/LG blends having E-beam irradiated lignin show better mechanical and thermal properties as compared to PLA/LG blends having unirradiated lignin. The PLA/LG-5% 30 kGy blend exhibits slightly more notched impact strength, elongation at break, HDT and less hydrolytic degradation than virgin PLA. Furthermore, the unirradiated and E-beam irradiated bamboo powder is melt blended with PLA to prepare PLA/bamboo powder (PLA/BP) composited. The epoxy silane is used to improve the compatibility between the PLA matrix and filler. Among all PLA/BP composites, PLA/EBP5/ES 5phr with 5 wt% E-beam irradiated bamboo powder and 5 phr epoxy silane exhibits good tensile properties and highest notched impact strength which is 12% more than pure PLA.

Acknowledgements

It gives me immense pleasure and delight to express my deep sense of gratitude and indebtedness to my research supervisor Dr. T. Venkatappa Rao, Associate Professor, Department of Physics, National Institute of Technology, Warangal, for his support and inspiring guidance. His dedication to science and integrity has inspired me to reach this stage. I am grateful to him for teaching me how to think innovatively in setting up the experiments. His guidance went beyond science and helped me to grow as a strong independent person.

I am expressing my gratitude and profound thanks to Prof. S.V.S. Ramana Reddy for his inspiring guidance. The friendliness and cordiality I enjoyed in his association will carried along all through my career.

My special thanks to Dr. Subhendu Ray Chowdhury, Scientist, Isotope and Radiation Application Division (IRAD), Bhabha Atomic Research Centre, Mumbai, India for guiding me through my doctoral research work. Fruitful discussions with him on a number of occasions and constructive suggestions I received at various stages have been immense help to me.

It is my bounded responsibility to place on record the technical support extended and the facilities provided to me by Prof. K.V.G. Reddy present Head, Department of Physics and Chairman of the Doctoral Scrutiny committee, Prof. R.L.N. Sai Prasad and Prof. L.R.G. Reddy, former Heads of the Department for their support and encouragement.

My sincere thanks to doctoral scrutiny committee members Dr. A. Seshagiri Rao, Dr. P. Abdul Azeem and Dr. P. Syam Prasad for their valuable suggestions and for evaluating my research work at each stage.

I immensely thank Prof. N.V. Ramana Rao, Director, NIT Warangal, a good researcher himself, popularly hailed by all the NIT'ians as a good teacher and especially as a brilliant inspiring person to research scholars. I ever remember him for his generosity in allowing me to be part of this wonderful institution and pursue this enterprising research.

I take this opportunity to express my gratitude to all the faculty members of the Department viz., Prof. M. Sai Shankar, Prof. D. Dinakar, Dr. B. Sobha, Dr. Sourabh Roy, Dr. D. Haranath, Dr. K. Thanga Raju, Dr. Kusum Kumari, Dr. V Jayalakshmi, Dr. D. Paul Joseph and Dr. R. Rakesh Kumar for their valuable advice, encouragement and moral support in my research.

I place on record, my deepest thanks to Shri. K.S.S. Sharma, former Head Board of Radiation and Isotope Technology (BRIT), Mumbai and Shri S. Abdul Khader, Officer-Incharge, SO, Electron Beam Accelerator Facility (ILU-EBA), BRIT, BARC Mumbai for providing Electron beam facility. I would like to thank Dr. S. Dutta, Programme Officer, BRNS and Co-ordinator, KSKRA & DGFS and Mr. Parsad of BRNS for their kind assistance. I am also grateful to Prof. Suresh Rayala, Department of Biotechnology, IITM, Chennai for his help and encouragement.

My special thank to Prof. K.B. Joshi, Central University of Himachal Pradesh and Prof. Aniruddha Chakraborty, IIT Mandi, Himachal Pradesh, who encouraged and motivated me at the early stage of my research career. I also thank Dr. B. Sanjeeva Rao, Retired Principal, Govt. Degree College, Rangasaipet, Warangal for inspiring me and critical discussions about my research work.

I sincerely thank my senior scholars Dr. S. Rajkumar, Dr. Himamahesh, Dr. P.V.N. Kishore and Dr. Diwaker for encouraging and supporting me during the course of my work.

I thank all my co-scholars for their moral support during my stay and for being very good friends.

All these loving souls credited to my account apart, what I am today is nothing but the forehead shed drops of the sweat of my parents, Smt. Mangla Devi and Shri. Parmod Singh, who have tilled the land with me as a grain. I would like to thank, my sisters and brothers-in-law Mamata Devi and Satpal, Lalita Devi and Vijay Kumar, and Monika Rani and Sanjeev Kumar for their motivation, support and love.

I am very much grateful to BRNS, since the research work presented in this thesis was carried out with the financial support from the research project sanctioned by the **Board of Research in Nuclear Sciences (BRNS),** Department of Atomic Energy, Government of India [**Sanction Number 35/14/55/2014-BRNS**].

I gratefully acknowledge everyone who has invariably contributed for my success.

Place: NIT Warangal **(Ashish Kumar)**

Contents

List of Figures

List of Tables

Notations

T_g	glass transition temperature
T_m	melting temperature
T_{cc}	cold crystallization temperature
ΔH_{cc}	crystallization enthalpy
ΔH_m	melting enthalpy
X_C	% crytallinity
MPa	megapascal
MeV	megaelectronvolt
kGy	Kilogray
σ_{Tr}	true stress
σ_{Eng}	engineering tensile stress
ε_{Eng}	engineering tensile strain
Ω	angular precession velocity
Γ	gyromagnetic ratio
N	electromagnetic frequency
H	applied magnetic field
Λ	wavelength of incident beam
Θ	angle of incidence
d_{hkl}	spacing between lattice planes of crystalline material
kV	Kilovolt

Abbreviations

PHA	poly (hydroxyalkonoates)
ASTM	American Society for Testing and Materials
PLA	poly (lactic acid)
ROP	ring opening polymerization
PLLA	poly (L-lactide)
PDLA	poly (D-lactide)
PDLLA	poly (DL-lactide)
sc-PLA	stereocomplex PLA
LG	lignin
PHB	poly (3-hydroxybutyrate)
PP	poly (propylene)
PCL	poly (ε-caprolactone)
PBS	Poly (butylenes succinate)
SA	succinic acid
BD	1, 4-butanediol
PET	poly (ethylene terephthalate)
HDT	heat deflection temperature
TAIC	triallyl isocyanurate
DCP	dicumyl peroxide
TMAIC	trimethallyl isocyanurate
TMPTA	trimethylolpropane triacrylate
HDDA	1, 6-hexanediol diacrylate
GM	glycidyl methacrylate
BF	bamboo fiber
WF	wood flour
BF	bamboo flour
GNP	graphene nanoplatelets and
MWNT	multi-walled carbon nanotubes
MWNT-OH	hydroxyl functionalized multi-walled carbon nanotubes
PVA	poly (vinyl acetate)
PMMA	poly (methyl methacrylate)
PEG	poly (ethylene glycol)
DSC	differentiation scanning calorimeter

DMA	dynamic mechanical analysis
LDPE	low-density polyethylene
PEGM	poly (ethylene-co-glycidyl methacrylate)
PHBV	poly (3-hydroxy butyrate-co-hydroxyvalerate)
TPS	thermoplastic starch
HBN	hexagonal boron nitride
ES	3-Glycidyloxypropyle trimethoxysilane
E-beam	electron beam
BP	bamboo powder
EBP	E-beam irradiated bamboo powder
DSC	differential scanning calorimetry
TGA	thermo gravimetric analysis
XRD	X-ray diffraction
FT-IR	fourier tranforms infrared spectroscopy
NMR	Nuclear magnetic resonance spectroscopy
SEM	scanning electron microscope
SE	secondary electrons
BSE	backscattered electrons
PBS	phosphate-buffer solution

Chapter 1

Introduction

This chapter comprises a brief introduction of the research topic chosen along with the motivation and scope of the present investigation. The various bio-based and bio-degradable polymers were described briefly. The pros and cons of these polymers over existing petrochemical polymers are also mentioned. Further, the development in the properties of the commercially available bio-based and biodegradable polymer i.e. poly (lactic acid) for different kind of applications is also described. The evolution and organization of the thesis is also propounded.

1.1 General Introduction

Numerous polymeric materials are available in nature. Lignin (major constituent in all plants), cellulose, starch (in corn, potatoes), natural rubber (poly-cis-isoprene), proteins and DNA are a few examples. The degree of sophistication of natural processes to synthesize these materials is far beyond the conventional synthetic polymerization processes, for instance, polymerization of amino acids into protein at ambient temperature and pressure. These natural materials cannot serve mankind directly for commodity and engineering applications, as conventional petrochemical-based plastic materials. This is because conventional thermoplastic polymers/plastics have more heat stability than their natural counterpart and are usually processed via molten state into any complex desired shape as per applications, however, natural polymeric materials such as lignin, cellulose, and starch cannot be heated into molten state due to thermal degradation or decomposition. There are ample advantages of the conventional polymer/plastics than the natural counterparts such as low cost, simple chemical structure, good barrier properties for endues applications, ease to process into complex shapes and excellent performance etc. [1,2]. However, petrochemical-based non-biodegradable polymers/plastics have acute environmental issues which severely affect the life of wild species and also spoil the scenes due to its virtually endless applications. The increasing insecurity of petrochemical resources, increasing oil prices and growing concerns about greenhouse gas emissions are also thought-provoking issues. Hence, from the past few decades, the synthesis of bio-based and biodegradable polymers from the renewable resources has gained great interest in both industries as well as in academia. Further, as schematically represented in the Fig. 1.1, the biopolymers based on their source of origin can be classified into three major categories [3,4]: natural polymers which are obtained by direct extraction from biomass viz. cellulose, lignin, starch and proteins; synthetic polymers which are retrieved by microbial fermentation of biomass and then extraction viz. poly (hydroxyalkonoates) (PHA); and synthetic polymer synthesized from natural monomers viz. poly (lactic acid). Moreover, synthetic biopolymers can be processed by conventional processing equipment and are known as bio-plastic. The synthetic bio-polymers/plastics are not necessarily bio-degradable. The bio-degradable polymer/plastic must be mineralized completely by the action of microorganism in the natural environment (i.e. landfill) and return to the environment within a short time (<one year) after disposal. The compostable polymers/plastics are also similar to bio-degradable polymers/plastics, as they both decompose into natural elements and return to nature safely. However, compostable polymer/plastic requires a special composting environment and conditions in accordance with

defined standard viz. ASTM-D-6400-04, ISO-17088 and EN-13432 [4–6]. The compostable polymers also furnish nutrients to the earth after complete degradation. The bio-compostable polymers are further briefly described as below: (properties, advantages and disadvantages, structure and applications)

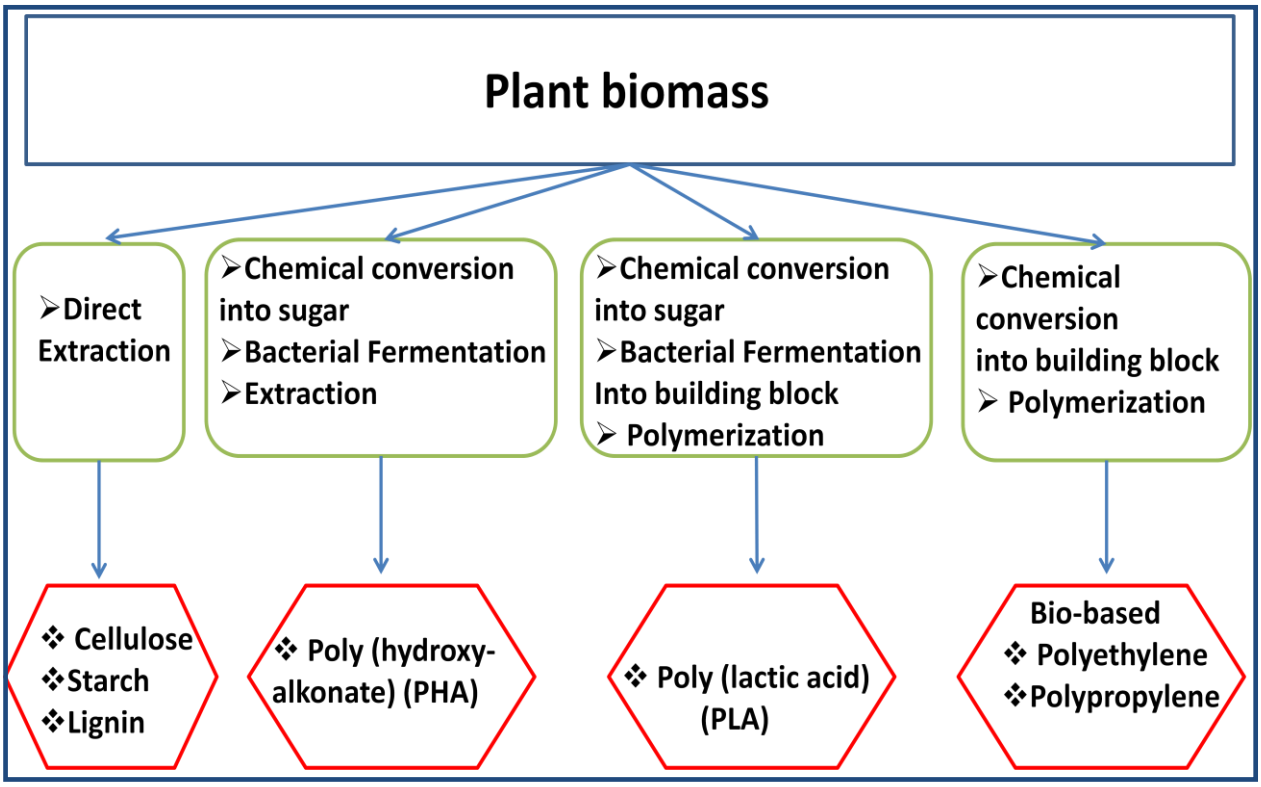

Fig.1.1 Production of biopolymers from different routes [4].

1.1.1 Poly (lactic acid)

The bio-based, bioresorbable and biodegradable poly (lactic acid) (PLA) is the linear polyester synthesized from lactic acid (2-hydroxypropanoic acid)/lactide (3,6-dimethyl-1,4-dioxane-2,5-dione) monomers through solid state polycondensation/ring opening polymerization (ROP) process [6]. The lactic acid/lactide monomers are derived from the natural feed stocks i.e. sugarcane, potato starch, corns and tapioca by the fermentation process. PLA synthesized via polycondensation process has a low molecular weight which leads to poor mechanical properties and is not acceptable for many commercial applications. This is because it is tedious to remove the water, which is a byproduct of this equilibrium reaction, as viscosity increases during the polymerization process. Hence, PLA having high molecular weight is usually synthesized via ROP process [7]. This two step process which normally involves extra purification step leads to increases in the production cost. However, this is the most favored and commercially adaptable process to make high molecular weight PLA because of precise control of chemistry and hence resulting polymer properties can be

broadened in more a restrained manner. Different forms of PLA (Fig. 1.2) i.e. poly (L-lactide) (PLLA), poly (D-lactide) (PDLA) and poly (DL-lactide) (PDLLA) depends on the chiral nature of their lactide monomers i.e. L-lactide, D-lactide, and DL-lactide, respectively (Fig. 1.2) [8,9]. Stereochemical purity of PLA depends on the stereochemical purity of the lactide monomers.

Further, due to stereoregularity of backbone polymer chains and enantiomeric purity of their building block (virgin monomers) the PDLA and PLLA are crystalline in nature possessing crystallinity of about 35%, glass transition temperature (T_g) ~ 50°C to 70 and melting temperature (T_m) ~ 170°C to 190°C [10,11]. In contrast, PDLLA is completely amorphous in nature because of its random polymer chain structure and consists of low T_g and T_m i.e. 34 °C and 155°C respectively. The stereocomplex PLA (sc-PLA) which is a resultant of blending PLLA and PDLA exhibits high T_m 230°C [12]. The mechanical properties of semicrystalline PLA such as yield strength, tensile modulus, deformability, notched Izod impact strength, flexural modulus and heat deflection temperature (HDT) are around 50-70 MPa, 3000-4000 MPa, 2-10%, 2.0-3.0 kJ/m^2, 4000-5000 MPa, and 51-60 °C respectively [13]. The commercial grade PLA was introduced in 2003 and found ample commercial applications [14]. The NatureWorks (USA) is a leading company which produces different series of commercial grades of PLA as per applications viz. 2000 series for extrusion and thermoforming, 3000 series for injection molding applications, 4000 series for films and cards, 6000 series for fibers and nonwovens and 7000 series for blow molding etc. Further, Purac, Teijin and Jiuding companies from Netherlands, Japan and China respectively are also some current leading producers of PLA. The commercial grade of PLA consists PLLA and a small percentage of PDLLA [15].

In some aspects such as carbon dioxide (CO_2) emission, energy consumption and end up life possibility, the PLA is much better than many petrochemical-based polymers [6,16]. However, PLA is not fit for many commercial applications, mainly hot-packaging applications and durable applications, due to its low deformation at the break, poor toughness and low thermal stability. Hence, these properties of PLA are required to improve for increasing its commercial applications in the diverse fields and also enable it to compete with existing petrochemical polymers [17,18].

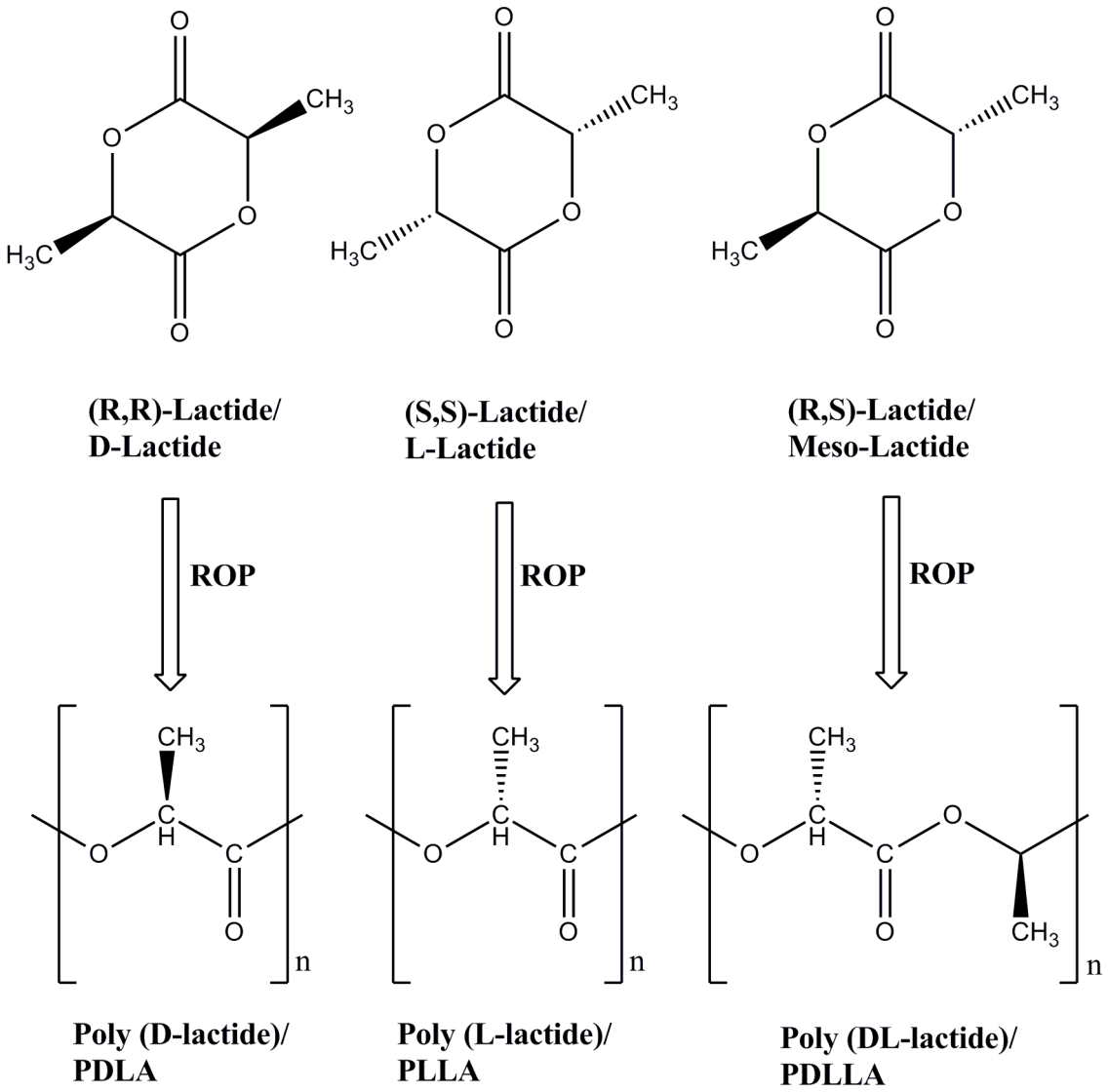

Fig. 1.2 Molecular Structures of a distinct form of PLA with respect to their chiral monomers [6].

1.1.2 Lignin

Lignin (LG) is the most plentiful biopolymer, next to cellulose, present in Mother Nature. It is the main constituent of all plants and furnishes them with mechanical support, rigidity, nutrients and safety from attacking microorganisms. Further, it also acts as an interface to hold the cellulose and hemicellulose in the polysaccharide matrix of biomass [19,20]. Lignin is produced from monolignols i.e. guaiacyl alcohol (hardwood and softwood), syringyl alcohol (hardwood) and p-coumaryl alcohol through radical-induced endwise polymerization in the plants [21,22]. The chemical structure of lignin depends on the extraction techniques viz. soda process, kraft process, sulfite process, organosolv process and steam explosion [23]. The typical model structure of lignin and its precursors are shown in Fig. 1.3. The chemical structure of lignin which consists of a number of functional groups

determines its compatibility with other polymers [21,24,25]. The large number of polar functional groups present in the lignin leads to the robust self-interaction of lignin molecules and decreases its miscibility in the hydrophobic polymers. The presence of large phenolic moieties in the complex lignin structure and self-interaction of polymer chains leads to high T_g ~ 97-165 °C [19,23]. The elastic modulus of lignin is 4500 MPa [26].

Since lignin is a by-product produced massively in the paper mills and in cellulose ethanol industries, the price of lignin is quite low as compared to oil-based materials. The lignin is being produced more than 70 % annually from the papermaking industries [27]. It cannot be processed directly by conventional polymers processing techniques because of its cross-linked structure and low thermal degradation temperature which is less than its melting point. However, lignin is a low-price inexhaustible material available in nature and being used as filler with many polymers to produce new kind of green plastic products. It can also be used as an antioxidant and UV light protective additive in the plastics [23,28]. The global lignin market, North America (US), Europe (UK, Germany, France), Asian Pacific (China, Japan, India), Latin America (Brazil) and the Middle East, Africa, is expected to reach around from 775 million USD to 900 million USD by 2020 [23].

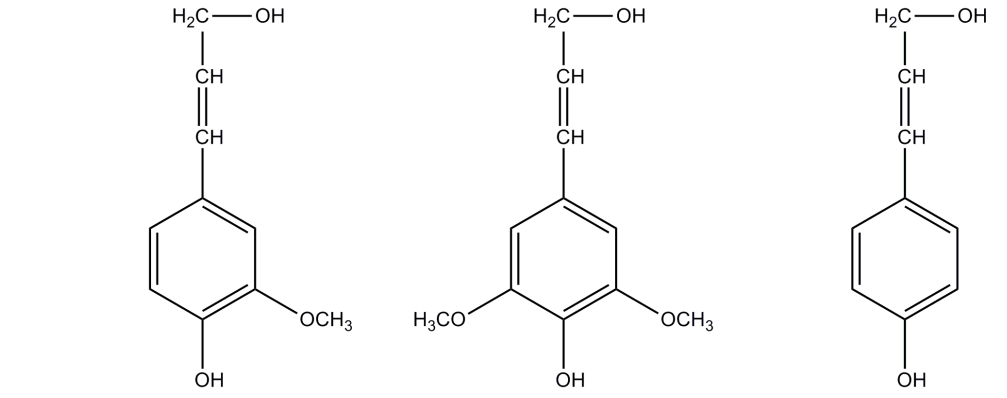

(a)

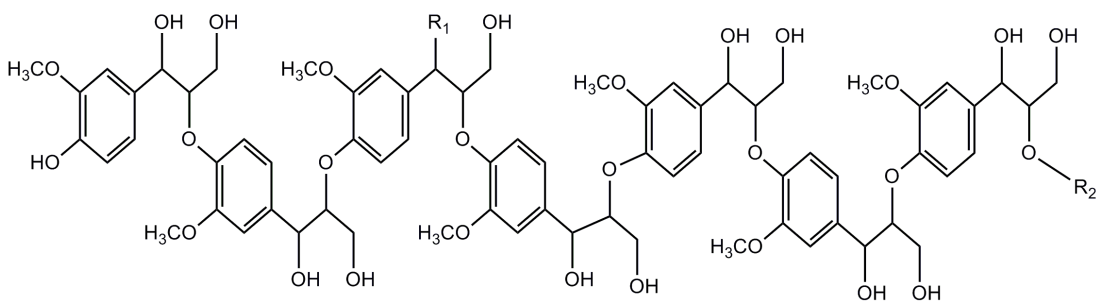

(b)

Fig. 1.3 (a) The different monolignols of lignin and (b) typical model structure of lignin [23].

1.1.3 Poly (hydroxyalkonoates)

The poly (hydroxyalkonoates) (PHA) belongs to polyester polymer family and is synthesized from the biomass through microorganisms viz. varieties of Gram-negative and Gram-positive bacteria [29,30]. The chemical structure of PHAs is depicted in Fig. 1.4. Based on the number of carbon atoms present in the branching polymer, the PHAs can be classified into two main categories i.e. short-chain and medium chain length PHAs. The short-chain length PHAs consist of three to five carbon atoms, for instance, poly (β-hydroxybutyrate)/poly (3-hydroxybutyrate), poly (4-hydroxybutyrate), poly (3-hydroxyvalerates) and their copolymers. However, medium-chain length PHAs consist of 6 to 14 or more than 14 carbon atoms, for instance, poly (3-hydroxyhexanoate), poly (3-hydroxyoctanoate) and their copolymers [31].

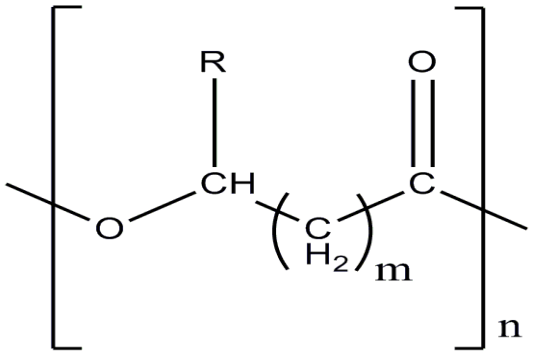

Fig. 1.4 General chemical structure of PHAs [30,32].

Further, the weight average molecular weight of PHAs is upto 3×10^6 Da [30,33]. The T_g and T_m of PHAs vary from -50 °C to 4 °C and 60 °C to 177 °C respectively. Among all PHAs the poly (3-hydroxybutyrate) (PHB) is more famous and most commonly used industrial polymer produced by bacteria from sugar and starch; it is discovered by Lemoigne in 1926. The mechanical properties of PHB are similar to poly (propylene) (PP), however, its major drawbacks i.e. brittleness, low thermal stability, poor crystallization rate and high cost restrict its commercial applications [30]. PHB has good biocompatibility and fast bio-composting rate. PHB based bio-plastic can be biodegraded aerobically and anaerobically into carbon dioxide (CO_2) and water (H_2O) or methane (CH_4). The main producers of PHB and its copolymers are PHB Industrial of Brazil, Kaneka Co., Tellen, Metabolix and Tianjin Green Bioscience of China.

1.1.4 Poly (ε-caprolactone)

The poly (ε-caprolactone) (PCL) is aliphatic polyester synthesized from cyclic ester caprolactone or ε-caprolactone (haxeno-6-lactone) through ring opening polymerization (ROP) process. It is synthesized in the presence of aluminum peroxide catalyst [34,35]. The chemical structure of PCL is given in Fig. 1.5. The molecular weight of PCL varies from 530 to 63, 000 M_n/Da and it is a semi-crystalline polymer and can be crystallized upto 69%. The T_g and T_m of PCL lie in the range -60 to -65 °C and 56 to 65 °C respectively. The mechanical properties of PCL i.e. tensile strength, Young's modulus and deformation at break are in the range 4 - 785 MPa, 210 - 440 MPa and 20 - 1000 % respectively [36].

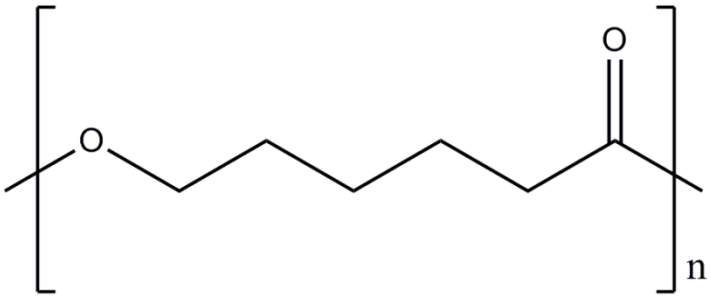

Fig. 1.5 The chemical structure of poly (ε-caprolactone) [36].

PCL has significant importance in industries and medical fields because of its biodegradability, biocompatibility, mechanical properties and miscibility with other polymers. However, its low T_g is a disadvantage for some applications. Hence, PCL is normally blended with other polymers or chemically modified and crosslinked by chemical or physical methods (radiation crosslinking) [37–40]. Dow Chemical and Daicel Corporations are the main producers of PCL.

1.1.5 Poly (butylene succinate)

Poly (butylene succinate) (PBS) is a biodegradable and bio-compostable polymer synthesized from the monomers succinic acid (SA) and 1, 4-butanediol (BD). These monomers are normally derived from fossil sources. However, interestingly, these can also be derived from the natural resources by fermentation process [41]. Hence, it may be expected bio-based in the near future. The chemical structure of PBS is shown in Fig. 1.6. The T_g and T_m of PBS are around -30 °C and 112 °C respectively [42,43]. The PBS can be exploited to manufacture mulch films, packaging films and hygienic products due to its interesting

thermo-mechanical properties and good biodegradability. However, low transparency, poor impact strength and high production cost are the hurdles for its commercialization [42].

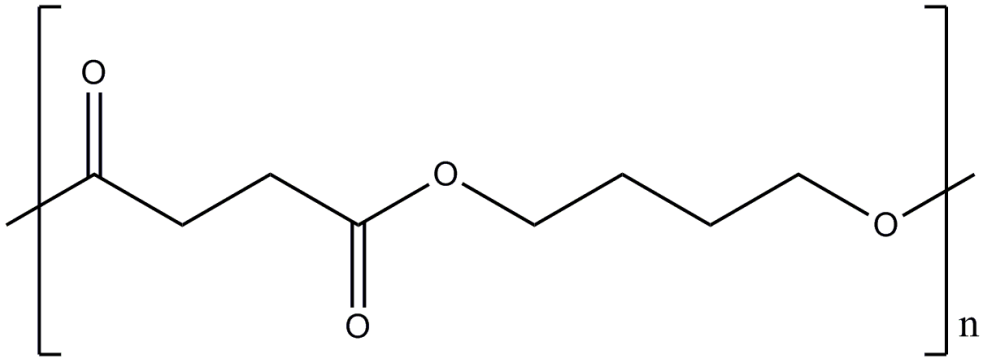

Fig. 1.6 Chemical structure of poly (butylene succinate) [41].

Since 1993, the PBS is commercially available with trade name Bionolle™ by Showa-Denko K.K. and its main manufacturers are Hexing Chemical (China), Mitsubishi Gas Chemicals (Japan), Ire Chemicals (Korea) and Showa Highpolymers (Japan).

In conclusion, among all bio-polymers and bio-compostable polymers described above, PLA exhibits superb biocompatibility, simple processability, good stiffness and transparency similar to poly (propylene) (PP) and poly (ethylene terephthalate) (PET) [6]. So, it can be used for various applications in diverse fields such as packaging, automotive and biomedical industries. However, its inherent brittleness, low elongation, poor thermal stability and high cost limit its widespread practical applications in many cases [17]. Further, the increasing demand of plastics in the society, as well as the escalating concerns about environmental problems generated due to petrochemical-based plastic, and increasing insecurity of fossil fuel resources are thought-provoking matters which insist the modification of PLA properties as per applications. Hence, the development of PLA based durable and green plastic for various applications has magnetized the interest of the global plastic market especially [44,45].

1.2 Literature Survey

Although the PLA exhibits good stiffness, excellent biodegradability and fine transparency the widespread application of PLA is still restricted due to its poor toughness, short extensibility, low heat deflection temperature (HDT) and more cost. So, there are several methods, viz. blending with other polymers, crosslinking of PLA matrix through chemical and physical process, chemical copolymerization and reinforcement of PLA matrix

with fibers and particles etc., has been used and described in the literature to overcome these drawbacks of PLA and make it more feasible for commercial applications as briefly discussed below.

1.2.1 Chemical copolymerization

Copolymerization is the process in which two or more than two different types of monomers are simultaneously polymerized and the resulting polymer consists of more than one repeating units [1]. The advantage of chemical copolymerization is that there is an ample number of monomers and polymers (both petrochemical and bio-based) available and can be copolymerized with PLA to manufacture a new material with average properties of both polymers. Hence, it is reported in the literature that the different polymers from petrochemical-based to bio-based, bio-compostable to non-compostable and amorphous to crystalline were exploited to copolymerize with PLA to produce new plastics as per applications [46].

Yui et al. [47] synthesized PLLA-b-PDLA diblock type copolymers (sb-PLA) from L-lactide and D-lactide monomers through ring-opening polymerization initiated by aluminium tris (2-propanolate). They found that this diblock copolymer easily promotes stereocomplex crystallization. The stereocomplex PLA (sc-PLA) comprises of both enantiomeric PLAs (PLLA and PDLA). The sc-PLA exhibits T_m 230° C which is greater than the T_m of PLLA and PDLA (i.e. 180° C). Hence, sc-PLA can act as a high-performance polymer [48].

Ohya et al. [49] proposed and reported a synthesis method for graft-polymerization of lactic acid on various types of polysaccharides by employing trimethylsilyl-protected polysaccharides. They were reported that the PLA-grafted polysaccharides copolymer showed more degradability due to reduced crystallinity as compared to PLA. They were also reported that this method can be used in graft-polymerization with other polyesters, glycolide and lactones on polysaccharides. The graft-copolymers obtained by this method may be used as biodegradable biomedical materials. Further, poly (lactic-glycolic acid) copolymer is accepted by FDA for clinical purposes.

A. K. Saleem et al. [50] synthesized and reported the poly (lactic acid)-poly (ethylene glycol)-biotin copolymer which has applications in the medical fields.

D.C. Aluthge et al. [51] synthesized triblock copolymer of poly (lactic) and poly (hydroxybutyrate) (PHB) i.e. PLA-PHB-PLA. The preparation of PLLA-PDLLA-PLLA and

PLLA-PDLLA-PDLA by sequential addition was also reported. The mechanical and rheological properties of prepared copolymers were investigated and reported. It was found that the rheological properties of PLLA-PDLLA-PLLA and PLLA-PDLLA-PDLA are similar to the PLLA and PDLA. However, triblock PLLA-PHB-PDLA exhibited more elastic nature having poor tensile strength and with remarkable enhancement in the deformation at the break.

From the literature, it is also observed that many authors had synthesized various copolymers of different polymers to enhance the miscibility of the PLA based polymer blends [52,53]. For instance, C.H. Kim et al. [54] synthesized poly (L-lactic acid-co-ε caprolactone) copolymer and discussed briefly the effect of concentration of synthesized copolymer on the compatibilization and crystallization behavior of PLLA/PCL blend. The details of the effect of different PLA based copolymers on the mechanical, thermal and degradation properties of PLA blends will be discussed in the section 1.2.4.

Hence, from the literature it can be concluded that the copolymerization is the best technique to develop new kind of materials from PLA for different applications in the diverse fields and this technique is broadening the PLA applications too. However, the long reaction tenure, cumbersome synthesis steps and cost of other constituents are the drawbacks of this technique to use for more commercial applications [52].

1.2.2 Chemical and radiation crosslinking of PLA matrix

In order to enhance the thermal stability of PLA, it is needed to strengthen the intermolecular interaction between PLA chains. A common solution to do that is to introduce crosslinking among the polymer chains of PLA matrix by chemical reactions [55]. The irradiation with UV-rays, X-rays and γ-rays is also one of the methods used to crosslink the polymer matrix. However, this method is not feasible for PLA because PLA degrades upon irradiation. Hence, recently, some authors have studied and reported the crosslinking of the PLA matrix by employing electron beam irradiation in the presence of various crosslinking agents [56–59]. The chemical and electron beam (E-beam) irradiation induced crosslinking of the PLA matrix in the presence of the crosslinking agents also strengthens the mechanical and thermal properties of PLA.

S. Yang et al. [55] employed the chemical treatment to induce the crosslinking of the PLA matrix. They melt blended polyfunctional molecules i.e. triallyl isocyanurate (TAIC) and

PLA along with a reaction initiator dicumyl peroxide (DCP). From the analyzed results they reported PLA matrix crosslinking was initiated with little addition of TAIC or DCP. Further, crosslinked PLA showed a decrement in the crystallinity and a remarkable enhancement in the thermal degradation temperature and mechanical properties of PLA.

N. Nagasawa et al. [56,57] irradiated the PLLA film to the electron beam in the presence of different crosslinking agents i.e. triallyl isocyanurate (TAIC), trimethallyl isocyanurate (TMAIC), trimethylolpropane triacrylate (TMPTA) and 1, 6-hexanediol diacrylate (HDDA). The concentration of crosslinking agents was taken as 1 wt%, 3 wt% and 5 wt% in the film. The PLLA film containing crosslinking agents were irradiated to the electron beam with different doses 20 kGy, 40 kGy and 50 kGy. From these studies, it was reported that TAIC is an excellent crosslinking agent for PLLA at optimized percentage i.e. 3 wt% and optimized radiation dose i.e. 50 kGy. PLLA film with 3 wt% of TAIC and at 50 kGy dose showed maximum gel fraction and good heat resistance properties as compared to other compositions.

B. Y. Shina et al. [58] modified the properties of PLA through E-beam irradiation in the attendance of functional monomer glycidyl methacrylate (GM). They were reported both chain scission and branching of the PLA upon irradiation, however, the formation of long chain branching of PLA is more prominent as compared to PLA chains scission, if the GM is present in the system. Hence, the thermo-mechanical properties were significantly enhanced due to the formation of long polymer chains. It was also reported that PLA containing 3 phr GM and 20 kGy absorbed dose showed 100 times more storage modulus and 10 times more complex viscosity as compared to pure PLA.

M. Salvatore et al. [59] prepared the poly (lactic acid)/montmorillonite nanocomposites for food packaging applications. The prepared nanocomposite films with loaded clay at 1, 3 and 5 wt % were irradiated to electron beam doses of 1 kGy and 10 kGy. From the acquired results, they reported that the electron beam irradiated samples show increment in the tensile modulus, T_g and decrement in the oxygen permeability as compared to unirradiated samples of nanocomposites. This is because electron beam irradiation brought the polymer crosslinking in the nanocomposites and hence increase the T_g of irradiated films. Further, the introduction of the clay to PLA creates a sinuous path to passage of oxygen through film and hence leads to decrement in the oxygen permeability.

Therefore, from the above findings, it can be inferred that the crosslinking of PLA matrix through the physical or chemical method is useful to improve the thermal stability of the PLA and also increase the tensile and storage modulus. However, the deformability and impact toughness of PLA are still inferior even after crosslinking of the PLA matrix [60].

1.2.3 Poly (lactic acid) composites

The polymer composites are often prepared to tailor the properties of the polymer matrix and/or reduce the cost of the final polymer product [6]. A composite comprises a polymer matrix (continuous phase) and reinforcement (discontinuous phase) agents i.e. either particles or fibers. The polymer matrix binds the fibers together and helps to transfer the applied stress from one to another which keeps the fibers at the desired location and orientation. The matrix also shields them from erosion and environmental damage. The most common type of reinforcement to prepare the polymer composites is fibers. In the literature several authors have reinforced the PLA with various natural and synthetic fibers; organic and inorganic fillers and whiskers in order to tailor the mechanical, thermal and degradation properties for diverse applications as well as to bring down the high cost of PLA [61].

Many authors have employed various natural fibers viz. kenaf, flax, hemp, bamboo, jute, abaca, pineapple, leaf and wood fibers to prepare fully bio-based and biodegradable PLA-fiber composites [62]. Some of the authors have reported the use of synthetic fibers i.e. glass fibers, PAN-based carbon fibers etc. to reinforce the PLA matrix. The fibers (natural and synthetic) are normally pretreated with different methods i.e. alkali treatment, esterification, cyanoethylation and silane treatment to improve the matrix fibers adhesion [63,64]. Further, organic fillers i.e. wood flour, starch, rice hulls, sugar beet pulp etc. and inorganic fillers i.e. hydroxyapatite, talc, carbon black, carbon nanotubes, hexagonal boron nitride etc. were also exploited to manufacture PLA composites for various applications [64–66]. The main difference between polymer composite and polymer blend is the polymer composite is made up of two or more distinct constituents or phases resulting multiphase system, whereas, the polymer blend is prepared by blending two or more polymers to get single phase system. The development and properties of some best PLA composites are discussed below:

H.M. Akil et al. [67] reported that the kenaf fiber-reinforced PLA composites consist of excellent mechanical, thermal properties and good fibers-PLA matrix adhesion when alkali and silane treated fibers were exploited. These composites have also shown significant improvement in the heat deflection temperature (HDT) from 64.5 °C to 170.3 °C and

174.8 °C (when alkali treated fiber were used). It was reported that the improvement in these properties is mainly derived from the increases in modulus as well as good interaction between matrix and fibers. It was further reported that the kenaf fibers promotes the crystallization and prevent the deformation of PLA/kenaf composites which lead to the higher HDT.

B. Bax et al. [68] reported that PLA reinforced with cordenka rayon fibers (30 % by weight) exhibits highest impact strength i.e. 72 kJ/m^2 and tensile strength 58 MPa. However, PLA matrix reinforced with flax fibers (30 % by weight) consists of highest Young's modulus. These composites have possible applications in automotive and electronic industries.

R. Tokoro et al. [69] prepared the poly (lactic acid)/bamboo fiber (BF) composites. They incorporated the different BF i.e. alkali treated pulp, steam exploded pulp and short BF to PLA matrix. They found that the PLA matrix reinforced with steam-exploded pulp fibers composites have shown a significant improvement in the bending strength, impact strength and heat resistance of virgin PLA. They also reported that the incorporation of bamboo fibers also increased the crystallinity of PLA. Further, the thermal properties and HDT of PLA/BF composites were significantly enhanced after annealing the prepared samples at 110 °C for 5h.

S.N. Lee et al. [70] synthesized PLA/wood flour composites and studied the effect of bamboo flour addition on the mechanical and thermal properties of PLA. The wood flour (WF) was incorporated utpo 40 wt% into the PLA along with silane (1 wt% and 3wt %) coupling agent to improve the interfacial affinity between PLA and WF. It was observed that the T_g and thermal degradation temperature decreased slightly as the wood flour content increased. This is attributed to poor interfacial compatibility between wood flour and PLA matrix. However, the addition of silane coupling agent in the PLA/WF composites at 1 wt% was enhanced the interfacial bonding between matrix and filler which resulted in improvement in the tensile modulus, tensile strength, T_g and thermal degradation temperature.

Y. Wang et al. [71] incorporated bamboo flour (BF) into PLA matrix to enhance its mechanical and thermal properties. The PLA-g-glycidyl methacrylate copolymer was first synthesized and blended along with PLA and BF in the PLA/BF bio-composite to achieve the good adhesion and better dispersion of fillers in the polymer matrix. From the results it was found that the PLA/BF composite consist of PLA (85 wt %), BF (15 wt %) and PLA-g-

glycidyl methacrylate (15 phr) showed significant improvement in thermal decomposition temperature, tensile modulus and tensile strength and small increment in the impact strength as compared to PLA/BF composites without compatibilizer.

Debrupa Lahiri et al. [65] have reinforced the polylactide-polycaprolacton copolymer (PLC) with boron nitride nanotubes. The boron nitride nanotubes were incorporated in three different concentrations i.e. 0, 2 and 5 wt% to reinforce PLC for orthopedic applications. It was reported that the addition of 5 wt% boron nitride nanotubes remarkably increases the elastic modulus and tensile strength of PLC to 1370% and 109% respectively. It was also reported that incorporation of boron nitride nanotubes into PLC does not have any adverse effect on its ductility.

M. Li et al. [66] studied the degradation behavior of PLA reinforced with different inorganic fillers i.e. titanium dioxide (TiO_2), graphene nanoplatelets (GNP), multi-walled carbon nanotubes (MWNT) and hydroxyl functionalized multi-walled carbon nanotubes (MWNT-OH). They reported that the incorporation of inorganic fillers at optimal concentration significantly increases the crystallization rate in the resulting composites. This is because the nanofillers in the resulting composites act as nucleating agents and increase the crystallization rate. Among all composites, PLA/TiO_2 was shown high degradation rate as compared to pure PLA due to the poor interfacial interaction between matrix and particles. Moreover, PLA/MWNT-OH composite was shown a decrement in the degradation rate as compared to PLA. This is because the surface treated MWNT has better interfacial bonding with matrix than untreated MWNT or other particles. The PLA/MWNT composite has also shows small increment in the tensile strength as compared to other composites and pure PLA.

Hence, it can be concluded that the reinforcement of the PLA matrix with various fibers and fillers leads to an improvement in the tensile, flexural, heat resistance and degradation properties of PLA. However, the some of PLA composites exhibit the impact properties and deformation at break usually less than pure PLA [6]. So, there is a need to improve these properties in the case of PLA-composites. Therefore, the use of relevant fibers reinforcement to PLA tailors the properties of PLA for desired applications (from biomedical to commercial applications) and incorporation of suitable low-cost fillers to PLA reduce the cost of PLA.

1.2.4 Poly (lactic acid) blends

The blending of the PLA with other polymers is the most adaptable and convenient method to overcome the drawbacks of PLA and hence tailors its properties for desired applications. Generally, blending of various plasticizer and small molecules with PLA leads to significant improvement in the deformation at break and impact toughness. The physical bending of PLA with other polymers furnishes the best results if the comments of the prepared blend are properly miscible (i.e. miscible blend). The compatibilization techniques are used to achieve the good compatibility among the different phases of incompatible or immiscible polymer blend. The interfacial phase compatibility and miscibility of blend components decide the performance of the resulting blend. The term compatibility is defined on the bases of phase morphology and properties profile of the resulting blend. If a partially miscible or immiscible blend exhibits a fine morphology and combined properties of the blended polymers then the compatibility between the blend components is good and it is said to be compatible blend. However, if blend consists of coarse phase morphology and inferior properties then it is said to be an incompatible blend. The compatibility between different phases of an incompatible blend can be enhanced by a suitable approach usually known as compatibilization. Thus the incompatible blend can be transformed to compatible blend by altering the blend coarse phase morphology to fine phase morphology and improving properties from poor to superior after compatibilization. Hence, in the literature, various compatibilizers and copolymers were blended with PLA along with selective polymer to improve the compatibility of resulting blend [52,72]. The main task of the compatibilizer in the blend is to decrease interfacial tension between the blend components and minimizes the size of the dispersed phase by reduction of and hampering the coalescence of the dispersed phase. Further details of various PLA blends and their compatibilization strategies are discussed as follows.

A. M. Gajria et al. [73] reported partly bio-based and bio-compostable blend of PLA and poly (vinyl acetate) (PVA). The PVA was melt blended with PLA by employing single screw extruder. The miscibility of prepared samples were characterized by physical properties, phase morphology and degradation properties. The prepared blend exhibits single T_g and claimed as miscible. The PLA/PVA blends (from 5 wt% to 15 wt% PVA) also show higher tensile strength and PLA/PVA blend (with 5 wt% PVA) shows significant increment in the elongation at break (i.e. utpo 200%) due to positive interaction between PLA and PVA phases in the resulting blend. They also analyzed the enzymatic degradation test results and found that the addition of PVA to PLA results in a drastic fall in the degradation rate.

G. Zhang et al. [74] blended poly (methyl methacrylate) (PMMA) with poly (DL-lactide) (PDLLA) and poly (L lactide) (PLLA). They studied the miscibility, crystallization behavior and interactions of the blend components. From the DSC results, they found a single value of T_g for the resulting blend which lies in between the T_g of two individual polymers, that signifies the miscibility of blend components. They also reported that the addition of amorphous PMMA strongly restricts the crystallization of PLLA.

M. Sheth et al. [75] prepared and characterized the PLA and poly (ethylene glycol) (PEG) blends with different weight ratios i.e. 100:0, 90:10, 70:30, 50:50 and 30:70 (PLA/PEG). Authors asserted that the miscibility of PLA/PEG blend depends on the weight ratio of the two polymers in the blends which were confirmed from the differential scanning calorimeter (DSC) and dynamic mechanical analysis (DMA) results. They reported that the blending of PEG with PLA leads to miscible blend if the weight ratio of PEG is less than 50% and partially miscible for above 50%. The T_g and tensile modulus of PLA decreased with increasing PEG concentration upto 50 %. However, the elongation at break increases due to the plasticization effect of PEG. Further, the crystallinity of PLA is found to increase with the blending of PEG above 50 wt%. Hence, PLA/PEG blends (PEG > 50%) with improved crystallinity showed the increment in the tensile modulus and drastic decrement in the elongation at break.

Y. Wang et al. [76] have reported the PLLA/ LDPE (Low-density polyethylene) binary and PLA/LDPE/PE-b-PLLA ternary blends. In the first step, they had synthesized a diblock copolymer PE-b-PLLA from L-lactide and PE-OH (hydroxyl terminated PE) through the ROP process. The weight ratio of PLLA and LDPE was fixed (i.e. 80:20) in the prepared binary blend. Moreover, PE-b-PLLA block copolymer was further incorporated into a prepared binary blend with weight percentage that varied from 2 wt% to 10 wt% in order to prepare PLLA/LDPE/PE-b-PLLA ternary blend. They have analyzed the effect of varying concentration of added block copolymer on the morphology and other properties of the prepared blend. From the morphology results it was observed that the PLLA/LDPE binary blend exhibited large average particle size i.e. 25.7 µm of dispersed LDPE phase and wide size distribution (4 to 150 µm) due to poor compatibility of the blend components. The PLLA/LDPE blend showed a decrement in the tensile modulus, tensile strength and impact resistance; however, it showed increment in the elongation at break. The addition of 2 wt% PE-b-PLLA copolymer to the PLLA/LDPE blend significantly on average reduced the particle size of dispersed LDPE phase to 3.5 µm and narrow down the particle distribution (1

to 15 µm). This is because the PE-b-PLLA block copolymers acted as a compatibilizer and increased the interfacial adhesion of the blended polymers. As the wt % of block copolymer increases the average particle size of dispersed phase further decreased. The PLLA/LDPE/PE-b-PLLA ternary blend has shown increment in the impact strength, elongation at break and small decrement in the tensile modulus and tensile strength.

N.S. Choi et al. [77] prepared a PLLA/PCL blend with fixed weight ratio 70:30. They further incorporated a random copolymer PLLA-co-εCL and block copolymer PLLA-b-εCL to PLLA/PCL blend and studied their effect on the morphology and degradation properties. It was noticed that the size of dispersed PCL phase in the blend decreased noticeably from 10 µm - 3µm with the incorporation of 5phr PLLA-co-εCL copolymer. This indicates that the PLLA-co-εCL copolymer acted as a compatibilizer and enhanced the miscibility of PLLA/PCL blend. In the case of PLLA-b-εCL, the size of the dispersed PCL phase decreased with increasing block copolymer content upto 10 phr. Hence, both copolymers significantly enhanced the compatibility among dispersed PCL phase and PLLA matrix in the resulting blend.

H.T. Oyama [78] proposed the super though PLA/ poly (ethylene-co-glycidyl methacrylate) (PEGM) blend which was synthesized by reactive blending of PLA with PEGM. He noticed a significant enhancement in the deformation at break and notched impact strength. It was asserted that during melt blending the PLA-g-PEGM graft copolymers are formed at the interface which compatibilized the resulting blend. It was further reported that the annealing of PLA/PEGM blend at 90 °C for 2.5 h increased the impact strength 50 times than neat PLA which confirmed that the matrix crystallization has a major contribution in toughening.

H. Bai et al. [38] reported the effect of crystallization of the polymer matrix on the impact toughness of PLA/PCL blend. The concentration of nucleating agent and dispersed PCL phase varied to achieve a wide range of matrix crystallinity (10 to 50 %) in PLLA/PCL blend. The effect of different mold temperatures in injection molding on the crystallinity of prepared blends was also studied. The impact toughness of resulting blend was tailored by controlling the crystallization of PLLA matrix. They reported that the PLLA/PCL blend exhibits poor crystallinity in injection molding at both mold temperatures i.e. 50 °C and 130 °C. However, the incorporation of the nucleating agent to PLLA and PLLA/PCL blend significantly increased the matrix crystallinity upto 50 %, at mold temperature 130 °C. The remarkable enhancement in the impact toughness upto 28.9 kJ/m^2 was achieved for

PLLA/PCL blend with highly crystallizing PLLA matrix. It was also noticed that there is a straight relationship between matrix crystallization and toughness. Further, it was also asserted that crystallization of PLLA matrix has a major contribution in improving the impact toughness rather than interfacial adhesion or average size and distribution of dispersed PCL phase.

Several authors [72] had used and blended various heat resistant polymers and copolymers viz. poly (carbonate), nylon, poly (oxymethylene) and poly (acrylonitrile-butadiene-styrene) etc. with PLA to improve its heat resistance property as well as impact toughness. For instance, K. Zhang et al. [79] synthesized a ternary blend of PLA, poly (3-hydroxy butyrate-co-hydroxyvalerate) (PHBV) and poly (butylene succinate) PBS which showed the balance stiffness and toughness along with improved heat deflection temperature (HDT) ~ 72 °C.

Many authors had also employed directly extracted biopolymers such as lignin and starch to make fully bio-based and biodegradable PLA blends for single use applications. These biopolymers were used as cheap fillers to reduce the cost of PLA because these polymers are abundant in nature. However, blending of these biopolymers with PLA is not straightforward because it results in poor miscibility of resulting blend components which leads to a dramatic loss of mechanical and thermal properties of PLA. Hence, various approaches, i.e. chemical modification, use of plasticizers, use of compatibilizers and copolymers, were exploited to increases the miscibility of these polymers into the PLA matrix which results in a compatible blend with improved mechanical and thermal properties [23,80].

Zhang et al. [81] synthesized PLA and wheat starch blend compatibilized by maleic anhydride (MA). An initiator L101 was employed to start the reaction among compatibilizer and polymers. The PLA/Starch blend was compatibilized with MA and L101 which shown significant improvement in the mechanical properties as compared to virgin PLA/starch blend. This signifies that the compatibilizer significantly improved the interfacial bonding between both polymer phases.

J.M. Ferrri et al. [82] reported PLA and thermoplastic starch (TPS) blend compatibilized by maleinized linseed oil. The weight percentage of TPS is fixed i.e. 30 %, however, compatibilizer i.e. maleinized linseed oil was added as parts per hundred from 0 phr to 8 phr. They found that the small amounts of compatibilizer positively improved the compatibility of matrix and dispersed phase as well as ductility of the resulting blend due to

its combined compatibilization-plasticization effect. The PLA/TPS blend with 6 phr maleinized linseed oil exhibited the elongation at break upto 160 % and high charphy's impact strength 9.5 kJ/m^2. The decrement in the tensile strength, modulus and T_g were noticed due to the plasticization effect of a compatibilizer.

Xiong et al. [83] compatibilized the incompatible PLA/Starch blend by utilizing epoxide soybean oil (ESO). The compatibility of resulting blend was increased on replacing the starch with MA grafted starch. This is because the reaction possibility of ESO with MA-g-starch was more as compared to virgin starch. The formation of actual compatibilizer i.e. PLA-ESO-Starch copolymer during the melt blending leads to the better compatibility and improved properties of resulting blend.

J. Li et al. [84] investigated the mechanical and thermal properties of PLLA/lignin blend. The lignin was incorporated at four levels i.e. 10, 20, 30 and 40 wt% to prepare PLLA/lignin blend. They noticed the decrement in the tensile strength, elongation at break and thermal degradation temperature as the lignin contents reaches 20 wt% in the resulting blend, however, Young modulus remained intact. From the results, they also asserted the existence of intermolecular interaction among PLLA and lignin molecules. It was stated that the direct blending of PLLA and lignin would mix the blend components at a macroscopic level, not at the molecular level.

Jalel Labidi et al. [24] reported the chemical modification of lignin by using the acetylation process and its blending with PLA. They found that the acetylated lignin has shown better miscibility and good compatibility with PLA into the PLA/Lignin blend as compared to unmodified lignin. Hence, significant improvement in the initial degradation temperature, hydrolytic degradation and contact angle was noticed in the case of PLA/lignin blend having acetylated lignin. However, its mechanical properties decreased as the concentration of acetylated lignin increased from 5% to 20%.

E. S. Sattely et al. [26] have synthesized lignin-lactide copolymer and reported that it can be employed as dispersion modifier in PLA/lignin-lactide composite. They observed improvement in the mechanical properties at low concentration of lignin i.e. 0.9 wt %, however, the decrement in the mechanical properties was noticed as the concentration was changed to 4.4 wt %.

Recently, Y. Liu et al. also synthesized and characterized dodecylated lignin-g-PLA graft copolymer and used it for significant toughening of PLA [85]. They incorporated this

graft copolymer to PLA and found a significant improvement in elongation at break, tensile strength and Young's modulus at low lignin % (w/w) (i.e. 1.8 %). However, the significant decrement was observed in the elongation at break, as the concentration of lignin-g-PLA graft copolymer was increased, with the increment in lignin % (w/w) (i.e. 4.5 %).

Hence, from the above discussion, it can be concluded that the blending of PLA is the best approach to overcome the drawbacks of PLA and it can be feasible to tailor various properties of PLA for different applications. Further, blending other most abundant natural polymers with PLA by exploiting suitable methods is appreciable to decrease the price of PLA and robust it to compete with existing petrochemical plastics in the global plastic market.

1.3 Scope and outline of the thesis

It is firmly believed that in the near future, there is more scope to replace the petrochemical-based plastic with PLA as compared to other bio-based and bio-compostable polymers because some of its properties such as stiffness, clarity and processability are similar to the existing most commonly used petrochemical-based plastics viz. polypropylene (PP) and poly (ethylene terephthalate). So, efforts are being made by various researchers in both academia and research laboratories and entrepreneurs in the industries to circumvent the other drawbacks of PLA i.e. poor toughness, less deformability, low heat resistance and high cost. Blending of PLA with polymers is the suitable approach to improve its inferior properties. However, miscibility of blend components and their interfacial compatibly are key parameters that decide the performance of prepared blend. The incorporation of copolymers of blending polymers can compatibilize the resulting blend effectively, but, also increase the cost of the final product due to tedious preparation methods and/or additional cost of copolymers.

The principal aim of the thesis is to furnish the probable methods to refine the properties of PLA with the main emphasis on improvement in the toughness, heat resistance and cost reduction. Hence, PLA based in-situ compatibilized blends were prepared by various simple and physical routes. The pros and cons of the developed methods are also described in the thesis. The remaining parts of the thesis are organized as follows:

Chapter 2 presents the materials and methodologies used to prepare PLA blends and blend-composites as well as the brief description of various tests used to characterize the

prepared materials. The physical treatment of used natural polymers by electron beam irradiation is also described in this chapter.

Chapter 3 elucidates the formation of PLA/PEGM graft copolymers during melt blending of PLA and poly (ethylene-co-glycidyl methacrylate) (PEGM) which acts as an interface between two polymer matrices and compatibilize the resulting blend. The mechanical and thermal properties of compatibilized PLA/PEGM blend are discussed. Further, the effect of reinforcement of PLA/PEGM blend with hexagonal boron nitride particles (HBN) on the mechanical and thermal properties of PLA/PEGM blend are also investigated.

Chapter 4 The PLA/PEGM blend and PLA/PEGM/HBN blend-composites, which were discussed in chapter 3, were irradiated to the electron beam. The optimization of mechanical, thermal and hydrolytic degradation properties of PLA/PEGM/HBN blend-composites through electron beam irradiation was performed. The optimized blend-composite with better mechanical, thermal and degradation properties was reported.

Chapter 5 describes a green physical approach to compatibilize biobased and biodegradable poly (lactic acid)/lignin (PLA/LG) blends for better mechanical, thermal and degradation properties. The biopolymer lignin was first treated with an electron beam and reported the changes due to irradiation. The PLA/LG blend with unirradiated lignin and electron beam irradiated lignin were prepared and characterized. The in-situ formation of PLA-TAIC-Lignin crosslinked structures which compatibilized the PLA/LG blend was elucidated.

Chapter 6 deals with the preparation and characterization of PLA/bamboo powder (BP) composites. The bamboo powder was irradiated to electron beam before blending with PLA. The effect of electron beam irradiation and epoxy silane agent on the miscibility of BF into PLA matrix was investigated.

Chapter 7 presents the concluding remarks on methodologies described in the thesis. A comparative analysis for mechanical, thermal and hydrolytic degradation properties of PLA and optimized compositions of prepared PLA blends and blend-composites has been executed in this chapter.

Chapter 2

Materials and Methods

This chapter describes different polymers, compatibilzers and additives which are used in the preparation of blends and blend-composites. The methods used to prepare the blends and blend-composites, sample preparation methods and various characterization techniques used to test the prepared samples are also discussed in detail.

2.1 Materials Used

- **Poly (lactic acid) (PLA),** a commercial Ingeo biopolymer 3052D grade, having melt flow rate (MFR) 14g/10 min (210°C, 2.16 kg), glass transition temperature (T_g) 55-60°C and crystalline melt temperature 145-160°C, was supplied by Natur-Tec India Pvt. Ltd.
- **Poly (ethylene-co-glycidyl methacrylate) (PEGM)** pellets, containing 8 wt% Glycidyl Methacrylate and having melt flow rate 5g/10min (192°C, 2.16 kg) were purchased from Sigma-Aldrich.
- **Hexagonal boron nitride (HBN)** powder with particle size 1μm was procured from Sigma-Aldrich.
- **Alkali lignin (LG)** a commercial grade (consists of low sulphonate contents, pH-10.5 and Mw~ 10,000) was obtained from Sigma-Aldrich.
- **Triallyl isocyanurate (TAIC) (1,3,5-Triallyl-1,3,5-triazine-2,4,6(1H,3H,5H)-trione)** a crosslinking agent contains 500 ppm tert-butylhydroquinone as inhibitor, boiling point 149-152 °C and density 1.159 g/ml was bought from Sigma-Aldrich.
- **3-Glycidyloxypropyle trimethoxysilane (Epoxy silane),** melting point < -70 °C, boiling point 119-121 °C and density 1.072 g/ml, was purchased from Alfa Aesar.
- **Bamboo granules** were supplied by "Maharashtra Bamboo Development Board, Nagpur, India" and ultra fine bamboo powder (BP) was prepared by using bamboo granules. The average particle size is 3-5 μm measured by employing Malvern particle size analyzer.
- **Phosphate buffer** powder was purchased from Sigma-Aldrich.
- **Deuterated chloroform ($CDCl_3$)**
- **Dimethyl sulfoxide-d_6 (DMSO-d_6)**
- **Chloroform (Trichloromethane) ($CHCl_3$)** was from Finar Ltd. India
- **Methanol (CH_3OH)** was from Finar Ltd. India.
- **Sodium phosphate monobasic anhydrous** was from Finar.
- **Sodium phosphate dibasic dihydrate** was from Finar.
- **Hydrochloric acid (HCL)** 0.1 N solution was from Finar.
- **Sodium Hydroxide (NaOH)** was from Finar.
- **De-ionized Water**

2.2 Methodology

The desired blends and blend-composites are prepared by melt-blending. The processes are opted to meet the desired purposes as follows.

2.2.1 Micro-compounding

Micro-compounding is a well-known technique to process or mix the raw polymer with various chemicals, additives or another polymer in the molten state at a very minute level i.e. 2 ml to 15 ml. The typical ingredients i.e. curatives or crosslinking agents, reinforcements, colorants, plasticizers and fillers used during micro-compounding strengthen the raw polymer and impart desired properties to the final product [18,86–88]. Micro-compounding is generally executed by using twin screw micro-compounder. The typical photographs of twin screw micro-compounder and extruder along with schematic workflow are shown in Fig 2.1 and 2.2 respectively. The micro-compounder comprises of an electrical barrel heater, a hopper with the piston for material feeding, conical screws, a motor for rotating screws, temperature and speed controller digital display, and manual valve and nozzle for exiting polymer melt etc. In the batch micro-compounder, the recirculation mixing time can be controlled by a manual valve. The resulted melt can be flushed out for the formulation of strand, injection molders and fiber line. The twin screw micro-compounder has significant advantages in the research and development (R&D) because it gives faster and better mixing and needs material in small quantity with less investment to prepare samples which are very essential to boost the innovation process.

2.2.1.1 Preparation of PLA/PEGM blend and PLA/PEGM/HBN blend-composites

The poly (lactic acid) (PLA)/poly (ethylene-co-glycidyl methacrylate) (PEGM) blend and Poly (lactic acid) (PLA)/Poly (ethylene-co-glycidyl methacrylate) (PEGM)/hexagonal boron nitride microcrystalline powder (HBN) blend-composites were prepared by using twin-screw Micro compounder, X-Plore, DSM, Netherlands which has clockwise co-rotating assembly. PLA pellets were vacuum dried at 70 °C for 12 hours before blending because drying of PLA resins normally takes place in the range of 60–90 °C. The required drying time is dependent on the drying temperature and opted as per the literature [6]. During the preparation of blend-composites, the processing conditions such as processing temperature, 210 ˚C, mixing time (10 minutes) and screw speed 80 rpm were kept constant for all compositions. The weight ratio of the blends was fixed at 80:20 (PLA: PEGM). However, the

hexagonal boron nitride (HBN) was incorporated with various amounts- 1 phr, 5 phr and 10 phr to prepare required blend-composites.

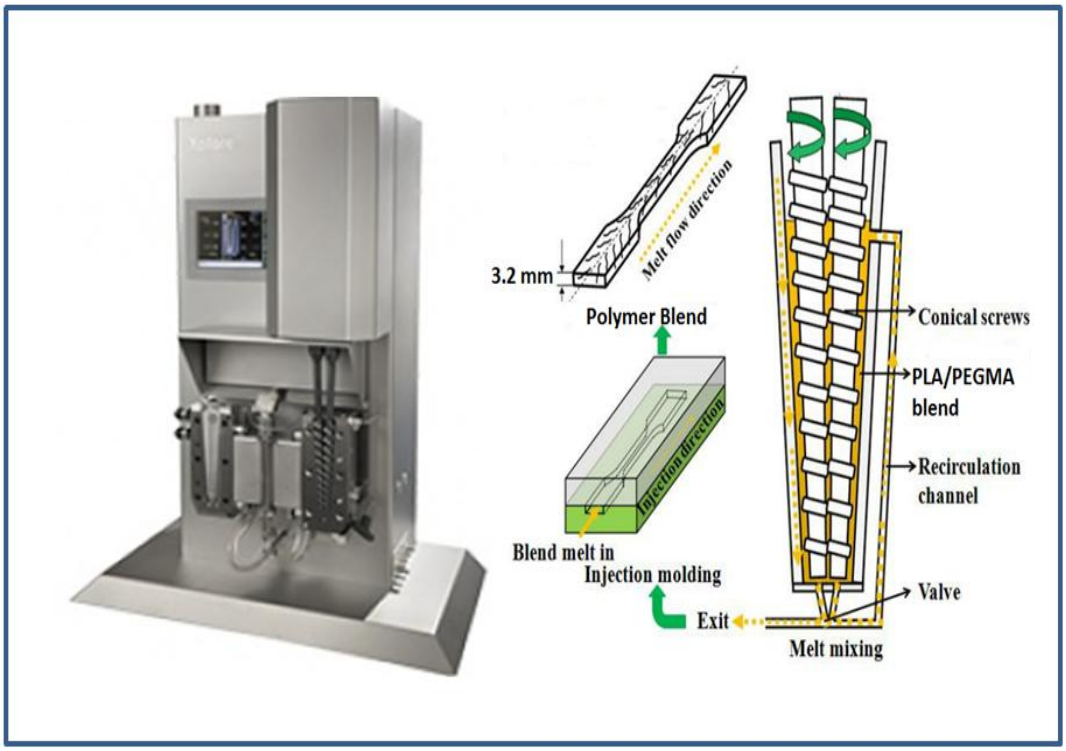

Fig. 2.1 Twin-screw Micro compounder, X-Plore, DSM, Netherlands and schematic workflow to prepare blend and blend-composites [89].

2.2.1.2 Preparation of poly (lactic acid)/lignin blends

The E-beam irradiated lignin with different doses along with TAIC at 3 phr were mixed thoroughly with PLA separately and then extruded by exploiting, THERMO HAAKE model twin screw extruder. PLA pellets were vacuum dried at 70 °C for 12 hours before extrusion. All E-beam irradiated lignins having different doses were processed with same processing parameters such that the feed zone temperature 162 °C, compression zone temperature 165 °C, metering zone temperature 165 °C and at a screw speed of 50 rpm. The extruded wires were then pelletized and kept in a vacuum oven at 70 °C and dried for 12 hours before injection molding. The selected TAIC percentage is most effective for crosslinking process as reported in the literature [55,56]. The PLA/LG blends having E-beam irradiated lignins and TAIC at 3phr were synthesized with two different lignin percentages, 5% and 20% (w/w). The PLA/LG blends having unirradiated lignin with two different lignin percentages, 5% and 20% (w/w) were also prepared by the same process.

2.2.1.3 Preparation of poly (lactic acid)/bamboo powder composites

The twin screw extruder, THERMO HAAKE model, was deployed to prepare PLA/bamboo powder and PLA/E-beam irradiated bamboo powder composites. PLA pellets were vacuum dried at 70 °C for 12 hours prior to use. Then E-beam irradiated bamboo powder (EBP) having 30 kGy absorbed dose and was mixed thoroughly along with the coupling agent 3-Glycidoxypropyltrimethoxy silane in the polythene bag prior to extrusion. The EBP has been melt blended with PLA in two different concentrations 5 wt% and 10 wt% along with coupling agent (epoxy silane (ES) as part per hundred (phr)). The unirradiated bamboo powder was also extruded with PLA. The processing parameters, i.e. feed zone temperature 120 °C, compression zone 170 °C and metering zone temperature 170 °C, are identical for all composites having E-beam irradiated and unirradiated bamboo powder. The extruded wires of composites were pelletized and then obtained pellets were dried at 70 ° C for 12 hours under vacuum condition.

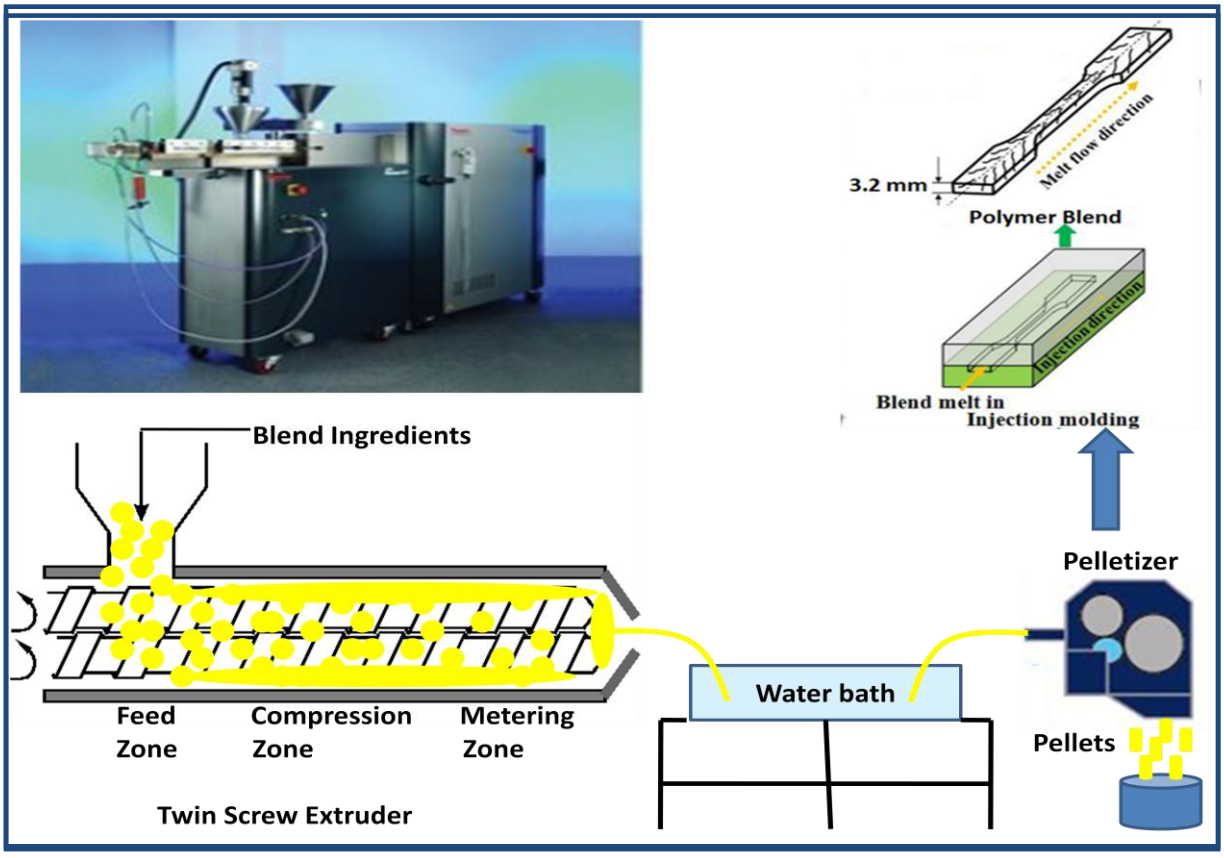

Fig. 2.2 Twin-screw extruder, THERMO HAAKE model, Japan and schematic workflow to prepare blend and blend-composites [86]

2.2.2 Injection molding

Injection molding a popular conventional process that involves the melting of thermoplastics near or above their melting temperature by extrusion and injecting the polymer

melts into the desirable mold then cool it below glass transition temperature and ultimately eject the prepared product. The injection moulders are similar to an extruder the only difference is the screws of an injection moulders do not only rotate but also move to and fro as per steps of the molding cycle [90]. Further, the mold in the injection moulders furnished with a cooling system gives the appropriate cooling to solidify the injected melt. The injection molding is used to prepare conventional plastic products viz. food trays, containers, bottles etc. The commercial injection-mold grade (i.e. 3052D) PLA can be injection molded by conventional molding machines. In the present case, all the samples of prepared blend and blend-composites are manufactured by employing Xplore microinjection moulder with less capacity 12 ml and fit seamlessly with micro-compounder.

After the preparation of blends and blend-composites by micro-compounder and mini extruder, the multipurpose test specimens -ASTM D638 of resulting blend and blend-composites are prepared by injection molding with mold temperature 32 °C. Furthermore, some test specimens -ASTM D256 were also prepared for the notch impact test. The dimensions of tensile specimens are (150 mm x 12.7 mm x 3.2 mm). Flexural and HDT specimens have the dimensions (127 mm x 12.7 mm x 3.2 mm) and the specimens used for notched impact test have the dimensions (63.5 mm x 12.7 mm x 3.2 mm).

2.3 Electron Beam Irradiation

The electron beam (E-beam) irradiation of prepared blends and blend-composites is carried out by employing electron ILU-EB accelerator, with beam energy 4.51 MeV and penetration depth 20 mm, at IRAD, Bhabha Atomic Research Center (BARC), Trombay, Mumbai, India. Some of the virgin materials are also irradiated to electron beam before blending. The schematic representation of E-beam irradiation is depicted in Fig. 2.3. Before E-beam irradiation, all set of samples or materials are packed in polythene cover which is filled with helium gas to avoid the oxidation during the irradiation process. The packet of samples/material was kept on the conveyor belt and its speed was selected as 3.00 m/minute. The distance between the samples and the E-beam source is 41.2 cm. The successive passes of the conveyor in the radiation zone determine the dose absorbed by the samples. In each pass, the dose absorbed by the samples is 5 kGy as measured by film dosimetry. In this manner, the numbers of passes are selected to achieve the desired dose.

The prepared specimens of neat PLA, PLA/PEGM blend and PLA/PEGM blend-composites are irradiated to the electron beam. It can be assumed that the E-beam irradiation

results in homogenous changes through the sample because the sample thickness is less than the penetration depth. Three sets of samples are irradiated to the electron beam with different doses of 20 kGy, 60 kGy and 100 kGy respectively.

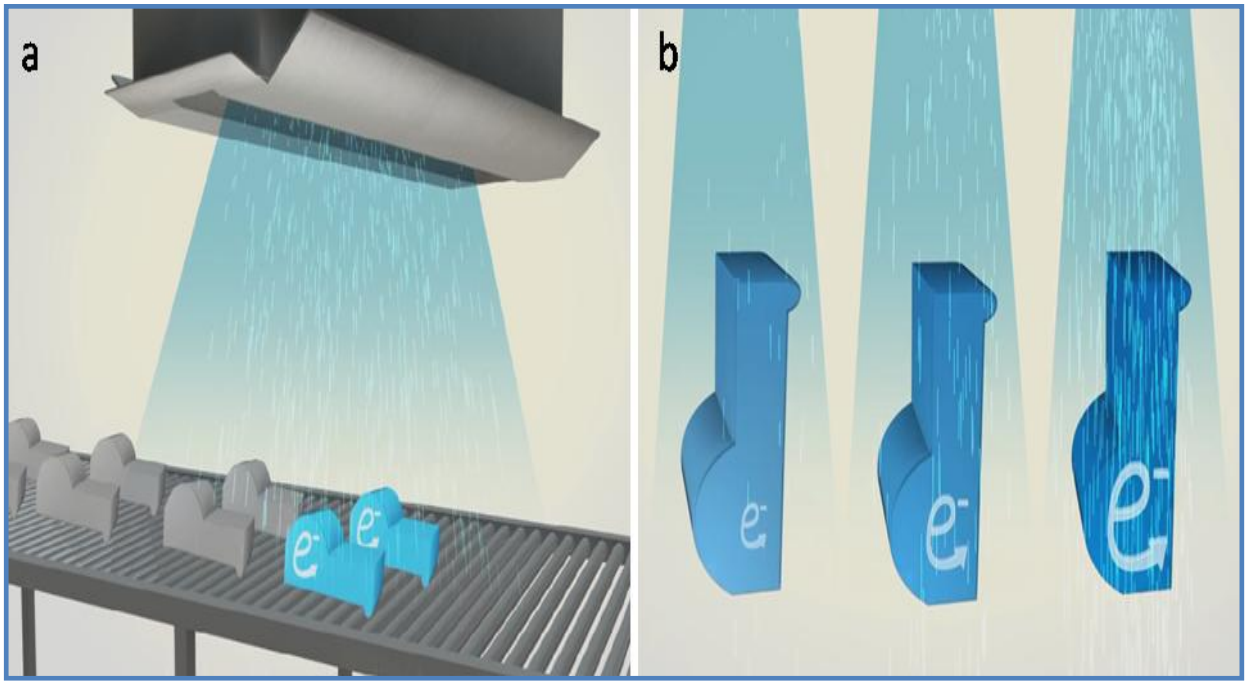

Fig. 2.3 (a) Schematic representation of electron beam irradiation of prepared samples, (b) samples irradiated to three different doses.

The commercial lignin and ultrafine bamboo powder are irradiated to an electron beam before blending with PLA. The virgin lignin is first filled into three polythene bags and these bags were further filled with helium gas then sealed. Further, these lignin bags were kept in the tray and then on a conveyor belt having speed 3 m/min. In each successive pass under radiation territory, the dose absorbed by lignin is 5 kGy. Hence, the determined passes are chosen to irradiate these lignin bags to the E-beam with three different doses of 30 kGy, 60 kGy and 90 kGy respectively. Moreover, the similar conditions were opted for E-beam irradiation of the bamboo powder.

2.4 Characterization Techniques

2.4.1 Mechanical tests

2.4.1.1 Tensile test

Tensile testing of newly manufactured material is an important aspect to choose a material for engineering and commercial applications. The polymers are viscoelastic in nature and exhibit properties like a viscous liquid and elastic solid, thus, the tensile properties of polymeric materials straight away depend on the temperature and time-scale of deformation. The tensile testing of synthesized polymeric materials is generally performed as per international standard procedures of testing viz. ASTM and ISO etc. The tensile specimens are prepared with dimensions as per standards, for instance, the multipurpose test specimens - ASTM D638 (Fig. 2.4a) have dimensions (150 mm x 12.7 mm x 3.2 mm).

The blend-composites are mechanically tested by Universal Testing Machine (UTM), INSTRON-3382. The tensile properties were measured by using ASTM D638 method with a speed of 10 mm min^{-1}. For each composition, five specimens were tested. In the tensile testing, the sample was fixed between the two clamps of the UTM machine and subjected to tension [91,92]. The force (load) (F) applied to the sample is normally described in relation to stress (σ) as given below

$$\sigma_{Tr} = \frac{F}{A} \quad 2.1$$

Here σ_{Tr} is the true stress and A is the area of cross-section. However, for practical purposes the continual changes in the A as consequences of applied force is ignored and the initial area of the cross-section (A_0) of the sample is considered to calculate the engineering tensile stress (σ_{Eng})

$$\sigma_{Eng} = \frac{F}{A_0} \quad 2.2$$

Similarly, the engineering tensile strain (ε_{Eng}) is also known as elongation at break defined as

$$\varepsilon_{Eng} = \frac{\Delta L}{L_0} \quad 2.3$$

Where$\Delta L = L - L_0$; L and L_0 are the final and initial length of the sample respectively.

From the stress-strain graph (Fig. 2.4d) of the tested polymeric sample, the following properties can be determined i.e. yield strength, tensile or Young's modulus, tensile strength, tensile toughness, elongation at break etc.

Yield strength [1,91] is defined as the maximum stress in the elastic region at which polymeric material deform elastically and return its original shape once the stress is released, however, after this stress value i.e. yield point, the polymeric material starts to deform

permanently or plastically and not recover its original shape. It is an important property used in structural engineering or material-working techniques (reshape material i.e. rolling, bending, pressing and hydro-forming) as it gives the extreme limit to the force that can be executed without permanent deformation.

Tensile modulus [1,91] is another critical material property which determines the stiffness of the material. It is calculated from the stress-strain curve and equivalent to the slope of the stress-strain curve in the linear elastic region. Generally, in the elastic region, the stress-strain relationship is defined by Hooke's law

$$\sigma = E\,\varepsilon \tag{2.4}$$

Here E is the Young's or tensile modulus.

The stiff materials have high tensile modulus and show very small deformation for the corresponding stress. The stiffness of material straight depends on chemical bonding among the atoms of the material.

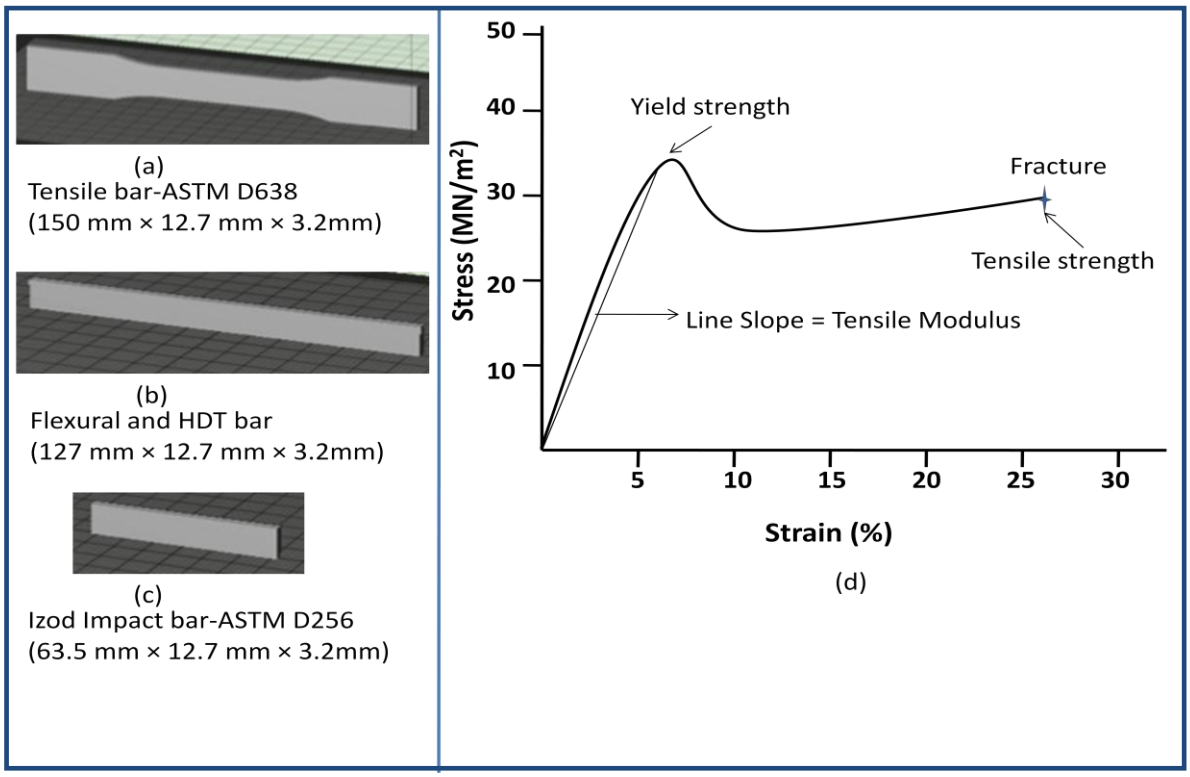

Fig. 2.4 Schematic representation of (a) tensile bar, (b) flexural and HDT bar, (c) Izod impact bar and (d) stress-strain curve for a typical polymer [91]

Tensile strength [1,91] is defined as the maximum load that can be sustained by polymeric samples before fracture or break. It is also known as ultimate tensile strength. It is measured in term of maximum stress that a polymeric material can wear upon stretching prior to fracture (Fig. 2.4d).

Tensile toughness [1,91] is generally very crucial material property than the tensile strength. It is defined as the amount of energy soaked by material prior to fracture. Tough materials consist of good strength and high ductility and offer high resistance to crack propagation. The tensile toughness can be calculated from the stress-strain graph and equal to the area under the stress-strain curve.

Elongation at break represents the capability of a material to withstand the changes in the shape without crack formation. The elongation at break is estimated from the stress-strain graph and equal to engineering strain.

2.4.1.2 Flexural test

Flexural was executed by Universal Testing Machine (UTM), INSTRON-3382. The flexural modulus was determined by following ASTM D790 procedure at a speed of 2 mm min^{-1}. To estimate the flexural modulus the five flexural specimens with dimensions 127 mm × 12.7 mm × 3.2 mm were tested.

Flexural modulus [1,92] is also known as bending modulus and defined as the ratio of stress to strain in the flexural deformation. It can also be determined from the slope of the stress-strain curve obtained due to flexural deformation. It expresses the ability of a material to bend without permanent deformation.

2.4.1.3 Impact test

Impact toughness is the crucial property of a polymeric material for durable/engineering applications. The impact toughness is measured in terms of impact strength and describes the ability of a material to absorb mechanical shocks. It is defined as the amount of impact energy absorbed by the sample prior to fracture and can be calculated by dividing impact absorption with a cross-section of the test specimen [93]. Further, similar to impact strength the notch impact strength can also be governed by employing a notched impact specimen and enhance the sensitivity of the test method because tri-axial stress may be introduced with the notch. Generally, the impact strength of a specimen is measured by two

different methods viz. Izod impact test and Charpy test. A V-shape notch is engraved on the sample with a rectangular cross-section. In the Izod method, the test specimen is clamped vertically on one side and a sudden load is applied on the front top side of the specimen by pendulum hammer facing the notch and break specimen at the notch point (Fig. 2.5). However, in the Charpy test, the test specimen is placed horizontally supported at both ends and the notch facing is away from the pendulum hammer [94]. For polymeric materials, the Izod impact test method is more often used. The impact tester and schematic represent for Izod impact testing are depicted in Fig. 2.5.

The Notched Izod impact test is performed by using the ASTM D256 test method with the help of TINIUS OLSEN-515 (USA), impact tester. Five specimens having dimensions (63.5 mm × 12.7 mm × 3.2 mm) of each composition were tested to determine the notched impact strength.

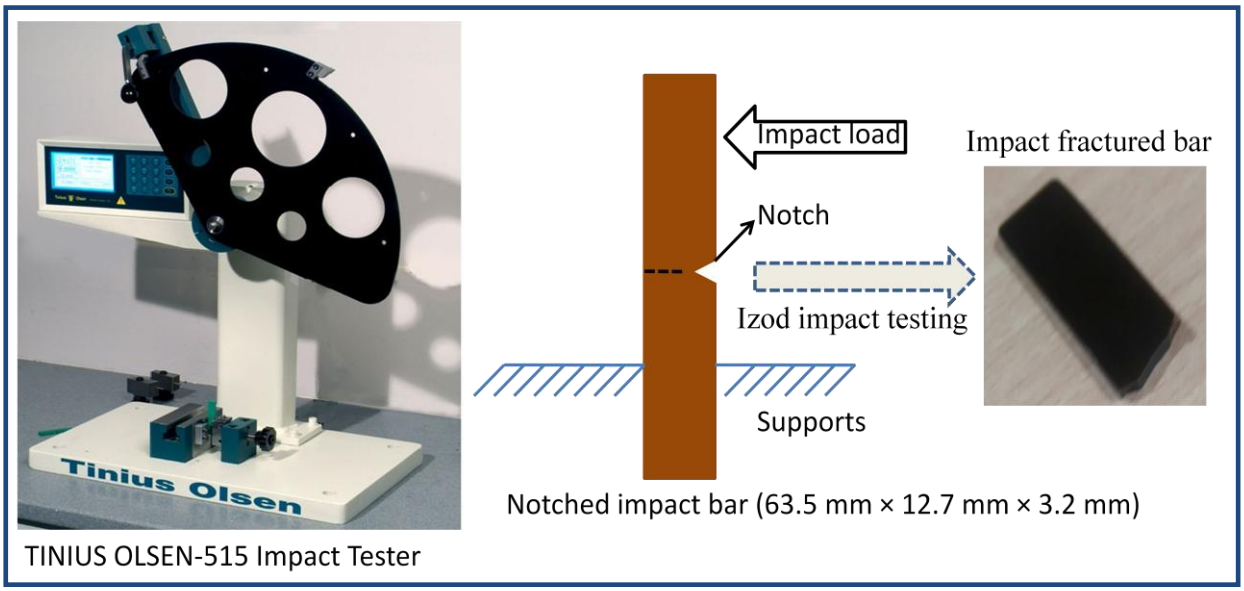

Fig. 2.5 Impact tester and schematic representation of Izod impact testing.

2.4.1.4 Heat deflection temperature

Heat deflection temperature (HDT) is defined as the temperature at which the plastic sample deforms or loses its load bearing capacity under a specific load [95]. It is useful to know the heat resistance of the prepared polymer product, which can be defined as the ability of the material to maintain the desired properties at maximum service temperature. It is also known as temperature dependent flexural modulus. HDT of the polymer depends on the degree of crystallinity and crystallization behavior [72].

Heat deflection temperature (HDT) of prepared specimens is determined by ASTM D256 test method with a load of 1.82 MPa at a heating rate of 2 °C per minute with the help of GOTECH HV-2000-C3 HDT/VSP testing machine. Three specimens with dimensions (127 mm × 12.7 mm × 3.2 mm) of each composition were used to measure the HDT.

2.4.2 Thermal analysis

2.4.2.1 Differential scanning calorimetry

Differential scanning calorimetry (DSC) is one of the most popular thermal analysis techniques to examine the thermal event in the materials upon heating or cooling without exchange of mass with surroundings. It is most commonly used technique in various fields to determine the phase transitions and thermodynamic properties such as glass transition temperature (T_g), cold crystallization temperature (T_{cc}), melting temperature (T_m), cold crystallization enthalpy (ΔH_{cc}), melting enthalpy (ΔH_m) and heat capacity [96]. The differential scanning calorimeter instrument principally measures the heat flow difference among the sample and reference. There are two mostly employed DSC instruments viz. heat flux DSC and power compensated DSC. In heat flux DSC one directly measures the temperature difference between the sample and reference and then converts it into heat flow difference. However, power compensated DSC directly measures the enthalpy changes of material in the thermal event [96,97]. For this thesis work, the power compensated DSC instrument (Perkin-Elmer 7) (Fig. 2.6) was used to determine the melting and crystallization behaviors of neat PLA, blend and blend-composites. A sample of about 5-10 mg was first heated from 40 °C to 200 °C at a heating rate of 10 °C per minute and hold on for three minutes in order to cancel previous thermal history; later the samples were cooled down to 40 °C and reheated to 200 °C at 10 °C/minute under argon atmosphere.

As shown in the Fig.2.6 the power compensated DSC instrument consist of two separate pans i.e. one for sample and other is reference connected to the individual heating element to regulate temperature. The temperature of the sample pan and reference pan is always maintained same (i.e. thermal null state, $\Delta T=0$) by the instrument during the thermal analysis. During thermal analysis initially, the heating rate for sample and reference is same; however, when thermal event occurs in the sample then the power of the heater for sample pan has to regulate in order to keep the sample temperature identical as that of reference. The exothermic events give off heat causing a decrease in the power of the sample heater to cool the sample. However, endothermic events absorb the heat causing an increase in the power to

heat the sample. The number of power variations for sample heater should be equal to the energy of heat flow to compensate the heat gain or release by the sample during the thermal event. A typical DSC graph consists of various thermal events is schematically represented in Fig. 2.7.

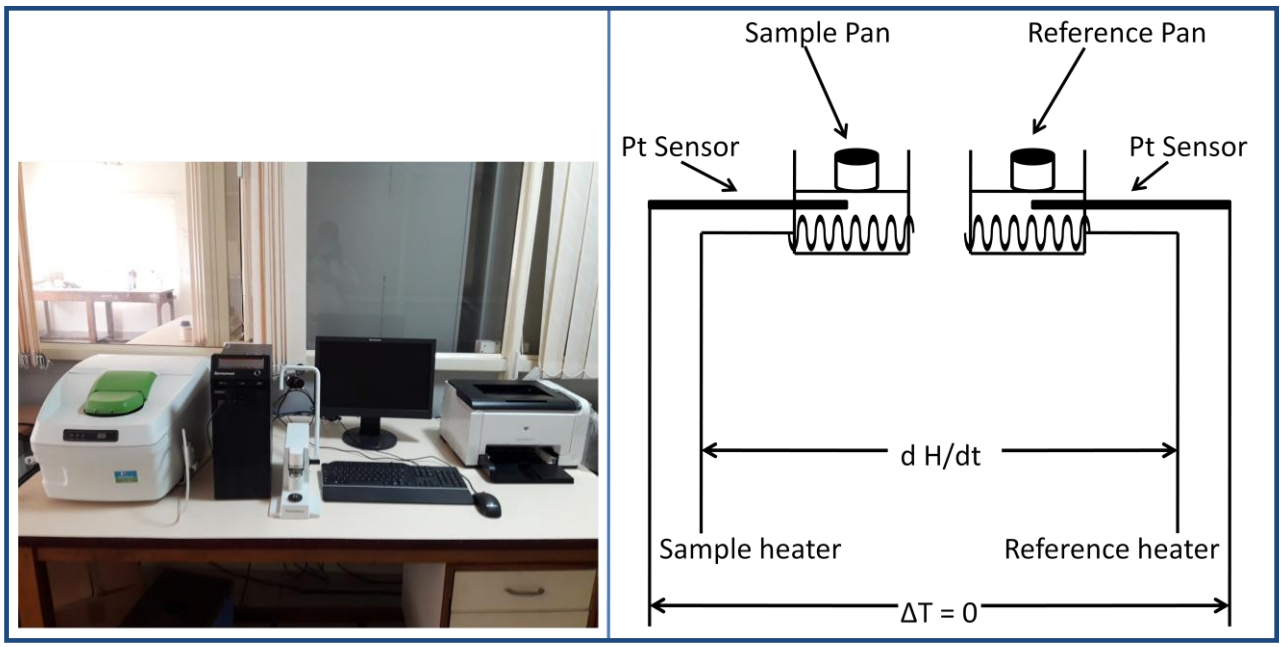

Fig. 2.6 Power compensated DSC instrument (Perkin-Elmer 7) and its schematic representation [96].

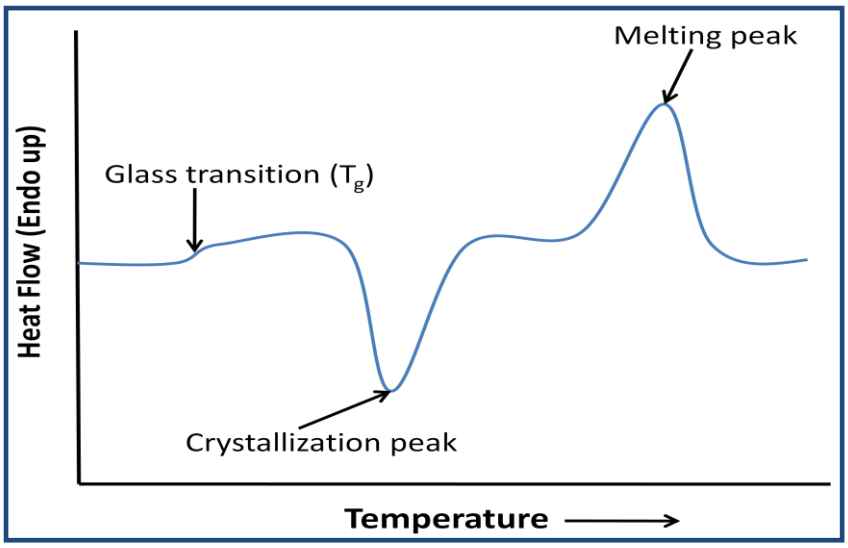

Fig. 2.7 The typical DSC curve for polymeric material.

The percentage of crystallinity of neat PLA, blend and blend-composites were calculated by the Eq. 2.5 [98]:

$$\%\text{Crystallinity} = X_c(\%) = \frac{(\Delta H_m - \Delta H_{cc})}{(\Delta H_m^0 \times w)} \times 100 \quad 2.5$$

Where ΔH_m = melting enthalpy, ΔH_{cc} = crystalline enthalpy, w is the weight fraction of PLA in the blend and ΔH^0_m is the enthalpy of fusion for 100% crystalline PLA i.e. 93 J/g [99,100].

2.4.2.2 Thermo gravimetric analysis

Thermo Gravimetric Analysis (TGA) is a popular technique to measure decomposition of materials and thermal stability by observing changes in the mass of a sample as a function of temperature. The measurement is usually performed in the inert atmosphere to avoid the sample oxidation. TGA instrument is mainly composed of four units i.e. microbalance, furnace, temperature controller and computer [96]. The schematic representation of the instrument is given in Fig. 2.8. The typical microbalance is most important and is heart of the TGA instrument. It is a null-point type and can measure the very minute mass change ±1 µg of the sample. The null-type microbalance keeps the sample in a vertical position and senses the vertical displacement of sample pan due to change in the mass of sample by an optical unit. To study the thermal degradation of material a pan loaded with the sample is placed along with the reference pan in the furnace and the change in the mass of the sample is detected by the microbalance. The temperature of the furnace and scanning rate are controlled by the computer system. Schematic representation of the weight loss of a sample as a function of temperature is depicted in Fig. 2.9.

TGA was also carried out to test the thermal stability of the neat PLA, blends and blend-composites by using TGA Q 50, TA Instruments, USA. Observations were carried out from 25 °C to 500 °C at a heating rate of 10 °C min^{-1}.

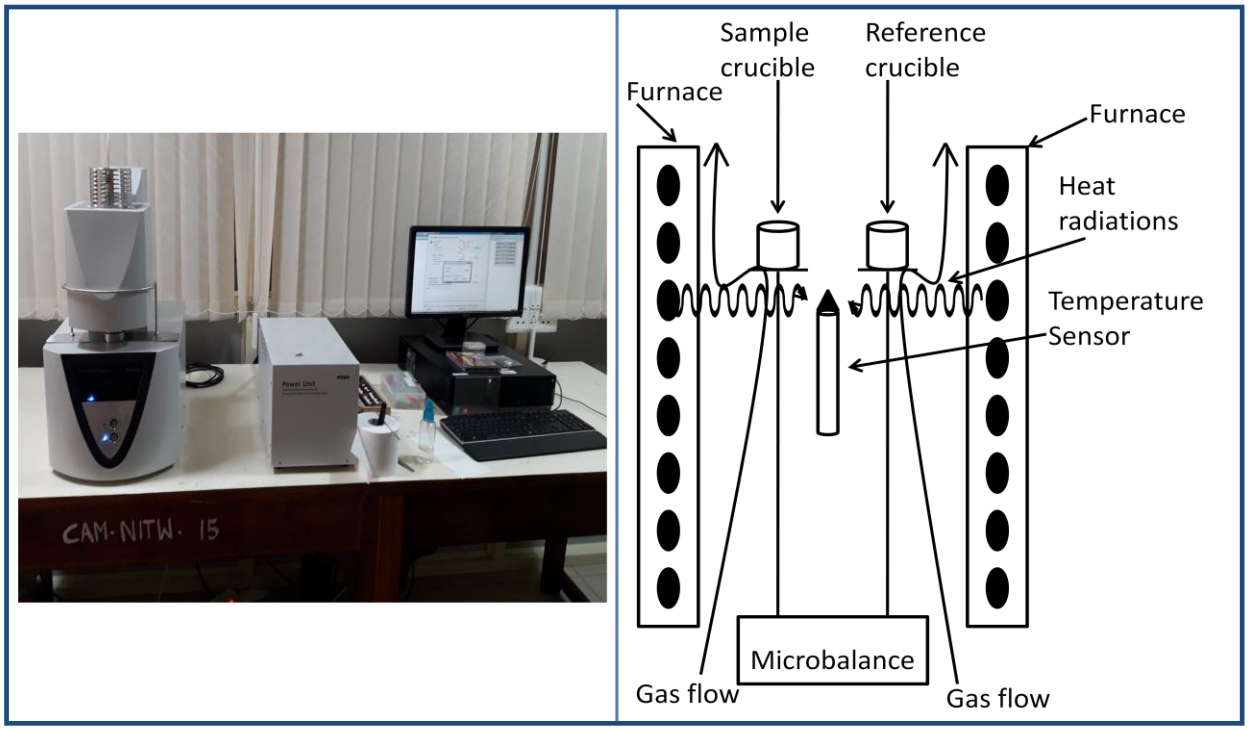

Fig. 2.8 TG instruments setup (TGA Q 50, TA Instrument, USA) and its schematic representation [96].

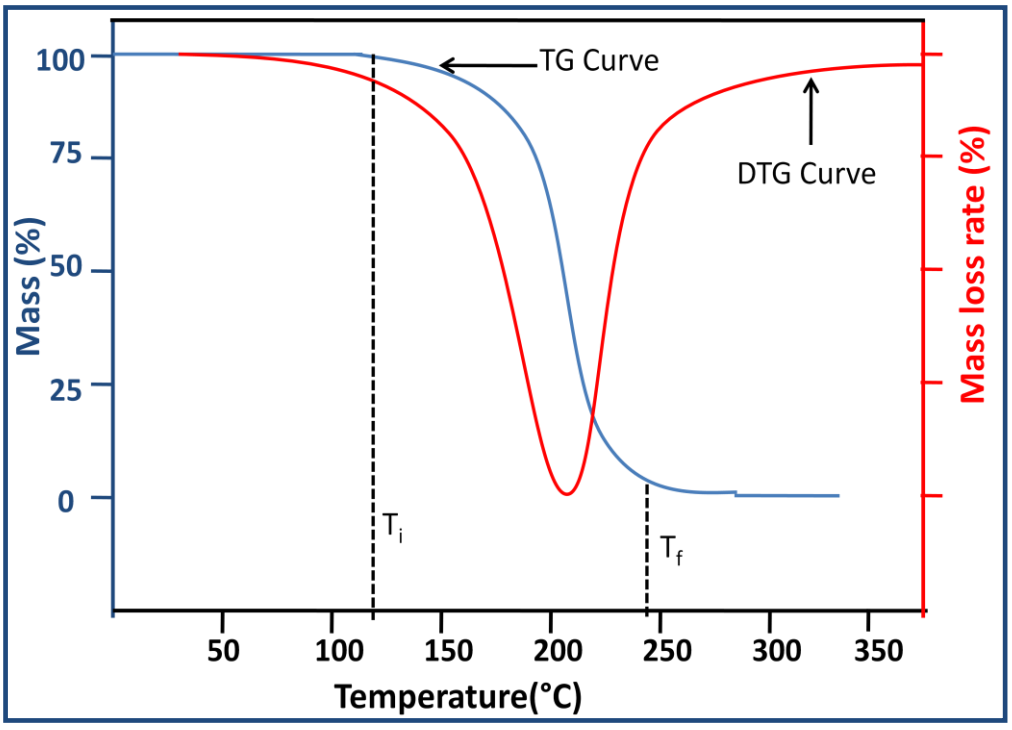

Fig. 2.9 Typical TG and DTG thermograms for the polymer, T_i and T_f are initial and final degradation temperature.

2.4.3 FT-IR spectroscopy

FT-IR is one of most popular and widely used techniques to determine the chemical structure of unknown compound (organic and inorganic). It can also be employed for quantitative analysis of some components present in the compound [101]. It is often used to determine the functional groups present in the chemical structure of organic molecules. Vibrational-rotational energy levels of most of the organic molecules lie in the infra-red (IR) region of electromagnetic waves. So, when organic sample exposes to infra-red radiations the sample molecules absorb the radiations and are excited from the ground state to higher vibrational-energy state. All the bonds/groups in the molecule will not absorb the infra-red radiation, however, only the bonds/groups which exhibit asymmetric stretching and have dipole moment absorb the IR radiations. Such vibration transitions are called IR active transitions. Further, various molecular bonds/groups present in the molecules vibrate at different frequencies that rely on the type of bonds and connected atoms. For individual IR active molecular bond/group there is a characteristic frequency which it absorbs in the IR regions and exhibits the corresponding absorption peak in the IR-spectra. Hence, there are several peaks that can be observed corresponding to different polar groups present for the organic compound in the IR-region. The optical diagram of the FT-IR instrument is given in Fig. 2.10.

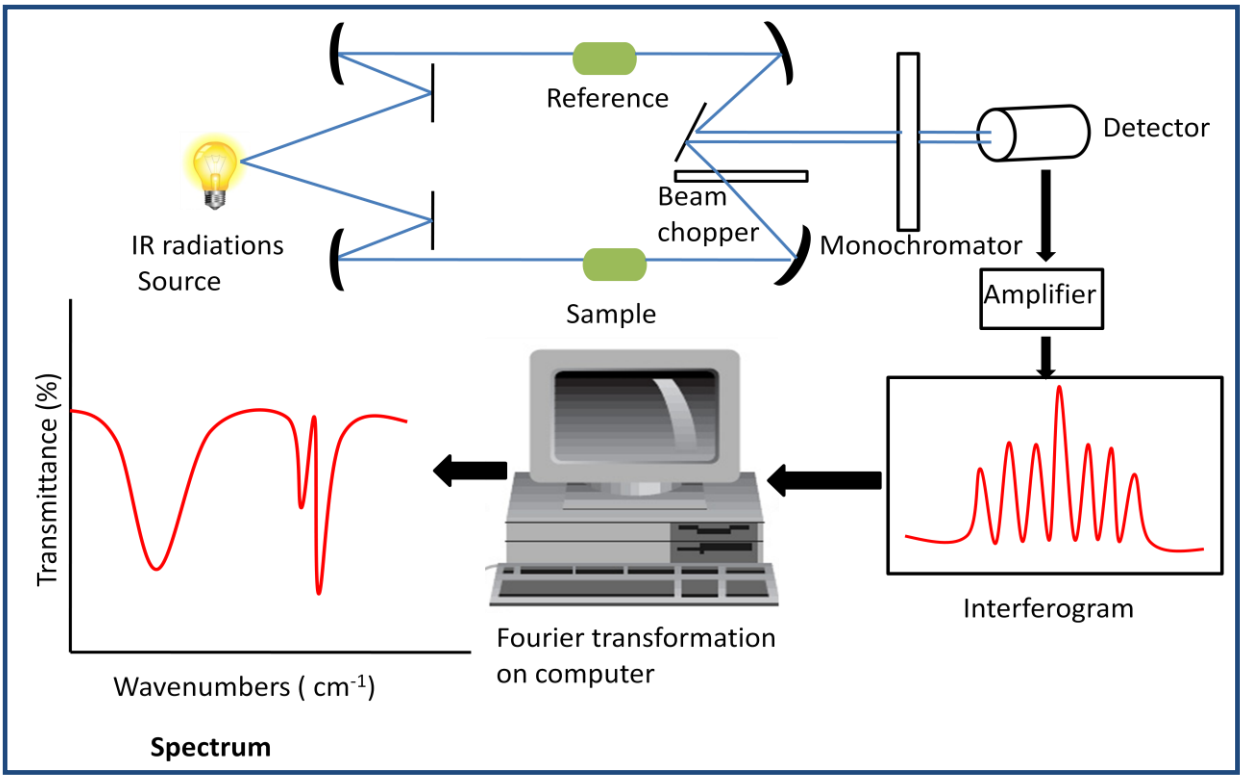

Fig. 2.10 Schematic diagram for FT-IR spectrometer [101].

The chemical structure of neat PLA, prepared blend and blend-composites were studied by ATR-FTIR spectroscopy using Perkin Elmer (model S 100) spectrometer. The spectrum was taken from a range of 400 cm^{-1} to 4000 cm^{-1}. For each sample, about 20 scans were gathered in the transmission mode with a resolution of 4 cm^{-1}.

2.4.4 Nuclear magnetic resonance (^{1}H NMR) spectroscopy

Nuclear magnetic resonance spectroscopy (NMR) is a powerful non-destructive tool to determine the structural information of the organic molecules and also help to find the contents and purity of a sample [102–104]. Among ^{1}H NMR, ^{13}C NMR and ^{31}P NMR techniques the proton (^{1}H) NMR is used most commonly [105]. The nuclear magnetic resonance entailed the interaction of the oscillating magnetic field of electromagnetic radiations with the nuclei precessing in the external magnetic field. All the nuclei with integral spin quantum number (I > 0) precess around the direction of the applied magnetic field (H). In detail, when a hydrogen atom (proton) is placed in the external applied magnetic field it behaves like a tiny magnet and starts to precess around the direction of the applied magnetic field with angular velocity [102] given below

$$\omega = \gamma H \qquad 2.6$$

ω and γ are the angular precession velocity and gyromagnetic ratio respectively.

As per fundamental NMR equation which associates the applied magnetic field with electromagnetic frequency (ν) is given below

$$2\pi\nu = \gamma H \qquad 2.7$$

From the above two equations, it can also be inferred that ν is the precessional frequency of tiny magnet (nucleus) in the applied magnetic field. Hence, when the frequency of applied electromagnetic beam match with the precessional frequency of the tiny magnet the resonance occurs and leads to transition of nucleus from one spin state to another spin state [105,106] as shown in Fig. 2.11. The frequency of electromagnetic radiation required for nuclear magnetic resonance lies in the radio-wave region. The protons which have same chemical environment are called equivalent protons. The different protons or set of equivalent protons precess at different frequencies. This is because the variation in their chemical environment leads to variation in the effective applied magnetic field strength they face. Thus we can either steadily vary the frequency of electromagnetic radiations or change the applied magnetic field strength.

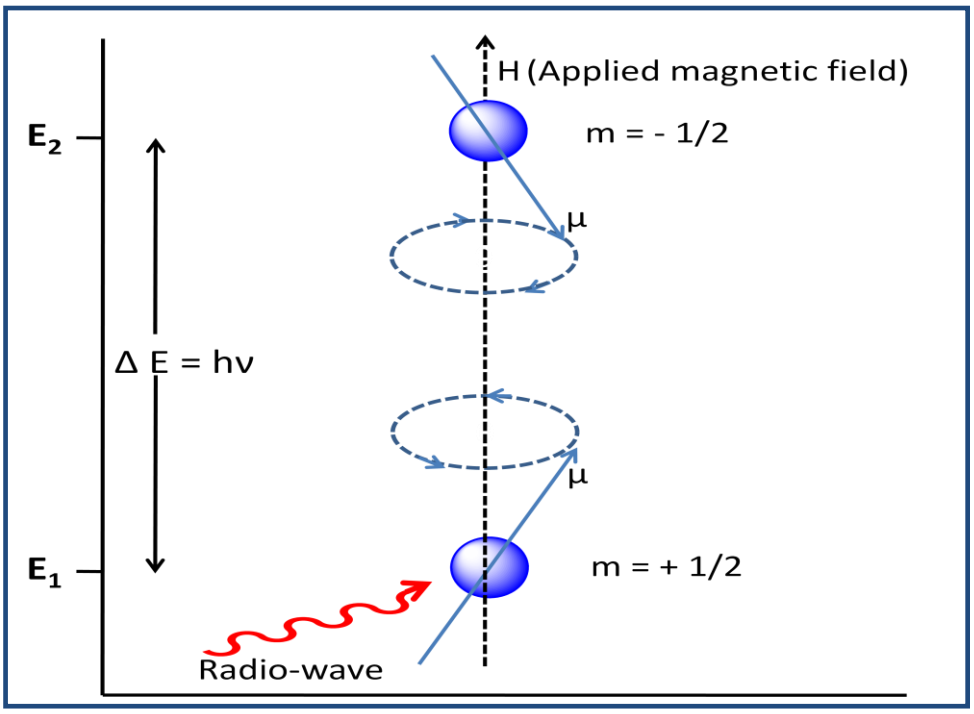

Fig. 2.11 Excitation of a precessing proton from one spin state to another spin state at resonance [106]

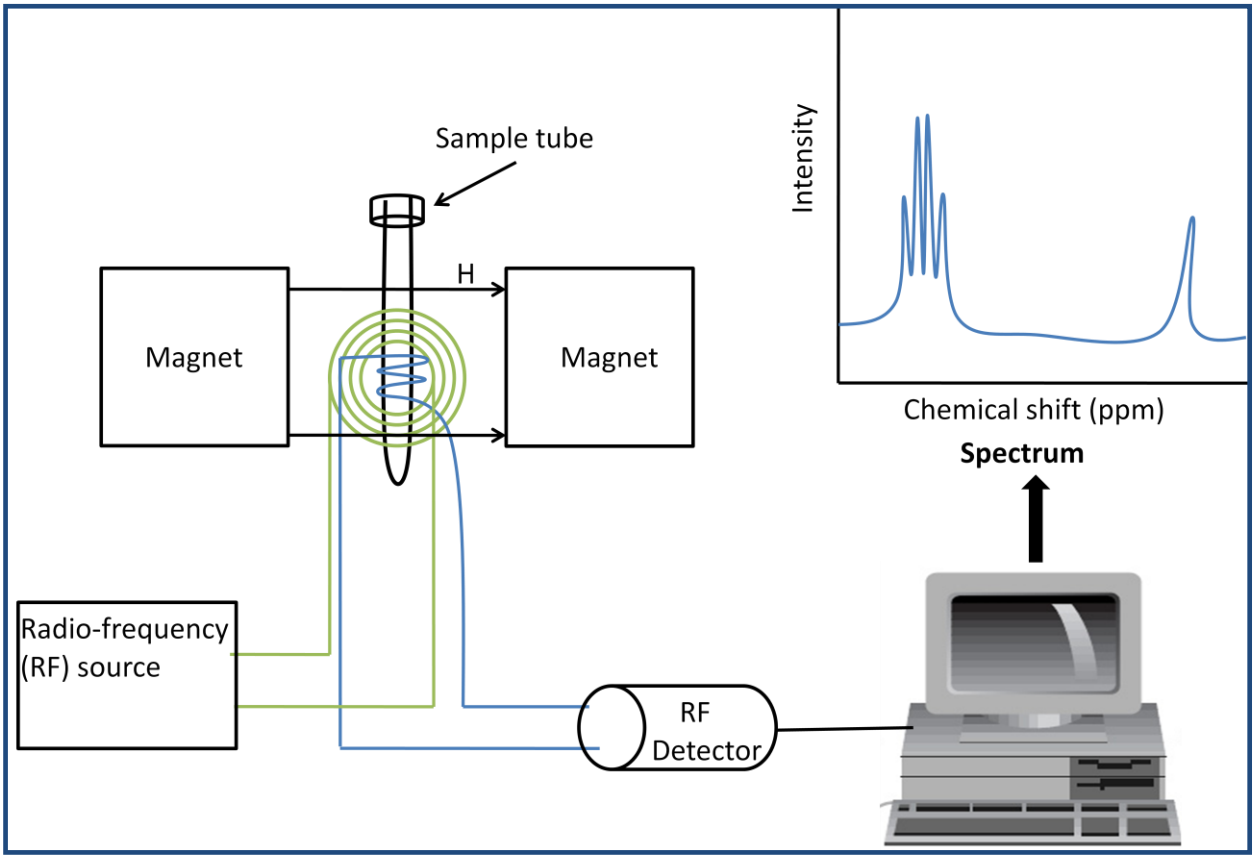

Fig. 2.12 The schematic diagram of Nuclear magnetic resonance spectrometer [105]

Generally for convenience, the radio-frequency is kept constant and applied magnetic field strength is varied to generate the same effective magnetic field strength for different protons to cause the absorption (resonance). Hence, absorption peaks versus corresponding measured applied magnetic field strengths for different sets of protons are plotted. Further, in NMR spectroscopy the absorption peaks of a different set of equivalent protons at different applied magnetic field strength are measured and plotted in term of chemical shift (δ) with respect to reference peak (i.e. peak due to tetramethylsilane (TMS)) [107,108]. The difference in the absorption position of the proton with respect to reference peak is known as chemical shift. The schematic diagram of NMR spectrometer is depicted in Fig. 2.12.

The ^{1}H NMR spectra of neat PLA, blend and blend composites were recorded at room temperature by using Bruker Ascend-400 MHz spectrometer, Switzerland. The $CDCl_3$ was used as a solvent for dissolving PLA and a mixture of solvents i.e.$CDCl_3$ + DMSO-d_6 was used as a solvent for PLA/PEGM blend and PLA/PEGM/HBN blend-composites for NMR study. The tetramethylsilane (TMS) was used as a standard for the chemical shift. For each measurement, a sample of about 7-8 mg was dissolved in the relevant solvent to take the proton NMR spectra. All the NMR data were processed and analyzed with the Bruker Top-Spin 3.2 software.

2.4.5 X-ray diffraction

The X-ray diffraction (XRD) is the most effective and widely used technique to know the structural features of a material. It determines the identity of a compound from its crystalline structure, not from its chemical composition [96,109,110]. Thus, the material with the same composition which exists in the different phases can be determined. In the case of semi-crystalline polymers, this technique is employed to find the crystalline nature of polymers and percentage of crystalline phase available in the polymers. It also helps to find the effect of nucleating agents on the crystallinity of the prepared polymer composites.

The K_α characteristic X-rays are used for X-ray diffractometry. X-ray diffraction method obeys the Bragg's law equation [96] as shown below

$$n\lambda = 2d\ \sin\theta \qquad 2.8$$

The above equation can simply be obtained from Fig. 2.13; the path difference between two incident beams relies on the angle of incidence (θ) and distance (d) between the parallel planes of a crystal.

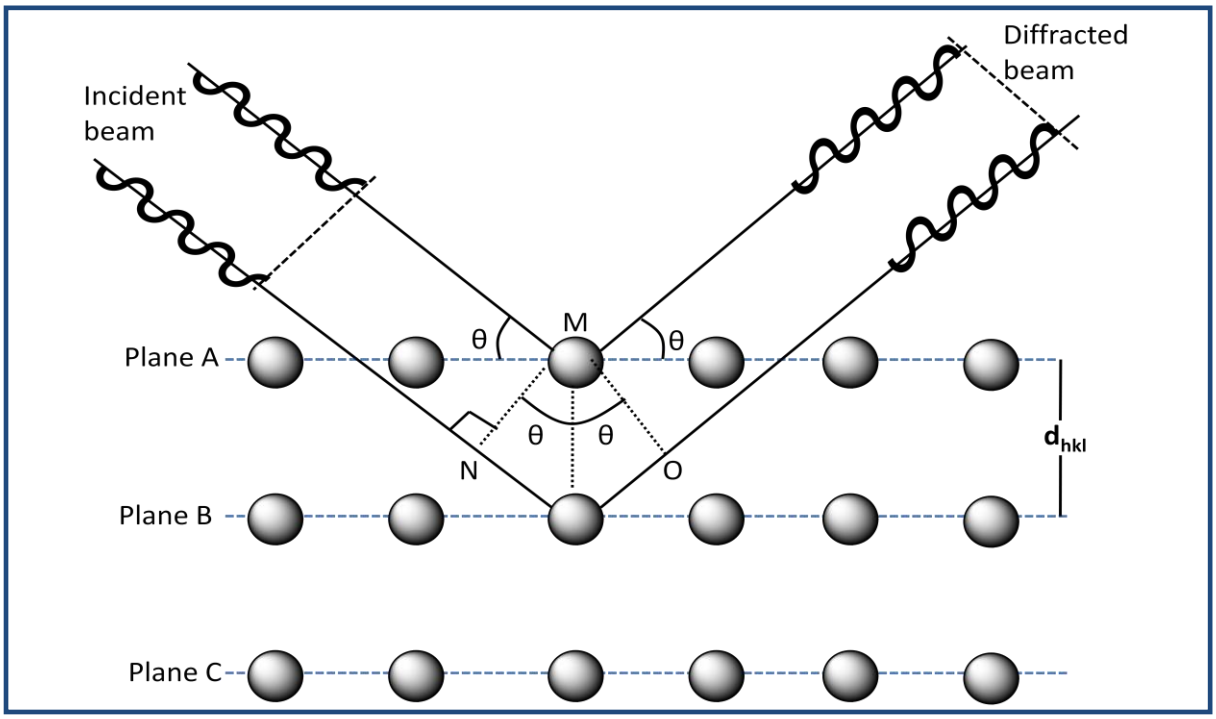

Fig. 2.13 Bragg diffraction of incident X-rays by planes of the crystal [109].

Based on the above equation, the information about distance among crystal planes can be determined when constructive interference occurs, provided incident beam wavelength (λ) and angle of incidence are known. Hence, once the spacing (d_{hkl}) between lattice planes of crystalline material is retrieved; the crystal structure of crystalline materials can be detected. For instance, in the case of a cubic crystal, the lattice plane spacing is related with its lattice parameter (a) [109] by an equation given below

$$d_{hkl} = \frac{a}{\sqrt{h^2 + k^2 + l^2}} \qquad 2.9$$

For a given crystal structure, the (hkl) is the Miller indices which represents the set of parallel planes in a crystal lattice having spacing d_{hkl}. So, the combination of the above two equations results in a new equation which gives the relationship between diffraction data and crystal parameters for cubic crystal [109] i.e.

$$\sin^2\theta = \frac{\lambda^2 (h^2 + k^2 + l^2)}{4a^2} \qquad 2.10$$

X-ray diffraction patterns were obtained for neat PLA, blends and blend-composites using Pan-analytical X'Pert instrument with Cu K_α radiation at a scanning speed of 2.5° min^{-1} in the angular region (2θ) of 6° to 40°. The Pan-analytical X'Pert instrument is θ-θ X-ray diffractometer in which both X-ray tube and detector are rotated at a rate of θ°/minute,

however, the sample position is fixed as shown in its geometrical representation (Fig. 2.14) [96,111].

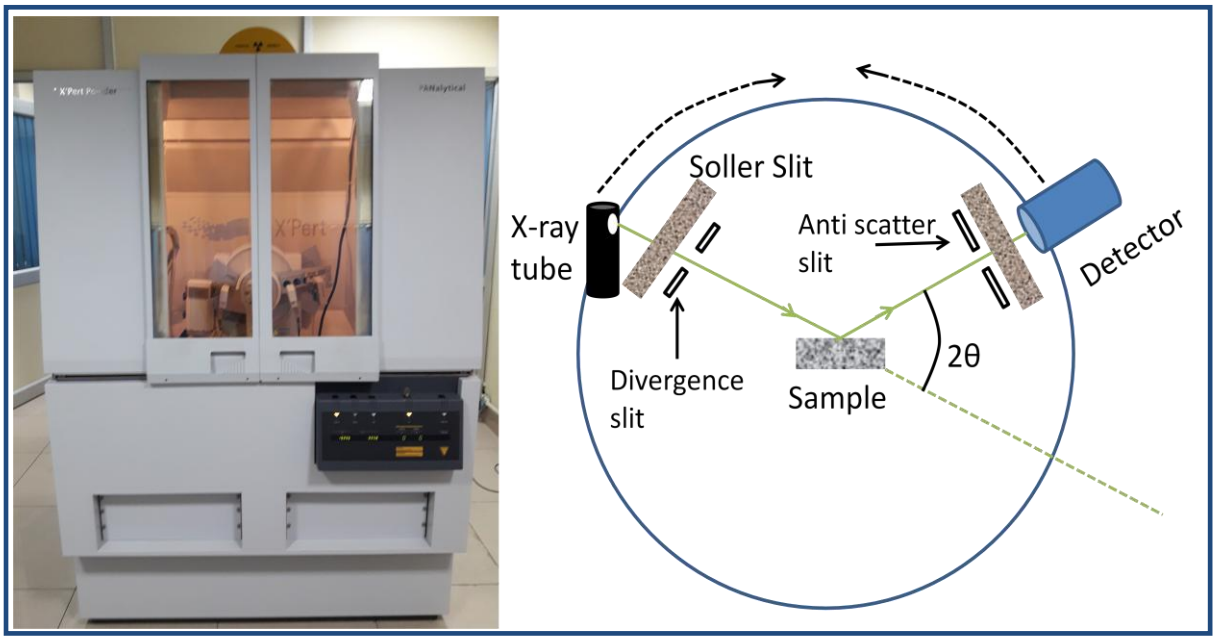

Fig. 2.14 Pan-analytical X'Pert instrument and geometric arrangement of θ-θ X-ray diffractometer [96,111].

2.4.6 Scanning Electron Microscopy

Scanning electron microscopy is one of the most favored techniques used for the topographical study of materials. In the scanning electron microscope (SEM) electron beam is employed to study the surface features of a sample [112]. The SEM comprises a large depth of field and is able to reach 1 μm at 10^4 × magnification as compared to the optical microscope [96,113]. When the surface of the specimen is walloped by an electron beam the following events occur (Fig. 2.15) (i.e. scattering of electrons by atoms of sample and production of characteristics X-rays etc.) below the surface of the sample. The scattering of electrons by the atoms of the sample under the sample surface leads to the production of secondary electrons (SE) and backscattered electrons (BSE). SE and BSE are the principal sources to generate SEM images. The secondary electrons mainly contribute for the surface topographical micrographs, however, backscattered electrons mainly contribute for producing composition micrographs [96,112].

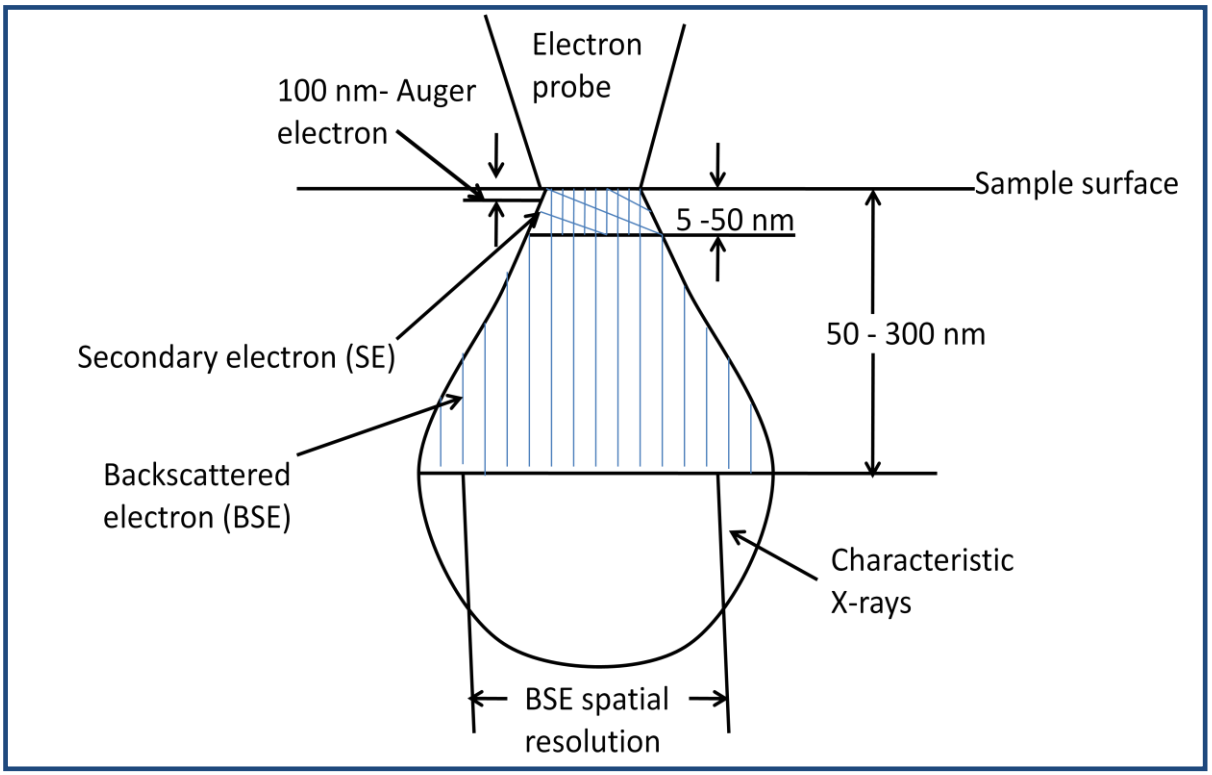

Fig. 2.15 The various events occur in the interaction zone of electrons and atoms under the surface of the sample [96].

To know the degree of compatibility among the PLA matrix and dispersed phases the cryo-fractured and notched impact fracture surfaces of prepared blends and blend-composites were analyzed with Carl Zeiss EVO 18 scanning electron microscope (SEM) at an operating voltage of 10 kV. For some of the compositions, the cryo-fractured and notched impact fractured surfaces were analyzed with TESCAN (VEGA 3LMU) at an operating voltage of 5 kV. All the specimen surfaces are sputtered with gold before going for characterization.

2.4.7 Hydrolytic degradation

Polymer chains with ester or amide functional groups in their backbone usually experiences random chain scission by hydrolysis. These groups present in the polymer chain backbone can be easily hydrolyzed in alkaline media. However, when these functional groups are available as side groups of polymer chain then hydrolyses leads changes only in the side groups of the polymer chain but not degradation of the polymer. This kind of reactions which lead to the changes only in the side functional groups without affecting the degree of polymerization is known as polymer analogue reactions [2].

The hydrolytic degradation studies of neat PLA, blends and blend-composites are carried out in phosphate-buffer solution (PBS), having pH = 7.1, at 58 °C [114,115]. The selected temperature is the standard temperature for biodegradation tests [116,117]. Further, in natural media, the degradation process of PLA stimulates between 25 °C to 58 °C has been reported in the literature [114,118]. The weight of the samples was carefully measured before the test. The samples were periodically removed, washed with distilled water, dried in a vacuum oven for 24 hours. Finally, the weight of dried samples was measured precisely to assess the degree of hydrolytic degradation. The weight loss (%) was estimated by exploiting the equation [24,66] given below.

$$\%\,\text{Weight loss} = \frac{(W_0 - W_t)}{W_0} \times 100 \qquad 2.11$$

Where W_0 = initial weight of the sample and Wt = weight of the dried sample

The test is performed in triplicate and the results are represented as the mean ± SE of weight loss percentage.

Chapter 3

In-situ compatibilization of PLA/PEGM blend and refinement of its thermal and mechanical properties

---

In this chapter, the formation of PLA/PEGM graft copolymers during the melt blending of poly (lactic acid) (PLA) and poly (ethylene-co-glycidyl methacrylate) (PEGM), which act as an interface between two polymer matrices, is illustrated by the epoxide ring-opening mechanism. There are two coupling reaction mechanisms of glycidyl methacrylate (GM) unit of PEGM with the terminal groups of PLA. The analysis of FTIR and ^{1}H NMR spectra elucidates the chemical reaction of GM unit of PEGM with carboxylic and hydroxyl terminal groups of PLA. FTIR analysis also confirms that the carboxylic terminal groups of PLA are more likely to react with GM group of PEGM. Hence, PLA grade having carboxyl terminal groups is more compatible with PEGM as compared to the PLA grade having hydroxyl and ester terminal groups. The hexagonal boron nitride (HBN) is incorporated with various labels such as 1 phr, 5 phr and 10 phr to prepare PLA/PEGM/HBN blend-composites. The blend-composite with low HBN content i.e. 1 phr shows better mechanical and thermal properties than neat PLA, PLA/PEGM blend and other blend-composites. This is attributed to the formation of covalent bond between polymer chains and HBN crystal layers and also due to the intermolecular interaction between the hydrogen atoms of polymer chains with the nitrogen atoms of HBN, which is confirmed by the FTIR and ^{1}H NMR studies. TG/DTG, SEM, XRD analysis and the improvement in the mechanical and thermal properties of the prepared blend also asserts the interfacial compatibility between PLA and PEGM in the blend and chemical interaction of HBN particles with the polymer matrix.

Publication:

1. **Ashish Kumar**, T.Venkatappa Rao, S. Ray Chowdhury, S.V.S Ramana Reddy, "Compatibility confirmation and refinement of thermal and mechanical properties of Poly (lactic acid)/Poly (ethylene-co-glycidyl methacrylate) blend reinforced by hexagonal boron nitride", **Journal of Reactive and Functional Polymers 117 (2017) 1–9 (Impact Factor 3.151).**

3.1 Introduction

PEGM is one of the most well-known polymers to make reactive blending and compatibilize other polymers with PLA as reported by many authors [119–121]. In general, for modification of toughness of PLA with rubbery polymers the feed ratio of PLA and blend components is usually fixed at 80:20 [122–124]. The reactive blending of PEGM with PLA was studied by H. T. Oyama [78] and reported an appreciable improvement in the mechanical properties of PLA with 20% weight percentage of PEGM in the prepared blend after annealing it at 90˚C for 2.5 hours. In the above studies, the exact interfacial reaction between PEGM and PLA was not studied, which has a significant effect on the compatibility strength of PEGM on the tailored properties of PLA based blend and composites. Apart from this, the post-annealing is also not industrially advisable. Hence, to overcome these deficiencies, in the current work, an attempt is made to explain the interfacial reaction mechanism between PLA and PEGM by preparing PLA/PEGM blend with weight ratio 80:20 and using FTIR, ^{1}H NMR, SEM, XRD measurements along with mechanical and thermal properties of the prepared blend. These studies reveal that the compatibilized strength of PEGM depends on the type of terminal groups present in the PLA chains (i.e. hydroxyl or carboxylic acid) in the PLA based blend. The study also shows that the PLA chains having carboxylic acid terminal groups most probably undergo a chemical reaction with an epoxidized group of PEGM and hence are more compatible with PEGM. Thus from these findings, it may be confirmed that the compatibilized strength of PEGM in the PLA based blend and composite depends on the PLA grade and purity of PLA. In addition to it, PLA/PEGM blend is also embodied with hexagonal boron nitride (HBN) as part per hundred (phr). For a PLA/PEGM/HBN blend-composite with 1phr, it is observed that the mechanical properties (such as impact strength and elongation at break) and heat deflection temperature (HDT) are further improved without much change in the other properties.

The details of experimental setup and method used to prepare the PLA/PEGM blend and PLA/PEGM/HBN blend-composites are given in the **Chapter 2, Section 2.2.1.1.** All the blends and blend-composites are designated and tabulated in Table 3.1.

Table 3.1

Nomenclature and compositions of sample.

Composition name	Percentage of PLA (%)	Percentage PEGM (%)	Addition of HBN as part per hundred (phr)
PLA	100	0	0
PLA/PEGM	80	20	0
PLA/PEGM/HBN 1phr	80	20	1 phr
PLA/PEGM/HBN 5phr	80	20	5 phr
PLA/PEGM/HBN 10phr	80	20	10 phr

3.2 Results and Discussion

3.2.1 Compatibility confirmation

To study the compatibility confirmation of PEGM and PLA and to know the factors influencing the compatibility of PEGM with PLA, blend of PLA and PEGM has been prepared with a weight ratio 80:20, since PEGM with 20% weight percentage in PLA/PEGM blend shows better compatibility along with excellent mechanical properties [78]. To elucidate the reaction mechanisms of interfacial bonding between PLA and PEGM, the normalized FTIR spectra of all the prepared compositions are recorded. The important wave numbers and band identifications of PLA, PLA/PEGM blend and their blend-composites are depicted in Fig. 3.1 The diverse characteristic peaks were present in the neat PLA spectra (Fig. 3.1a), carbonyl group (C=O) stretching appears at 1757cm^{-1}, C-O-C asymmetric stretching appears at 1184cm^{-1}, two different peaks are observed at 3656cm^{-1} and 3501cm^{-1} which correspond to O-H stretching of hydroxyl and carboxylic acid terminating groups respectively [98]. Also, a doublet of C-H stretching for the CH_3 group appears at 2998-2946cm^{-1}, (C-CH_3) stretching appears at 956 cm^{-1} and (-C-C-) stretching in amorphous and crystalline phases of PLA at 870 cm^{-1} and 757 cm^{-1} respectively [125,126]. In the FTIR spectra (Fig. 3.1b) of PLA/PEGM blend, the intensity of absorbance for C=O and C-O-C groups are increased and simultaneously slight suppression of O-H peak of the carboxylic acid terminal group, the slight increment in O-H peak of the alcoholic group are also observed. In addition, the peaks at 993 cm^{-1} and 852 cm^{-1} corresponding to an epoxy ring of PEGM [126,127] were also absent. This signifies that the terminal carboxylic group of PLA reacts with the epoxide group of PEGM through epoxide ring-opening mechanism as illustrated in (Fig. 3.2a) [128], leads to an increase in number of ester groups and addition of

new alcoholic groups because in the PLA/PEGM graft copolymers the PLA and PEGM are linked by ester linkage (i.e. new ester group) clearly shown as dotted circle in Fig. 3.2a. A new peak is also observed in the FTIR spectra at 2852cm^{-1} which corresponds to C-H stretching. However, as depicted in Fig. 3.2b, if epoxide group reacts with hydroxyl terminal group of PLA leads to the increment only in the (C-O-C) group because it introduces the ether linking (i.e. new ether group) unit between PLA and PEGM, results in an increment in the relative peak intensity of (C-O-C) group and O-H peak of alcohol group. But this is not consistent with FTIR spectra of PLA/PEGM blend because the increment in the intensity of absorbance for C=O group has also been observed. This shows that the probability of reacting carboxylic terminal group of PLA with an epoxide group of PEGM is more as compared to the hydroxyl terminal group. Thus, the interfacial compatibility of PEGM polymer depends on the type of terminal groups of PLA chains. Hence, the PLA grade which contains more PLA chains terminating with carboxylic groups is more compatible with PEGM as compared to PLA grade having terminating groups other than carboxylic acid.

With the incorporation of hexagonal boron nitride (HBN) particles along with PLA/PEGM to prepare PLA/PEGM/HBN blend-composites, leads to the breakage of polymer chains induced by HBN. This can be asserted by observing a reduction in the peak intensities of the carbonyl group (C=O) stretching as well as (C-O-C) group asymmetric stretching in the FTIR spectra (Fig. 3.1 c, d and e). However, the FTIR spectra of all these blend-composites show the simultaneous suppression of hydroxyl peak which can be attributed to the chemical interaction of HBN with the hydroxyl group and carbonyl groups of polymer chains. Moreover, the FTIR spectra (Fig. 3.1c) of PLA/PEGM/HBN 1phr (i.e. with the addition of hexagonal boron nitride as 1 part per hundred to prepare blend-composite) shows extinction of hydroxyl peak which confirms hydroxyl groups of polymer chains undergo chemical reaction with HBN and lead to formation of covalent bonds between the HBN layers and polymer chains. The same covalent bond formation between hydroxyl groups and hydrogen atoms with the boron atoms and nitrogen atoms respectively of the HBN layers has already been studied [129]. The increasing concentration of HBN from 1phr to 5 phr in the blend-composite leads to enhance the polymer chain scission which can be confirmed by a further decrement in the peak intensity of (C=O) group as well as (C-O-C) group in the FTIR spectra. Incidentally, this spectrum also shows the increasing concentration of HBN in the blend-composites diminishes the interaction between the polymer chains and HBN layers which may be asserted from the reappearance of hydroxyl peak in the FTIR spectra Fig. 3.1d and e. Indeed, the spectra (Fig. 3.1e) shows again increment in peak intensity of (C=O) group and

(C-O-C) group which are slightly more than the pure PLA and intensity of hydroxyl peaks are fairly decreased as compared to pure PLA. Hence with the loading of 10 phr HBN, it has very least interaction with polymer chains and has similar properties as PLA/PEGM blend may be due to poor dispersion of HBN particles in the polymer matrix and aggregation of HBN particles.

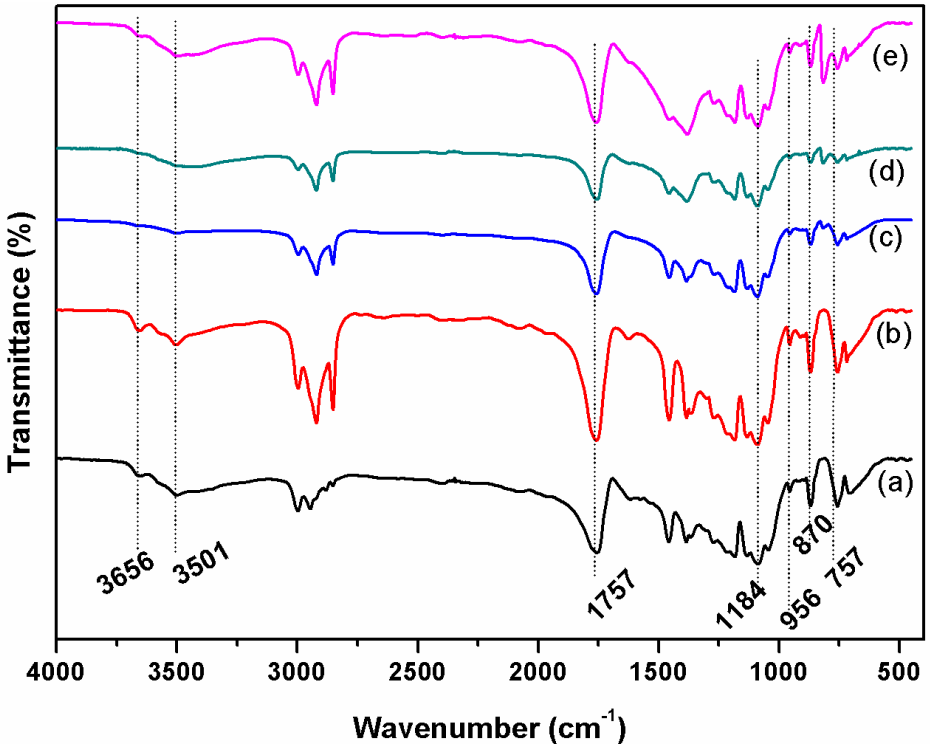

Fig. 3.1 Normalized FTIR spectra of PLA and their blends: (a) PLA, (b) PLA/PEGM (80:20), (c) PLA/PEGM/HBN 1phr, (d) PLA/PEGM/HBN 5phr, (e) PLA/PEGM/ HBN 10 Phr.

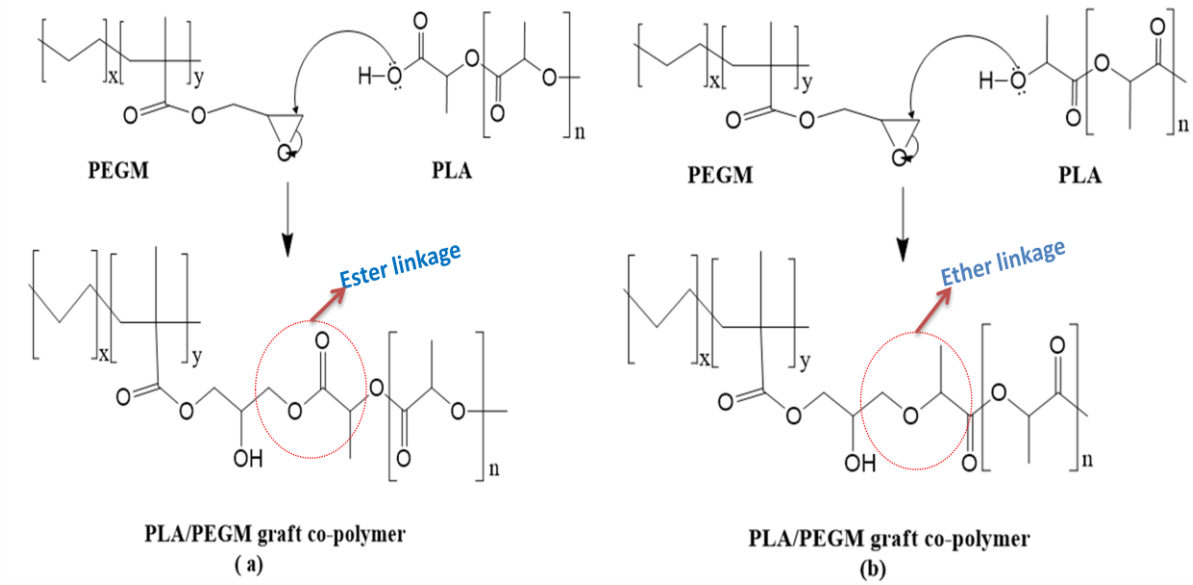

Fig. 3.2 Possible interfacial reaction mechanisms between PLA and PEGM polymers. The formation of PLA/PEGM graft co-polymer trough epoxide ring-opening mechanism (a) by the formation of new ester linkage and (b) by the formation of an ether linkage.

3.2.2 ^{1}H NMR spectroscopy analysis

The proton NMR study is performed to know the chemical structure of pristine PLA, PLA/PEGM blend and interaction of the hexagonal nitride (HBN) particles dispersed in the polymer matrix of PLA/PEGM/HBN 1phr blend-composite. The ^{1}H NMR spectra of neat PLA, PLA/PEGM blend and PLA/PEGM/HBN 1phr blend-composites are depicted in Fig. 3.3. It can be seen from the literature that the proton NMR spectra of the interior of the polymers are found as a single set of positional averaged peaks [130,131]. The characteristics resonance signals of methine and methyl group belong to PLA were observed at (5.14-5.19) ppm as a quartet (q, 1H) and (1.57-1.59) doublet (d, 3H) respectively [107,108,132,133] in the ^{1}H NMR spectra of neat PLA as shown in Fig. 3.3. In the ^{1}H NMR spectra of PLA/PEGM blend four eminent peaks, apart from the characteristic peaks of PLA, can be observed in inset enlarged zone of the spectrum. The resonance peaks at 1.25 ppm and 2.17 ppm correspond to characteristic hydrogen proton of a backbone methylene group (-CH_2-) of ethylene unit [130] and methacrylate unit [126] respectively for Poly (ethylene-co-glycidyl methacrylate) (PEGM). Further, the proton resonance signal at 2.97 ppm could be assigned to (-C (O)-OCH_2-) of glycidyl methacrylate. Fascinatingly, the two new resonance signals at 2.88 ppm and 3.38 ppm have been found in the inset enlarge the zone of ^{1}H spectra of PLA/PEGM blend in Fig. 3.3 which could be assigned to methine group proton and hydroxyl group proton respectively [126,130] of linking unit of PLA/PEGM graft copolymer formed during the melt blending of PLA and PEGM. The formation of the PLA/PEGM graft copolymers has also been determined by FTIR study. The PLA/PEGM graft copolymer formed during the melt blending of PLA and PEGM located at the interface between PLA and PEGM matrix thus improved their compatibility and hence shows the good mechanical and thermal properties in case of PLA/PEGM blend as compared to neat PLA. The ^{1}H NMR spectra of PLA/PEGM/HBN 1phr blend composite also shows the characteristic resonance signals of neat PLA and PLA/PEGM blend. However, the absence of a peak at 3.38 ppm corresponding to hydroxyl proton and peak at 2.17 ppm corresponding to backbone methylene group clearly indicates the hydroxyl group of PLA/PEGM graft copolymers reacted with the boron atoms and protons of methylene group reacted with nitrogen atoms of HBN. In addition, the proton resonance signal of methine group corresponding to PEGM shifted from 2.88 ppm to high chemical shift 3.28 ppm due to the hydrogen bonding with nitrogen atoms of HBN. The hydrogen bonding involves electron cloud transfer from the hydrogen atom to neighbouring electronegative atom (i.e. N atom of HBN) experiences a net deshielding effect which leads to high chemical shift [134,135]. Thus ^{1}H NMR spectra of PLA/PEGM/HBN 1phr composite

also elucidate the chemical interaction of dispersed HBN particles with the polymer matrix of PLA/PEGM blend which leads to further improvement in the notched impact strength and heat deflection temperature as compared to the PLA/PEGM blend.

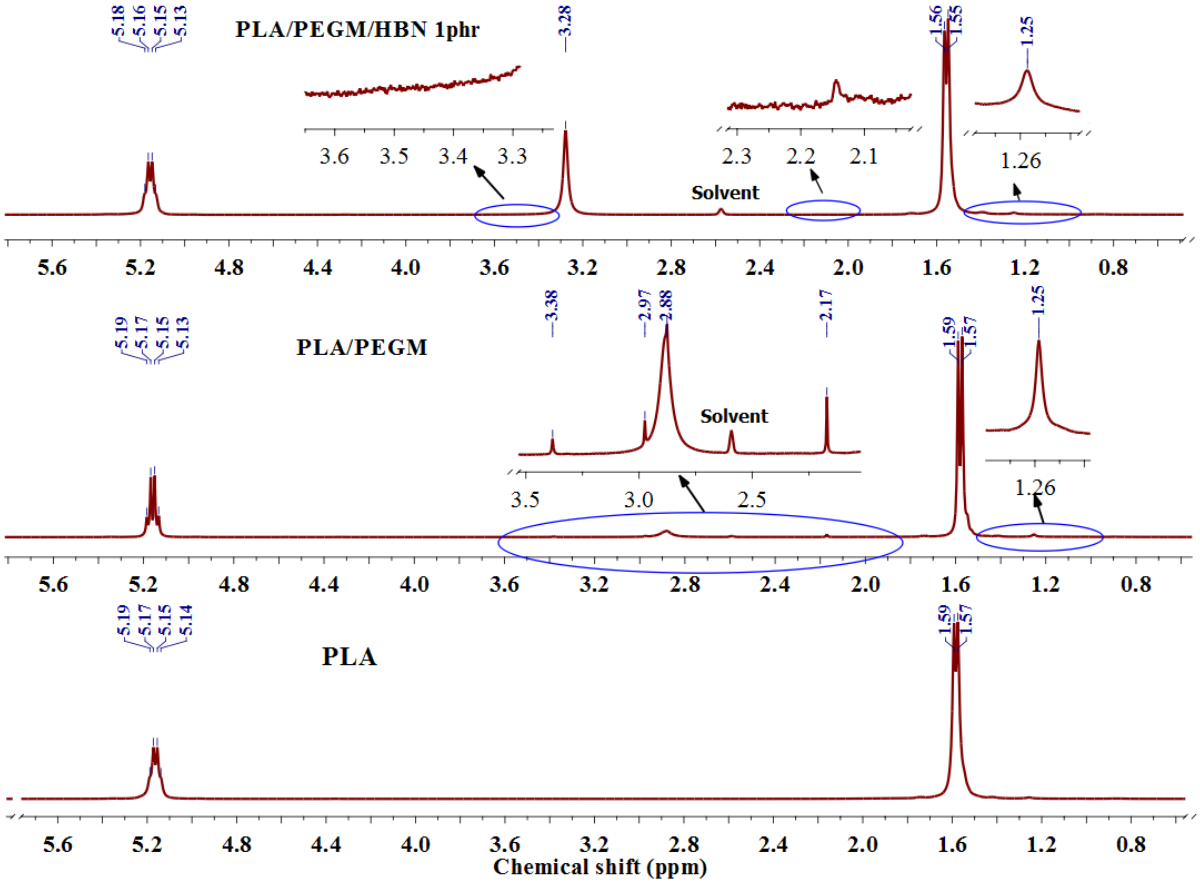

Fig. 3.3 ^{1}H NMR spectra of pristine PLA, PLA/PEGM blend and PLA/PEGM/HBN 1phr blend-composite.

3.2.3 X-ray diffraction

The interaction of HBN layers with the polymer chains in the blend-composites have also been analyzed from the X- ray diffraction pattern manifested in Fig.3.4. It is observed from the graph that pure PLA exhibit large broad halo amorphous peak [136]. However, PLA/PEGM blend shows two crystalline peaks of PLA at 2θ= 20.5˚ and 22.7˚, correspond to (110) and (200) planes [137–139], which indicates PEGM in the blend helps to improve the crystallinity to a small extent. The blend-composites i.e. PLA/PEGM/HBN 1phr, PLA/PEGM/HBN 5phr and PLA/PEGM/HBN 10phr are showing the additional characteristic sharp intense peaks corresponds to (200) planes of HBN at 26.2˚ , 26.7˚ and 26.9˚ respectively which are shifted from their original position i.e. 2θ= 26.6˚ [65,140], can be evidently seen in the inset of Fig. 3.4. The shifting in the position of crystalline peaks of PLA has also been

noticed after addition of HBN. Thus shifting the position of the characteristic peak of HBN and the crystalline peaks of PLA signify the chemical interactions between polymer chains and crystal layers of HBN. Furthermore, the diffraction pattern for the PLA/PEGM/HBN 1phr shows the large shift in the characteristic peak of HBN towards lower angle side which is due to the large strain produced in the crystal structure of HBN [96] may be caused by introduction of covalent bond between polymer chains and HBN crystal layers or may be due to strong intermolecular interaction between the hydrogen atoms of polymer chains with the nitrogen atoms of crystal layers of HBN [129], such covalent bonds formation has been already discussed in the FTIR, ^{1}H NMR studies. The diffraction pattern of blend-composites with a higher concentration of HBN, i.e. 5phr and 10phr, has shown very small displacement in the characteristic peak of HBN towards higher angle attributed to very little stress produced in the crystal structure of HBN by polymer chains. This small shift also signifies the weak interaction of HBN layer and polymer chains.

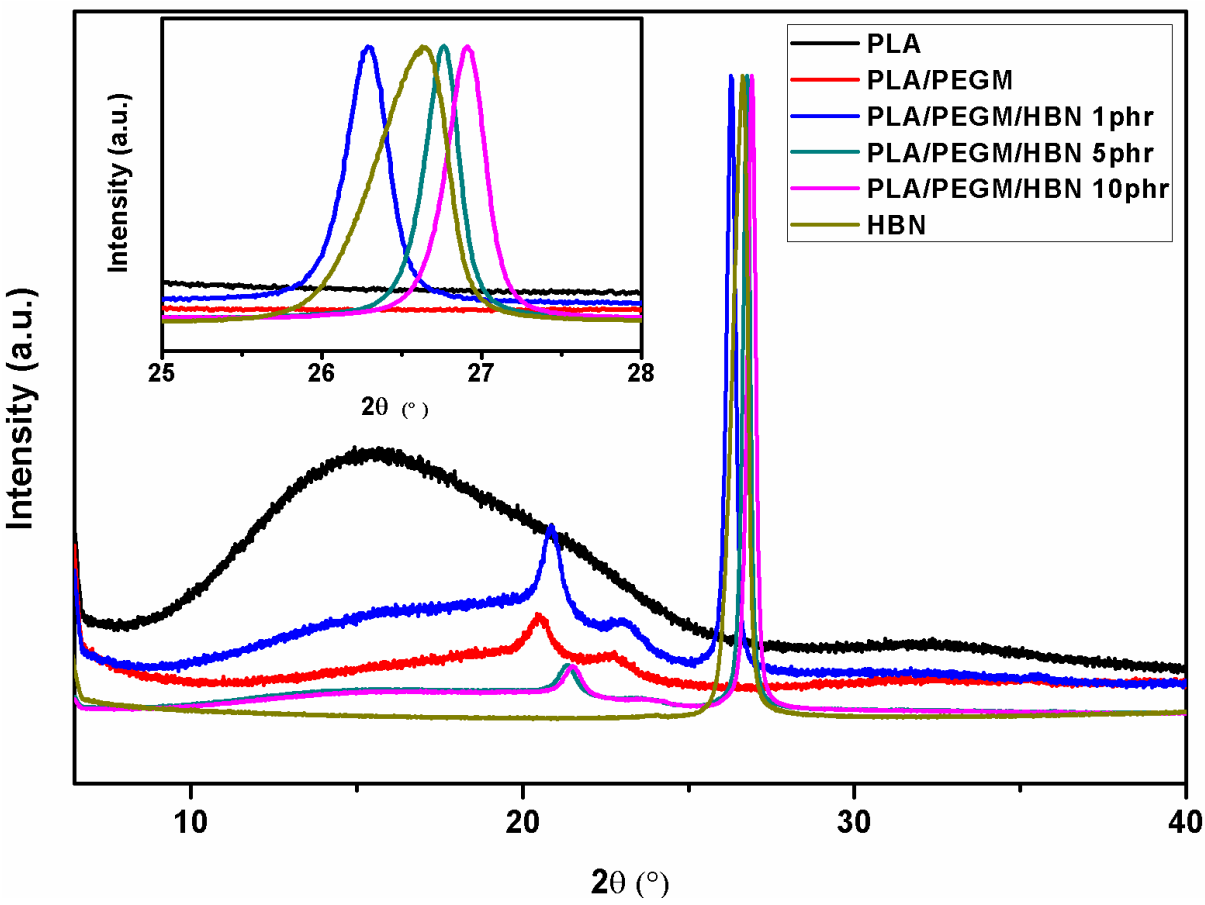

Fig. 3.4 XRD patterns of neat PLA, PLA/PEGM blend and PLA/PEGM/HBN blend-composites.

3.2.4 Mechanical properties

Mechanical properties such as tensile modulus, yield strength, elongation at break, tensile toughness of prepared PLA/PEGM blend and PLA/PEGM/HBN blend-composites are measured with tensile test and notch impact strength is measured by notch Izod impact test, and the results are tabulated in Table 3.2. The tensile stress-strain curves for neat PLA, PLA/PEGM blend and PLA/PEGM/HBN blend-composites are shown in Fig. 3.5. The flexural modulus of PLA, PLA/PEGM blend and PLA/PEGM/HBN blend-composites was also given in Table 3.2. The virgin PLA, processed under those same processing conditions as the PLA/PEGMA blend and blend-composites, gives tensile modulus, yield strength, flexural modulus, tensile toughness and elongation at break respectively as 2300.00 MPa, 65.00 MPa, 3767.00 MPa, 2.70 MJ/m^3 and 5.76%. The low elongation at break of neat PLA ascribes its brittleness. Obviously, it is observed from Table 3.2, that the addition of PEGM reduces the brittleness of PLA leads to a significant increase in the elongation at break. The interfacial interaction between PLA and PEGM, which has been observed by the FTIR and ^{1}H NMR studies, helps to reduce the brittleness and make it tougher. However, the decrement in the tensile modulus, yield strength and flexural modulus has been identified with increment in the elongation at break. It can be noticed from the Table 3.2, that the prepared PLA/PEGM blend has shown a remarkable change in the elongation at break from 5.76% to 157.40% which is 28 times higher than neat PLA and tensile toughness from 2.70 MJ/m^3 to 36.82 MJ/m^3. The elongation at break and tensile toughness were further improved with the addition of HBN, in case of PLA/PEGM/HBN 5 phr, which are 1.5 times more than PLA/PEGM blend. The improvement in the tensile toughness is achieved in case of PLA/PEGM/HBN 5phr because it shows the large elongation at break as compared to other specimens and yield strength near to PLA/PEGM/HBN 10phr blend-composite. Hence, HBN acts as a good plasticizer for PLA/PEGM blend. A general trend of improvement in the elongation at break and tensile toughness with a decrement in other tensile properties have been reported earlier [141,142]. The addition of HBN also increases the HDT as compared to the neat PLA and PLA/PEGM blend. This improvement is due to the chemical interaction of HBN crystal layers with polymer chains, which is more in the case of PLA/PEGM/HBN 1phr, may be due to a fine dispersion of HBN particles in the polymer matrix at low loading and hence this composition shows the high value of heat deflection temperature.

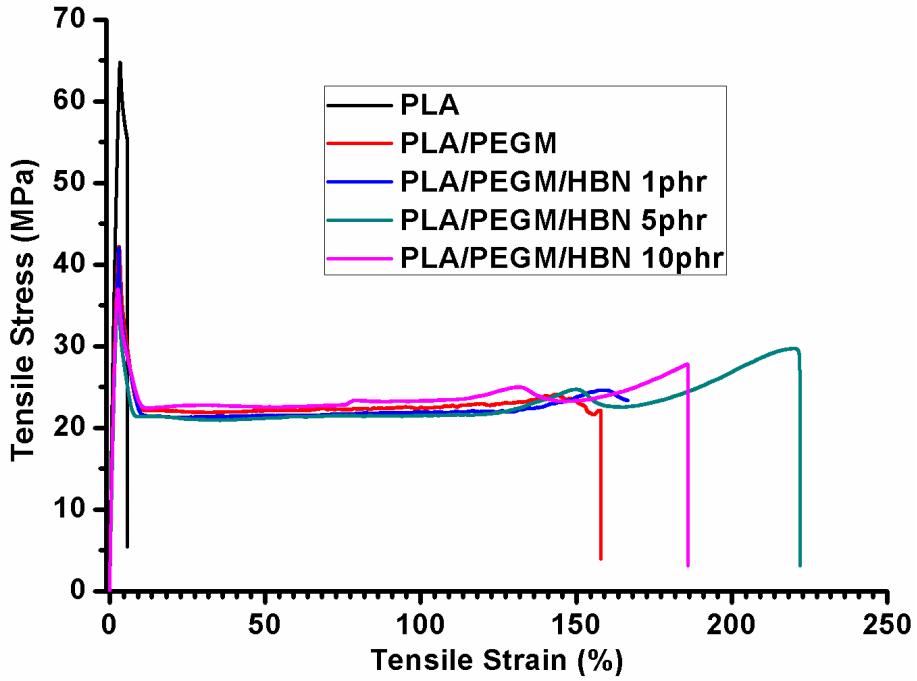

Fig. 3.5 Representative stress-strain curves for PLA, PLA/PEGM blend and PLA/PEGM/HBN blend-composites.

Moreover, from the results of the notched impact test listed in Table 3.2, the neat PLA shows the low impact strength. The addition of PEGM increases the impact strength of PLA through reactive blending. The PLA/PEGM/HBN 1phr blend-composite has shown the highest notched impact strength which is 1.5 times to the impact strength PLA/PEGM blend. This can also be confirmed by studying the surface morphology of impact fractured surfaces of neat PLA, PLA/PEGM blend and PLA/PEGM/HBN 1phr. The SEM micrographs of impact fractured surfaces of PLA/PEGM blend and PLA/PEGM/HBN 1phr blend-composite are as shown in Fig. 3.6. The neat PLA shows brittle fracture surface morphology [132] without sufficient distortions. In spite of it, the PLA/PEGM and PLA/PEGM/HBN 1phr exhibited rough morphology as compared to neat PLA and denoting the fracture transition from brittle to tougher. Furthermore, SEM micrograph of PLA/PEGM/HBN 1phr reveals the higher rough morphology as compared to PLA/PEGM blend which indicates that PLA/PEGM/HBN 1phr has absorbed more impact energy as compared to PLA/PEGM blend because HBN dispersed in the polymer matrix exhibits the chemical interaction with the polymer chains [132,143] and hence it has more notched impact strength which is in agreement with the above results. The SEM micrographs of impact fractured surfaces of PLA/PEGM/HBN 1phr and PLA/PEGM/HBN 10phr blend-composites with high magnification are displayed in Fig. 3.7. The high magnification SEM micrographs of PLA/PEGM/HBN 1phr blend-composite, Fig. 3.7a and a', show the uniform phase with good

interfacial adhesion. This could be attributed to the interaction of HBN particles with the polymer matrix and fine distribution of HBN particles in the polymer matrix. However, at high concentration of HBN (i.e. PLA/PEGM/HBN 10 phr), the highly magnified SEM micrographs (Fig. 3.7b and b') exhibit the phase separation and void formation which is due to the agglomeration of HBN particles that in turn causes poor reactivity and week interfacial adhesion. The agglomeration of the HBN particles, marked by dotted circles, in the polymer matrix can be seen clearly from the Fig. 3.7b', which leads to the decrement in the mechanical and thermal properties [142,144,145].

Table 3.2

Tensile and Flexural properties of neat PLA and PLA blend-composites.

Composition name	Tensile Modulus (MPa)	Yield Strength (MPa)	Elongation at break (%)	Tensile toughness (MJ/m^3)	Notched Izod Impact Strength (kJ/m^2)	Flexural Modulus (MPa)	HDT (˚C)
PLA	2300±24.91	65±0.25	5.76±0.44	2.70±0.24	2.65±0.32	3767±20.85	52.60±0.45
PLA/PEGM	1797±36.08	43±0.91	157.40±4.16	36.82±1.48	5.91±0.25	2545±4.50	51.90±0.58
PLA/PEGM/ HBN 1phr	1754±35.82	42±1.79	166.50±34.29	37.73±7.94	8.89±0.50	2337±71.52	54.50±1.07
PLA/PEGM/ HBN 5phr	1615±14.75	37±0.65	225.81±2.29	54.70±1.90	4.71±1.10	2340±14.69	53.90±0.53
PLA/PEGM/ HBN 10phr	1651±31.36	38±0.58	180.23±4.22	43.91±0.56	4.62±0.90	2394±36.78	51.00±0.89

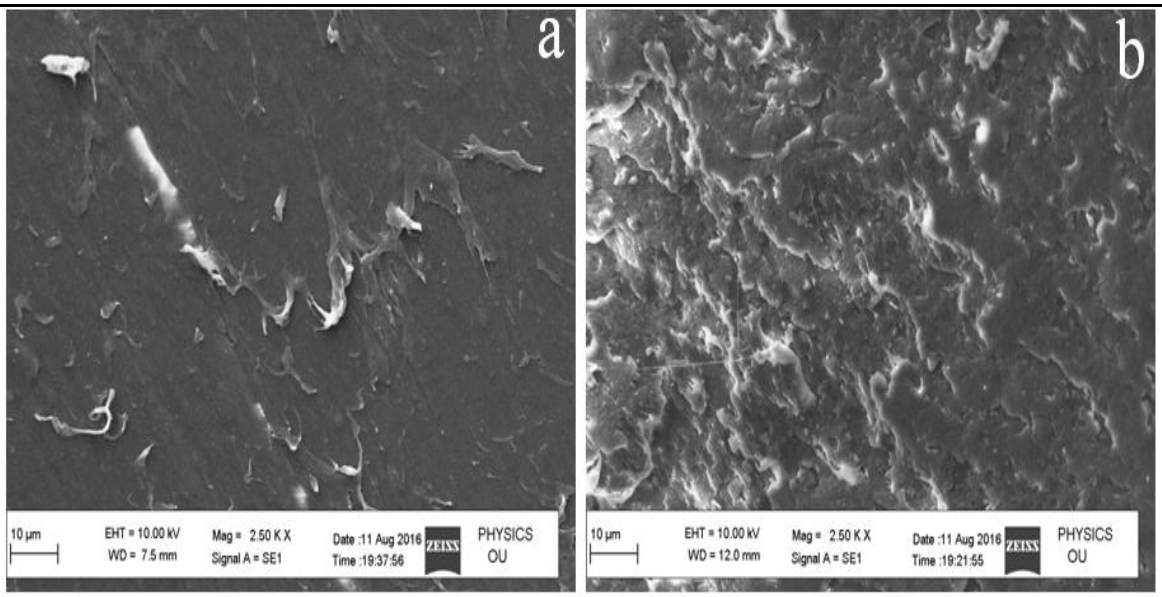

Fig. 3.6 SEM micrographs for the notched impact fractured surfaces for (a) PLA/PEGM blend and (b) PLA/PEGM/HBN 1phr. The scale bar is 10 µm.

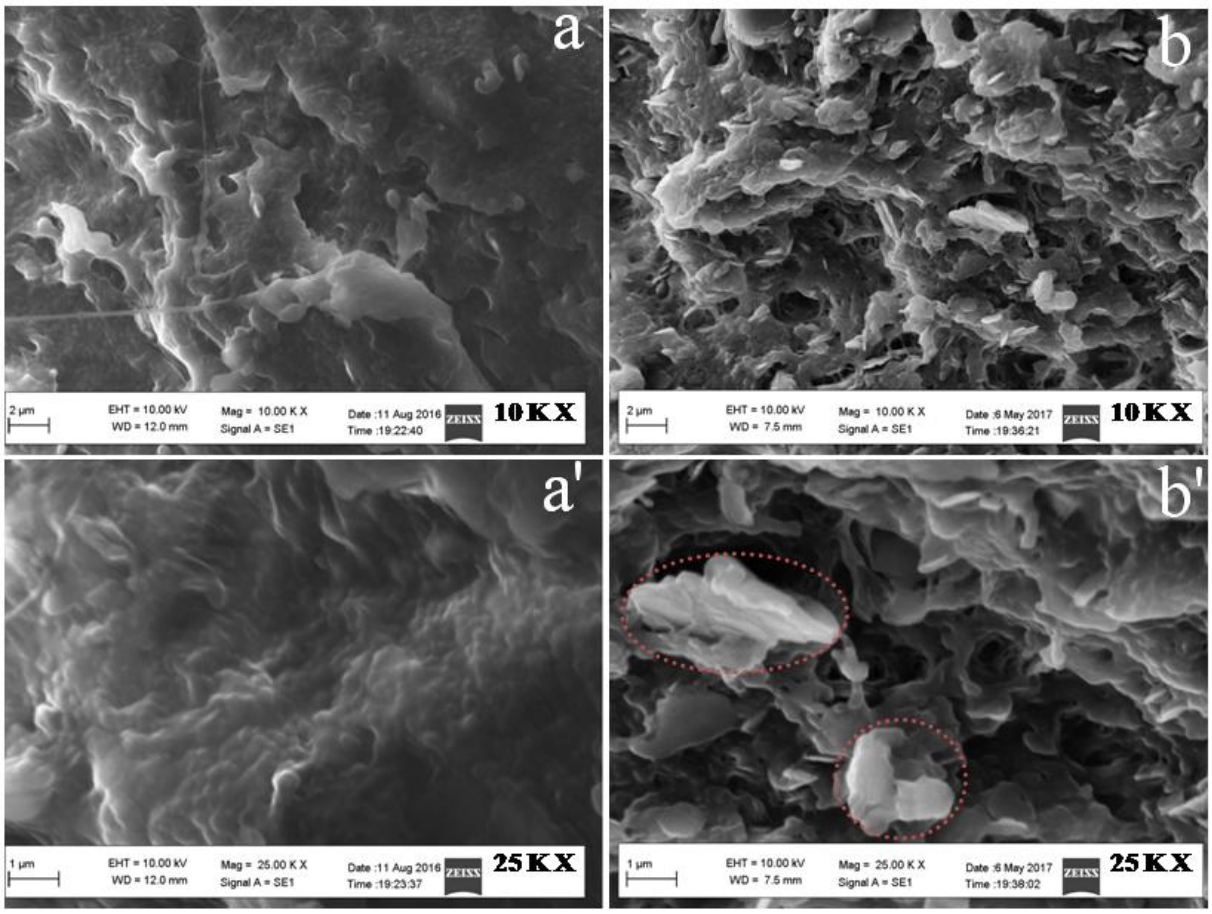

Fig. 3.7 High magnification SEM micrographs for the notched impact fractured surfaces for (a/a') PLA/PEGM/HBN 1phr and (b/b') PLA/PEGM/HBN 10phr. The scale bar for (a and b) is 2 µm and for (a' and b') is 1 µm.

Fascinatingly, several authors have studied the effect of crystallization on the impact strength of blends having PEGM after annealing because PEGM promotes the crystallization of PLA during the thermal annealing process [78,121]. Hence, to see the effect of crystallization, the notched impact strength of annealed specimens (annealed at 90 °C for 2 hours) of PLA/PEGM blend and PLA/PEGM/HBN blend-composites have been measured and shown in Fig. 3.8. It can be observed that after annealing the impact strength of all compositions are increased significantly. The PLA/PEGM/HBN 1phr still shows the highest notched impact strength as compared to PLA/PEGM blend and other blend-composites. These results evinced that at low concentrations HBN helps to improve the mechanical properties.

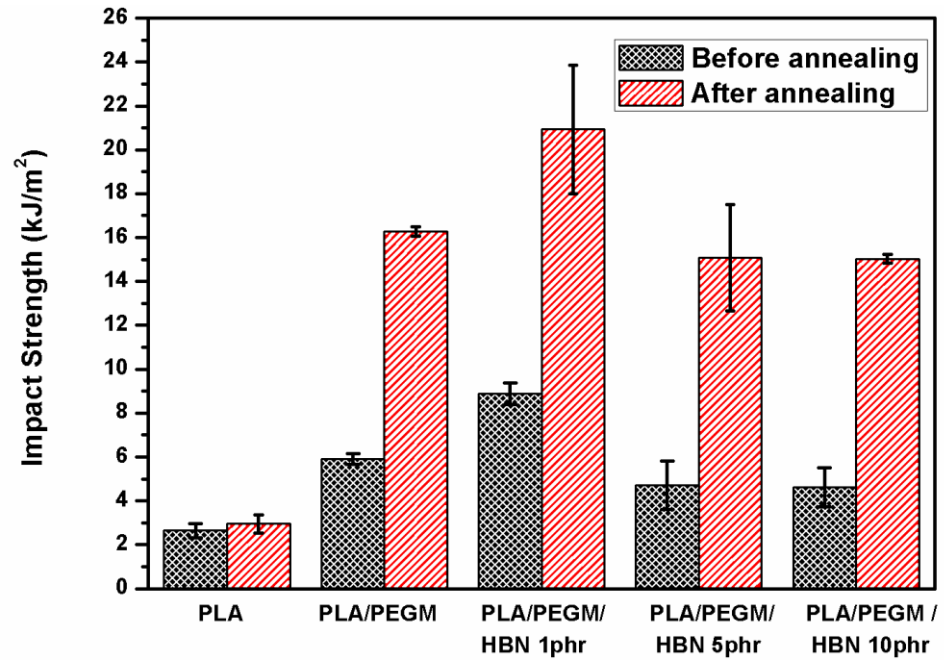

Fig. 3.8 The notched impact strength of neat PLA and PLA blend-composites with different percentage of HBN before and after annealing all specimens at 90˚C for two hours.

3.2.5 Thermal properties

The DSC curves of neat PLA, PLA/PEGM blend and PLA/PEGM/HBN blend-composites are shown in Fig. 3.9. The essential parameters such as glass transition temperature (T_g), cold crystallization temperature (T_{cc}), melting temperature (T_m), cold crystallization enthalpy (ΔH_{cc}), melting enthalpy (ΔH_m) and % of crystallinity (X_c) (Eq. 2.5) are reported in Table 3.3. The small but significant change in the glass transition temperature (T_g) of samples are found. It can be seen that glass transition temperature of PLA/PEGM blend shifted slightly to lower temperature compared to virgin PLA, signifies the compatibility between PLA and PEGM as noticed earlier from FTIR and ^{1}H NMR studies. However, PLA/PEGM/HBN 1phr shows the shift in glass transition temperature to the higher value as compared to neat PLA. This may be due to chemical interactions between crystal layers of HBN and polymer chains which restrict their local segmental motion. The blend-composites with 5phr and 10phr HBN shows the lower glass transition temperature as compared to neat PLA but higher than PLA/PEGM blend. The cold crystallization temperature of the PLA blend and blend-composites have shown an increase and the normalized heat of fusion is decreased as compared to neat PLA. This is because the HBN chemical interactions with polymer chains affect the interaction among the polymer chains that leads to less mobility of polymer chains and hence shows higher crystallization temperature. The DSC thermograms shown in Fig. 3.9 have two melting peaks for all

specimens. Similar results have been reported by other authors [24,146,147]. The double peaks of PLA samples are due to the two crystalline phases formed in the cold crystallization stage and re-crystallization stage. The two crystallization phases are normally attributed to different crystallization structures i.e. crystallization regions of different size and perfection or stability.

Table 3.3

Thermal transition data of prepared blend and blend-composites.

Composition name	T_g (˚C)	(T_{cc}) (˚C)	(ΔH_{cc}) (J/g)	(T_m) (˚C)	(ΔH_m) (J/g)	(X_c) (%)
PLA	55.43	96.05	48.05	145.82, 154.05	52.75	5.05
PLA/PEGM	53.91	96.90	28.88	144.83, 152.68	35.00	8.23
PLA/PEGM/HBN 1phr	55.88	98.04	19.53	146.03, 153.93	23.75	5.73
PLA/PEGM/HBN 5phr	54.49	98.67	12.90	145.33, 152.86	18.03	7.24
PLA/PEGM/HBN 10phr	54.91	98.98	15.15	145.30, 152.87	21.82	9.86

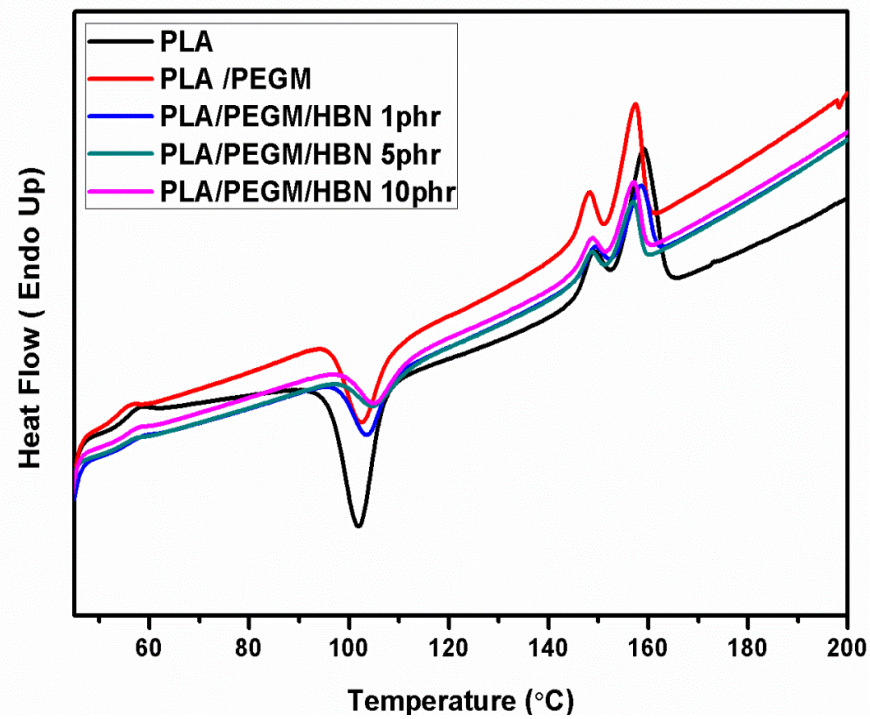

Fig. 3.9 DSC thermogram for the as injected moulded samples of neat PLA, PLA/PEGM blend and PLA/PEGM/HBN blend-composites.

The TG and DTG curves, under a nitrogen atmosphere, of pure PLA and blend-composites are displayed in Fig. 3.10 and corresponding data such as initial degradation temperature ($T_{5\%}$), maximum weight loss temperature (T_{max}) and mass loss rate at T_{max} are

summarized in Table 3.4. The addition of PEGM improves the thermal stability of PLA and PLA/PEGM shows higher $T_{5\%}$ and lower mass loss rate than neat PLA. The higher thermal stability of PLA/PEGM blend is due to the formation of PLA/PEGM graft-copolymers, which act as an interface between PLA and PEGM, and hence increase the chemical linkage. The PLA/PEGM/HBN 1phr and PLA/PEGM/HBN 10phr also show better thermal stability than neat PLA due to higher $T_{5\%}$ and lower mass loss rate than neat PLA. However, these blend-composites show the slightly low thermal stability than PLA/PEGM blend because the addition of HBN also leads the PLA chains scission. This effect is more pronounced in the case of PLA/PEGM/HBN 5phr, which is also confirmed by FTIR study, and as a result, it has low thermal stability as compared to neat PLA.

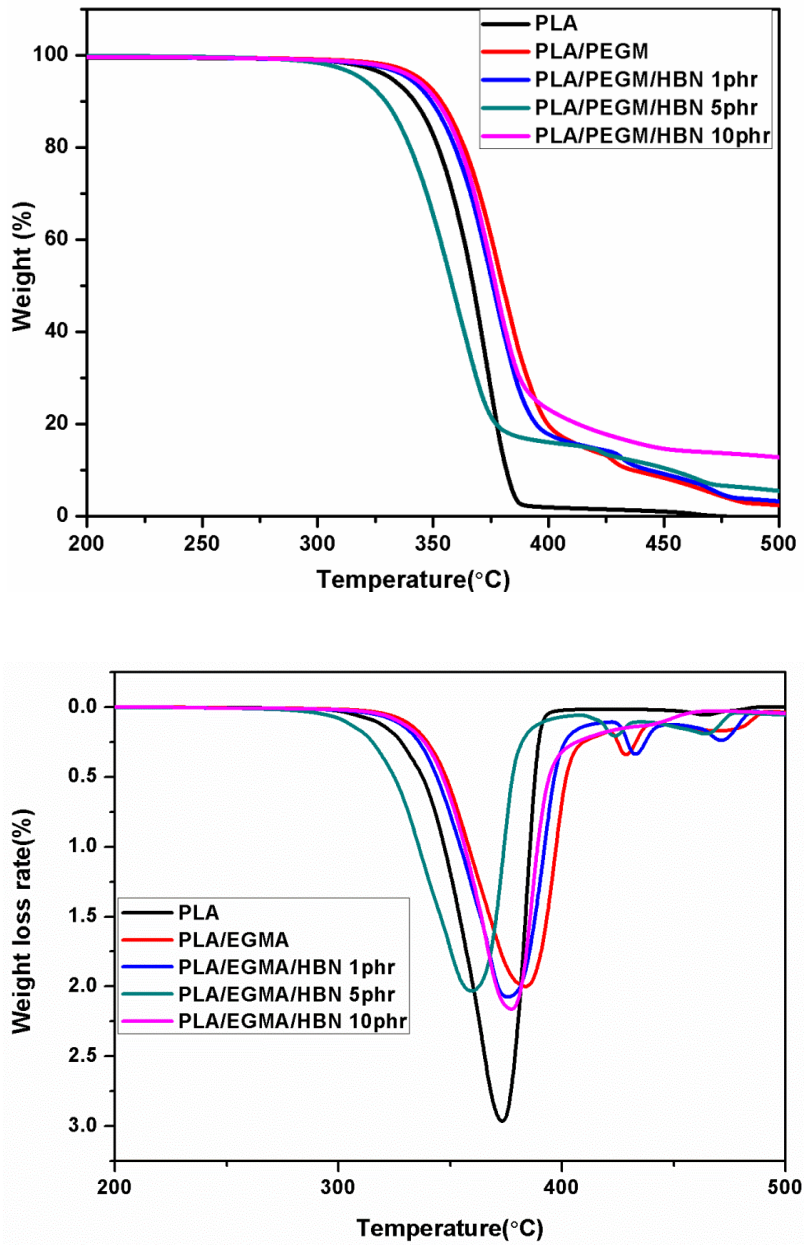

Fig. 3.10 TG and DTG curves of PLA, PLA/PEGM blend and PLA/PEGM/HBN blend-composites.

Table 3.4

TG and DTG data of neat PLA, PLA/PEGM blend and PLA/PEGM/HBN blend composites.

Composition name	$T_{5\%}$ (˚C)	T_{max} (˚C)	Mass loss rate at T_{max} (wt %/ ˚C)
PLA	331.74	373.35	2.96
PLA/PEGM	344.06	383.68	2.00
PLA/PEGM/HBN 1phr	339.41	375.64	2.07
PLA/PEGM/HBN 5phr	318.70	359.46	2.03
PLA/PEGM/HBN 10phr	341.77	377.24	2.16

3.3 Conclusions

The interfacial compatibly between PLA and PEGM took place due to PLA/PEGM graft copolymers which act as an interface between PLA and PEGM to improve their compatibility. The formation of PLA/PEGM graft copolymers through epoxide ring-opening mechanism has been studied using FTIR and ^{1}H NMR analysis. From the FTIR studies, it can be inferred that the probability for reacting of epoxide group of PEGM with the carboxylic terminal group is more as compared to the hydroxyl terminal group of PLA chains. Hence, the PLA grade having carboxyl terminal groups is more compatible with PEGM as compared to the PLA grade having hydroxyl terminal groups. Furthermore, many researchers used to follow post-annealing for improving the mechanical properties of PLA and PEGM based polymer blends. In general, the post-annealing is not industrially advisable. Hence to improve the mechanical properties of the PLA-PEGM blend, the HBN has been incorporated. From the results, it can be observed that the blend-composite with low HBN content i.e. PLA/PEGM/HBN 1phr on an average shows better mechanical and thermal properties than neat PLA, PLA/PEGM blend and other blend-composites. By optimizing the concentration of HBN, the combination of high impact strength and large strain to failure in tension can be achievable.

Chapter 4

Optimization of mechanical, thermal and hydrolytic degradation properties of PLA/PEGM/HBN blend-composites using electron beam irradiation

---

In this chapter, the influence of electron beam irradiation on mechanical, thermal and hydrolytic degradation properties of Poly (lactic acid) (PLA)/Poly (ethylene-co-glycidyl methacrylate) (PEGM)/Hexagonal boron nitride (HBN) blend-composites are investigated. The previous studies have reported that the blending of PLA and PEGM with weight ratio (PLA: PEGM) (80:20) reduce the brittleness and improve the toughness. However, the heat deflection temperature (HDT) and other tensile properties are found to be reduced. It is found that HDT can be improved with the incorporation of HBN particles. So far, the effect of PLA/PEGM blending on the hydrolytic degradation properties of PLA has not been studied. Hence, in the present work, the hydrolytic degradation test on a prepared blend and blend-composites is performed. It is observed that the blending of PEGM with PLA significantly retards the hydrolytic degradation of PLA. Further reduction in the hydrolytic degradation of PLA was observed in the blend-composites. Hence, the E-beam is employed to optimize the mechanical, thermal and degradation properties of the final product as per the desired applications.

Publications:

1. **Ashish Kumar**, T.Venkatappa Rao, S. Ray Chowdhury, S.V.S Ramana Reddy, "Optimization of mechanical, thermal and hydrolytic degradation properties of Poly (lactic acid)/Poly (ethylene-co-glycidyl methacrylate)/Hexagonal boron nitride blend composites through electron-beam irradiation", **Nuclear Inst. Methods in Physics Research B 428 (2018) 38-46 (Impact Factor 1.323).**

2. Ashish Kumar, T.Venkatappa Rao, S. Ray Chowdhury, S.V.S Ramana Reddy, "Effect of electron beam irradiation on thermal and mechanical properties of poly (lactic acid) / poly (ethylene-co-glycidyl methacrylate) blend", **AIP Conference Proceedings 1849(1):020039 · June 2017, DOI: 10.1063/1.4984186.**

4.1 Introduction

The consumer and biomedical applications of PLA depend on its bulk properties (e.g. toughness, degradation rate etc.) and surface properties (hydrophobicity, roughness, and reactive functionalities). The surface modification of PLA has been undertaken by researchers for medical applications [148,149]. The toughness and elongation at break of PLA are being improved for commercial applications and the improvement in the degradation rate has advantages in both consumer as well as medical applications. Many authors have attempted to improve the elongation at break and toughness of PLA through blending [52]. The PEGM is a pronounced polymer to improve the toughness and elongation at break of PLA through reactive blending [78,121]. However, the reactive blending of PLA and PEGM leads to decrease in the HDT and other tensile properties of PLA.

M.S. Cairns et.al has used the electron beam (E-beam) irradiation to get the controlled degradation of PLA for medical applications [150]. It has been reported that the electron beam can be used to induce the crosslinking among the polymer chains of PLA in the presence of various crosslinking agents to improve the mechanical and thermal properties of PLA [56,59,60,151]. B.Y. Shin et.al has reported, the E-beam irradiation of PLA in the presence of glycidyl methacrylate induce both crosslinking and branching of PLA chains [58]. In the present work, the effect of E-beam irradaition on mechnical, thermal and hydrolytic dgeradtion properties of prepared PLA/PEGM blend and PLA/PEGM/HBN blend-comsposites is studied. To observe the effect of E-beam irradiation on PLA/PEGM blend and PLA/PEGM/HBN blend-composites the prepared test specimens of the blend and blend-composites were further treated by E-beam irradiation with various radiation doses (e.g. 20 kGy, 60 kGy and 100 kGy). It has been noticed that the E-beam irradiation improves the toughness and HDT of PLA/PEGM/HBN blend-composites as compared to the unirradiated PLA/PEGM/HBN blend-composites. The irradiated samples of PLA/PEGM/HBN 5 phr and 10 phr blend-composites reveal the high notched impact strength and HDT as compared to unirradiated and E-beam irradiated PLA, PLA/PEGM blend and PLA/PEGM/HBN 1 phr blend-composite. These improvements with the application of E-beam could be attributed to the introduction of polymer chains scission and polymer chain branching in the PLA/PEGM/HBN blend-composites which enhance the physical interaction of HBN particles with polymer chains asserted by DSC analysis. This also leads to the fine dispersion of the HBN particles in the polymer matrix which in turn uniform phase morphology with good interfacial adhesion asserted by SEM analysis. Further, the hydrolytic degradation studies

revealed the blending of PLA with PEGM markedly restricts the hydrolytic degradation of PLA. From the hydrolytic degradation results, it can also be observed that the E-beam irradiation of prepared specimens leads to significant increment in the degradation as compared to unirradiated specimens. Among all compositions, the irradiated PLA/PEGM/HBN 5 phr blend-composite has shown high hydrolytic degradation rate as well as good mechanical and thermal properties which are useful for both commercial and medical applications. Hence, in the present work, the mechanical, thermal and degradation properties of PLA have been optimized with the help of E-beam irradiation.

4.2 Results and Discussion

4.2.1 Thermal properties

Fig. 4.1 shows the thermal transition curves of E-beam irradiated PLA, PLA/PEGM blend and PLA/PEGM/HBN blend-composites. These thermal transition values are given in Table 4.1 and compared with the thermal transition data of unirradiated PLA, PLA/PEGM blend and blend-composites.

In comparison, it has been observed that the glass transition temperature (T_g) and cold crystalline temperature (T_{cc}) of PLA, blend and blend-composites are increased with E-beam irradiation. This is due to the E-beam irradiation which causes the polymer chains scission, polymer chains branching and partial crosslinking network in the amorphous region of the polymer matrix [58,150]. The crosslinking restricts the local segmental polymer chains motion reflect an increase in T_g values and difficulty in crystallization [60]. In the case of E-beam irradiated PLA and PLA/PEGM blend the crosslinking is more pronounced as compared to polymer chain scission at low radiation dose 20 kGy which made the samples difficult to crystallize during the heating scan can be asserted by observing the high T_g and low ΔH_{cc}. Further, at high radiation dose, i.e. 60 kGy and 100 kGy the polymer chains scission is greater which made them crystallize easily and hence show increment in the ΔH_{cc} with an increase of radiation dose. It is also observed that the sample crystallinity increases with increasing radiation dose.

The E-beam irradiated PLA/PEGM/HBN blend-composites show the high T_g value and crystallinity (X_c) as compared to unirradiated blend-composites. In the case of blend-composites, the ΔH_{cc} was also increased with E-beam irradiation. This can be attributed the E-beam irradiation of blend-composites leads to polymer chains scission which in turn improved the physical interaction of HBN particles, act as nucleating agent, with polymer chains and

promotes the crystallization [98]. The ΔH_{cc} is increasing with radiation dose can be seen in Table 4.1. The E-beam irradiated PLA/PEGM/HBN 5 phr and 10 phr blend-composites samples show high T_g as compared to all E-beam irradiated PLA/PEGM blends and PLA/PEGM/HBN 1 phr blend-composites. Further, the improvement difference in ΔH_{cc} is also more in the case of PLA/PEGM/HBN 5 phr and 10 phr blend-composites. This is due to the E-beam irradiation improved the physical interaction of HBN particles with polymers chains leads to a fine dispersion of HBN particle in the polymer matrix and hence restricts the localized motion of polymer chains. The improved interaction of HBN particles with polymer chains in the polymer matrix helps them to enhance their nucleating ability and hence sample crystallizes more during non-isothermal melt crystallization. This can also be asserted by observing the high crystallinity (X_c) in PLA/PEGM/HBN 5 phr and 10 phr blend-composites.

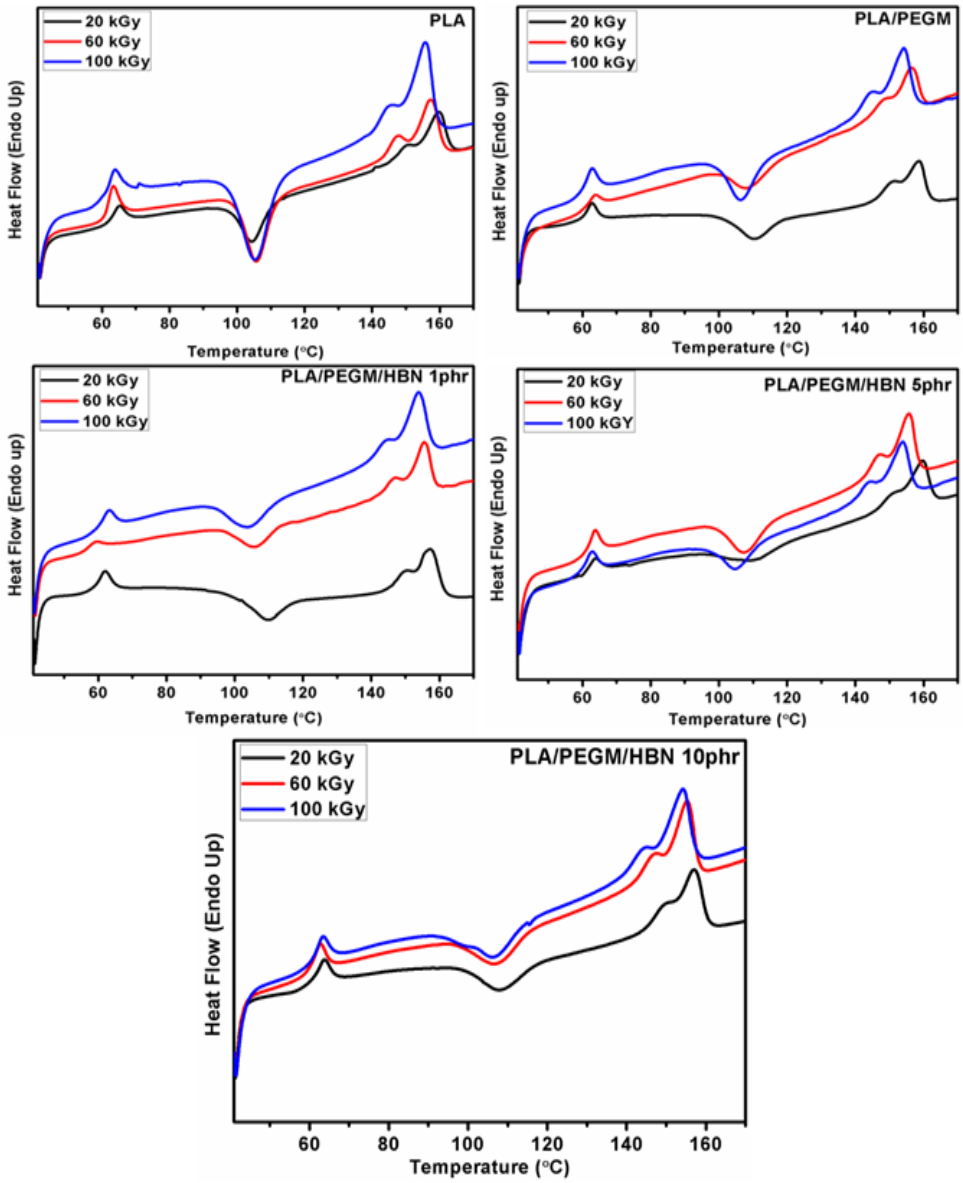

Fig. 4.1 Thermal transition plots of E-beam irradiated PLA, PLA/PEGM blend and PLA/PEGM/HBN blend-composites.

Table 4.1

Thermal transition data of unirradiated and E-beam Irradiated PLA, PEGM/HBN blend and PLA/PEGM/HBN blend-composites.

Composition name	T_g (°C)	(T_{cc}) (°C)	(ΔH_c) (J/g)	(T_m) (°C)	(ΔH_m) (J/g)	(X_c)* (%)
PLA Unirradiated	55.43	96.05	48.05	145.82, 154.05	52.75	5.05
PLA 20 kGy	61.28	97.86	45.36	147.06, 159.82	47.10	1.87
PLA 60 kGy	60.29	99.55	58.80	144.04, 150.54	62.44	3.92
PLA 100 kGy	61.69	97.73	86.26	147.59, 141.62	95.77	10.26
PLA/PEGM Unirradiated	53.91	96.90	28.88	144.83, 152.68	35.00	8.23
PLA/PEGM 20 kGy	59.67	101.29	27.60	147.31, 150.40	39.94	16.58
PLA/PEGM 60 kGy	59.88	100.22	26.80	144.47, 149.54	39.62	17.23
PLA/PEGM 100 kGy	62.75	99.41	41.05	140.38, 145.83	57.26	21.78
PLA/PEGM/HBN 1phr Unirradiated	55.88	98.04	19.53	146.03, 153.93	23.75	5.73
PLA/PEGM/HBN 1 phr 20 kGy	59.32	100.79	25.36	147.34, 151.72	42.61	23.42
PLA/PEGM/HBN 1 phr 60 kGy	56.55	97.19	20.76	143.53, 150.17	33.14	16.81
PLA/PEGM/HBN 1 phr 100 kGy	60.71	94.14	29.78	140.50, 146.95	51.06	28.89
PLA/PEGM/HBN 5 phr Unirradiated	54.49	98.67	12.90	145.33, 152.86	18.03	7.24
PLA/PEGM/HBN 5 phr 20 kGy	61.26	96.47	19.08	147.51, 151.70	31.76	17.89
PLA/PEGM/HBN 5 phr 60 kGy	61.23	99.60	25.75	143.24, 149.02	41.32	21.97
PLA/PEGM/HBN 5 phr 100 kGy	59.84	97.30	26.49	140.86, 146.40	39.62	18.53
PLA/PEGM/HBN 10 phr Unirradiated	54.91	98.98	15.15	145.30, 152.87	21.82	9.86
PLA/PEGM/HBN 10 phr 20 kGy	60.75	99.99	21.78	147.26, 149.99	37.88	23.81
PLA/PEGM/HBN 10 phr 60 kGy	60.06	96.67	26.84	142.94, 148.95	41.15	21.15
PLA/PEGM/HBN 10 phr 100 kGy	60.81	96.76	30.48	140.13, 146.44	44.89	21.30

*The percentage of crystallinity was calculated by the formula given in the chapter 2 (Eq. 2.5).

4.2.2 Morphology

The PLA/PEGM blend and PLA/PEGM/HBN 1 phr blend-composites exhibit good compatibility and uniform phase was asserted by FTIR, ^{1}H NMR and SEM measurements in the previous chapter. However, the high magnification SEM images of blend-composites, having magnification scale 2 µm and 1 µm, revealed that the blend-composite with a high concentration of HBN particles exhibits the phase separation and voids formation due to

agglomeration of HBN particles which leads to less interfacial adhesion. Hence, blend-composite specimens with high HBN concentration were shown poor performance upon mechanical and thermal testing discussed in the previous chapter.

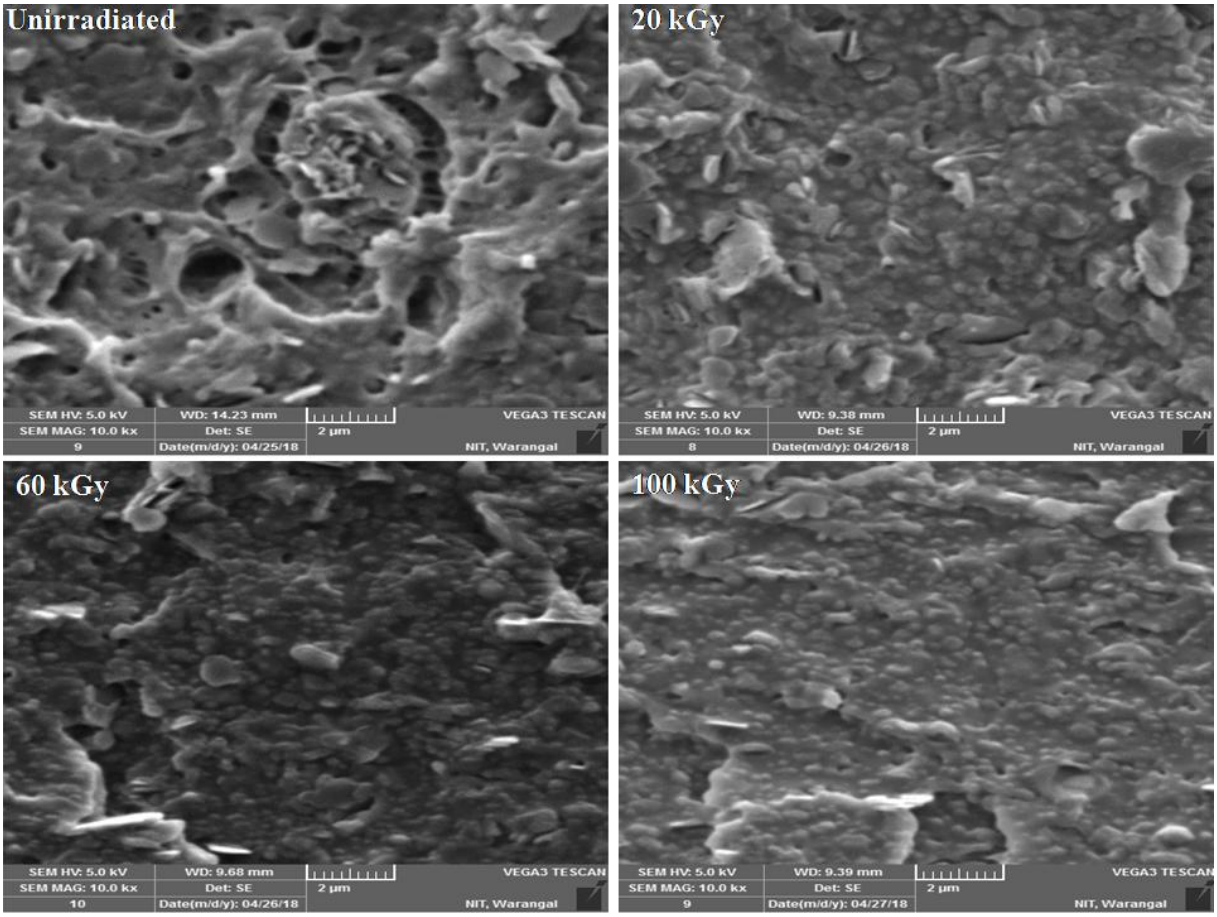

Fig. 4.2 The high magnification SEM micrographs for the notched impact fractured specimens of unirradiated and E-beam irradiated PLA/PEGM/HBN 5 phr blend-composite. The scale bar is 2 µm.

The high magnification SEM micrographs of notched impact fractured specimens of unirradiated and E-beam irradiated PLA/PEGM/HBN 5 phr blend-composite are presented in Figs. 4.2 and 4.3. It can be elucidated from the Figs. 4.2 and 4.3 that the unirradiated PLA/PEGM/HBN 5 phr blend-composite consists of phase separation and voids in the resulting blend-composite. It is due to the high concentration of HBN particles in the blend-composite results in agglomeration of particles in the polymer matrix which affect the reactivity and diminished the interfacial adhesion. Hence, leads to poor mechanical properties [144,145]. The Figs. 4.2 and 4.3 are also manifested the uniform phase morphology with better interfacial adhesion and disappearance of voids in the case of E-beam irradiated PLA/PEGM/HBN 5 phr blend-composite. The uniformity in the phase of the blend-composite

is increased with increasing radiation dose. This could be attributed to a fine dispersion of HBN particles caused by the E-beam irradiation. The E-beam irradiation led to the polymer chains scission and improved their interaction with HBN particles which in turn improved the dispersion of HBN particles into the polymer matrix. Hence, E-beam irradiation of PLA/PEGM/HBN 5 phr blend-composite assisted to improve the interfacial adhesion and dispersion of HBN particles in the polymer matrix of resulting blend-composite. These results are consistent with DSC results.

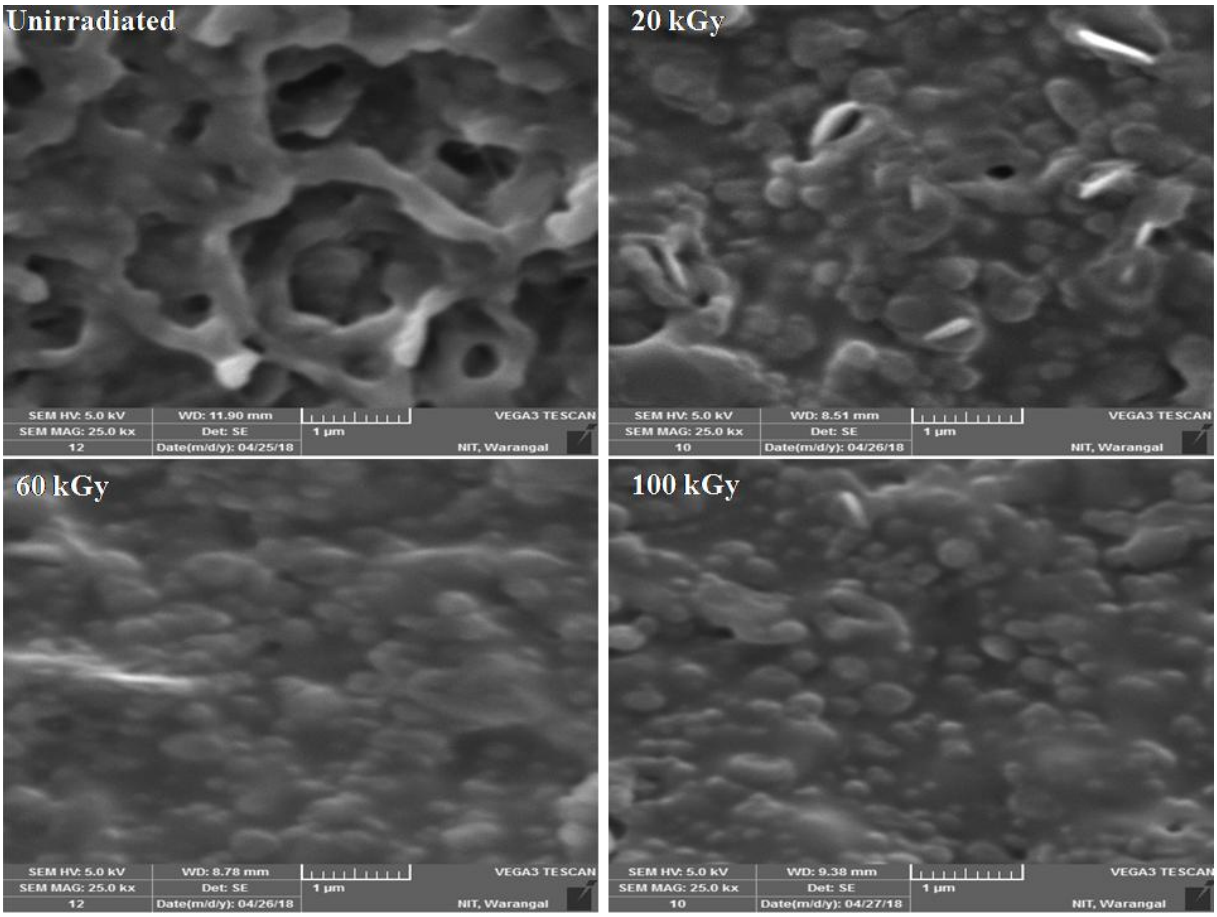

Fig. 4.3 The high magnification SEM micrographs for the notched impact fractured specimens of unirradiated and E-beam irradiated PLA/PEGM/HBN 5 phr blend-composite. The scale bar is 1 µm.

4.2.3 Mechanical properties

The impact strength is one of the most crucial properties of polymer blends and composites for commercial and medical (i.e. in orthopedic fracture fixation) applications [148]. The notched impact strength of unirradiated and E-beam irradiated neat PLA, PLA/PEGM blend and PLA/PEGM/HBN blend-composites are tested with ASTM D256

method and shown in Fig. 4.4. From Fig. 4.4 it can be seen that the neat PLA shows the poor notched impact strength i.e. 2.65 ± 0.32 kJ/m^2 but the reactive blending of PEGM with PLA increase the notched impact strength of PLA up to 5.91 ± 0.25 kJ/m^2. Further addition of HBN particles at low concentration i.e. 1 phr has still improved notched impact strength to 8.89 ± 0.50 kJ/m^2. However, the addition of HBN particles at high concentrations i.e. 5 phr and 10 phr leads to a small reduction in the notched impact strength as compared to PLA/PGEM blend and PLA/PEGM/HBN 1 phr blend-composite. The above results were reported and discussed briefly in the previous chapter. In the present study, with the execution of E-beam irradiation, the notched impact strength of PLA/PEGM/HBN 5 phr and PLA/PEGM/HBN 10 phr blend-composites appreciably increased which can be seen in the Fig. 4.4. The neat PLA specimens irradiated at 20 kGy also show the better impact strength as compared to unirradiated PLA because electron beam irradiation results in chain branching and partial crosslinking among the PLA chains [56,60,150,152] but with high radiation dose, i.e. 60 kGy and 100 kGy PLA chains scission is more prominent than crosslinking. Hence, the notched impact strength of irradiated PLA samples has been decreased with increasing the irradiation dose. The impact strength of PLA/PEGM blend and PLA/PEGM/HBN 1 phr blend-composite are also decreased with E-beam irradiation due to polymer chains scission. In these cases, the impact strength is not improved significantly with increasing irradiation dose. However, in the case of PLA/PEGM/HBN blend-composites 5 phr and 10 phr, the E-beam irradiation significantly improves the notched impact strength up to 6.50 ± 0.13 kJ/m^2 for PLA/PEGM/HBN 5 phr at 100 kGy and 6.68 ± 0.44 kJ/m^2 for PLA/PEGM/HBN 10 phr at 60 kGy. The impact strength of E-beam irradiated PLA/PEGM/HBN 5 phr blend-composite increases with increasing radiation dose. The PLA/PEGM/HBN 5 phr and 10 phr blend composites show high impact strength at high radiation doses i.e. 100 kGy and 60 kGy respectively which is more as compared to E-beam irradiated PLA, PLA/PEGM blend and PLA/PEGM/HBN blend-composites. This improvement can be attributed to polymer chains scission which elude the particle agglomeration at high HBN particles concentration and also improve the physical interaction of HBN particles with polymer chains. This leads to the uniform phase with good interfacial adhesion and fine dispersion of HBN particles into the polymer matrix asserted by SEM analysis.

The mechanical properties such as tensile modulus and yield strength of unirradiated and E-beam irradiated PLA, PLA/PEGM blend and PLA/PEGM/HBN blend-composites are shown in Fig. 4.5. The reactive blending of PEGM with PLA reduced the yield strength and tensile modulus which can be seen from the Fig. 4.5. The unirradiated PLA/PEGM/HBN

blend-composites also show the low yield strength and tensile modulus as compared to unirradiated PLA and PLA/PEGM blend. However, the irradiated samples PLA/PEGM/HBN blend-composites show the improvement in the yield strength and tensile modulus with radiation doses. Thus E-beam irradiation also helps to improve these tensile properties of PLA/PEGM blend and PLA/PEGM/HBN blend-composites.

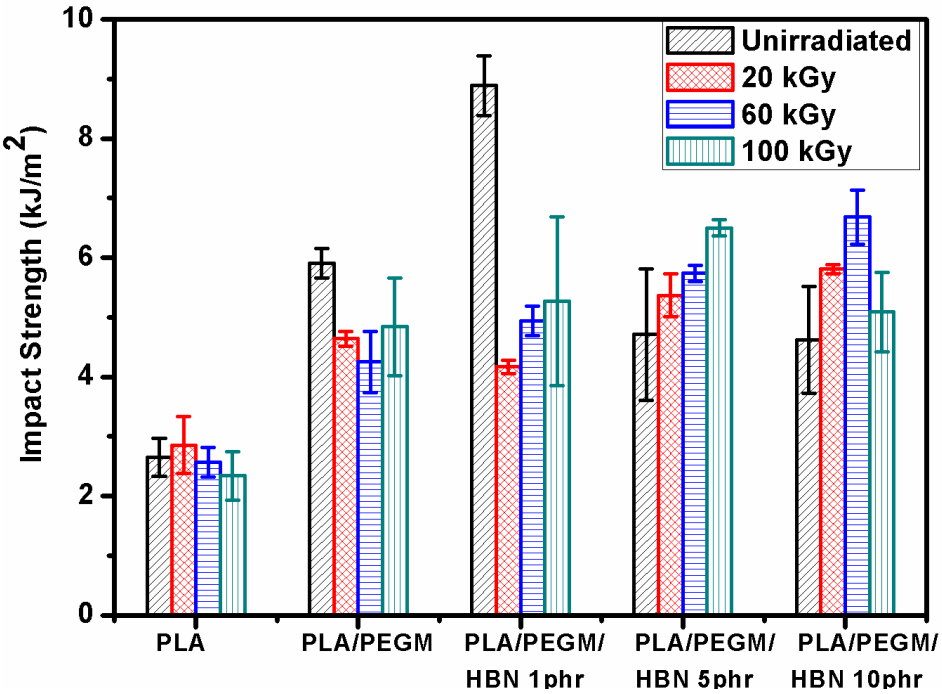

Fig. 4.4 The notched impact strength of unirradiated and E-beam irradiated neat PLA, PLA/PEGM blend and PLA/PEGM/HBN blend-composites.

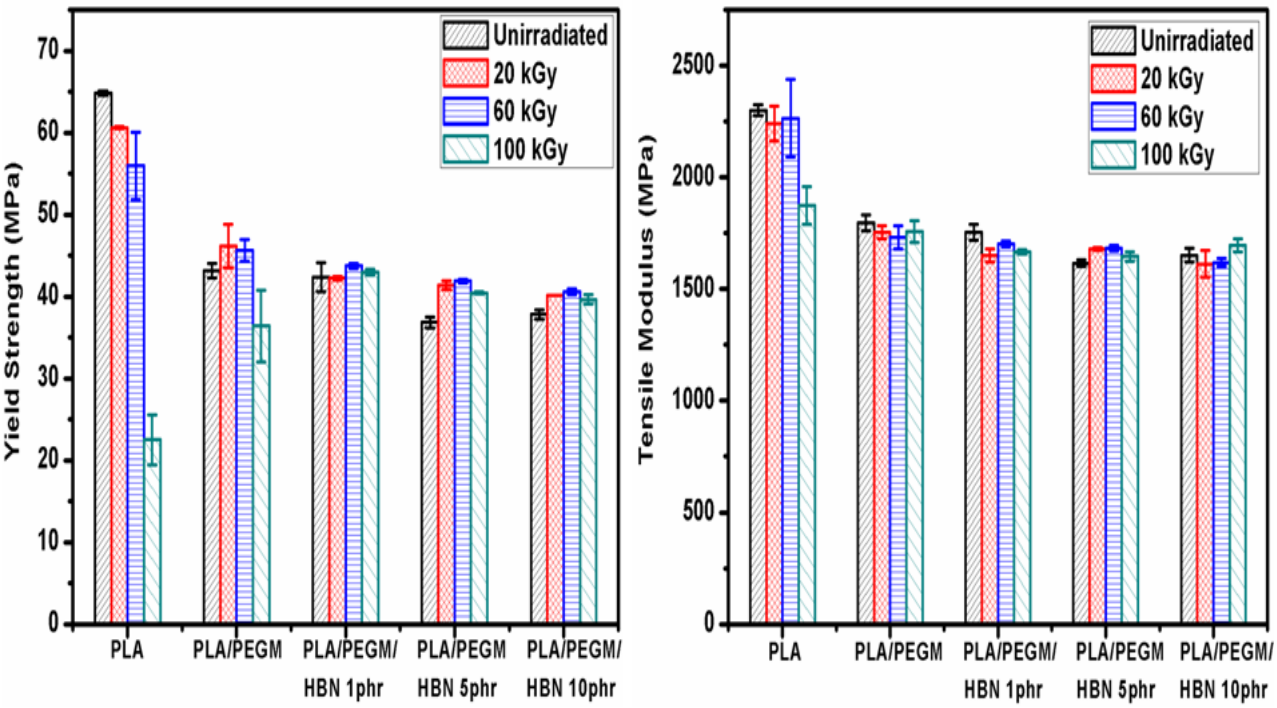

Fig. 4.5 The yield strength and tensile modulus of unirradiated and E-beam irradiated neat PLA, PLA/PEGM blend and PLA/PEGM/HBN blend-composites.

The heat deflection temperature (HDT) is one of the important thermal properties of a polymer product applied in many aspects such as product design, engineering and manufacture of products. It is also known as heat resistant index (an index of strength i.e. elastic modulus at high temperature). Thus, the HDT of unirradiated and E-beam irradiated PLA, PLA/PEGM blend and PLA/PEGM/HBN blend-composites are measured and shown in Fig. 4.6. It can be observed from Fig. 4.6, the unirradiated samples viz., neat PLA, PLA/PEGM blend, PLA/PEGM/HBN 1 phr, PLA/PEGM/HBN 5 phr and PLA/PEGM/HBN 10 phr show 52.60 °C, 51.90 °C, 54.50 °C, 53.90 °C and 51.00 °C respectively. The Fig. 4.6 elucidates the E-beam irradiation significantly improves the HDT of neat PLA, PLA/PEGM blend and PLA/PEGM/HBN blend-composites. This improvement can be attributed to the establishment of the polymer chain branching and improvement in crystallinity with the application of E-beam irradiation [121,143]. The E-beam irradiated PLA/PEGM/HBN 5 phr blend-composite shows the highest value of HDT i.e. 58.80 °C at a low dose (20 kGy) among all unirradiated and E-beam irradiated samples.

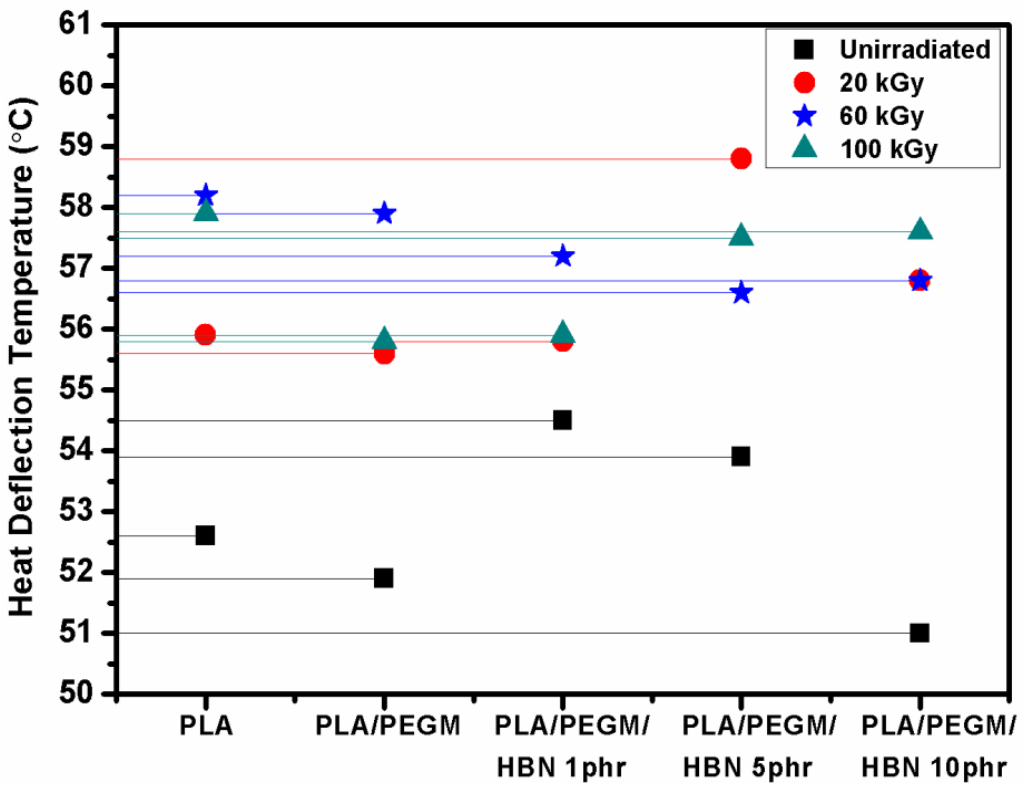

Fig. 4.6 The heat deflection temperature (HDT) of unirradiated and E-beam irradiated neat PLA, PLA/PEGM blend and PLA/PEGM/HBN blend-composites.

4.2.4 Hydrolytic degradation

The controlled degradation of PLA along with good mechanical and thermal properties is indispensable to promote it's various biomedical, commercial and agriculture applications. Some of its applications favor fast hydrolytic degradation rate, however, in other applications stability of the product over a long time is desirable [118,148,153]. The blending of PLA with other polymers and additives affect its hydrolytic degradation rate. In the present chapter, the effects of blending of PEGM and further incorporation of HBN particles on hydrolytic degradation of PLA were studied. The weight loss (%) was estimated by exploiting the Eq. 2.11 (chapter 2). After the first week of immersion into the PBS, all the specimens have shown small weight gain because of moisture absorbed during the process. This can be attributed to the high diffusion rate of water molecules into specimens during initial days of the test. After the second week of the hydrolytic degradation test, the weight loss by neat PLA and PLA/PEGM blend and PLA/PEGM/HBN blend-composites were observed gravimetrically and visually (Fig. 4.7). The weight loss by all specimens is increasing with degradation time. The neat PLA hydrolyzed rapidly and showed maximum weight loss after four weeks of test. However, it can be noticed that the reactive blending of PLA with PEGM significantly controlled its hydrolytic degradation rate (Fig. 4.7). It is reported that PLA hydrolyzes into low molecular weight water-soluble oligomers and the hydrolytic degradation of PLA takes place due to the presence of hydrolyzable ester functional groups in its backbone [15,114,118]. Hence, hydrolysis of ester linkages of PLA and its blend samples leads to the formation of low molecular weight water-soluble oligomers and shown the weight loss. The hydrolysis of PLA has been assumed to be self-catalyzed and self-maintained process due to the catalytic action of its carboxylic acid terminal groups [114,118,154,155]. The reactive blending of PLA with PEGM leads to the formation of PLA/PEGM graft copolymer, through epoxide ring-opening mechanism in which carboxylic terminal group PLA is more prone to react with an epoxide group of PEGM has been studied by using FTIR and ^{1}H NMR studies in the previous chapter. This results decrement in the carboxylic terminal group in the resulting PLA/PEGM blend and suppressed the self-catalyzed action of PLA. Hence, significantly retard the hydrolytic degradation of PLA. Moreover, Fig. 4.7 also shows that after 14 days of immersion period the PLA/PEGM/HBN 1 phr and PLA/PEGM/HBN 5 phr have slightly more weight loss percentage as compared to PLA/PEGM blend. This is due to the addition of HBN particles among PLA/PEGM to prepare blend-composites induced small chain breakage which initially helps to slightly more degradation of the specimens. However, the PLA/PEGM/HBN 10 phr blend-composite have less weight loss percentage as

compared to PLA/PEGM blend because of the least interaction of HBN particles and polymer chains. Further, after third and fourth weeks of immersion study, the PLA/PEGM/HBN blend-composites have shown less weight-loss percentage as compared to PLA/PEGM blend. The weight loss percentage with degradation time is decreased with increasing the concentration of HBN particles. This could be attributed to the high physical and chemical interaction of HBN particles in the blend-composites with the hydroxyl and hydrogen ions of immersion medium. Such kind of interaction has been studied and reported in the literature [129,156]. Thus the availability of water molecules of immersion media to hydrolyzable ester linkage of PLA chains in PLA/PEGM/HBN blend-composites was reduced and hence shown the more stability, decrement in the weight loss percentage, as compared to PLA/PEGM blend. The increase in the concentration of HBN particles causes more interaction and least availability of hydroxyl and hydrogen ions of immersion media and hence the weight loss percentage of the specimens was decreased with increasing concentration of HBN particles in blend-composites.

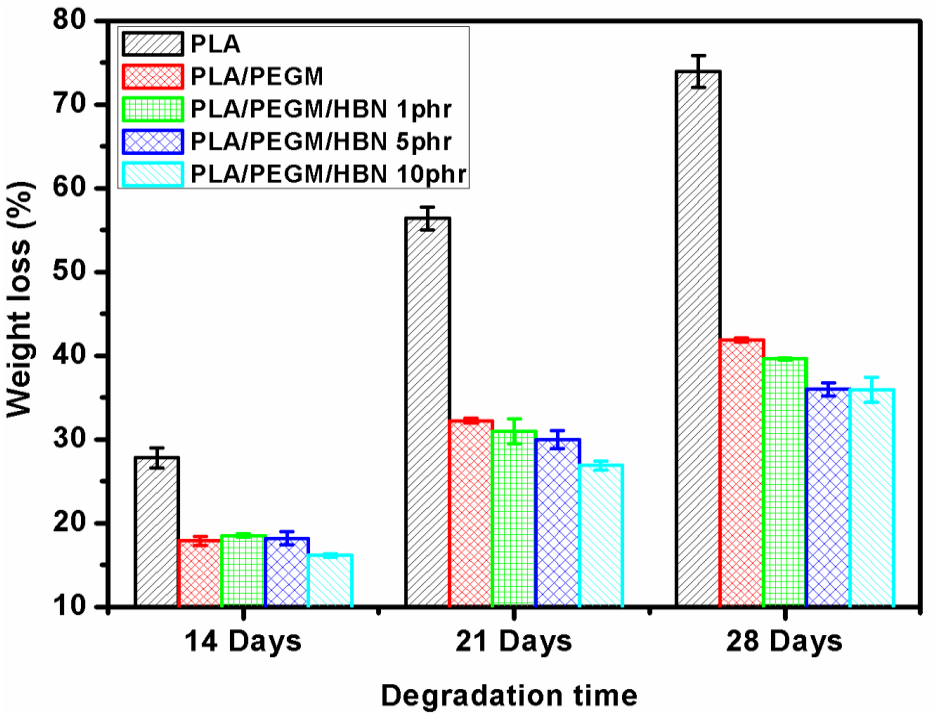

(a)

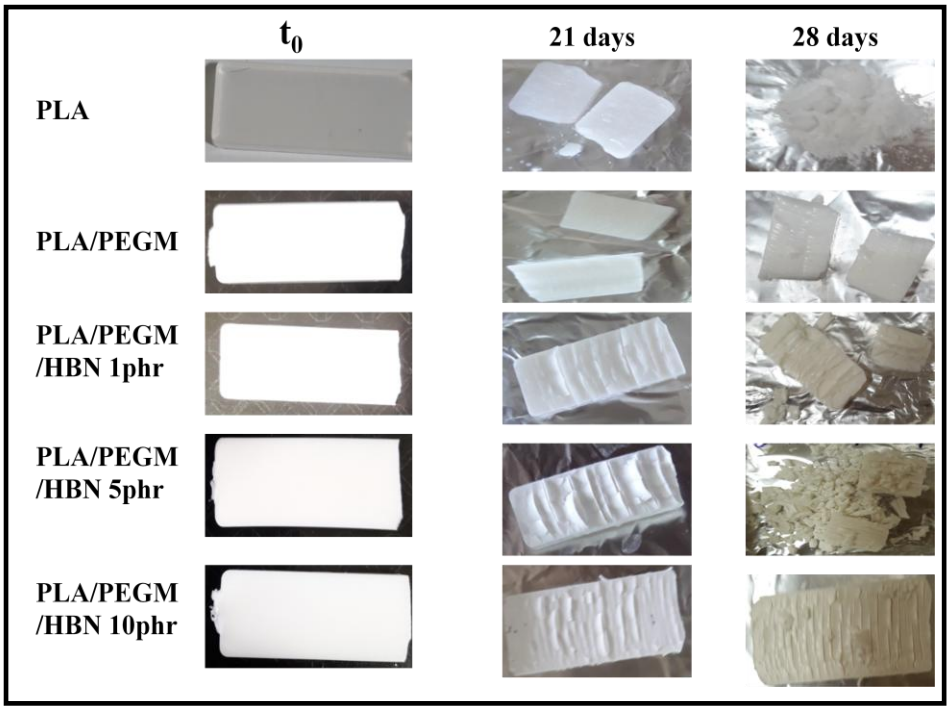

(b)

Fig. 4.7 Hydrolytic degradation of neat PLA, PLA/PEGM blend and PLA/PEGM/HBN blend-composites, (a) weight loss percentage (b) optical images of hydrolyzed samples, with degradation time in PBS at 58ºC.

The effect of electron beam (E-beam) irradiation on hydrolytic degradation of PLA/PEGM blend and PLA/PEGM/HBN blend-composites has also been studied and the results are shown in Fig 4.8. Fig. 4.8 shows that at 20 kGy dose the degradation process starts

earlier for E-beam irradiated PLA/PEGM blend and blend-composites as compared to unirradiated blend and blend-composites. The weight loss percentage is significantly increased with the E-beam irradiation for PLA/PEGM blend and all blend-composites (Fig. 4.8). The E-beam irradiation of blend and blend-composites leads to the polymer chains scission, asserted by DSC analysis. The polymer chains scission assists the water diffusion in the polymer matrix and accelerated the hydrolytic degradation. The E-beam irradiated PLA/PEGM/HBN 5 phr blend-composite at 100 kGy shows the fast degradation and maximum weight loss (Fig. 4.9). The E-beam irradiated PLA/PEGM/HBN 5 phr blend-composites also show the good yield strength, better tensile modulus, HDT and high notched impact strength at 60 kGy and 100 kGy as compared to other E-beam irradiated blend and blend-composites.

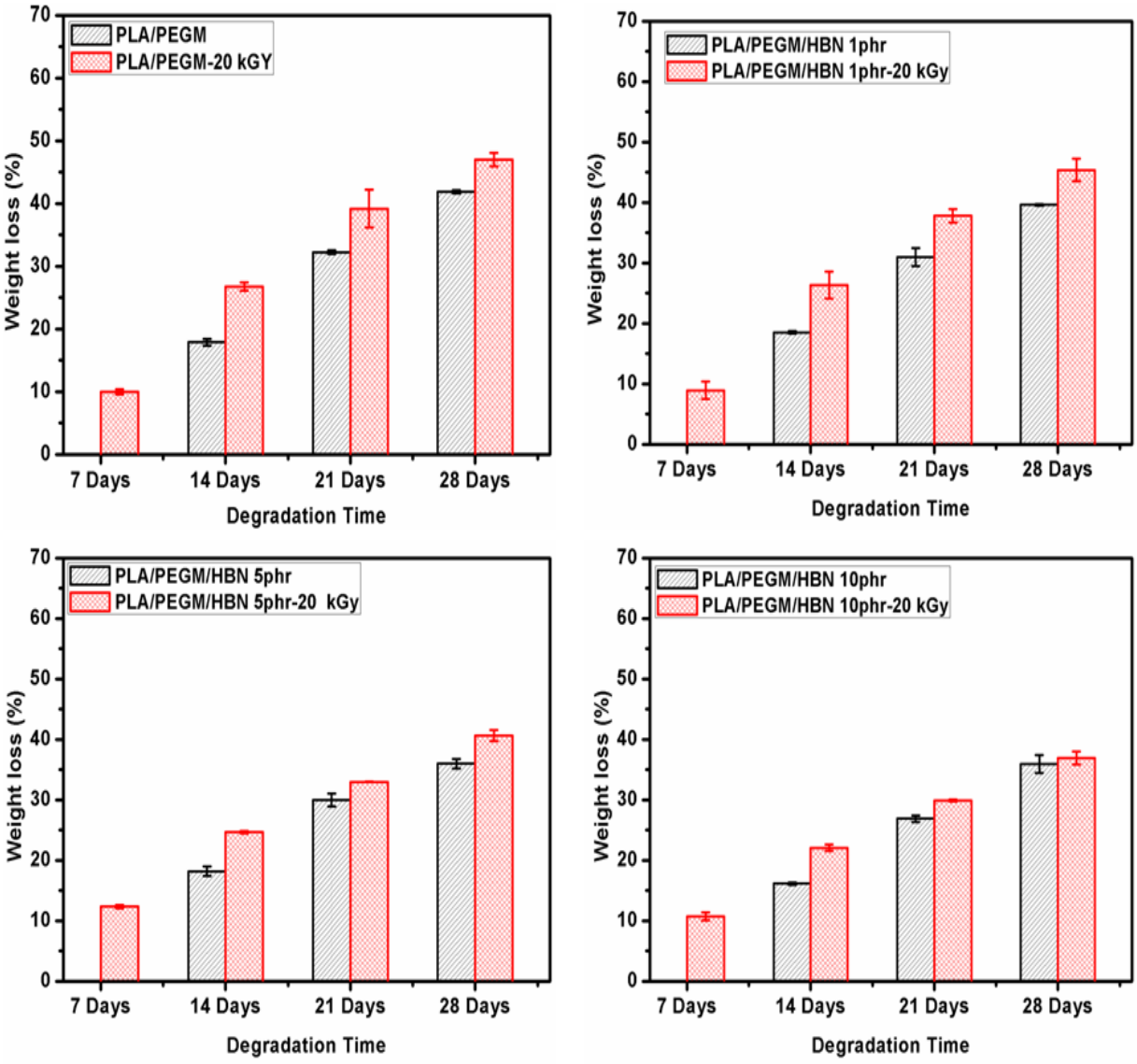

Fig. 4.8 The effect of E-beam irradiation, at 20 kGy dose, on hydrolytic degradation of PLA/PEGM blend and PLA/PEGM/HBN blend-composites.

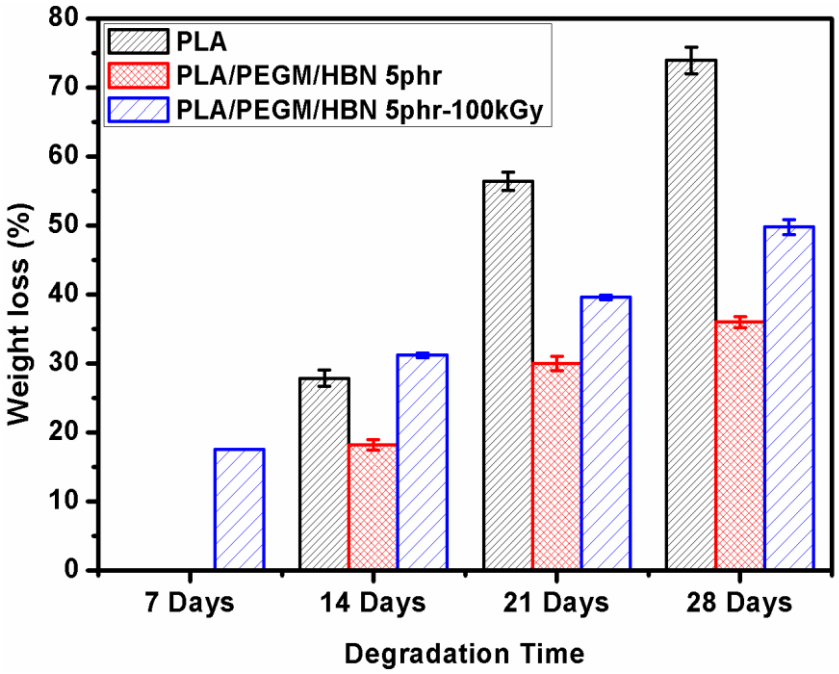

Fig. 4.9 The hydrolytic degradation of neat PLA, PLA/PEGM/HBN 5 phr and PLA/PEGM/HBN 5 phr-100 kGy blend-composites.

4.3 Conclusions

The good impact strength and controlled degradation rate of PLA is essential for various commercial and medical applications. As reported in the previous chapter, the blending of PEGM with PLA reduces the brittleness, improves the toughness; decreases the tensile modulus, yield strength and HDT of PLA. The improvement in the HDT was obtained with the incorporation of HBN particles without sacrificing other properties. In the present work, an attempt has been made to optimize the mechanical, thermal and hydrolytic degradation properties with the help of E-beam irradiation. The E-beam irradiation significantly improves the mechanical properties and HDT of PLA/PEGM/HBN 5 phr and 10 phr blend-composites. The E-beam irradiated PLA/PEGM/HBN 5 phr blend-composites show high notched impact strength, HDT and other tensile properties as compared to other E-beam irradiated blend and blend-composites. It is also found that the blending of PEGM with PLA and incorporation of HBN particles significantly controlled the hydrolytic degradation of PLA. However, the E-beam irradiation of blend and blend-composites enhance the degradation rate of irradiated blend and blend-composites. The E-beam irradiated PLA/PEGM/HBN 5 phr blend-composite has shown the maximum impact strength at 100 kGy and also exhibits fast degradation rate. Hence, it can be concluded that the reactive blending and further incorporation of HBN particles (at low concentration i.e. 1 phr) help to

improve the mechanical, thermal properties of PLA and also control its hydrolytic degradation which is useful for the applications that require the good mechanical properties and stability over a long period of time. In contrast to it, the E-beam irradiated blend-composites 5 phr and 10 phr are useful for applications that need good mechanical properties and fast hydrolytic degradation rate.

Chapter 5

In-situ compatibilization of a bio-based poly (lactic acid)/lignin blend for better mechanical, thermal and degradation properties

---

In this chapter, the lignin (LG) is blended with poly (lactic acid) (PLA) to develop green plastic. However, the blending of lignin with PLA leads to incompatible blend with poor mechanical and thermal properties. Hence, in the present work, a green and simple approach is employed to make PLA/LG compatible blend with high lignin percentage (5 and 20%). The E-beam irradiated lignins having different absorbed dosages are blended with two different percentages 5 and 20 with PLA in the presence of 3phr triallyl isocyanurate (TAIC). FTIR and DSC studies have confirmed the formation of PLA-TAIC-Lignin crosslinked structures which act as an interface between the dispersed lignin phase and PLA matrix and hence improved their compatibility in the resulting blend. The compatibility of resulting blends was further validated by the morphology study, Glass transition temperature (T_g) behavior of PLA/LG blends and by observing the significant improvement in the mechanical, thermal and hydrolytic degradation properties.

Publication:

1. Ashish Kumar, T.Venkatappa Rao, S. Ray Chowdhury, S.V.S Ramana Reddy, "A green physical approach to compatibilize a bio-based poly (lactic acid)/lignin blend for better mechanical, thermal and degradation properties", **International Journal of Biological Macromolecules 121, 588-600 (2019) (Impact Factor 3.929).**

5.1 Introduction

Lignin, as it is the second most inexhaustible and low cost biopolymer [19], can be used as an additive to manufacture new kind of plastics [23,157–159]. Also, lignin can be used as a natural antioxidant additive for plastics and helps to prevent the UV light degradation has been reported in the literature [160–162]. Thus several authors have been exploited lignin as an additive for PLA to reduce its price and get a significant economic gain in the plastic industry [23,24,26,84]. However, due to the strong intermolecular interaction of lignin molecules caused by the availability of an ample number of polar functional groups leads to the poor miscibility of lignin into PLA/lignin blend and hence severely decrease the mechanical properties of PLA [19,23,28,160]. Thus, generally, the chemical modification of lignin before incorporation to PLA has been reported in the literature. Jalel Labidi et al. chemically modified the lignin by employing the acetylation process and blended it with PLA [24]. They reported that the acetylation of lignin assists to improve the compatibility of lignin with PLA into PLA/Lignin blend which shows the improvement in thermal degradation temperature, hydrolytic degradation, and contact angle. However, the mechanical properties were decreased at high concentration (from 5% onward) of lignin even with acetylated lignin. Further, E. S. Sattely et al. have synthesized lignin-lactide copolymer and reported that it can be employed as dispersion modifier in PLA/lignin-lactide composite. They observed the improvement in the mechanical properties at low concentration of lignin i.e. 0.9 wt %, however, the decrement in the mechanical properties was noticed as the concentration was changed to 4.4 wt % [26]. Recently, Y. Liu et al. also synthesized and characterized dodecylated lignin-g-PLA graft copolymer and used it for significant toughening of PLA [85]. They incorporate this graft copolymer to PLA and found the significant improvement in elongation at break, tensile strength and Young's modulus at low lignin % (w/w) (i.e. 1.8 %). However, the significant decrement was observed in the elongation at break, as the concentration of lignin-g-PLA graft copolymer was increased, with the increment in lignin % (w/w) (i.e. 4.5 %). R. Liu et al. synthesized lignin-graft-PLA copolymers and further blended these copolymers with PLA upto 10 % (w/w) to improve the miscibility of resulting blend [163,164]. Hence, lignin-g-PLA graft copolymer also limits the toughening of PLA at low concentration of lignin. Thus from the above findings, it can be noticed that the chemical modification of lignin to compatibilize PLA/lignin blend is useful at low concentration of lignin and it also involves the cumbersome steps i.e. acetylation, grafting and then blending with PLA. Hence, the present work deals with the new green and simple approach, which was not reported earlier in the literature, to a significant compatibilization of PLA/LG blend even

with high lignin percentage i.e. 5% and 20% (w/w). In this approach, Kraft lignin was first irradiated to the electron beam with three different doses 30 kGy, 60 kGy and 90 kGy. Then electron beam (E-beam) irradiated lignins were blended with PLA with two different percentages (5% and 20%) along with the triallyl isocyanurate (TAIC) as 3 phr (parts per hundred) to prepare PLA/LG blends. The 3 phr concentration of TAIC is most effective for crosslinking reaction was reported in the literature[55,56]. The E-beam irradiation of lignin generates the peroxy radicals and poly-conjugated radicals which are stable up to high temperature i.e. 403K to 453K was confirmed by ESR, FTIR in previous studies [165]. These free radicals present in the irradiated lignin can initiate the reaction with TAIC and then resulting polymer molecules further react with the PLA chains [55,56,60,155], as per proposed reaction mechanism, which leads to the formation of PLA-TAIC-Lignin crosslinked structures. These crosslinked structures act as an interface between PLA and lignin phases and hence improve their miscibility in the resulting blend. The validity of the proposed possible reaction mechanism and compatibility of PLA/LG blends have been evidenced by FT-IR, DSC and SEM analysis. The significant improvement in the mechanical and thermal properties is noticed in the case of PLA/LG blends having E-beam irradiated lignin as compared to PLA/LG blends having unirradiated lignin. Further, the hydrolytic studies of prepared PLA/LG blends also reveal that the blending of E-beam irradiated lignin with PLA along with TAIC restricts the hydrolytic degradation of PLA as compared to the simple blending of virgin lignin with PLA. The PLA/LG blend having 5% E-beam irradiated lignin with 30 kGy absorbed dose shows slightly more impact strength, elongation at break, HDT and less hydrolytic degradation as compared to pure PLA without scarifying any other mechanical properties significantly.

The details of experimental setup and method used to prepare the PLA/lignin blend are given in the **Chapter 2, Section 2.2.1.2.** All the blends having a different percentage of lignin (unirradiated and E-beam irradiated lignin) are designated and tabulated in Table 5.1.

Table 5.1

Nomenclature and compositions of sample.

Composition name	Percentage of PLA (%)	Percentage of lignin (%)	E-beam dose absorbed by lignin (kGy)	Addition of TAIC as part per hundred (phr)
PLA	100	0	0	0
PLA/LG-5%	95	5	0	0
PLA/LG-20%	80	20	0	0
PLA/LG-5% 30 kGy	95	5	30	3 phr
PLA/LG-20% 30 kGy	80	20	30	3 phr
PLA/LG-5% 60 kGy	95	5	60	3 phr
PLA/LG-20% 60 kGy	80	20	60	3 phr
PLA/LG-5% 90 kGy	95	5	90	3 phr
PLA/LG-20% 90 kGy	80	20	90	3 phr

5.2 Results and Discussion

5.2.1 FT-IR analysis of unirradiated and E-beam irradiated lignin

Lignin is a natural biopolymer which is produced from monolignols viz. guaiacyl alcohol (G), syringyl alcohol (S) and p-coumaryl alcohol (H) by the dehydrogenative polymerization in plants [19]. The several characteristic absorption peaks correspond to lignin structure can be seen in the normalized FTIR spectra (Fig. 5.1). Both unirradiated and E-beam irradiated lignins show a broad intense O-H stretching peak of the hydroxyl group at 3422 cm^{-1} and 3434 cm^{-1} respectively. Further, C-H stretching peaks at 2935 cm^{-1} and 2850 cm^{-1} correspond to methyl and methylene groups respectively. The characteristic absorption peaks at 1597 cm^{-1}, 1509 cm^{-1} belong to C=C of aromatic skeletal vibrations and the absorption peak at 1464 cm^{-1} attributable to C-H deformation of methyl and methylene groups in the lignin molecules. The aromatic ring breathing at 1266 cm^{-1}; aromatic C-H in-plane deformation at 1137 cm^{-1} (S) and 1041 cm^{-1} (G>S) and C-C stretching peak at 1215 cm^{-1} were observed [24,25,166]. In the structure of commercial lignin guaiacyl units (G) are greater than syringyl units (S). The E-beam irradiation of lignin has shifted the absorption peak of hydroxyl group towards the high absorption frequency can be seen from Fig. 5.1a and broadness of hydroxyl peak also decreased in the case of E-beam irradiated lignin (Fig. 5.1b).

It should be attributed to the decrement of hydrogen bonding among lignin molecules with E-beam irradiation because weaker the hydrogen bonding, greater is the absorption peak shift towards high absorption frequency. The relative intensities of absorption peaks correspond to aromatic and aliphatic groups of lignin decrease in the case of E-beam irradiated lignin as compared to unirradiated lignin (Fig. 5.1b). This could be due to the involvement of some of these structural groups of lignin in the formation of free radicals [165,167], as per the proposed reaction mechanism.

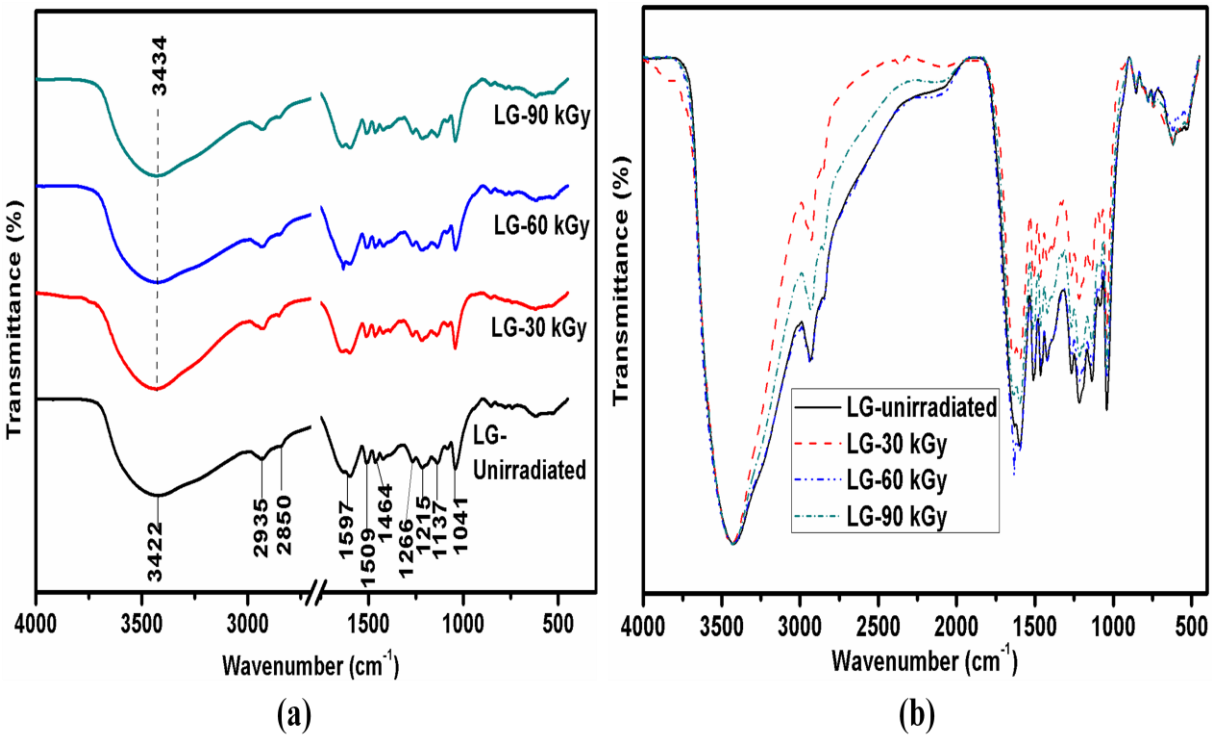

Fig. 5.1 Normalized FTIR spectra of unirradiated and E-beam irradiated lignin (a) representation of characteristic absorption peaks of lignin structure (b) comparison of relative intensities of absorption peaks.

5.2.2 Interfacial compatibilization through in-situ formed PLA-TAIC-Lignin structures

FTIR spectra of neat PLA and all PLA/LG blends are shown in Fig. 5.2 and 5.3. All the important wavenumbers are depicted in the normalized FTIR spectra. For quantitative evaluation, the normalized absorption peak intensities corresponding to some important wavenumbers are also depicted in Fig. 5.2 and Fig. 5.3. The peaks at about 1757 cm^{-1} and 1184 cm^{-1} correspond to C=O stretching and C-O-C asymmetric stretching of PLA respectively [55,98,168]. Further, the peaks at 3656 cm^{-1} and 3501 cm^{-1} belong to O-H

stretching of hydroxyl and carboxylic acid terminal groups of PLA, respectively. The other characteristic peaks of PLA are reported in our previous studies [168].

The direct blending of lignin with PLA leads to polymer chain scission at the C-O linkage can be asserted by observing decrement in the C-O-C peak intensity of PLA/LG-5% blend as compared to neat PLA (Fig. 5.2b). It occurs because C-O-C linking units are reduced due to polymer chain scission. The C=O stretching peak shift to lower absorption frequency i.e. 1752 cm^{-1} and new peak corresponds to C=C at 1631cm^{-1} was also noticed in case PLA/LG-5% blend. This is due to the PLA chain scission at C-O linkage disproportionate and two small polymer chains having carboxylic acid (-C (O)-OH) and alkenes (CH_2=C (O)-) terminal groups are formed [58]. These alkenes (CH_2=C (O)-) terminal groups form conjugation with C=O (carbonyl) groups of PLA backbone and hence lower its absorption frequency due to inductive effect [96]. The small increment in the O-H peak intensity of carboxylic acid terminal group was also found in the case of PLA/LG-5% blend. This is because the PLA polymer chain scission at C-O linkage leads to decrement in the polymer chain length and hence increases the carboxylic acid terminal groups [58]. FTIR spectra of PLA/LG-5% 30 kGy (Fig. 5.2c) blend exhibit new absorption peaks at 1698 cm^{-1} and 1631 cm^{-1} correspond to C=O stretching and C=C stretching respectively of TAIC molecule [169]. The blending of PLA and 5% E-beam irradiated lignin having 30 kGy absorbed dose along with TAIC resulted in the suppression of carbonyl C=O peak, C-O-C peak as well as a small decrement in the O-H peak intensity (shown in Fig. 5.2c). The PLA/LG-5% 30 kGy blend also does not show any shift of C=O absorption peak of PLA from its original value i.e. at 1757 cm^{-1}. This can be attributed to the evolution of the covalent bond between PLA, TAIC, and E-beam irradiated lignin [170]. The cause of formation of covalent bonds is further elucidated, as the E-beam irradiated lignin owns peroxy and poly-conjugated radicals were confirmed by the EPR (electron paramagnet resonance spectroscopy) and FTIR analysis in previous studies [165,167,171]. These lignin radicals above glass transition temperature gain the thermal energy and react with TAIC molecules and breaks the double bond of allyl groups of TAIC and from two kinds of radical sites [55,57]. The addition of E-beam irradiated lignin to PLA leads to polymer chain scission at the C-O linkage of PLA and produce radical sites at PLA polymer chains viz., (R-C (O)-$O^{\bullet}$) and (-$^{\bullet}$CH (CH_3)-C (O)-R), R represents the remaining polymer chain [58,172,173]. At the same time, R-C (O)-$O^{\bullet}$ and (-$^{\bullet}$CH (CH_3)-C (O)-R) units of PLA after chain scission combine with the radical site of TAIC generated after reaction with lignin radicals and form a PLA-TAIC-Lignin crosslinking structure. The possible reaction mechanism of in-situ formation of PLA-TAIC-Lignin crosslinking structure

is depicted in Fig. 5.4. Hence, it is clear that the radical sites at PLA polymer chains formed due to the addition of E-beam irradiated lignin did not undergo disproportionation as in the case of PLA/LG-5% blend. This could be, further, asserted by observing no peak shift of C=O stretching in the case of PLA/LG-5% 30 kGy blend. These crosslinking structures act as an interface between PLA and Lignin phases in PLA/LG-5% 30 kGy blend and hence improve the compatibility between two phases.

Moreover, the PLA/LG-5% 60 kGy and PLA/LG-5% 90 kGy blends show the increment in the absorption peak intensities of C=O stretching (of PLA) and hydroxyl group (O-H) stretching which is increasing with the addition of high dose E-beam irradiated lignin (Fig. 5.2d and e). The decrement in the (C=C) stretching of TAIC was also observed with the addition of high dose E-beam irradiated lignin. The FTIR spectra of PLA/LG-5% 90 kGy (Fig. 5.2e) blend shows the extinction of (C=C) stretching peak belongs to TAIC. The poly-conjugated and peroxy radicals of E-beam irradiated lignin increases with increasing absorbed dose were asserted by EPR analysis in the previously reported studies [165,167]. The presence of excess lignin radicals in the case of PLA/LG-5% 90 kGy blend leads to cleavage of all allyl (C=C) bonds of TAIC molecules followed by lignin self-crosslinking and hence reduce the formation of PLA-TAIC-lignin crosslinking structure. This results in a decrement in the compatibility between PLA and lignin in case of high dose absorbed E-beam irradiated PLA/LG blend as compared to low dose absorbed E-beam irradiated PLA/LG blend.

The effect of increasing concentration of E-beam irradiated lignin on the compatibility of PLA/LG blend is also studied. The FTIR spectrum of PLA/LG-20% 30 kGy blend was depicted in Fig. 5.3. The addition of E-beam irradiated lignin in high percentage (i.e. 20%), to prepare PLA/LG-20% 30 kGy, leads to the increment in peak intensity of C=O group (carbonyl group of PLA) as compared to PLA/LG-5% 30 kGy and disappearance of C=C group of TAIC can be evidently seen from the inset of Fig. 5.3. This could be due to increasing concentration of E-beam irradiated lignin in the resulting blend increase the number of lignin free radicals. The presence of excess lignin radicals induce lignin self-crosslinking and hence reduce the formation of PLA-TAIC-lignin crosslinking structure as observed in the case of PLA/LG-5% 90 kGy blend. Hence, the compatibility between PLA and lignin in PLA/LG blend is also decreased with increasing concentration of E-beam irradiated lignin.

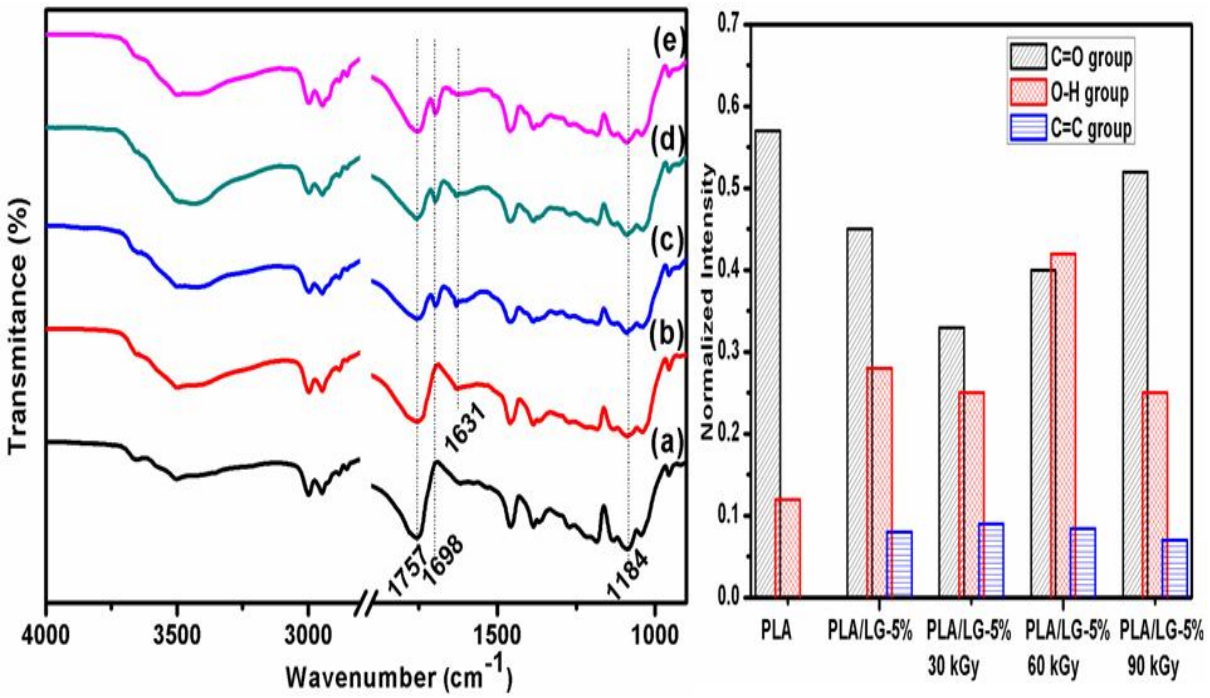

Fig. 5.2 Normalized FTIR spectra of pure PLA and PLA/LG blends: (a) Virgin PLA, (b) PLA/LG-5%, (c) PLA/LG-5% 30 kGy, (d) PLA/LG-5% 60 kGy and (e) PLA/LG-5% 90 kGy.

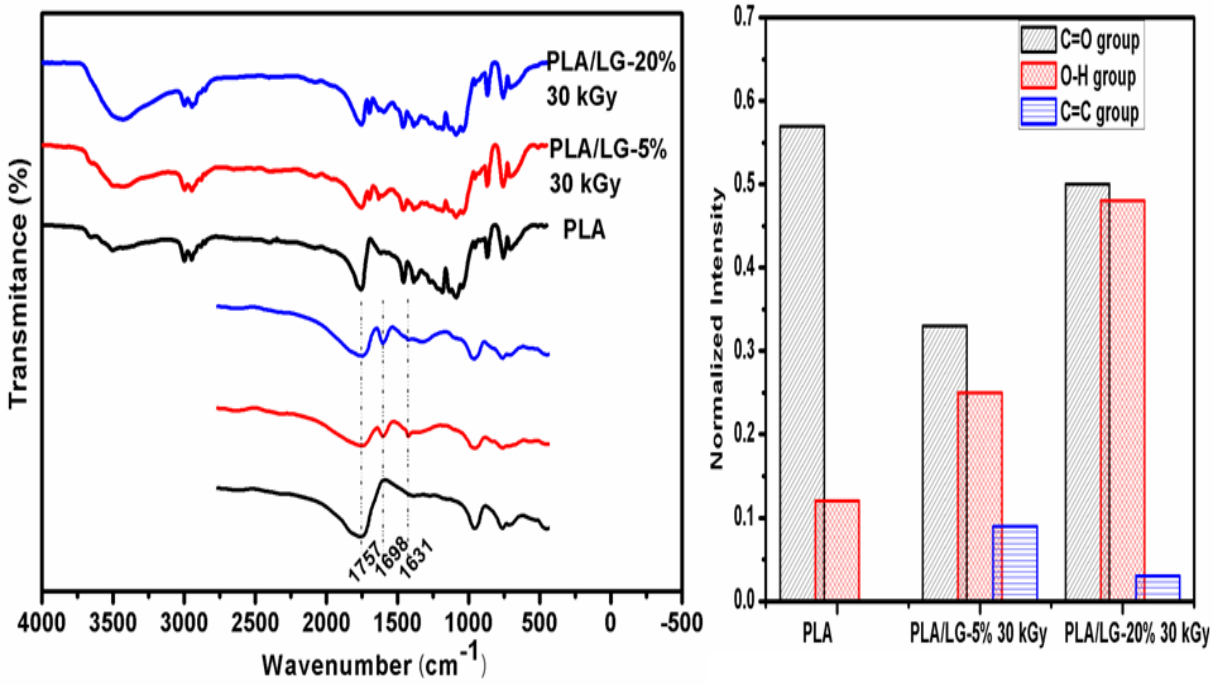

Fig. 5.3 Normalized FTIR spectra of neat PLA, PLA/LG-5% 30 kGy and PLA/LG-20% 30 kGy blends.

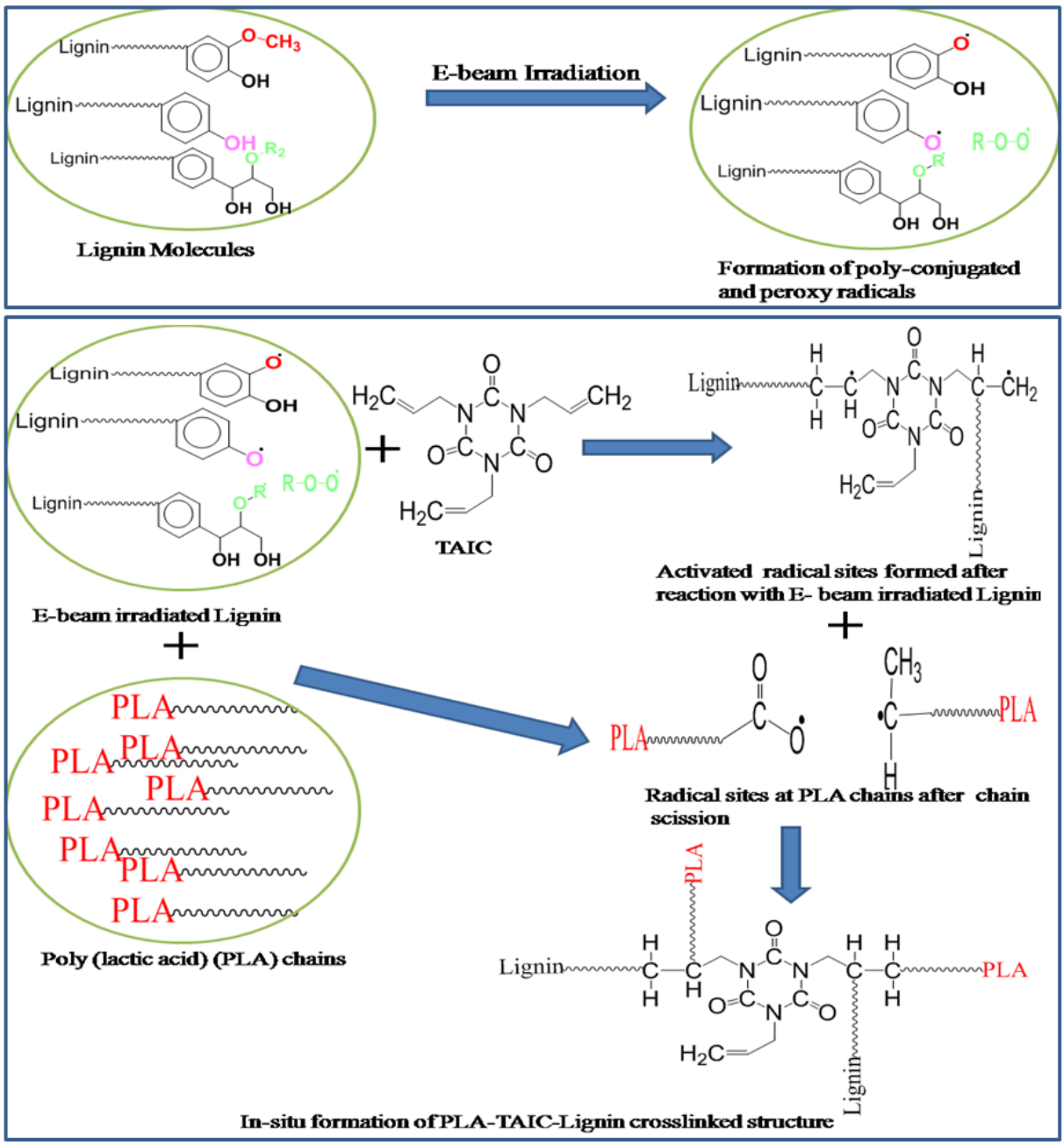

Fig. 5.4 A possible reaction mechanism for the in-situ formation of PLA-TAIC-Lignin crosslinked structure**.**

5.2.3 Thermal properties

The non-isothermal DSC experiment is conducted to observe the effect of the addition of unirradiated and E-beam irradiated lignin on thermal transition properties of blends. Fig. 5.5 shows the non-isothermal transition curves of PLA/LG blends having unirradiated and E-beam irradiated lignin with two different concentrations. Thermal transition data i.e. glass transition temperature (T_g), cold crystallization temperature (T_{cc}), cold crystallization enthalpy (ΔH_{cc}), melting temperature (T_m), melting enthalpy (ΔH_m) and percentage of crystallinity (X_c)

(Eq. 2.5) corresponding to each curve is tabulated in Table 5.2. The non-isothermal DSC scan of neat PLA with similar scanning method was studied and reported in our previous report [168]. The midpoint (midpoint type: half height) of glass transition event was considered as the T_g. Further, the onset temperature of crystalline and melting peaks was defined as the T_{cc} and T_m respectively. The complex structure of lignin consists of rigid phenol moieties involves the hydrogen bonding leads to the self-interactions of lignin molecules. The self-interaction among the lignin molecules and presence of condensed rigid phenolic moieties restrict the local segmental motion of the lignin molecules which results in high T_g of lignin i.e.~ 150-165 °C [23,26] as compared to the PLA. Two melting peaks were observed in the case of neat PLA and PLA/LG blends can be attributed to the two different crystalline phases formed during crystallization and re-crystallization stages [24,98,168].

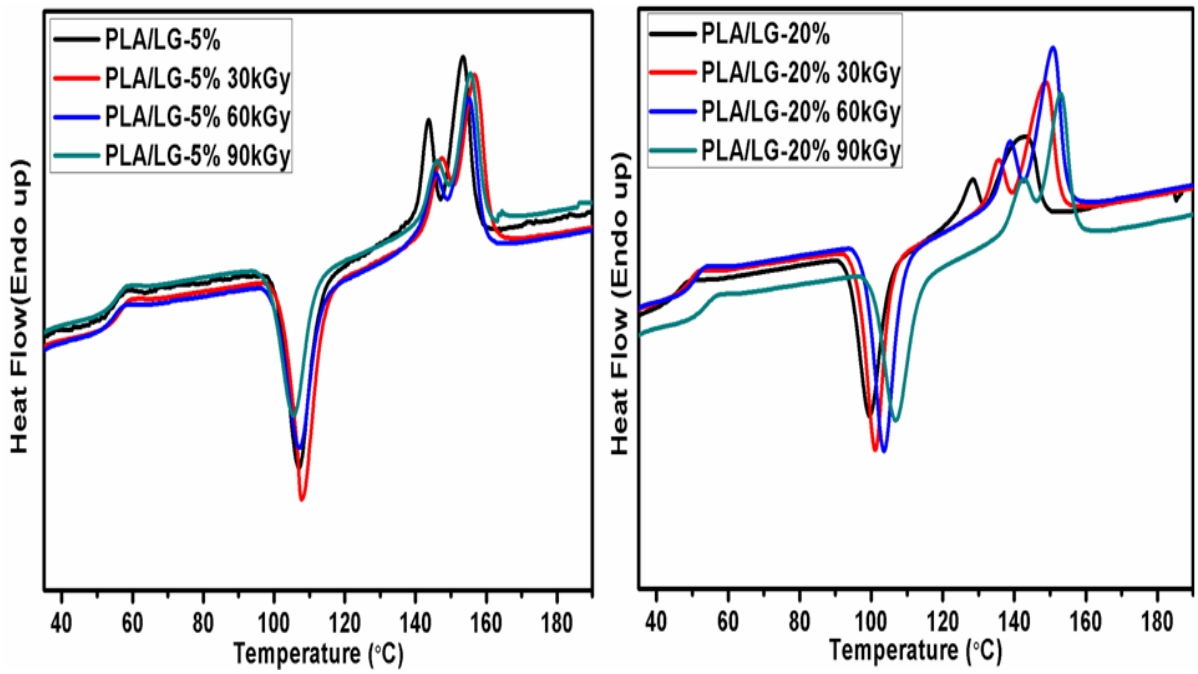

Fig. 5.5 DSC thermograms of injection molded PLA/LG blends with two different concentration of unirradiated and various E-beam dose absorbed lignin.

The blending of unirradiated lignin with PLA results decrement in the T_g and T_m of resulting blends (i.e. PLA/LG-5% and PLA/LG-20%) as compared to neat PLA can be seen in Table 5.2. The diminution of T_g is token of week favorable interaction between the blend components [174]. The decrement in the T_g and T_m was observed with increasing the unirradiated lignin percentage in the blend. This is due to the addition of lignin leads to the PLA chains scission followed by a shortening of PLA chains length, asserted by FTIR study. As a consequence, it facilitates the local segmental chain motions and also polymer chains mobility upon melting. Further, the T_g of PLA/LG-5% 30 kGy blend is shifted to a higher

temperature as compared to neat PLA, it can be attributed to the in-situ formation of PLA-TAIC-Lignin crosslinked structure [132,175]. The presence of the crosslinked structure also impeded the mobility of PLA chains and interfered with the crystallization process [55]. Hence, the T_{cc} of PLA/LG-5% 30 kGy blend shifted to a higher temperature and also showed the low percentage of crystallinity (X_c) as compared to neat PLA. The formation of PLA-TAIC-Lignin crosslinked structures, during melt blending in the case of PLA/LG-5% 30 kGy blend was also asserted by FTIR study, acts as an interface between PLA and lignin phases and hence improved their compatibility. The PLA/LG-5% 60 kGy and PLA/LG-5% 90 kGy blends were shown nearly the same T_g as neat PLA. This was due to the blending of PLA with E-beam irradiated lignin with higher absorbed radiation doses slow down the formation of PLA-TAIC-Lignin crosslinked structure and hence decreased the compatibility, confirmed by FTIR study. The PLA/LG-20% 30 kGy blend also showed the higher T_g, $T_{cc,}$ and T_m as compared to PLA/LG-20% blend indicating the better compatibility of PLA and Lignin phases in PLA/LG-20% 30 kGy blend as compared to PLA/LG-20% blend.

The further information about the miscibility and quality of interaction between the PLA and lignin phases of PLA/LG blends is obtained by exploiting the Gordon-Taylor equation[174,176] given below

$$T_g = \frac{\emptyset_1 T_{g^1} + K\emptyset_2 T_{g^2}}{\emptyset_1 + K\emptyset_2} \qquad 5.1$$

Here T_g^1, T_g^2 ~150 °C [26] and T_g are the glass transition temperature of PLA, lignin and PLA/LG blend respectively. $Ø_1$ and $Ø_2$ are weight fraction of PLA and lignin respectively. K indicates the quality of interaction and miscibility of blend components.

The value of K for PLA/LG-5%, PLA/LG-20% and PLA/LG-5% 30 kGy, PLA/LG-20% 30 kGy blends was calculated from the experimental data. The values of K for PLA/LG-5%, PLA/LG-20% and PLA/LG-5% 30 kGy, PLA/LG-20% 30 kGy blends are -0.17, -0.03 and 0.16 and 0.11 respectively. The PLA/LG blends have E-beam irradiated lignin with 30 kGy absorbed dose posses' better miscibility and strong intermolecular interaction between PLA and lignin phases as compared to PLA/LG blend having unirradiated lignin. This is because the more the value of K the stronger the interactions among the blend components and hence better their miscibility [174,176,177].

Table 5.2

Thermal transition data of neat PLA, PLA/LG blends having unirradiated and E-beam irradiated lignin**.**

Sample name	T_g (°C)	(T_{cc}) (°C)	(ΔH_{cc}) (J/g)	(T_m) (°C)	(ΔH_m) (J/g)	(X_c) (%)
PLA	55.4	96.0	48.05	145.8,154.0	52.75	5.05
PLA/LG-5%	54.5	100.7	28.88	140.5,148.1	36.28	8.62
PLA/LG-20%	46.0	93.9	18.92	123.3,132.7	22.37	4.77
PLA/LG-5% 30 kGy	56.2	103.7	32.18	143.3,152.0	35.82	4.24
PLA/LG-20% 30 kGy	49.0	95.9	21.55	131.5,140.7	28.97	10.26
PLA/LG-5% 60 kGy	54.6	100.2	26.77	141.8,150.2	32.18	6.31
PLA/LG-20% 60 kGy	50.7	97.9	25.17	134.6,144.0	31.55	8.83
PLA/LG-5% 90 kGy	55.3	98.9	23.25	142.3,151.0	28.15	5.71
PLA/LG-20% 90 kGy	53.7	100.4	21.05	138.0,147.7	27.17	8.47

5.2.4 X-ray diffraction

Fig. 5.6 illustrates the WAXD measurements of all PLA/LG blends. The diffraction pattern of neat PLA with similar scanning method is studied and reported in our previous report [168]. The PLA/LG blends with 5% unirradiated and E-beam irradiated lignin have shown the same large broad halo amorphous peak at 2θ = 16.5° and around 10.0° to 25.0° (Fig. 5.6a) as the neat PLA [168]. It can be attributed to the poor crystallinity of PLA in the PLA/LG blends with 5% unirradiated and E-beam irradiated lignin. However, PLA/LG-20% 30 kGy blend which was shown high crystallinity, exhibits the typical crystalline peak of PLA at 2θ = 16.5° (Fig. 5.6b), corresponds to (110) planes [12,132,163]. The results are in agreement with the DSC results. Hence, blending of unirradiated and E-beam irradiated lignins with PLA have not improved the crystallinity of PLA in the resulting blends, significantly.

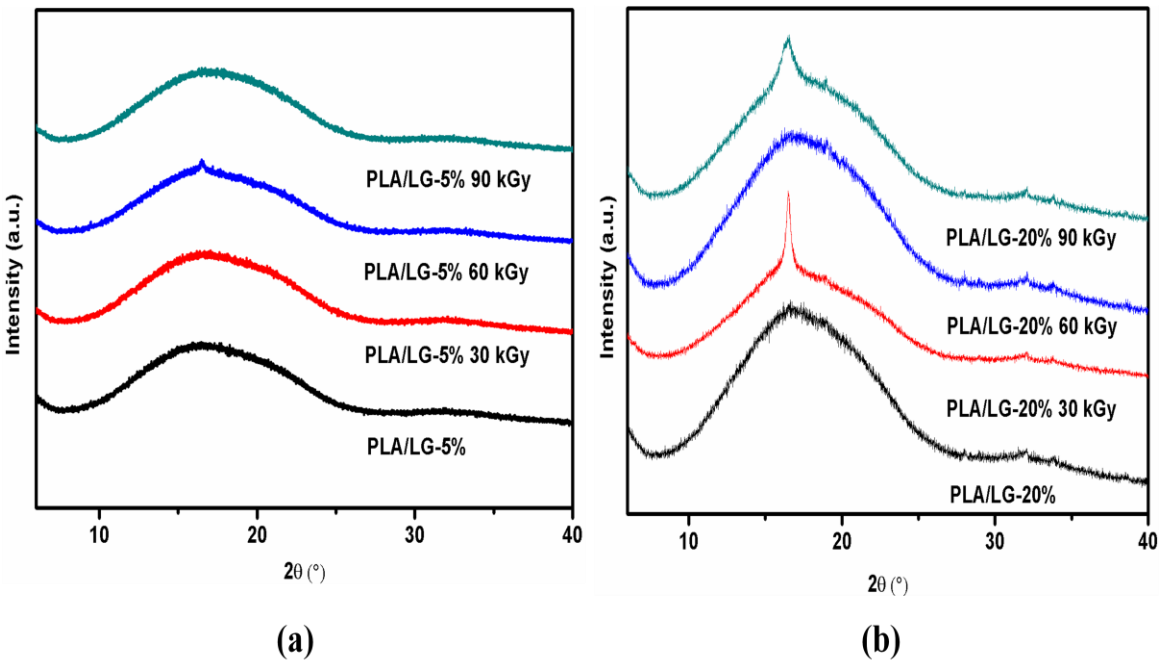

Fig. 5.6 XRD patterns of PLA/LG blends with two different concentration of unirradiated and various E-beam dose absorbed lignin.

5.2.5 Morphology

The morphology of PLA/LG blends containing unirradiated and E-beam irradiated (30 kGy dose) lignin was studied by cryogenically fractured surfaces of PLA/LG blend specimens. The blending of lignin with the PLA, i.e. PLA/LG-5%, leads to the heterogeneous and ruptured structure because of the immiscibility of lignin into PLA matrix [178] can be observed in Fig. 5.7a. This cause the large weaken space within the resulting blend and hence severely affect its mechanical properties. However, the blending of E-beam irradiated lignin (5%) along with TAIC (3phr) improves the miscibility of lignin into the PLA matrix. This can be asserted by observing the continuous phase, less distinct phase separation and diminishes of rifts [170] in the case of PLA/LG-5% 30 kGy blend (Fig. 5.7b). The addition of E-beam irradiated lignin to high percentage i.e. 20% also shows the crack formation as observed in case of PLA/LG-20% 30 kGy blends (Fig. 5.7c). Hence, it can be asserted that the incorporation of E-beam irradiated lignin to high percentage also reduces the compatibility between PLA and lignin in the resulting blend. Further, the high magnified cryo-fractured surfaces of PLA/LG-5% 30 kGy and PLA/LG-20% 30 kGy blends (Fig. 5.8) show that the addition of E-beam irradiated lignin at high percentage (i.e. 20%) leads to poor miscibility which can be asserted by observing particle appearance and agglomeration of particles (Fig. 5.8b). However, the addition of E-beam irradiated lignin with a low percentage (i.e. 5%)

shows good miscibility (Fig. 5.8a). The results are consistent with the earlier discussed FTIR and DSC results.

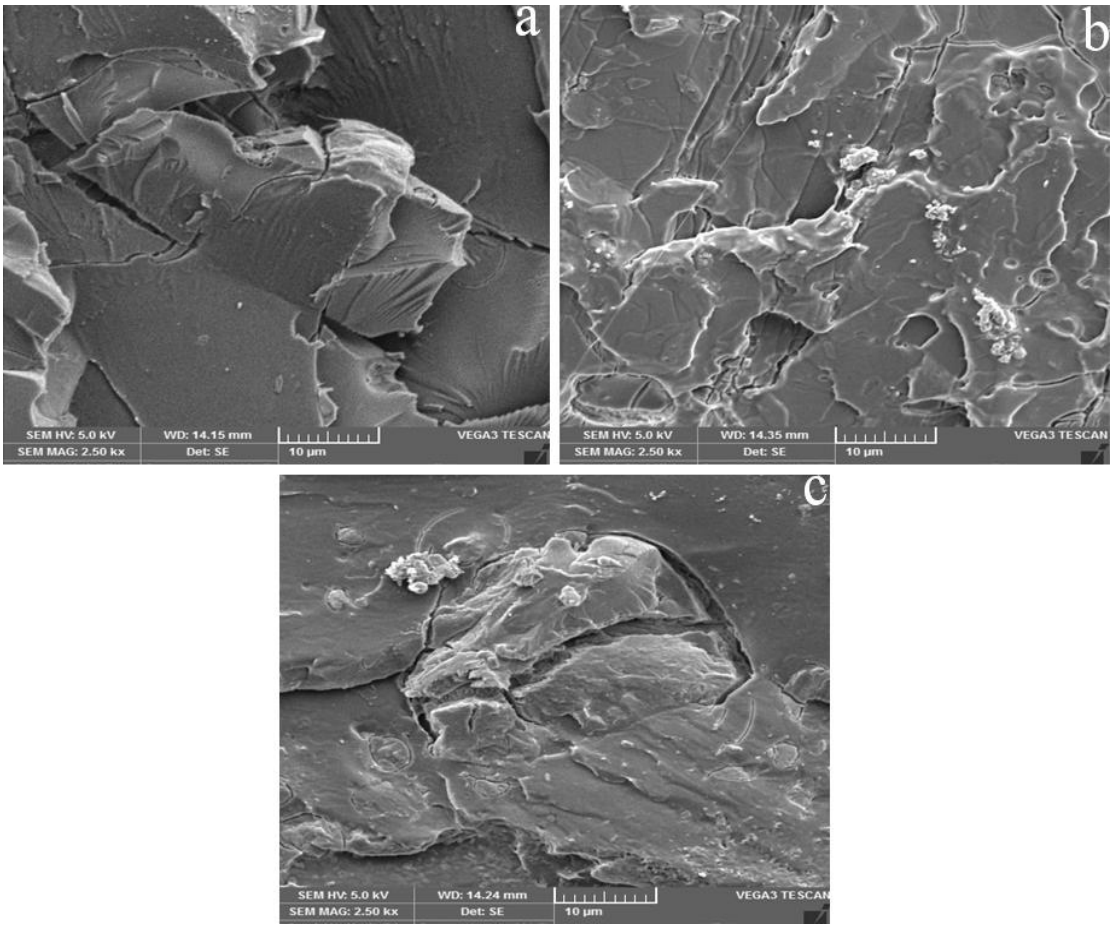

Fig. 5.7 SEM images of cryofractured PLA/LG blends: (a) PLA/LG-5%, (b) PLA/LG-5% 30 kGy and (c) PLA/LG-20% 30 kGy. The scale bar is 10 µm.

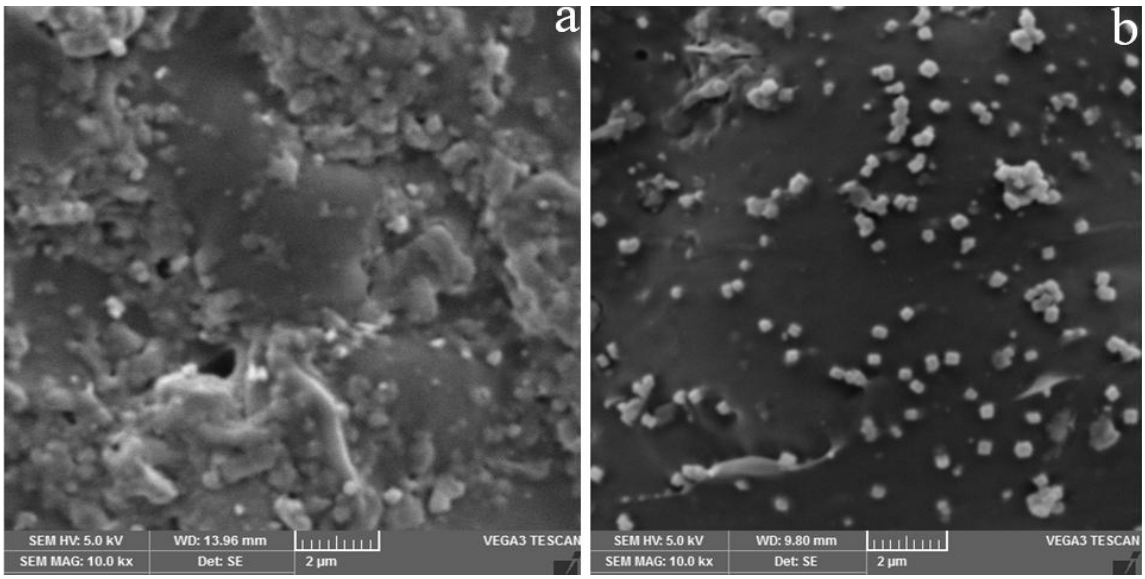

Fig. 5.8 High magnified SEM images of cryo-fractured PLA/LG blends: (a) PLA/LG-5% 30 kGy and (b) PLA/LG-20% 30 kGy. The scale bar is 2 µm.

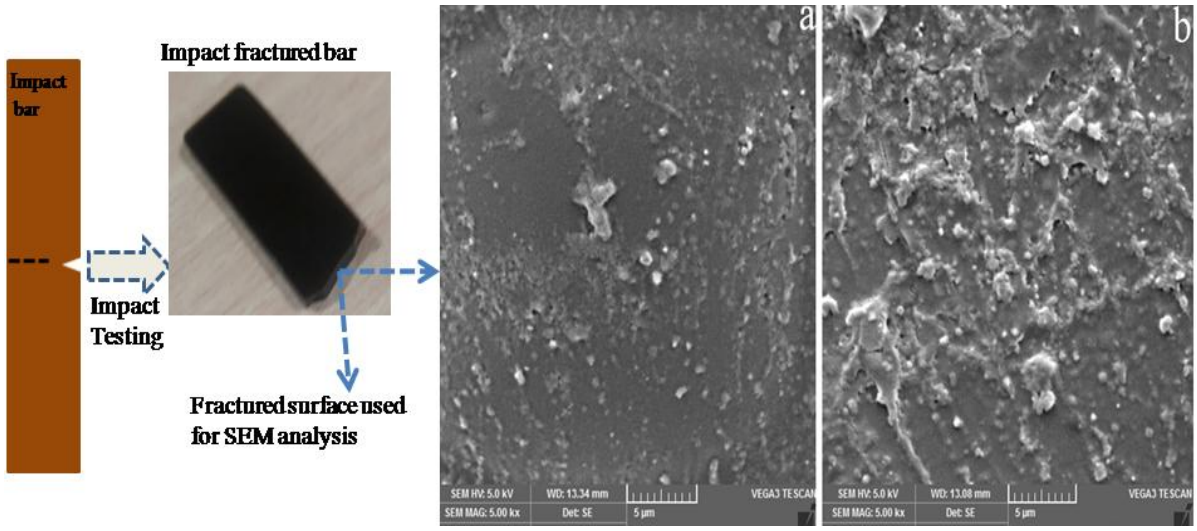

Fig. 5.9 SEM images of notched impact fracture surfaces of PLA/LG blends: (a) PLA/LG-5% and (b) PLA/LG-5% 30 kGy. The scale bar is 5 µm.

5.2.6 Mechanical properties

The blending of lignin with PLA increases the bio-content and assists to reduce the cost of the final product. In general, the blending of lignin with PLA significantly decreases the yield strength, elongation at break, impact strength and tensile modulus of the blend. The mechanical properties of PLA/LG blend become worsen with the insertion of a high percentage of lignin (i.e. 20 %) has been observed by many authors [24,84,85,179]. These authors claimed that the incorporation of lignin with high percentage impedes the formation of long rage continuous phase of PLA which results in a drastic decrement in the mechanical properties of resulting blend. In the present work, the mechanical properties of neat PLA and PLA/LG blend having unirradiated and E-beam irradiated lignin were tested and shown in Fig. 5.10. The corresponding data is given in Table 5.3. It can be noticed from the Fig. 5.10, the addition of unirradiated lignin significantly reduce the yield strength, elongation at break, notched impact strength and tensile modulus. The decrement in these properties is more prominent with increasing the percentage of lignin content in the resulting blend. This is due to the immiscibility and poor interfacial interaction between the dispersed lignin phase and PLA matrix as observed in SEM, DSC and FTIR studies. The flexural modulus is slightly increased with the addition of lignin. These results are consistent with the previous findings [24,84]. The addition of E-beam irradiated lignin along with TAIC (3phr) significantly improved the mechanical properties of PLA/LG blends as compared to blends having unirradiated lignin. This is because of good miscibility and improved interfacial interaction of dispersed lignin phase and PLA matrix determined by FTIR and SEM studies in the case of

PLA/LG blends consisting of PLA, E-beam irradiated lignin and TAIC. Fig. 5.10a shows the significant improvement in the yield strength of PLA/LG-5% 30 kGy, 60 kGy, 90 kGy blends as compared to the PLA/LG-5% blend; and also PLA/LG-20 % 30 kGy, 60 kGy, 90 kGy blends as compared to PLA/LG-20% blend. Among all the blends, the PLA/LG-5% 30 kGy blend shows significant enhancement in the elongation at break and notched impact strength and these values are still slightly more as compared to pure PLA (Fig. 5.10c and d). This can be attributed to the formation of PLA-TAIC-Lignin crosslinking structures which act as an interface between the dispersed lignin and PLA matrix lead to better compatibility between them. The neat PLA exhibits brittle fracture (smooth fracture surface) morphology with scanty distortions [132]. Fig. 5.9a reveals that the PLA/LG-5% blend also shows the brittle fracture morphology and hence absorbed low impact energy. However, the PLA/LG-5% 30 kGy blend exhibits the rougher morphology (Fig. 5.9b) and sufficient distortions as compared to PLA/LG-5% blend and neat PLA, indicating the enhanced impact strength through soaking up more impact energy [132,143].

The blending of PLA with E-beam irradiated lignin having high absorbed dose (containing more free radicals) decreases the compatibility between dispersed lignin phase and PLA matrix as discussed earlier in the FTIR studies. Hence, the decrement in yield strength, elongation at break and notched impact strength have been noticed in the case of PLA/LG-5% 60 kGy and PLA/LG-5% 90 kGy blends as compared to PLA/LG-5% 30 kGy (Fig. 5.10). The PLA/LG-20% 60 kGy and PLA/LG-20% 90 kGy blends have also shown the decrement in the mechanical properties as compared to PLA/LG-20% 30 kGy blend. Fig. 5.10 also shows that for a particular radiation dose, the increasing concentration of E-beam irradiated lignin (from 5% to 20%) into the blend decrease the value of these properties. Because FTIR and SEM analysis of prepared blends have shown that increasing concentration of E-beam irradiated lignin into the resulting blend decrease the compatibility between lignin and PLA matrix.

Fig. 5.10b shows that blending of unirradiated lignin at low percentage i.e. 5% with PLA slightly increases the tensile modulus of resulting blend as compared to neat PLA. Further, the blending of unirradiated lignin at high percentage i.e. 20% with PLA severely decreased the tensile modulus of resulting blend. Similar results were reported by other authors [24,170]. However, the blending of E-beam irradiated lignin at high percentage i.e. 20% with PLA (along with TAIC) (i.e. PLA/LG-20% 30 kGy, PLA/LG-20% 60 kGy and PLA/LG-20% 90 kGy) significantly improved the tensile modulus of resulting blend (Fig. 5.10b) as compared to PLA/LG blends having unirradiated lignin. Further, it can also be seen

from Fig. 5.10e, PLA/LG blends with E-beam lignin irradiated lignin show an insignificant decrement in the flexural modulus as compared to PLA/LG blends with unirradiated lignin.

Heat deflection temperature (HDT) is defined as the temperature at which the plastic sample deforms or loses its load bearing capacity under a specific load [95]. It is useful to know the heat resistance of the prepared polymer product, which can be defined as the ability of the material to maintain the desired properties at maximum service temperature. It is also known as temperature dependent flexural modulus. HDT of PLA depends on the degree crystallinity and crystallization behavior [72]. The HDT of neat PLA and PLA/LG blend having unirradiated and E-beam irradiated lignin was measured and tabulated in Table 5.3. It can be seen from Table 5.3 that the neat PLA exhibit HDT (52.60 ± 0.45) °C. The blending of lignin with PLA increased the HDT of resulting blend as compared to virgin PLA. This can be attributed to the intermolecular hydrogen bonding between phenolic hydroxyl groups of lignin molecules with the carbonyl groups of PLA [23,180]. The PLA/LG blends having E-beam irradiated lignin have shown the less HDT as compared to the PLA/LG blends having unirradiated lignin. This is because the blending of E-beam irradiated lignin along with TAIC results in a decrement of the carbonyl groups and hydroxyl groups of resulting blend which is observed in the FTIR study. Hence, the intermolecular hydrogen bonding was reduced in the resulting blend which leads to the decrement in the HDT.

Table 5.3

Mechanical properties and heat deflection temperature (HDT) of neat PLA, PLA/LG blends having unirradiated and E-beam irradiated lignin.

Sample name	Yield Strength (MPa)	Tensile Modulus (MPa)	Elongation at break (%)	Notched Impact Strength (kJ/m^2)	Flexural Modulus (MPa)	HDT (°C)
PLA	65.00±0.25	2300±25	5.76±0.44	2.65±0.32	3767±21	52.60±0.45
PLA/LG-5%	28.00±1.22	2933±32	1.00±0.04	1.28±0.02	4052±37	56.55±0.35
PLA/LG-20%	6.00±0.34	1422±272	0.58±0.19	0.97±0.04	4305±83	53.50±0.35
PLA/LG-5% 30 kGy	50.00±0.25	2001±68	7.32±0.34	2.89±0.03	3516±67	54.40±0.30
PLA/LG-20% 30 kGy	37.00±4.86	2826±70	1.49±0.35	2.31±0.33	3802±59	54.85±0.15
PLA/LG-5% 60 kGy	48.00±0.38	2021±96	4.79±0.77	2.41±0.14	3414±57	54.56±0.55
PLA/LG-20% 60 kGy	22.81±1.06	2767±9	0.73±0.20	2.15±0.36	3807±67	53.50±0.60
PLA/LG-5% 90 kGy	43.81±1.07	2292±69	3.36±0.37	2.06 ±0.51	3714±55	55.55±0.55
PLA/LG-20% 90 kGy	25.75±3.05	2366±61	1.21±0.17	2.29±0.57	3681±40	54.40±0.20

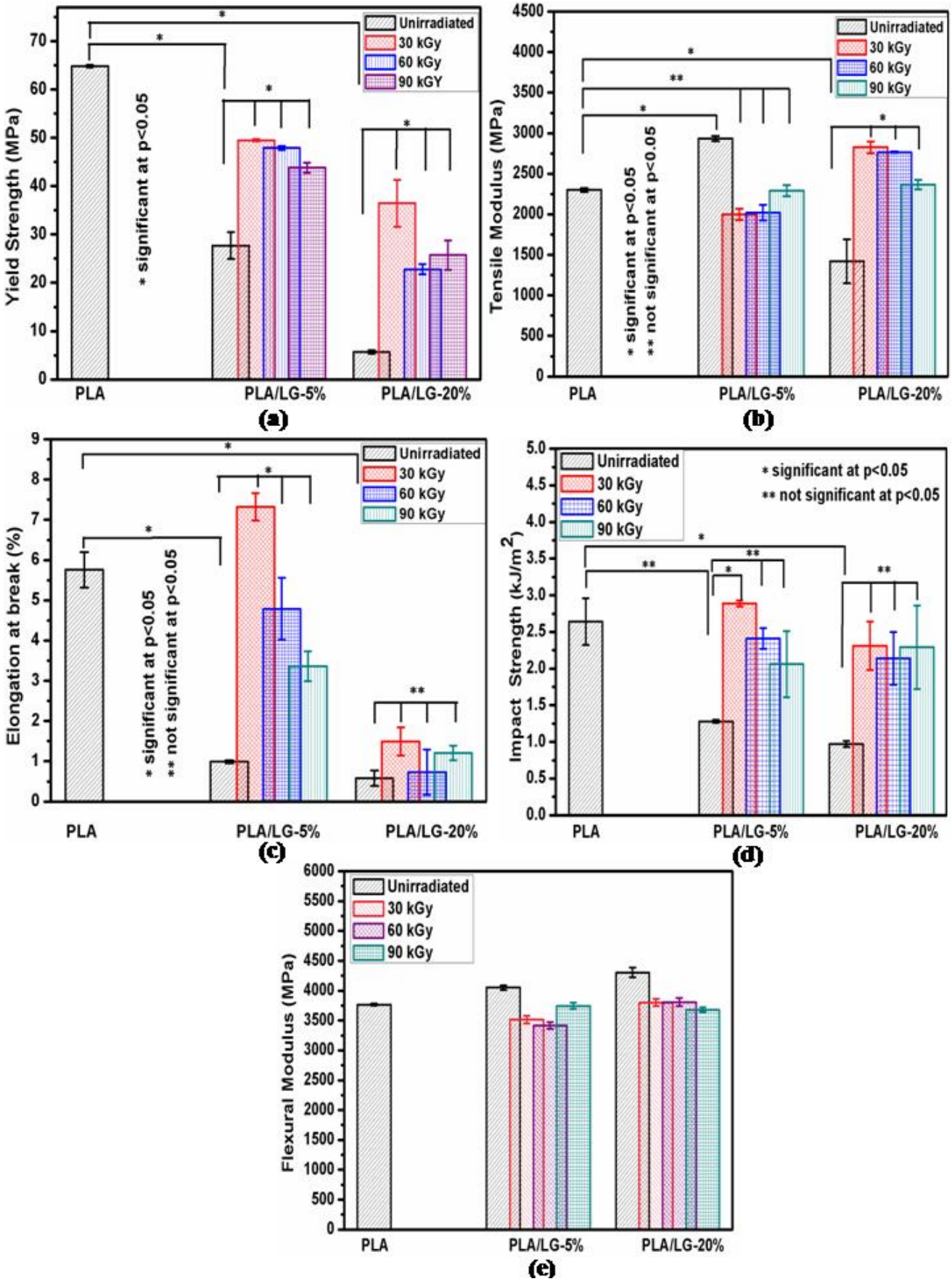

Fig. 5.10 Mechanical properties of PLA/LG blends: (a) Yield strength (b) Tensile modulus (c) Elongation at break (d) Notched Izod impact strength (e) Flexural Modulus.

5.2.7 Hydrolytic degradation

Fig. 5.11 shows that hydrolytic degradation of neat PLA and PLA/LG blends (having 5 wt% unirradiated and E-beam irradiated lignin) samples as a function of degradation time. Fig. 5.12 depicts the hydrolytic degradation of PLA/LG blends (having 20% unirradiated and E-beam irradiated lignin) samples as a function of degradation time. The weight loss (%) was estimated by exploiting the Eq. 2.11 (chapter 2). The weight loss by each sample with degradation time is tabulated in Table 5.4. After the first week of immersion in the phosphate buffer solution (PBS), the PLA samples showed small weight gain may be due to soaked moisture because diffusion of water molecules during initial days of the test is high. This can also be asserted by observing the loss of transparency by PLA samples after one week of immersion in PBS; similar hydrolytic degradation behavior of neat PLA during initial days of the test was observed and reported by Jalel labidi et.al. [24]. After the second and consecutive weeks of immersion time, the neat PLA shows the noticeable weight loss percentage which increased with increasing the degradation time. Whereas all the PLA/LG blends show the small weight loss after the first week of immersion. The PLA/LG-5% blend (having unirradiated lignin) shows the more weight loss (6.71 ± 0.07 %) as compared PLA/LG-5% 30 kGy blend (5.74 ± 0.24) after one week of the assay. It can also be noticed from Table 5.4 that the percentage weight loss by neat PLA, PLA/LG-5%, and PLA/LG-5% 30 kGy blends increasing with the increasing degradation time. The difference in the weight loss (%) between neat PLA and PLA/LG blends increase with increasing degradation time. After four weeks of the assay, the neat PLA has shown maximum weight loss (%) as compared to other prepared PLA/LG blends. It can be attributed to chemical hydrolysis of hydrolyzable ester linkage present in the backbone of PLA chains lead to the random chain scission of ester groups resulting in the decrement of the molecular weight [115,181]. The hydrolysis of PLA is self-catalyzed process due to the presence of carboxylic acid terminal groups of PLA and its oligomers. It leads to faster degradation of neat PLA [118]. The blending of lignin with PLA leads to decrement in the ester functional groups (ester linkage of PLA chains) in the resulting blend, determined by the FTIR analysis. Further, the hydroxyl groups present in the lignin could involve in the hydrogen bonding with water molecules of immersion media restrict the diffusion of water molecules and minimize their interaction with the ester linkage of PLA. Hence, PLA/LG blend samples show less weight loss as compared to neat PLA after four weeks of immersion in PBS. The incorporation of lignin retards the hydrolytic degradation of PLA was also proven by other authors [24]. The decrement in the hydrolyzable ester functional groups in the case of PLA/LG-5% 30 kGy was more, which can be asserted by

observing the more suppression of carbonyl and ester peak in FTIR study, as compared to other PLA/LG blends. Hence, the PLA/LG-5% 30 kGy blend exhibits the least weight loss (%) as compared to other blends and neat PLA. It showed 30 % less weight loss as compared to neat PLA after four weeks of test can be clearly seen from Table 5.4. Thus, the blending of PLA with 5% E-beam irradiated lignin having low absorbed dose (30 kGy) along with TAIC improved the compatibility between dispersed lignin phase and PLA matrix which leads to significant reduction of hydrolytic degradation of PLA.

Fig. 5.12 shows the effect of blending of PLA with 20 wt% (unirradiated and E-beam irradiated) lignin on the hydrolytic degradation of PLA. It can be noticed from Fig. 5.12 that the incorporation of unirradiated lignin to 20 wt% leads to significant weight loss i.e. (31.26 ± 0.29) % after the first week of the assay (Table 5.4). This is due to the incorporation of lignin with high percentage leads to incompatibility between PLA and lignin as seen by the drastic diminution in the mechanical properties. Further, the compatibility between PLA and lignin phases is more in the case of PLA/LG blends with E-beam irradiated lignin (along with TAIC), even up to 20 wt%, as compared to PLA/LG with unirradiated lignin has been confirmed by FTIR, SEM studies and also by seeing the improvement in the mechanical properties. Hence, PLA/LG blends with 20 wt% E-beam irradiated lignin show less weight loss (%) as compared to PLA/LG blend having 20 wt% unirradiated lignin. The PLA/LG-20% 30 kGy blend shows less weight loss, i.e. (23.89 ± 0.80) % after the first week of the test (Table 5.4), as compared to other blends (i.e. PLA/LG-20%, PLA/LG-20% 60 kGy and PLA/LG-20% 90 kGy) because of the better interfacial interaction of dispersed lignin phase and PLA matrix through the PLA-TAIC-Lignin crosslinking structures. After four weeks of the assay, the PLA/LG-20% blend exhibits weight loss (%) nearly equal to neat PLA. However, the PLA/LG-20% 30 kGy blend has shown 14.31 % less weight loss as compared to neat PLA.

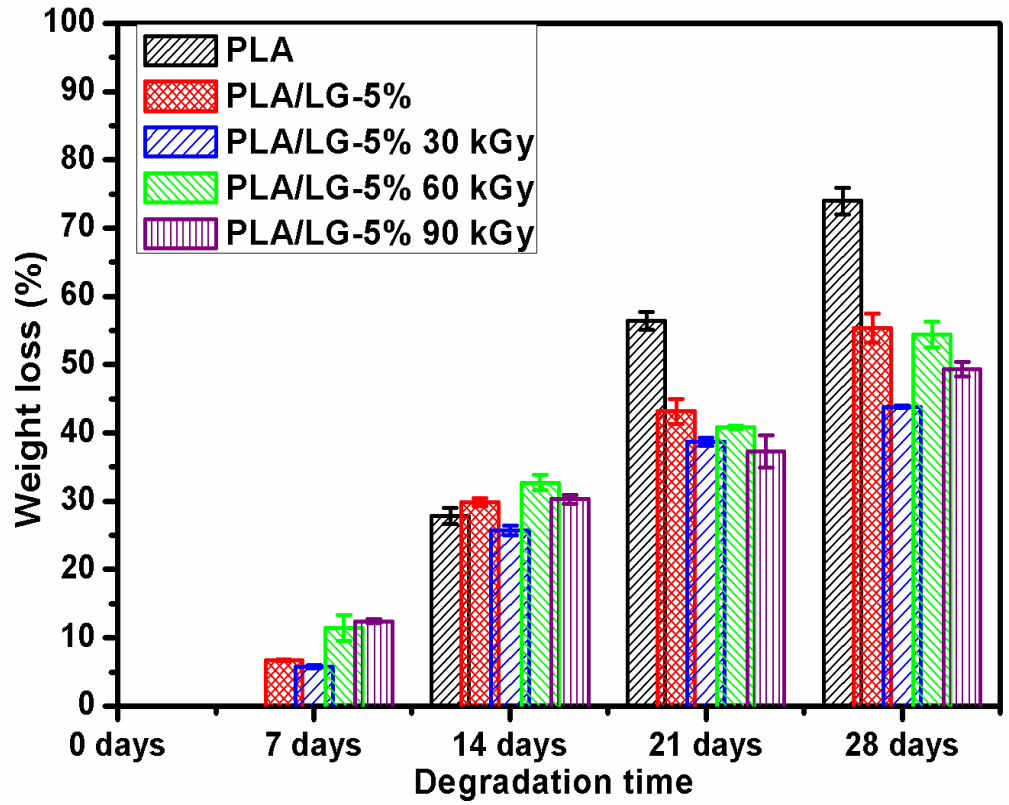

Fig. 5.11 Weight loss of neat PLA and PLA/LG blends (having 5 wt% unirradiated and E-beam irradiated lignin) as a function of degradation time.

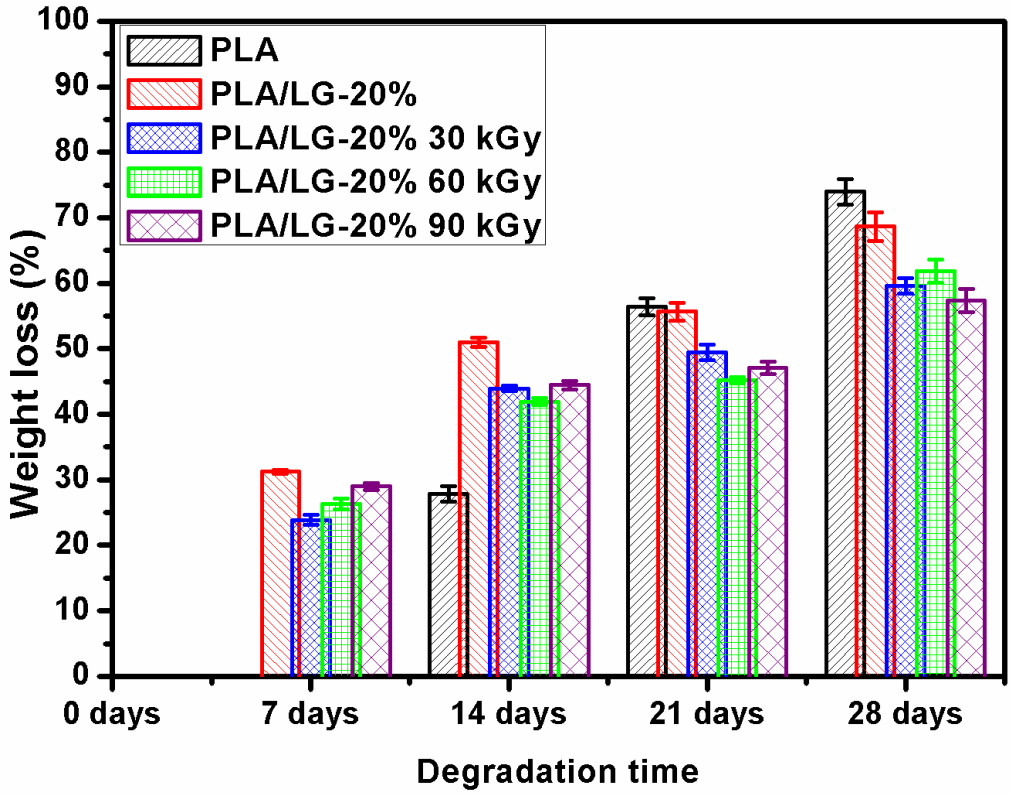

Fig. 5.12 Weight loss of neat PLA and PLA/LG blends (having 20 wt% unirradiated and E-beam irradiated lignin) as a function of degradation time.

Table 5.4

The hydrolytic degradation of neat PLA and all prepared PLA/LG blends samples as a function of degradation time.

Sample name	Weight loss (%) as a function of degradation time				Difference in weight loss (%) w.r.t. neat PLA
	7 days	14 days	21 days	28 days	
PLA	0	27.82 ± 1.18	56.40 ± 1.33	73.96 ± 1.93	
PLA/LG-5%	6.71 ± 0.07	29.85 ± 0.56	43.16 ± 1.82	55.38 ± 2.10	18.58
PLA/LG-20%	31.26 ± 0.29	51.01 ± 0.69	55.68 ± 1.37	68.67 ± 2.19	5.29
PLA/LG-5% 30 kGy	5.74 ± 0.24	25.74 ± 0.70	38.71 ± 0.55	43.83 ± 0.17	30.13
PLA/LG-20% 30 kGy	23.89 ± 0.80	43.95 ± 0.37	49.45 ± 1.19	59.65 ± 1.17	14.31
PLA/LG-5% 60 kGy	11.46 ± 1.91	32.72 ± 1.10	40.87 ± 0.22	54.39 ± 1.92	19.57
PLA/LG-20% 60 kGy	26.28 ± 0.83	41.95 ± 0.56	45.20 ± 0.44	61.83 ± 1.77	12.13
PLA/LG-5% 90 kGy	12.42 ± 0.27	30.29 ± 0.63	37.33 ± 2.37	49.31 ± 1.03	24.65
PLA/LG-20% 90 kGy	28.99 ± 0.53	44.44 ± 0.64	47.09 ± 0.99	57.40 ± 1.75	16.56

5.3 Conclusions

A new, simple and green approach is employed to enhance the miscibility of the PLA/lignin blend having the lignin contents to a high percentage (i.e. 20%). PLA-TAIC-Lignin crosslinking structures formed during melt blending of PLA, E-beam irradiated lignin and TAIC act as an interface between the dispersed lignin phase and PLA matrix, help to improve their miscibility. The glass transition temperature behavior of blends and Gordon-Taylor equation analysis assert that the PLA/LG blends having E-beam irradiated lignin with 30 kGy absorbed dose are compatible whereas PLA/LG blends having unirradiated lignin are not compatible. SEM analysis of PLA/LG blends having E-beam irradiated lignin with 30 kGy absorbed dose has also shown the continuous phase morphology without any significant phase separation. Hence, PLA/LG blends having E-beam irradiated lignin along with TAIC have shown significant improvement in the mechanical, thermal properties and slow hydrolytic degradation as compared to PLA/LG blends having unirradiated lignins. The obtained results also show that the E-beam irradiated lignin with 30 kGy absorbed dose is more suitable to enhance the miscibility of PLA/LG blends. This is because increasing E-beam absorbed dose leads to the production of the excess of radicals resulting in the enhancement of the self-intermolecular chain interactions of lignin, which was

confirmed by FTIR studies and reported in the previous literature. Hence, limits the formation of PLA-TAIC-Lignin crosslinked structures which act as an interfacial compatibilizer. The PLA/LG-5% 30 kGy blend exhibits slightly more notched impact strength, elongation at break and HDT as compared to the neat PLA. It also shows the significant improvement in the yield strength as compared to PLA/LG-5% blend without any significant decrement in the other mechanical properties. Further, the PLA/LG-5% 30 kGy blend shows the less weight loss (%) as compared to the neat PLA and other PLA/LG blends. The PLA/LG-20% 30 kGy shows the significant improvement in the yield strength and tensile modulus as compared to PLA/LG-20% blend. Hence, it can be concluded that the 30 kGy is the optimized radiation dose to enhance the miscibility of the PLA/Lignin blend.

Chapter 6

Physicochemical properties of the electron beam irradiated bamboo powder and its bio-composites with PLA

The high cost and low toughness are the main drawbacks of PLA which limit its commercial applications. However, the cost of PLA can be reduced by incorporating it with various bio-based low-priced fillers. The bamboo powder (BP), a lignocellulosic biomass, is promising green filler since it has high cellulose content and no competition with food. However, its poor compatibility with the polymers reduces the mechanical properties of the resulting composite. Hence, this work investigates the electron beam irradiation pretreatment of bamboo powder. Further, the electron beam irradiated bamboo powder was blended with PLA in two different concentrations (5% and 10%) along with epoxy silane (3-Glycidoxypropyltrimethoxy silane) as a compatibilizer. The FT-IR, XRD and TG/DTG analyses revealed that the irradiation demolishes aliphatic and aromatic moieties of bamboo powder followed by the formation of free radicals. The reduction in the intra and intermolecular hydrogen bonding among these moieties are also asserted. Moreover, mechanical and thermal properties of PLA/electron beam irradiated bamboo powder (PLA/EBP) composites are tested and the obtained results have shown the improvement in the notched impact strength as well as stability in other mechanical and thermal properties. The compatibility and dispersion of the electron beam irradiated bamboo powder in the PLA matrix were analyzed by SEM study. The hydrolytic degradation test of prepared composites was also performed.

Publication:

1. Ashish Kumar, T.Venkatappa Rao, "Physicochemical properties of fully bio-based and bio-degradable PLA/Bamboo powder composites", **Composites Part B: Engineering 175 (107098), 1-9 (2019) (Impact Factor 6.864).**

6.1 Introduction

Among all natural fillers, lignocellulosic biomass is the most favored bio-filler because of its large abundance and non-competition with food resources. Lignocellulosic biomass like bamboo fibers or flour have gained more popularity from last decade and being employed to prepare the green composites [5,182–184]. However, a large number of polar/hydrophilic groups (-OH) present in the molecular structure of bamboo powder decrease the interfacial bonding with the hydrophobic PLA matrix. To circumvent the heterogeneous interfacial problem among PLA matrix and bamboo fillers, compatibilizers have been used by many authors and also reported chemical modification of bamboo fillers prior to use such as surface modification of bamboo fillers with silane, sodium hydroxide (NaOH) and grafting of PLA molecules on the surface of bamboo fibers [71,185–191]. For instance, Ya-nan et al. [71] have synthesized and utilized the poly (lactic acid)-g-glycidyl methacrylate (PLA-g-GM) graft copolymer to enhance the interfacial adhesion between bamboo flour (BF) and PLA matrix in the PLA/BF composites. They have asserted that the PLA-g-GM act as a compatibilizer and effectively improved the mechanical properties of PLA/BF composite. Further, Jianyong Lin et al. [185] have reported the reinforcement of PLA with alkali treated bamboo fibers. They have compared the results of untreated bamboo fiber/PLA composite and alkali treated bamboo fibers/PLA composites and found that the alkali treatment enhanced the thermal and mechanical properties by introducing chemical interaction between fibers and PLA matrix. Recently, Y. Zuo et al. [186] have described the grafting of PLA onto bamboo fibers through in-situ solid state polycondensation. They have characterized the PLA-g-bamboo fibers and reported that the grafting enhanced the thermo-plasticity, thermal degradation stability and hydrophobicity of PLA-g-bamboo fibers. However, the tensile strength is slightly decreased. Moreover, S. Qian et al. [187] have reported the toughening of PLA with silane modified bamboo cellulose nanowhiskers. They have treated nanowhiskers with various concentration of silane (A-151) and blended with PLA at 2.5 w/w%. In their findings, they reported that the silane modification of nanowhiskers improved the compatibility of bio-composites, via interfacial bonding between nanowhiskers and PLA matrix, which leads to the noticeable improvement in the deformation at the break. However, other mechanical properties of bio-composites were decreased. Thus from the above-reported findings, it can be deduced that the chemical treatments of bamboo fillers improve the compatibility of PLA/bamboo filler composites. However, the chemical modification of bamboo fillers feasible only at lab scale because it entailed cumbersome steps and toxic

substances. Moreover, these strategies are complicated; increase the production cost and make hard to industrialize the final products.

Hence, the present work describes the simple and green method to modify bamboo powder (BP) and compatibilize PLA/bamboo powder composites. This method is similar to the one executed to compatibilize PLA/lignin blends [192] as described in the previous chapter. The objective of the present work is to prepare compatibilized PLA/Bamboo powder composites without any chemical modification of bamboo powder. In the present strategy, the bamboo powder is irradiated to electron beam (E-beam) with different doses 30 kGy, 60 kGy and 90 kGy. E-beam irradiated bamboo powders were analyzed with FTIR, XRD and TG/DTG techniques. In previous chapter, it was concluded that the 30 kGy is the optimized radiation dose to physically modify the organic fillers which enhance the miscibility of organic fillers into PLA matrix. Hence, the E-beam irradiated bamboo powder with 30 kGy absorbed dose was melt blended with PLA at two different concentrations i.e. 5 wt% and 10 wt% along with epoxy silane (3-Glycidoxypropyltrimethoxy silane) (ES). In the literature, it has been reported that the irradiation of wood powder to high energy radiations leads to the formation of free radicals in its lignocellulosic units [167,193]. During the melt blending of PLA, E-beam irradiated bamboo powder (EBP) and ES; the free radicals (RO˙) present in the EBP initiate the reaction between PLA and ES trough epoxide unit of ES and lead to in-situ grafting of ES molecules on the carboxyl end groups of PLA chains [52,58,194]. These in-situ formed PLA-g-ES copolymers act as a compatibilizer between the dispersed bamboo powder and PLA matrix by enhancing the interfacial bonding between them. This is because the alkoxy groups of PLA-g-ES copolymers are reactive toward hydroxyl groups present in the lignocellulosic units of bamboo powder and form silicon-oxygen-silicon bonds [187,188,190]. The interfacial compatibility of PLA/E-beam irradiated bamboo powder composites was validated with SEM, DSC analyses and by observing the improvement in the mechanical and thermal properties. Further, the blending of E-beam irradiated bamboo powder with PLA in the presence of 5phr ES leads to a 12 % improvement in the notched impact strength as compared to virgin PLA. The hydrolytic degradation test was also performed.

The details of experimental setup and method used to prepare the PLA/bamboo powder composites are given in the **Chapter 2, Section 2.2.1.3.** All synthesized composites were labeled and structured in the Table 6.1.

Table 6.1

Nomenclature of PLA/bamboo powder composites.

Sample name	Percentage of PLA (%)	Percentage of bamboo powder (%)	E-beam dose absorbed by bamboo powder (kGy)	Addition of (ES) as part per hundred (phr)
PLA	100	0	0	0
PLA/BP5	95	5	0	0
PLA/BP5/ES 5phr	95	5	0	5
PLA/EBP5/ES 5phr	95	5	30	5
PLA/EBP10/ES 5phr	90	10	30	5
PLA/EBP5/ES 10 phr	95	5	30	10

6.2 Results and Discussion

6.2.1 Characterization of E-beam irradiated bamboo powder

The bamboo powder is lignocellulosic biomass composed of three main constituents viz. hemicellulose, cellulose and lignin [195]. In lignocellulosic biomass, the hemicellulose part consists of random polymer chains which are rich of branches and as a consequence exhibit amorphous structure. In contrast to hemicellulose, the cellulose part comprises of long polymer chains of glucose arranged in good order and exhibit semi-crystalline structure [195,196]. Further, hydroxyl groups of glucose moieties of cellulose polymer chains also involve in the intermolecular hydrogen bonding. Finally, the lignin composed of phenylpropanoid moieties with different branches and exhibits three-dimensional network structures. Fig. 6.1 shows the normalized FTIR spectra of unirradiated and E-beam irradiated bamboo powders. The various characteristic peaks of bamboo powder constituents are depicted in the Fig. 6.1. The broad absorption peak at 3400 cm^{-1} is identified as a characteristic peak of stretching vibration of hydroxyl (O-H) groups. The absorption peak at 2917 cm^{-1} belongs to C-H stretching vibration frequency for ($-CH_3$) groups, the absorption peak at 1052 cm^{-1} attributed to starching vibration of C-O bond and the absorption peak at 1162 cm^{-1} assigned to glycosidic (C-O-C) bonds are the fingerprints of cellulose constituents [185–187,197,198]. Further, the absorption frequencies at 1734 cm^{-1}, 1247 cm^{-1} and 1515 cm^{-1} characteristics peaks of carbonyl groups (C=O) and acyl-oxygen stretching vibration in hemicelluloses and aromatic skeletal vibrations in lignin, respectively [25]. The

electron beam irradiated bamboo powders show the migration of hydroxyl group (O-H) stretching vibration frequency to higher wavenumbers i.e. 3412 cm^{-1}. So, it should be asserted that the E-beam irradiation of bamboo powder leads to a diminution of intermolecular hydrogen bonding among the cellulose molecules of bamboo powder. This could be due to the cleavage of glycosidic bonds of cellulose moieties or hydrogen abstraction from glucose molecules followed by the formation of free radicals [199]. The similar effect of E-beam irradiation on lignin was observed and reported in the previous studies [165,192].

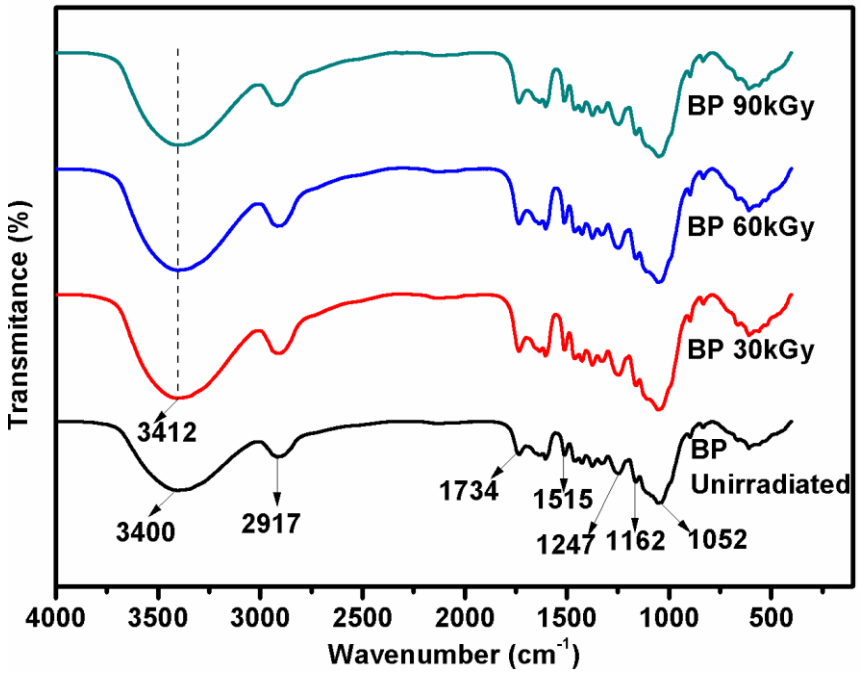

Fig. 6.1 Normalized FT-IR spectra of E-beam irradiated and unirradiated bamboo powder.

To see the effect of E-beam irradiation on the crystalline structure of bamboo powder the X-ray diffraction analysis was executed and the results are depicted in the Fig. 6.2. The unirradiated and E-beam irradiated bamboo powders show the diffractions peaks at 2θ = 16.1°, 21.72° and 34.69° correspond to (101), (002) and (040) crystal planes, respectively [185,186,200]. From the Fig. 6.2, it can be observed that the E-beam irradiation increased the peak intensity of (101) and (002) diffraction planes at low radiation dose (i.e. 30 kGy); however, the peak intensity of these diffraction planes is decreased with increasing radiation doses (i.e. 60 kGy and 90 kGy). So, it can be asserted that E-beam irradiation of bamboo powder at low dose enhances the crystallinity of bamboo powder. This is because the E-beam irradiation of bamboo powder, at a low absorbed dose, leads to the polymer chains scission in the cellulosic amorphous regions [201] which shortened the cellulose chains and help themselves to arrange in the order. This is also asserted by the FTIR study. Further, E-beam irradiated bamboo powder with 60 kGy and 90 kGy absorbed dose show the less

crystallinity as compared to unirradiated bamboo powder. Hence, the E-beam irradiation of bamboo powder to elevated doses results in polymer chains scission in both crystalline and amorphous regions of cellulose part due to the high percentage of cellulose contents and presence of long-chains structure get more irradiation exposure [202]. The polymer chains scission in the cellulosic crystalline region results in the disturbance in arraignment of the polymer chains as well as the formation of excess free radicals. These free radicals in the lignocellulosic biomass increases with increasing the absorbed dose are reported in the previous studies [165,201]. The excess free radicals in the high dose absorbed bamboo powder could recombine randomly and increase the amorphous regions of bamboo powder.

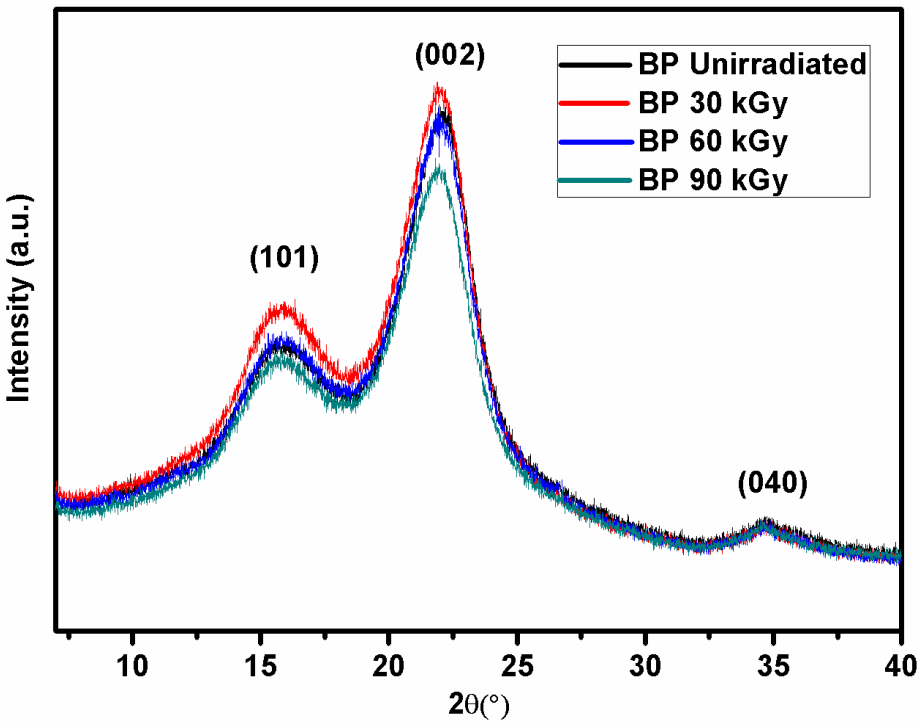

Fig. 6.2 XRD spectrum of unirradiated and E-beam irradiated bamboo powder.

Thermal gravimetric analysis of unirradiated and E-beam irradiated bamboo powders was carried out under an argon atmosphere to find the initial and maximum degradation temperatures. The Fig. 6.3 shows the TG and DTG graphs of these samples. The data such as initial degradation temperature ($T_{10\%}$), maximum weight loss temperatures (T_{max}) and weight loss rate were obtained from the graphs and tabulated in Table 6.2. The unirradiated and E-beam irradiated bamboo powders dehydrated at 70 °C to 100 °C can be seen from the Fig. 6.3. It can be noticed from Table 6.2 that the E-beam irradiation of bamboo powder at 30 kGy absorbed dose decreases the initial thermal degradation temperature and slightly increases the maximum degradation temperature. It is reported in the literature that the amorphous regions are usually thermal unstable and degrade prior to thermally stable crystalline regions in the

semi-crystalline polymers [203,204]. The FTIR and XRD studies revealed that the E-beam irradiation of bamboo powder at low absorbed dose ruptured the polymer chains in cellulosic amorphous regions; however, cellulosic crystalline regions are remaining intact. So, E-beam irradiation of bamboo powder at low dose leads to decrement only in the initial degradation temperature. It can also be seen from Table 6.2, the E-beam irradiation of bamboo powder to high doses causes a diminution in the maximum degradation temperature. This is because the E-beam irradiation of bamboo powder at high doses causes the polymer chains scission in the thermally stable cellulosic crystalline regions, as asserted by FTIR and XRD studies. It is further noticed that the irradiated bamboo powders with 60 kGy and 90 kGy absorbed dose exhibit the high initial degradation temperature as compared to irradiated bamboo powder with 30 kGy absorbed dose. The excess free radicals generated in the case of high dose absorbed bamboo powders recombined randomly and form an amorphous crosslinked structure. As a consequence, the initial degradation temperature which is degradation temperature for amorphous regions of bamboo powders is increased upon E-beam irradiation to high doses.

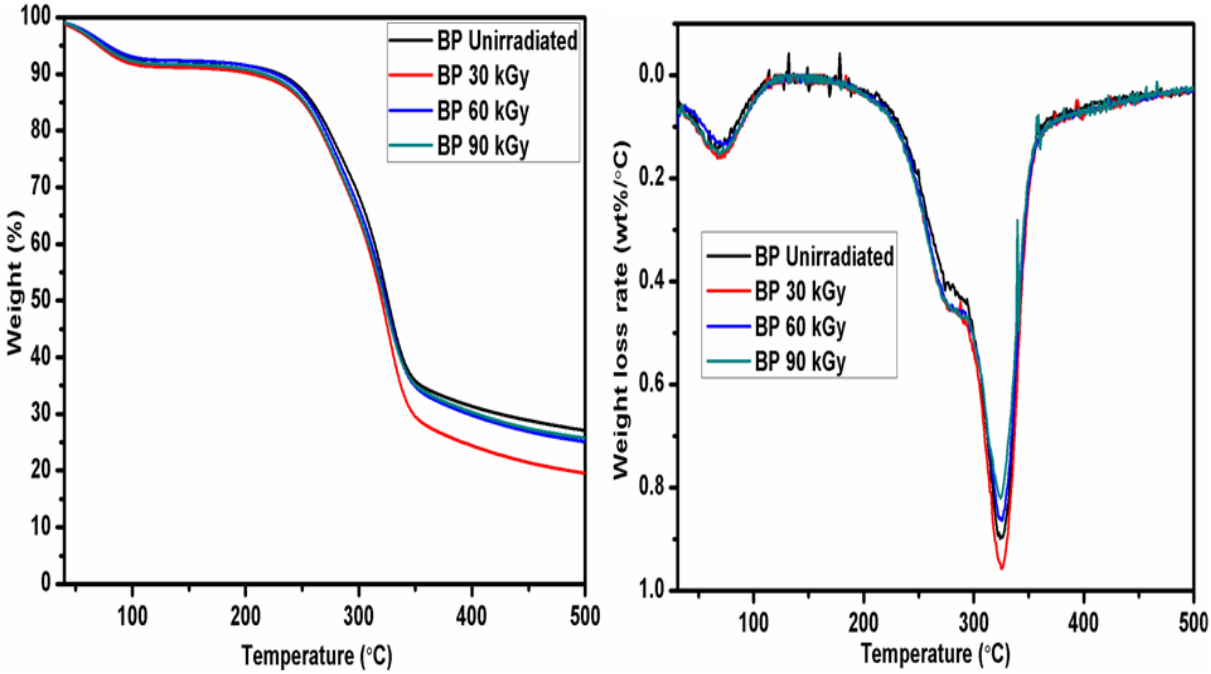

Fig. 6.3 TG and DTG thermograms of E-beam irradiated and unirradiated bamboo powder.

Table 6.2
TG and DTG data of unirradiated and E-beam irradiated bamboo powders.

Sample name	$T_{10\%}$ (°C)	T_{max} (°C)	Mass loss rate (wt%/°C)
BP Unirradiated	229.4	324.4	0.89
BP 30 kGy	204.0	325.6	0.96
BP 60 kGy	226.7	325.2	0.86
BP 90 kGy	215.8	322.3	0.82

6.2.2 PLA/E-beam irradiated bamboo powder composites

6.2.2.1 Mechanical properties

The melt mixing of bamboo powder with PLA helps to reduce the cost of bio-composites. The mechanical properties of prepared PLA/bamboo powder composites having unirradiated and E-beam irradiated bamboo powder were tested and tabulated in Table 6.3. The mechanical properties of pure PLA measured under similar conditions were discussed in chapter 3 [168] and also given in Table 6.3. The small reduction in the tensile properties is observed in the case of PLA/BP5 composite having 5 wt% unirradiated bamboo powder as compared to pure PLA. This is because the incorporation of unirradiated bamboo powder into the PLA matrix leads to the bad dispersion of bamboo powder and poor interfacial compatibility between dispersed bamboo powder and matrix which can be affirmed by observing the discontinuous phase morphology of PLA/BP5 composite from SEM micrographs Fig. 6.4a. The high magnification SEM micrograph (Fig. 6.5a) of PLA/BP composites also shows the appearance of bamboo powder particles due to poor interfacial interaction among bamboo powder and matrix. The poor compatibility causes the heterogeneous structure within the resulting PLA/BP composite and affects its mechanical properties [24,190]. The PLA/BP5/ES 5phr composite, having 5 wt% unirradiated bamboo powder along and 5 phr epoxy silane, exhibits better tensile properties as compared to PLA/BP5 composite. Further, PLA/EBP5/ES phr composite, having E-beam irradiated bamboo powder and epoxy silane, was shown the better tensile properties as compared to other PLA/BP composites. The addition of 5 wt% E-beam irradiated bamboo powder into the PLA matrix along with the 5phr epoxy silane improves the compatibility between filler and the matrix. Which can be asserted by observing continuous phase morphology in SEM micrograph of PLA/BP5/ES 5phr composite (Fig. 6.4b) and better dispersion of filler

encapsulated in the PLA matrix (seen in Fig. 6.5b). This could be due to the trapped free radicals in the E-beam irradiated bamboo powder which come on to the surface upon heating during melt blending with PLA and initiate the reaction between epoxide group of epoxy silane and carboxylic terminal groups of PLA. Hence, lead to the formation of PLA-g-ES copolymers [71,165,168,192]. The in-situ formed PLA-g-ES copolymers act as an interface between PLA matrix and bamboo filler to enhance their miscibility, because, the silane alkoxy groups of PLA-g-ES are highly reactive to the hydroxyl groups of bamboo powder [187]. The compatibility between matrix and fillers leads to continuous phase structure with the least gap between filler and matrix which assist the transfer of load under tensile force. Hence, the PLA/EBP5/ES 5phr composite exhibits better tensile properties as compared to PLA/BP5 composite. Moreover, PLA/EBP10/ES 5phr composite having 10 wt% E-beam irradiated bamboo powder and 5phr epoxy silane has shown the decrement in the tensile properties as compared to PLA/EBP5/ES 5phr composite. This is because as the concentration of E-beam irradiated bamboo powder is increased, the compatibility between filler and matrix is decreased. This can be asserted by observing the heterogeneous phase morphology in the case of PLA/EBP10/ES 5phr composite (Fig. 6.4c). The increasing concentration of epoxy silane also has an adverse effect on the mechanical properties of the composite which can be seen from Table 6.3.

Table 6.3

The mechanical properties and HDT of neat PLA and PLA/bamboo powder composites.

Sample name	Yield Strength (MPa)	Tensile Modulus (MPa)	Elongation at break (%)	Notched Izod Impact Strength (kJ/m^2)	HDT (°C)
PLA	65.00 ± 0.25	2300 ± 25	5.76 ± 0.44	2.65 ± 0.32	52.60 ± 0.45
PLA/BP5	57.00 ± 0.27	1996 ± 52	3.66 ± 0.15	2.95 ± 0.09	52.50 ± 0.08
PLA/BP5/ES 5phr	60.00 ± 0.20	2032 ± 26	3.78 ± 0.04	2.79 ± 0.05	52.33 ± 0.69
PLA/EBP5/ES 5phr	59.00 ± 0.20	2036 ± 17	3.76 ± 0.04	2.97 ± 0.16	52.13 ± 0.24
PLA/EBP10/ES 5phr	53.00 ± 1.00	2007 ± 43	3.30 ± 0.21	2.70 ± 0.1	48.76 ± 0.53
PLA/EBP5/ES 10 phr	48.00 ± 0.72	1806 ± 45	3.27 ± 0.16	2.65 ± 0.21	44.40 ± 0.37

The PLA has low notched impact strength and shows brittle fracture or smooth surface morphology without adequate wraps [132]. The incorporation of unirradiated and E-beam irradiated bamboo powder at 5 wt% enhance the notched impact strength of PLA as shown in

the Table 6.3. The PLA/BP5 and PLA/EBP5/ES 5phr composites have shown nearly 12 % more notched impact strength as compared to pure PLA. These results are verified by observing the surface morphology of notched impact surfaces of PLA/BP5 and PLA/EBP5/ES 5phr composites (Fig. 6.6). Both PLA/BP5 and PLA/EBP5/ES 5phr composites have shown the rougher morphology with adequate distortions which signifies the absorption of more impact energy. Because of the compatibility and interfacial bonding between the PLA matrix and filler, the PLA/EBP5/ES 5phr composite exhibits the high impact energy as compared to neat PLA and other composites. Further, the incorporation of E-beam irradiated bamboo powder to high percentage i.e. 10 wt% leads to the decrement in the notched impact strength because of interfacial compatibility among matrix and filler decrease with increasing the bamboo content as noticed from the SEM micrographs.

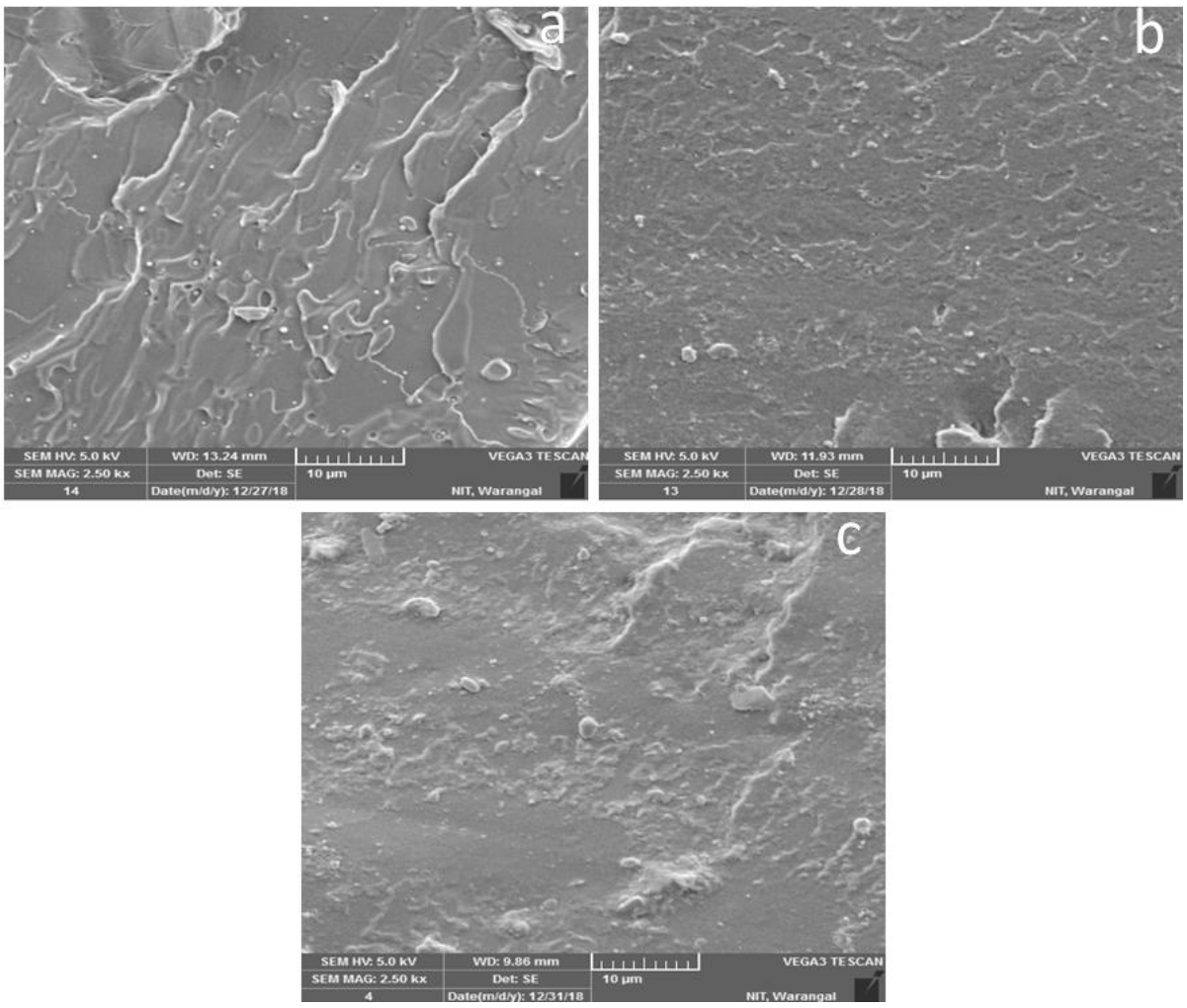

Fig. 6.4 SEM images of cryo-fractured PLA/bamboo powder composites: (a) PLA/BP5, (b) PLA/EBP5/ES 5phr and (c) PLA/EBP10/ES 5phr. The scale bar is 10 µm.

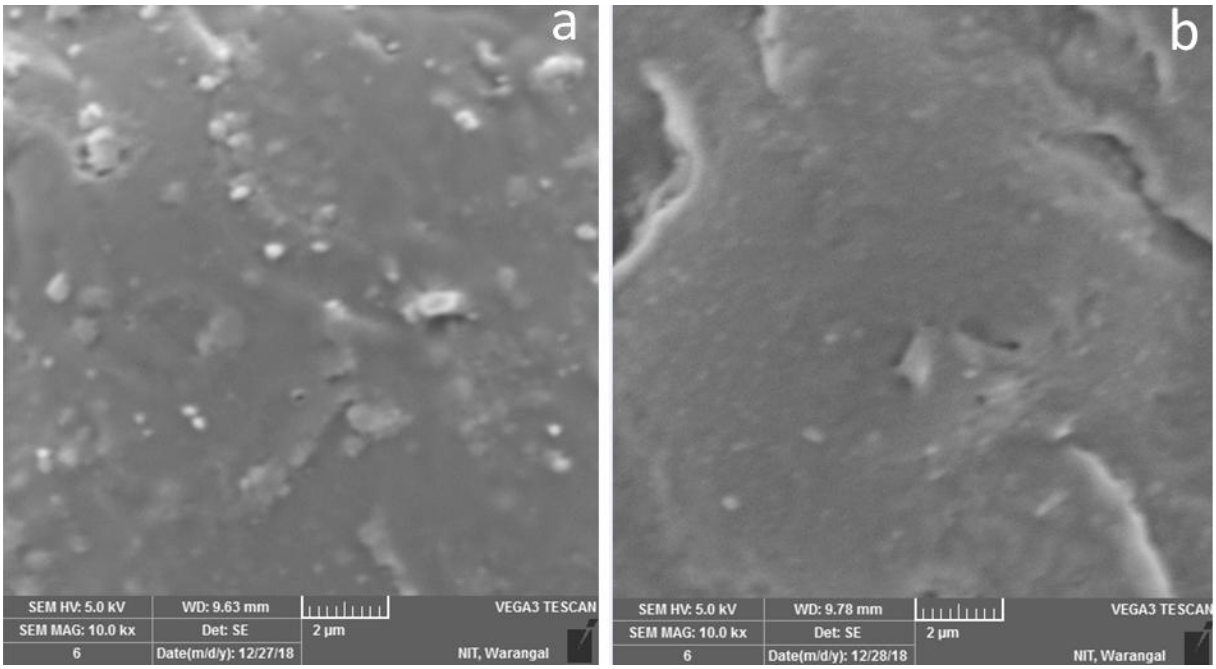

Fig. 6.5 High magnification SEM images of cryo-fractured PLA/bamboo powder composites: (a) PLA/BP5 and (b) PLA/EBP5/ES 5phr and. The scale bar is 2 µm.

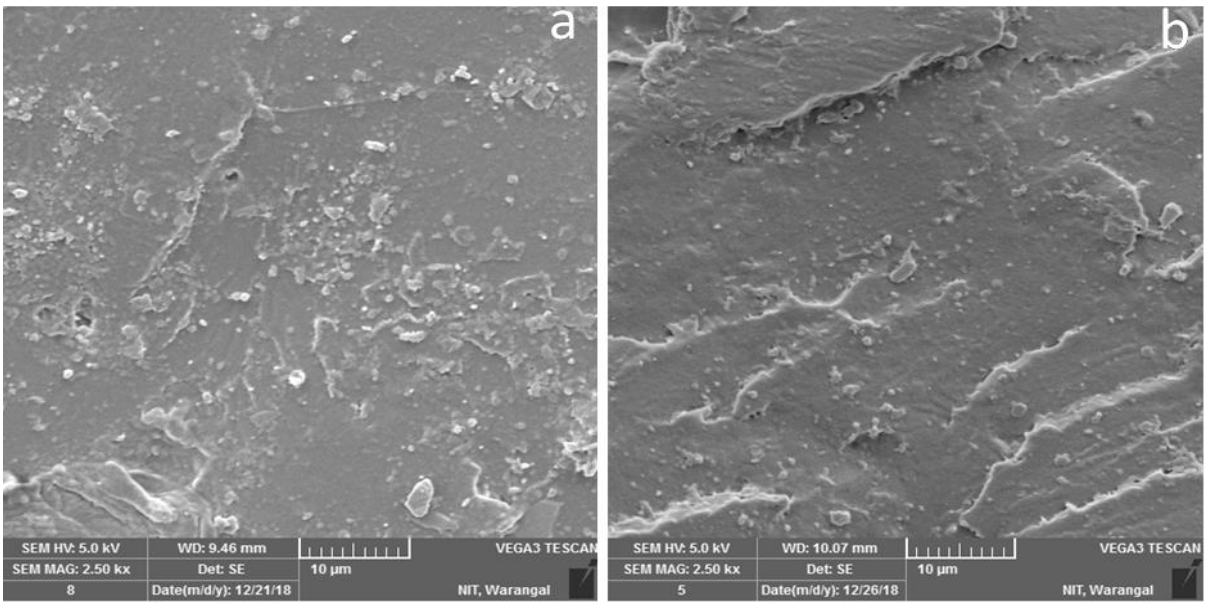

Fig. 6.6 SEM images of notched impact fracture surfaces of PLA/bamboo powder composites: (a) PLA/BP5 and (b) PLA/EBP5/ES 5phr. The scale bar is 10 µm.

The heat deflection temperature (HDT) is an essential property of a polymer product which defines the load bearing capability of the product under specific load and temperature [143]. The incorporation of unirradiated and E-beam irradiated bamboo powder at 5 wt% does not have much influence on the HDT compared to neat PLA as given in Table 6.3. However, the addition of E-beam irradiated bamboo powder at 10 wt% leads to decrement in the HDT.

This is due to less interfacial compatibility between matrix and filler in the case of PLA/EBP10/ES 5phr composite.

6.2.2.2 Thermal properties

The non-isothermal DSC profile of prepared PLA/BP composites having unirradiated and E-beam irradiated bamboo powder are depicted in Fig. 6.7. The indispensable parameters viz. glass transition temperature (T_g), cold crystallization temperature (T_{cc}), melting temperature (T_m), exothermic crystallization and endothermic melting enthalpies (i.e. ΔH_{cc} and ΔH_m respectively) belonging to various thermal events during thermal scan were calculated from the Fig. 6.7 and reported in Table 6.4. These parameters for pure PLA and the percentage of crystallinity (X_c) (Eq. 2.5) of PLA/BP composites were calculated as discussed in chapter 3 [168] and given in Table 6.4. It can be noticed from Fig. 6.7 and Table 6.4 that the addition of 5 wt% unirradiated bamboo powder increased the T_g, T_{cc} and T_m of resulting PLA/BP5 composite as compared to PLA. So, there should be some physical interaction or intermolecular hydrogen bonding between hydroxyl groups of PLA matrix and filler which hampered the localized motion of polymer segments resulting in high T_g. The presence of intermolecular hydrogen bonding also hindered the mobility of polymer chains and made it difficult to crystallize the PLA/BP5 composite, resulting in a high T_{cc} [23,190]. The two melting peaks of PLA/BP5 composite belong to two different crystalline phases formed due to crystallization and re-crystallization events in the thermal scan [98,146]. The PLA/EBP5/ES 5 phr composite exhibits a similar T_g as the PLA/BP5 composite, however, shows less T_{cc} and high percentage of crystallization (X_c) as compared to PLA/BP5 composite. The presence of PLA-g-ES copolymers in the case of PLA/EBP5/ES 5phr composite improves the compatibility and fine dispersion of the E-beam irradiated bamboo particles. These particles could cause heterogeneous nucleating effect and facilitated the polymer chains arrangement resulting in lower T_{cc} and more percentage of crystallization (X_c) [163]. The high percentage of E-beam irradiated bamboo powder i.e. 10 wt% further increased the percentage of crystallization (X_c). The PLA/EBP5/ES 10 phr having a high percentage of epoxy silane exhibits less compatibility between matrix and filler and shown low T_g, Tcc and ΔH_{cc} as compared to PLA/EBP5/ES 5phr.

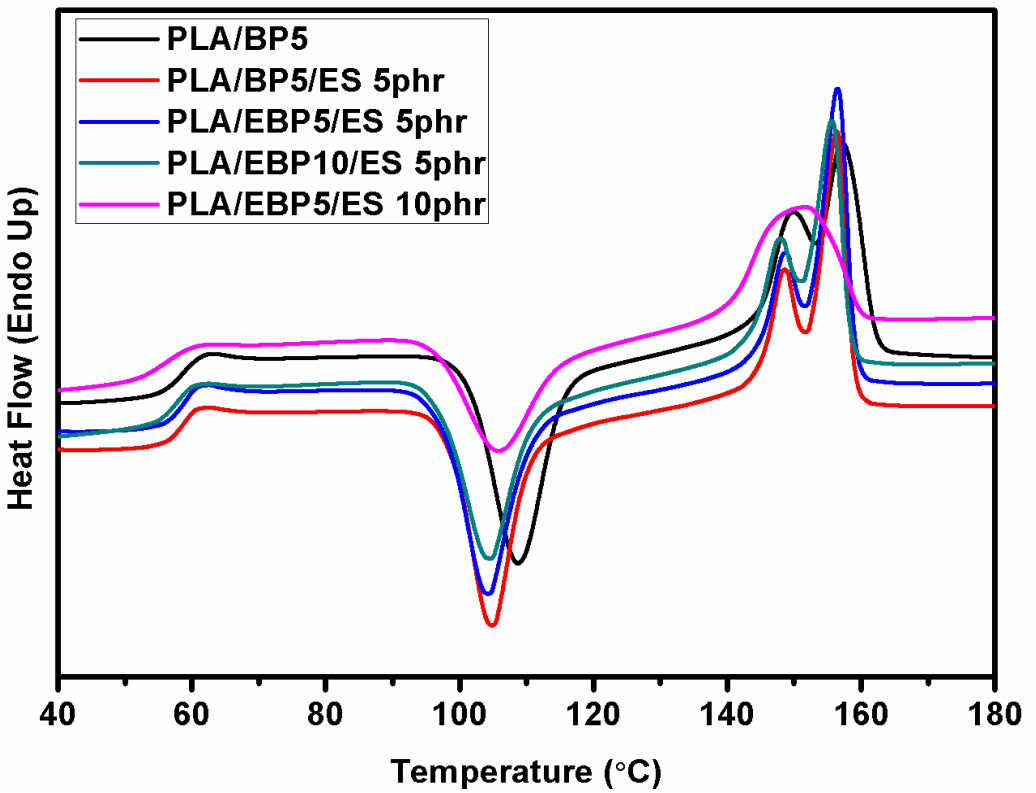

Fig. 6.7 DSC thermograms of injection molded PLA/bamboo powder composites having unirradiated and E-beam irradiated bamboo powder.

Table 6.4

Thermal transition data of neat PLA, PLA/bamboo powder composites having unirradiated and E-beam irradiated bamboo powder**.**

Sample name	T_g (°C)	(T_{cc}) (°C)	(ΔH_{cc}) (J/g)	(T_m) (°C)	(ΔH_m) (J/g)	(X_c) (%)
PLA	55.4	96.0	48.05	145.8,154.0	52.75	5.05
PLA/BP5	58.6	101.5	25.32	146.0,153.9	31.02	6.45
PLA/BP5 /ES 5phr	58.7	98.6	21.70	145.4,152.8	26.53	5.64
PLA/EBP5/ES 5phr	58.7	97.5	24.23	145.6,152.8	30.58	7.50
PLA/EBP10/ES 5phr	57.8	97.2	20.20	144.8,152.0	27.88	9.60
PLA/EBP5/ES 10 phr	56.8	96.8	15.99	139.9	21.65	7.08

6.2.2.3 X-ray diffraction

The wide angle X-ray diffraction (WAXD) patterns of prepared PLA/BP composites are shown in Fig. 6.8. Fig. 6.8 revealed that the PLA/BP composites having unirradiated bamboo powder exhibit the large halo amorphous peak at 2θ = 16.5° about 10.0° to 25.0° same as the virgin PLA [168]. However, PLA/EBP5/ES 5phr and PLA/EBP10/ES 5phr composites having E-beam irradiated bamboo powder were shown the characteristic crystallization peak of PLA at 2θ = 16.5° attributed to (110) planes [12]. The well dispersed E-beam irradiated bamboo particles cause a nucleating effect which helps to crystallize the samples of PLA/EBP5/ES 5phr and PLA/EBP10/ES 5phr composites during the injection molding process. The intensity of the characteristic crystallization peak belongs to PLA increased with increasing the percentage of E-beam irradiated bamboo powder. These results are consistent with the DSC results.

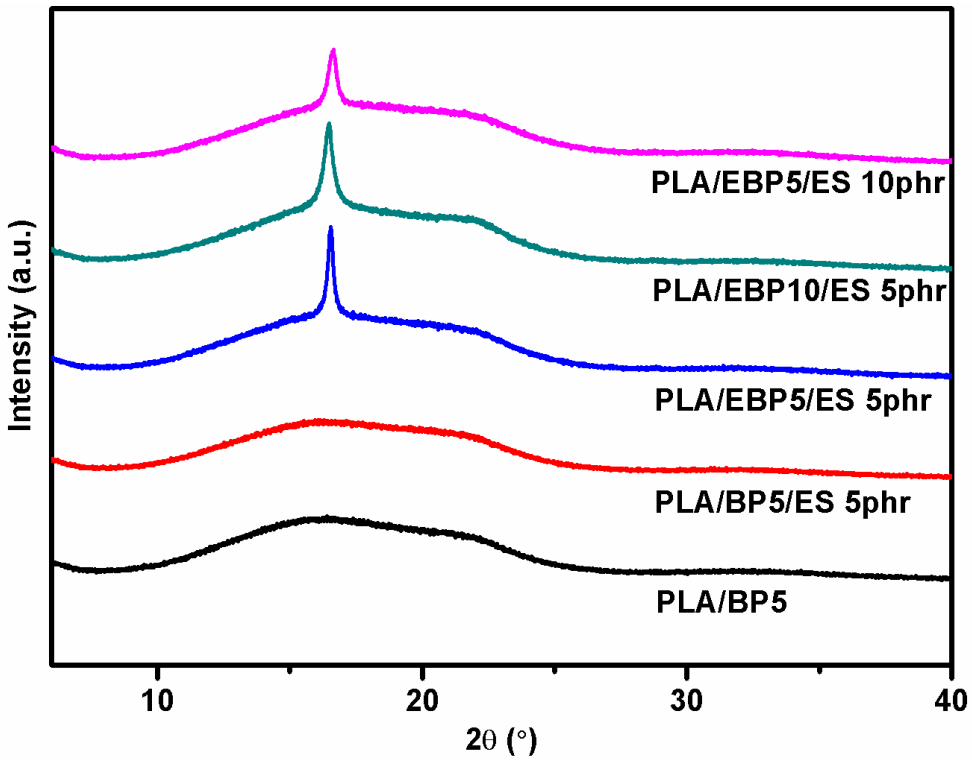

Fig. 6.8 XRD patterns of PLA/bamboo composites having unirradiated and E-beam irradiated bamboo powder.

6.2.2.4 Hydrolytic degradation analysis

The hydrolysis of PLA is the primary step of PLA bio-degradation followed by the biotic degradation process which involves the decomposition of PLA oligomers and monomers into CO_2, water and biomass under aerobic conditions [114,118]. The hydrolytic

degradation of PLA is feasible due to the presence of hydrolyzable ester repeating units in its backbone [115,118]. The hydrolytic degradation process of PLA is self-catalyzed by its carboxylic terminal groups [118]. The hydrolytic degradation of neat PLA and PLA/BP composites were carried out in phosphate buffer solution (PBS). The results are shown in Fig. 6.9 as a function of degradation time. The weight loss (%) was calculated (Eq. 2.11) for each sample after regular interval of time and tabulated in Table 6.5. After 7 days of immersion in the PBS, neither neat PLA nor PLA/BP composite samples were shown weight loss. After the 14 days of immersion and successive immersion time intervals, the virgin PLA was shown remarkable weight-loss percentage. All PLA/BP composites having unirradiated and E-beam irradiated bamboo powder shown less weight-loss percentage as compared to neat PLA, during the assay. This can be attributed to the intermolecular hydrogen bonding between hydroxyl groups of lignocellulosic moieties of bamboo powder with water molecules of immersion media which restricted the diffusion of water molecules and reduce their interaction with ester units of PLA. Hence, PLA/BP composites were shown less weight-loss percentage as compared to PLA. After 28 days of immersion, PLA has shown the maximum weight loss percentage i.e. (73.96 ± 1.93) %. Further after 28 days of immersion, PLA/BP5, PLA/BP5/ES 5phr, PLA/EBP5/ES 5phr and PLA/EBP10/ES 5phr composites were shown weight loss percentage (51.46 ± 1.57) %, (39.25 ± 0.17) %, (43.04 ± 1.06) % and (35.60 ± 0.27) % respectively. It is obviously noticed from the Table 6.5, the PLA/EBP5/ES 5phr composites having E-beam irradiated bamboo powder and epoxy silane is shown more difference in the weight loss percentage as compared to PLA/BP5 composite having unirradiated bamboo powder after 28 days of immersion. This is because the melt blending of E-beam irradiated bamboo powder and epoxy silane with PLA leads to the formation of PLA-g-ES copolymer and lessen the carboxylic acid terminal groups of PLA. Hence, the self-catalytic action of carboxylic terminal groups of PLA is decreased which slow down the hydrolytic degradation of PLA chains [118,192]. The PLA/EBP10/ES 5phr composite is shown the maximum difference in the weight loss percentage with respect to neat PLA. This is because the high concentration of E-beam irradiated bamboo powder (i.e. 10 wt %) increased the lignocellulosic contents in the resulting composite. So, the large number of hydroxyl groups associated with lignocellulosic moieties was involved in the intermolecular hydrogen bonding with water molecules of the immersion media. Hence, the diffusion of water molecules into the matrix is declined and their interaction with ester units of PLA backbone is also minimized which resulted in less weight loss percentage.

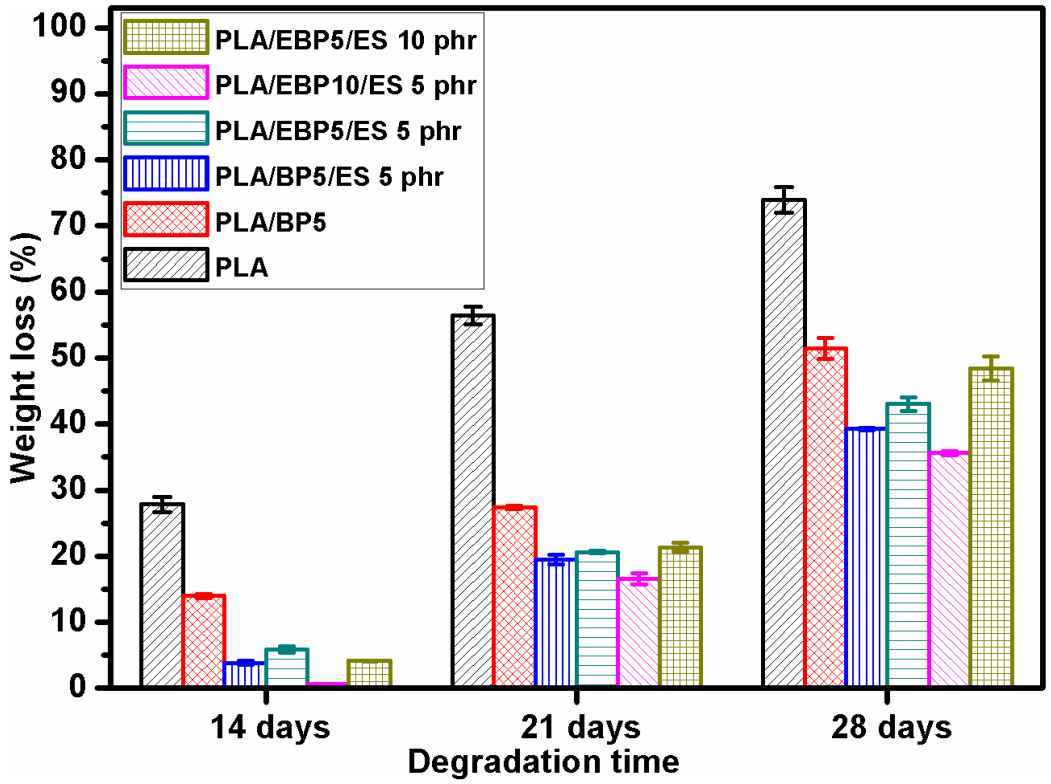

Fig. 6.9 Weight loss % of PLA and PLA/BP composites as a function of degradation time.

Table 6.5

The hydrolytic degradation of neat PLA and PLA/BP composites as a function of degradation time.

Sample name	Weight loss (%) as a function of degradation time			Difference in weight loss (%) w.r.t. neat PLA
	14 days	21 days	28 days	
PLA	27.82 ± 1.18	56.40 ± 1.33	73.96 ± 1.93	
PLA/BP5	13.98 ± 0.28	27.37 ± 0.22	51.46 ± 1.57	22.50
PLA/BP5 /ES 5phr	3.87 ± 0.25	19.51 ± 0.73	39.25 ± 0.17	34.71
PLA/EBP5/ES 5phr	5.85 ± 0.47	20.62 ± 0.20	43.04 ± 1.06	30.92
PLA/EBP10/ES 5phr	0.63 ± 0.03	16.56 ± 0.84	35.60 ± 0.27	38.36
PLA/EBP5/ES 10 phr	4.12 ± 0.03	21.37 ± 0.68	48.41 ± 1.87	25.15

6.3 Conclusions

The E-beam irradiation of bamboo powder at low irradiation dose i.e. 30 kGy ruptured the polymer chains in amorphous cellulosic regions of bamboo powder which resulted in the formation of free radicals and decrement in the intermolecular hydrogen bonding among the

cellulose molecules and was asserted by FTIR, XRD and TG/DTG results. However, E-beam irradiation of bamboo powder at high irradiation doses i.e. 60 kGy and 90 kGy leads to the polymer chain scission in both amorphous and crystalline regions of the cellulosic parts of bamboo powder. It leads to the formation of excess free radicals which recombine randomly and increase the amorphous regions in the bamboo powder as confirmed by XRD and TG/DTG results.

The PLA/BP5 composite with 5 wt% unirradiated bamboo powder is shown the decrement in the mechanical properties as compared to neat PLA due to poor interfacial compatibility between matrix and filler. However, PLA/EBP5/ES 5phr having 5 wt% E-beam irradiated bamboo powder and 5 phr epoxy silane is shown a better mechanical properties as compared to PLA/BP5 composite and also exhibits the highest notched impact strength which is 12% more than pure PLA. The PLA-g-ES copolymers formed during melt blending process act as an interface between matrix and filler and improved the interfacial compatibility of the resulting composite which was asserted by SEM analysis. PLA/EBP10/ES 5phr composite having 10 wt% E-beam irradiated bamboo powder and epoxy silane was also shown better impact strength as compared to neat PLA. Further, the addition of unirradiated and E-beam irradiated bamboo powder retarded the hydrolytic degradation of PLA. Hence, incorporation of E-beam irradiated bamboo powder with 30 kGy absorbed dose along with 5phr epoxy silane helps to improve the notched impact strength of PLA as well as reduce the cost of the final product.

Chapter 7

Summary and Conclusions

To overcome the problems involved in petrochemical polymers/plastics and to meet the increasing demand for commodity plastics, the green plastics should be developed by employing natural polymer resources. The PLA is the front runner synthetic biopolymer in the emerging bio-plastic market, can be used to replace the non-biodegradable petrochemical polymers/plastics. However, some of its drawbacks such as poor notched impact strength, brittleness and low HDT need to be improved along with the competitive cost of the product for commercial applications.

The thesis work is aimed at circumventing the drawbacks of PLA and making it acceptable for commercial applications. Initially, the efforts are given to enhance the notched impact strength, elongation at break and HDT of PLA. So, PEGM is melt blended with the PLA at fixed weight ratio 80:20. The melt blending of PLA and PEGM leads to the formation of PLA-g-PEGM graft copolymers which act as an interface between the dispersed PEGM phase and PLA matrix and enhance their compatibility. The PLA/PEGM compatible blend has exhibited elongation at break 28 times and notched impact strength 2.23 times more than neat PLA. Further, to improve the notched impact strength, elongation at break and HDT the HBN particles are incorporated at different concentrations such as 1 phr, 5 phr and 10 phr to prepare PLA/PEGM/HBN blend-composites. The PLA/PEGM/HBN 1phr blend-composite has shown better notched impact strength, elongation at break and HDT than neat PLA and PLA/PEGM blend. The notched impact strength of PLA/PEGM/HBN 1phr blend-composite is 1.5 times higher than PLA/PEGM blend and 3.36 times higher than neat PLA. The blending of PEGM with PLA and further incorporation of HBN particles retards the hydrolytic degradation of PLA. Hence, to increase the hydrolytic degradation rate as well as good mechanical properties the prepared samples of the blend and blend-composites are irradiated to E-beam with three different doses i.e. 20 kGy, 60 kGy and 100 kGy. The E-beam irradiated samples of the blend and blend-composites have shown fast degradation rate, better HDT and more weight loss percentage as compared to unirradiated samples. The PLA/PEGM/HBN 5phr 100 kGy blend-composite has shown high notched impact strength which is 2.45 times more than neat PLA and more weight loss percentage as compared to other irradiated blend and blend-composites.

Finally, the research has been extended to prepare fully bio-based and cost-effective PLA blends and composites with better mechanical and thermal properties. The commercial alkali kraft lignin is blended with PLA to develop green plastic. However, the blending of lignin with PLA causes incompatible blend which exhibits inferior mechanical and thermal

properties. Hence, the lignin is physically modified by irradiating it to E-beam with three different doses 30 kGy, 60 kGy and 90 kGy prior to blending. The unirradiated and E-beam irradiated lignins having different absorbed doses are blended with PLA in two different percentages i.e. 5 and 20 % (w/w). During the melt blending of PLA and E-beam irradiated lignin along with 3 phr TAIC the PLA-TAIC-Lignin crosslinked structures are formed which act as an interface between dispersed lignin phase and PLA matrix and hence compatibilize PLA/LG blend. Among all the PLA/LG blends, the blends having E-beam irradiated lignin with 30 kGy absorbed dose and TAIC are more compatible and exhibit better mechanical and thermal properties. PLA/LG-5% 30 kGy blend shows better elongation at break, notched impact strength and HDT than virgin PLA and stability in other mechanical properties. Further, the incorporation of lignin into PLA matrix retards the hydrolytic degradation of PLA.

Moreover, the ultra-fine bamboo powder is also used to prepare fully bio-based cost-effective PLA/bamboo powder composites. The bamboo powder is also physically modified, similar to lignin, prior to blending with PLA. The E-beam irradiated bamboo powder with 30 kGy absorbed dose is incorporated into PLA matrix in two different percentages i.e. 5 wt% and 10 wt% along with epoxy silane. The PLA/EBP5/ES 5phr and PLA/EBP10/ES 5phr composites are compatible and shown more notched impact strength as compared to PLA, without scarifying the other mechanical properties remarkably. The PLA/EBP5/ES 5phr composite shows 12% more notched impact strength than neat PLA. The incorporation of bamboo powder into the PLA matrix also restricts the hydrolytic degradation of PLA.

A comparative analysis has been executed for mechanical, thermal and hydrolytic degradation properties of PLA and optimized compositions of prepared PLA blends and blend-composites (Table 7.1).

Table 7.1

Comparative summary for mechanical, thermal and hydrolytic degradation properties of PLA and optimized compositions of prepared PLA blends and blend-composites.

PLA/Optimized Compositions	Yield Strength (MPa)	Tensile Modulus (MPa)	Elongation at break (%)	Notched Izod Impact Strength (kJ/m^2)	Flexural Modulus (MPa)	HDT (°C)	Hydrolytic Degradation (W_L %)$^{\#}$
PLA	65	2300	5.76	2.65	3767	52.6	73.96
PLA/PEGM/HBN 1phr	42	1754	166.00	8.89	2337	54.5	39.64
PLA/PEGM/HBN 5phr 100 kGy	37	1646	3.12	6.50	N.S.*	57.5	49.79
PLA/LG-5% 30 kGy	50	2001	7.32	2.89	3516	54.4	43.83
PLA/LG-20% 30 kGy	37	2826	1.49	2.31	3802	54.8	59.65
PLA/EBP5/ES 5phr	59	2036	3.76	2.97	N.S.*	52.1	43.04
PLA/EBP10/ES 5phr	53	2007	3.30	2.70	N.S.*	48.8	35.60

N.S.* represents Not Studied.

(W_L %) $^{\#}$ represents a Weight loss percentage after 28 days of immersion in the phosphate buffer solution (PBS).

To epitomize, it is scrutinized from the experimental findings that the blending of PEGM with PLA and incorporation of HBN particles at low percentage i.e. 1phr is beneficial to overcome the major drawbacks of PLA. However, it retards the hydrolytic degradation of PLA. Further, E-beam irradiation of samples can be employed to enhance the hydrolytic degradation. The PLA/PEGM/HBN 1phr blend-composite has shown good mechanical and thermal properties; however, it is not completely compostable and can be used for durable commercial applications. Moreover, the fully bio-based PLA/LG blends having E-beam irradiated lignin with 30 kGy absorbed dose and PLA/BP composites having E-beam irradiated bamboo powder with 30 kGy absorbed dose have better impact strength than PLA and with tensile proprieties similar to PLA. These compositions could be completely

compostable and can be used for commercial applications that need good mechanical properties and complete biodegradation.

Future Perspectives

The research findings show that the major drawbacks of PLA are ameliorated by melt blending it with different polymers and fillers. However, the improvement in the heat deflection temperature is not sufficient and needs to be further improved. Hence, research work will be extended and efforts will be given to enhance the heat deflection temperature of PLA along with other mechanical properties. The emphasis will also be given to compatibilize prepared compositions with high bio-contents and use other natural fillers into the PLA blends and composites which help to reduce the cost of the prepared product. The suitable bio-fillers or fiber reinforcements will be used which bring umpteen opportunities to tailors the product properties as per desire applications. The low-cost green plastics with high bio-contents will have numerous end-use applications from biomedical to conventional thermoplastics. The commodity plastics (namely disposal cups, plates, buckets, bags for carrying household waste and lamination films), sanitary products and diapers and so on are the major applications of the green plastics. The durable green plastic will generate a lot of interest for automotive applications such as car interiors and exteriors and electronic applications such as personal computer housing, chassis for mobiles and electronic casing. The bio-compatible and hydrolytic degradable green plastics will magnetize a lot of interest for biomedical applications such as sutures, bone screws, scaffolds, hydrogels, drug delivery devices, protein encapsulation and delivery systems and so on.

References

[1] D.I. Bower, An Introduction to Polymer Physics, First, Cambridge University Press, (2002) 1-425. www.cambridge.org/9780521631372.

[2] V.R. Gowariker, N. V. Viswanathan, J. Sreedhar, Polymer Science, First, New Age International Publishers, New Delhi, India, (2008) 1-493.

[3] R. Chandra, R. Rustgi, Pergamon Biodegradable Polymers, Prog. Polym. Sci. 23 (1998) 1273–1335. doi:10.1016/S0079-6700(97)00039-7.

[4] B. Geueke, Dossier – Bioplastics as food contact materials, Food Packag. Forum. (2014) 1–8. doi:10.5281/zenodo.33517.

[5] K.G. Satyanarayana, G.G.C. Arizaga, F. Wypych, Biodegradable composites based on lignocellulosic fibers-An overview, Prog. Polym. Sci. 34 (2009) 982–1021. doi:10.1016/j.progpolymsci.2008.12.002.

[6] H.T. Rafael Auras, Loong-Tak Lim, Susan E. M. Selke, Poly(Lactic Acid), John Wiley & Sons, Inc., Hoboken, NJ, USA, (2010) 1-487. doi:10.1002/9780470649848.

[7] D.J. Darensbourg, W. Choi, O. Karroonnirun, N. Bhuvanesh, Support Information for Ring-Opening Polymerization of Cyclic Monomers by Biocompatible Metal Complexes . Production of Poly (lactide), Polycarbonates and Their Copolymers ., Macromolecules. 40 (2007) 3521–3523. doi:10.1021/ma062780n.

[8] A.P. Gupta, V. Kumar, New emerging trends in synthetic biodegradable polymers - Polylactide: A critique, Eur. Polym. J. 43 (2007) 4053–4074. doi:10.1016/j.eurpolymj.2007.06.045.

[9] C.M. Chan, L.J. Vandi, S. Pratt, P. Halley, D. Richardson, A. Werker, B. Laycock, Composites of Wood and Biodegradable Thermoplastics: A Review, Polym. Rev. 58 (2018) 444–494. doi:10.1080/15583724.2017.1380039.

[10] T. Maharana, B. Mohanty, Y.S. Negi, Melt–solid polycondensation of lactic acid and its biodegradability, Prog. Polym. Sci. 34 (2009) 99–124. doi:10.1016/j.progpolymsci.2008.10.001.

[11] T.M. Ovitt, G.W. Coates, C.U. V, N. York, Stereoselective Ring-Opening

Polymerization of meso -Lactide : Synthesis of Syndiotactic Poly (lactic acid), J. Am. Chem. Soc. 121 (1999) 4072–4073. doi:10.1021/ja990088k.

[12] T. Kawai, N. Rahman, G. Matsuba, K. Nishida, T. Kanaya, M. Nakano, H. Okamoto, J. Kawada, A. Usuki, N. Honma, K. Nakajima, M. Matsuda, Crystallization and melting behavior of poly (L-lactic acid), Macromolecules. 40 (2007) 9463–9469. doi:10.1021/ma070082c.

[13] A. Södergård, M. Stolt, Properties of lactic acid based polymers and their correlation with composition, Prog. Polym. Sci. 27 (2002) 1123–1163. doi:10.1016/S0079-6700(02)00012-6.

[14] S. Saeidlou, M.A. Huneault, H. Li, C.B. Park, Poly(lactic acid) crystallization, Prog. Polym. Sci. 37 (2012) 1657–1677. doi:10.1016/j.progpolymsci.2012.07.005.

[15] R. Auras, B. Harte, S. Selke, An overview of polylactides as packaging materials, Macromol. Biosci. 4 (2004) 835–864. doi:10.1002/mabi.200400043.

[16] R.E. Drumright, P.R. Gruber, D.E. Henton, Polylactic acid technology, Adv. Mater. 12 (2000) 1841–1846. doi:10.1002/1521-4095(200012)12:23<1841::AID-ADMA1841>3.0.CO;2-E.

[17] R.M. Rasal, A. V. Janorkar, D.E. Hirt, Poly(lactic acid) modifications, Prog. Polym. Sci. 35 (2010) 338–356. doi:10.1016/j.progpolymsci.2009.12.003.

[18] L.-T. Lim, R. Auras, M. Rubino, Processing technologies for poly(lactic acid), Prog. Polym. Sci. 33 (2008) 820–852. doi:10.1016/j.progpolymsci.2008.05.004.

[19] M.N.S. Kumar, A.K. Mohanty, L. Erickson, M. Misra, Lignin and its applications with polymers, J. Biobased Mater. Bioenergy. 3 (2009) 1–24. doi:10.1166/jbmb.2009.1001.

[20] J.L. Wen, B.L. Xue, F. Xu, R.C. Sun, A. Pinkert, Unmasking the structural features and property of lignin from bamboo, Ind. Crops Prod. 42 (2013) 332–343. doi:10.1016/j.indcrop.2012.05.041.

[21] G. Gellerstedt, Softwood kraft lignin: Raw material for the future, Ind. Crops Prod. 77 (2015) 845–854. doi:10.1016/j.indcrop.2015.09.040.

[22] J. Ponomarenko, T. Dizhbite, M. Lauberts, A. Viksna, G. Dobele, O. Bikovens, G.

Telysheva, Characterization of softwood and hardwood lignoboost kraft lignins with emphasis on their antioxidant activity, BioResources. 9 (2014) 2051–2068. doi:10.15376/biores.9.2.2051-2068.

[23] D. Kun, B. Pukánszky, Polymer / lignin blends : Interactions , properties , applications, Eur. Polym. J. 93 (2017) 618–641.

[24] O. Gordobil, I. Egüés, R. Llano-Ponte, J. Labidi, Physicochemical properties of PLA lignin blends, Polym. Degrad. Stab. 108 (2014) 330–338. doi:10.1016/j.polymdegradstab.2014.01.002.

[25] F. Monteil-Rivera, M. Phuong, M. Ye, A. Halasz, J. Hawari, Isolation and characterization of herbaceous lignins for applications in biomaterials, Ind. Crops Prod. 41 (2013) 356–364. doi:10.1016/j.indcrop.2012.04.049.

[26] Y.L. Chung, J. V. Olsson, R.J. Li, C.W. Frank, R.M. Waymouth, S.L. Billington, E.S. Sattely, A renewable lignin-lactide copolymer and application in biobased composites, ACS Sustain. Chem. Eng. 1 (2013) 1231–1238. doi:10.1021/sc4000835.

[27] B. Kamm, P.R. Gruber, M. Kamm, Biorefineries – Industrial Processes and Products, in: Ullmann's Encycl. Ind. Chem., Wiley VCH Verlag GmbH & Co. KGaA, 2015: pp. 1–32. doi:10.1002/14356007.l04_l01.pub2.

[28] J. Wang, R.S.J. Manley, D. Feldman, Synthetic polymer-lignin copolymers and blends, Prog. Polym. Sci. 17 (1992) 611–646. doi:10.1016/0079-6700(92)90003-H.

[29] E. Bugnicourt, P. Cinelli, A. Lazzeri, V. Alvarez, Polyhydroxyalkanoate (PHA): Review of synthesis, characteristics, processing and potential applications in packaging, Express Polym. Lett. 8 (2014) 791–808. doi:10.3144/expresspolymlett.2014.82.

[30] A. Anjum, M. Zuber, K.M. Zia, A. Noreen, M.N. Anjum, S. Tabasum, Microbial production of polyhydroxyalkanoates (PHAs) and its copolymers: A review of recent advancements, Int. J. Biol. Macromol. 89 (2016) 161–174. doi:10.1016/j.ijbiomac.2016.04.069.

[31] S. Taguchi, Y. Doi, Evolution of Polyhydroxyalkanoate (PHA) production system by "enzyme evolution": Successful case studies of directed evolution, Macromol. Biosci. 4

(2004) 145–156. doi:10.1002/mabi.200300111.

[32] M. Koller, A. Salerno, A. Muhr, A. Reiterer, E. Chiellini, S. Casella, P. Horvat, G. Braunegg, Whey Lactose as a Raw Material for Microbial Production of Biodegradable Polyesters, in: Polyester, 2012: pp. 19–59. doi:10.5772/48737.

[33] K. Sudesh, H. Abe, Y. Doi, Synthesis, structure and properties of polyhydroxyalkanoates: Biological polyesters, Prog. Polym. Sci. 25 (2000) 1503–1555. doi:10.1016/S0079-6700(00)00035-6.

[34] M. Okada, Chemical syntheses of biodegradable polymers, Prog. Polym. Sci. 27 (2002) 87–133. doi:10.1016/S0079-6700(01)00039-9.

[35] M. Labet, W. Thielemans, Synthesis of polycaprolactone: A review, Chem. Soc. Rev. 38 (2009) 3484–3504. doi:10.1039/b820162p.

[36] Y. Ikada, H. Tsuji, Biodegradable polyesters for medical and ecological applications, Macromol. Rapid Commun. 21 (2000) 117–132. doi:10.1002/(SICI)1521-3927(20000201)21:3<117::AID-MARC117>3.3.CO;2-O.

[37] J. Odent, J.M. Raquez, P. Leclère, F. Lauro, P. Dubois, Crystallization-induced toughness of rubber-modified polylactide: Combined effects of biodegradable impact modifier and effective nucleating agent, Polym. Adv. Technol. 26 (2015) 814–822. doi:10.1002/pat.3513.

[38] H. Bai, H. Xiu, J. Gao, H. Deng, Q. Zhang, M. Yang, Q. Fu, Tailoring impact toughness of poly(L-lactide)/poly(ε-caprolactone) (PLLA/PCL) blends by controlling crystallization of PLLA matrix, ACS Appl. Mater. Interfaces. 4 (2012) 897–905. doi:10.1021/am201564f.

[39] Changyu Han Xianghai Ran Xuan Su Kunyu Zhang Nanan Liu Lisong Dong, Effect of peroxide crosslinking on thermal and mechanical properties of poly(ε-caprolactone), Polym. Int. 56 (2007) 593–600. doi:10.1002/pi.

[40] K. Gandhi, D. Kriz, R. Salovey, M. Narkis, R. Wallerstein, Crosslinking of polycaprolactone in the pre-gelation region, Polym. Eng. Sci. 28 (1988) 1484–1490. doi:10.1002/pen.760282209.

[41] M. Gigli, M. Fabbri, N. Lotti, R. Gamberini, B. Rimini, A. Munari, Poly(butylene

succinate)-based polyesters for biomedical applications: A review in memory of our beloved colleague and friend Dr. Lara Finelli., Eur. Polym. J. 75 (2016) 431–460. doi:10.1016/j.eurpolymj.2016.01.016.

[42] R. Wang, S. Wang, Y. Zhang, C. Wan, P. Ma, Toughening Modification of PLLA / PBS Blends via In Situ Compatibilization, Polym. Eng. Sci. 49 (2009) 26–33. doi:10.1002/pen.21210 Published.

[43] K. Chrissafis, K.M. Paraskevopoulos, D.N. Bikiaris, Thermal degradation mechanism of poly(ethylene succinate) and poly(butylene succinate): Comparative study, Thermochim. Acta. 435 (2005) 142–150. doi:10.1016/j.tca.2005.05.011.

[44] L. Yu, K. Dean, L. Li, Polymer blends and composites from renewable resources, Prog. Polym. Sci. 31 (2006) 576–602. doi:10.1016/j.progpolymsci.2006.03.002.

[45] S.P. Gautam, C. Pollution, C. Board, M.O.F. Environment, Bio-degradable Plastics-Impact on Environment, Cent. Pollut. Control BOARD Minist. Environ. For. Gov. INDIA. (2009) 1–46.

[46] K. Madhavan Nampoothiri, N.R. Nair, R.P. John, An overview of the recent developments in polylactide (PLA) research, Bioresour. Technol. 101 (2010) 8493–8501. doi:10.1016/j.biortech.2010.05.092.

[47] N. Yuia, J. Feijen, Stereo block copolymers of D and L-lactides, Makmmol. Chem. 488 (1990) 481–488.

[48] P. Ma, T. Shen, P. Xu, W. Dong, P.J. Lemstra, M. Chen, Superior Performance of Fully Biobased Poly(lactide) via Stereocomplexation-Induced Phase Separation: Structure versus Property, ACS Sustain. Chem. Eng. 3 (2015) 1470–1478. doi:10.1021/acssuschemeng.5b00208.

[49] Y. Ohya, S. Maruhashi, T. Ouchi, Preparation of poly(lactic acid)-grafted amylose through the trimethylsilyl protection method and its biodegradation, Macromol. Chem. Phys. 199 (1998) 2017–2022. doi:10.1002/(SICI)1521-3935(19980901)199:9<2017::AID-MACP2017>3.0.CO;2-9.

[50] A.K. Salem, S.M. Cannizzaro, M.C. Davies, S.J.B. Tendler, C.J. Roberts, P.M. Williams, K.M. Shakesheff, Synthesis and Characterisation of a Degradable Poly (

lactic acid) - Poly (ethylene glycol) Copolymer with Biotinylated End Groups, Biomacromolecules. 2 (2001) 575–580.

[51] D.C. Aluthge, C. Xu, N. Othman, N. Noroozi, S.G. Hatzikiriakos, P. Mehrkhodavandi, PLA−PHB−PLA Triblock Copolymers: Synthesis by Sequential Addition and Investigation of Mechanical and Rheological Properties, Macromolecules. 46 (2013) 3965–3974.

[52] J.-B. Zeng, K.-A. Li, A.-K. Du, Compatibilization strategies in poly(lactic acid)-based blends, RSC Adv. 5 (2015) 32546–32565. doi:10.1039/C5RA01655J.

[53] G. Kfoury, J.-M. Raquez, F. Hassouna, J. Odent, V. Toniazzo, D. Ruch, P. Dubois, Recent advances in high performance poly(lactide): from "green" plasticization to super-tough materials via (reactive) compounding, Front. Chem. 1 (2013) 32. doi:10.3389/fchem.2013.00032.

[54] C.H. Kim, K.Y. Cho, E.J. Choi, J.K. Park, Effect of P(lLA-co-εCL) on the Compatibility and Crystallization Behavior of PCL/PLLA Blends, J. Appl. Polym. Sci. 77 (2000) 226–231. doi:10.1002/(SICI)1097-4628(20000705)77:1<226::AID-APP29>3.0.CO;2-8.

[55] S. lin Yang, Z.H. Wu, W. Yang, M.B. Yang, Thermal and mechanical properties of chemical crosslinked polylactide (PLA), Polym. Test. 27 (2008) 957–963. doi:10.1016/j.polymertesting.2008.08.009.

[56] N. Nagasawa, A. Kaneda, S. Kanazawa, T. Yagi, H. Mitomo, F. Yoshii, M. Tamada, Application of poly(lactic acid) modified by radiation crosslinking, Nucl. Instruments Methods Phys. Res. Sect. B Beam Interact. with Mater. Atoms. 236 (2005) 611–616. doi:10.1016/j.nimb.2005.04.052.

[57] H. Mitomo, A. Kaneda, T.M. Quynh, N. Nagasawa, F. Yoshii, Improvement of heat stability of poly(l-lactic acid) by radiation-induced crosslinking, Polymer (Guildf). 46 (2005) 4695–4703. doi:10.1016/j.polymer.2005.03.088.

[58] B.Y. Shin, D.H. Han, R. Narayan, Rheological and Thermal Properties of the PLA Modified by Electron Beam Irradiation in the Presence of Functional Monomer, J. Polym. Environ. 18 (2010) 558–566. doi:10.1007/s10924-010-0198-8.

[59] M. Salvatore, A. Marra, D. Duraccio, S. Shayanfar, S.D. Pillai, S. Cimmino, C. Silvestre, Effect of electron beam irradiation on the properties of polylactic acid/montmorillonite nanocomposites for food packaging applications, J. Appl. Polym. Sci. 133 (2016) 1–12. doi:10.1002/app.42219.

[60] P. Rytlewski, R. Malinowski, K. Moraczewski, M. Zenkiewicz, Influence of some crosslinking agents on thermal and mechanical properties of electron beam irradiated polylactide, Radiat. Phys. Chem. 79 (2010) 1052–1057. doi:10.1016/j.radphyschem.2010.04.013.

[61] F.P. La Mantia, M. Morreale, Green composites: A brief review, Compos. Part A Appl. Sci. Manuf. 42 (2011) 579–588. doi:10.1016/j.compositesa.2011.01.017.

[62] N. Graupner, A.S. Herrmann, J. Müssig, Natural and man-made cellulose fibre-reinforced poly(lactic acid) (PLA) composites: An overview about mechanical characteristics and application areas, Compos. Part A Appl. Sci. Manuf. 40 (2009) 810–821. doi:10.1016/j.compositesa.2009.04.003.

[63] J. George, M.S. Sreekala, S. Thomas, A review on interface modification and characterization of natural fiber reinforced plastic composites, Polym. Eng. Sci. 41 (2001) 1471–1485. doi:10.1002/pen.10846.

[64] P.K. Bajpai, I. Singh, J. Madaan, Development and characterization of PLA-based green composites, J. Thermoplast. Compos. Mater. 27 (2014) 52–81. doi:10.1177/0892705712439571.

[65] D. Lahiri, F. Rouzaud, T. Richard, A.K. Keshri, S.R. Bakshi, L. Kos, A. Agarwal, Boron nitride nanotube reinforced polylactide-polycaprolactone copolymer composite: Mechanical properties and cytocompatibility with osteoblasts and macrophages in vitro, Acta Biomater. 6 (2010) 3524–3533. doi:10.1016/j.actbio.2010.02.044.

[66] M.-X. Li, S.-H. Kim, S.-W. Choi, K. Goda, W.-I. Lee, Effect of reinforcing particles on hydrolytic degradation behavior of poly (lactic acid) composites, Compos. Part B Eng. 96 (2016) 248–254. doi:10.1016/j.compositesb.2016.04.029.

[67] H.M. Akil, M.F. Omar, A.A.M. Mazuki, S. Safiee, Z.A.M. Ishak, A. Abu Bakar, Kenaf fiber reinforced composites: A review, Mater. Des. 32 (2011) 4107–4121. doi:10.1016/j.matdes.2011.04.008.

[68] B. Bax, J. Müssig, Impact and tensile properties of PLA/Cordenka and PLA/flax composites, Compos. Sci. Technol. 68 (2008) 1601–1607. doi:10.1016/j.compscitech.2008.01.004.

[69] R. Tokoro, D.M. Vu, K. Okubo, T. Tanaka, T. Fujii, T. Fujiura, How to improve mechanical properties of polylactic acid with bamboo fibers, J. Mater. Sci. 43 (2008) 775–787. doi:10.1007/s10853-007-1994-y.

[70] S.Y. Lee, I.A. Kang, G.H. Doh, H.G. Yoon, B.D. Park, Q. Wu, Thermal and mechanical properties of wood flour/talc-filled polylactic acid composites: Effect of filler content and coupling treatment, J. Thermoplast. Compos. Mater. 21 (2008) 209–223. doi:10.1177/0892705708089473.

[71] Y.N. Wang, Y.X. Weng, L. Wang, Characterization of interfacial compatibility of polylactic acid and bamboo flour (PLA/BF) in biocomposites, Polym. Test. 36 (2014) 119–125. doi:10.1016/j.polymertesting.2014.04.001.

[72] V. Nagarajan, A.K. Mohanty, M. Misra, Perspective on Polylactic Acid (PLA) based Sustainable Materials for Durable Applications: Focus on Toughness and Heat Resistance, ACS Sustain. Chem. Eng. 4 (2016) 2899–2916. doi:10.1021/acssuschemeng.6b00321.

[73] C.L. Yue, R.A. Kumar, R.A. Gross, S.P. McCarthy, Miscibility and biodegradability of poly(lactic acid)/poly(ethylene oxide) and poly(lactic acid)/poly(ethylene glycol) blends, J. Eng. Appl. Sci. 2 (1996) 1611–1615. doi:10.1016/0032-3861(96)82913-2.

[74] G. Zhang, J. Zhang, X. Zhou, D. Shen, Miscibility and phase structure of binary blends of polylactide and poly(vinylpyrrolidone), J. Appl. Polym. Sci. 88 (2003) 973–979. doi:10.1002/app.11735.

[75] S.P.M. Mihir Sheth, R. Ananda Kumar, Vipul Dave, Richard A. Gross, Biodegradable Polymer Blends of Poly (lactic acid) and Poly (ethylene glycol), J. Appl. Polym. Sci. 66 (1997) 1495–1505.

[76] Y. Wang, M.A. Hillmyer, Polyethylene-poly(L-lactide) diblock copolymers: Synthesis and compatibilization of poly(L-lactide)/polyethylene blends, J. Polym. Sci. Part A Polym. Chem. 39 (2001) 2755–2766. doi:10.1002/pola.1254.

[77] N.S. Choi, C.H. Kim, K.Y. Cho, J.K. Park, Morphology and hydrolysis of PCL/PLLA blends compatibilized with P(LLA-co-εCL) or P(LLA-b-εCL), J. Appl. Polym. Sci. 86 (2002) 1892–1898. doi:10.1002/app.11134.

[78] H.T. Oyama, Super-tough poly(lactic acid) materials: Reactive blending with ethylene copolymer, Polymer (Guildf). 50 (2009) 747–751. doi:10.1016/j.polymer.2008.12.025.

[79] M.H. Wise, I.J. Linn, C.R. Kennedy, A comparison of the feeding biology of Mink Mustela vison and otter Lutra lutra, J. Zool. 195 (1981) 181–213. doi:10.1111/j.1469-7998.1981.tb03458.x.

[80] J.J. Koh, X. Zhang, C. He, Fully biodegradable Poly(lactic acid)/Starch blends: A review of toughening strategies, Int. J. Biol. Macromol. 109 (2018) 99–113. doi:10.1016/j.ijbiomac.2017.12.048.

[81] J.F. Zhang, X. Sun, Mechanical properties of poly(lactic acid)/starch composites compatibilized by maleic anhydride, Biomacromolecules. 5 (2004) 1446–1451. doi:10.1021/bm0400022.

[82] J.M. Ferri, D. Garcia-Garcia, L. Sánchez-Nacher, O. Fenollar, R. Balart, The effect of maleinized linseed oil (MLO) on mechanical performance of poly(lactic acid)-thermoplastic starch (PLA-TPS) blends, Carbohydr. Polym. 147 (2016) 60–68. doi:10.1016/j.carbpol.2016.03.082.

[83] Z. Xiong, Y. Yang, J. Feng, X. Zhang, C. Zhang, Z. Tang, J. Zhu, Preparation and characterization of poly(lactic acid)/starch composites toughened with epoxidized soybean oil, Carbohydr. Polym. 92 (2013) 810–816. doi:10.1016/j.carbpol.2012.09.007.

[84] Jianchun Li.; Yong He.; Inoue Yoshio, Thermal and mechanical properties of biodegradable blends of poly(L-lactic acid) and lignin, Polym. Int. 52 (2003) 949–955. doi:10.1002/pi.1137.

[85] W. Ren, X. Pan, G. Wang, W. Cheng, Y. Liu, Dodecylated lignin-g-PLA for effective toughening of PLA, Green Chem. 18 (2016) 5008–5014. doi:10.1039/C6GC01341D.

[86] Z.V.G.G. Tadmor, Principles of Polymer Processing, Second, John Wiley & Sons, Inc., Hoboken, New Jersey Published, 2007.

[87] E.K. Silviya, S. Varma, G. Unnikrishnan, S. Thomas, Compounding and mixing of polymers, in: T.Y.W. Sabu (Ed.), Adv. Polym. Process. From Macro- to Nano-Scales, First, Elsevier, 2009: pp. 71–105. doi:10.1533/9781845696429.

[88] L.F.R. Valle, Principles of Polymer Processing, in: V. Enrique, Saldívar-Guerra; Eduardo (Ed.), Handb. Polym. Synth. Charact. Process., John Wiley & Sons, Inc., 2013: pp. 451–461. doi:10.1002/9781118480793.ch23.

[89] M.M. Chehimi, J. Pinson, Applied surface chemistry of nanomaterials, Nova Science Publishers, Inc. New York, 2013.

[90] M. Jamshidian, E.A. Tehrany, M. Imran, M. Jacquot, S. Desobry, Poly-Lactic Acid: Production, applications, nanocomposites, and release studies, Compr. Rev. Food Sci. Food Saf. 9 (2010) 552–571. doi:10.1111/j.1541-4337.2010.00126.x.

[91] J.R.Davis, Tensile Testing, 2004. doi:10.1002/jsfa.930.

[92] I.M. Ward, J. Sweeney, Mechanical Properties of Solid Polymers, Third, John Wiley & Sons, Ltd, Chichester, UK, 2012. doi:10.1002/9781119967125.

[93] W.G. Perkins, Polymer toughness and impact resistance, Polym. Eng. Sci. 39 (1999) 2445–2460. doi:10.1002/pen.11632.

[94] W.D. Callister Jr, Materials Science and Engineering - An Introduction, Eight, John Wiley & Sons, (2010) 1-800. http://www.emeraldinsight.com/doi/10.1108/acmm.2000.12847aae.001.

[95] L. Wang, Y. nan Wang, Z. gang Huang, Y. xuan Weng, Heat resistance, crystallization behavior, and mechanical properties of polylactide/nucleating agent composites, Mater. Des. 66 (2015) 7–15. doi:10.1016/j.matdes.2014.10.011.

[96] Y. Leng, Materials Characterization, John Wiley & Sons (Asia) Pte Ltd, (2008) 1-333.

[97] Z. Jiang, C.T. Imrie, J.M. Hutchinson, An introduction to temperature modulated differential scanning calorimetry (TMDSC): A relatively non-mathematical approach, Thermochim. Acta. 387 (2002) 75–93. doi:10.1016/S0040-6031(01)00829-2.

[98] P. Nanthananon, M. Seadan, S. Pivsa-Art, S. Suttiruengwong, Enhanced crystallization of poly (lactic acid) through reactive aliphatic bisamide, IOP Conf. Ser. Mater. Sci.

Eng. 87 (2015) 012067. doi:10.1088/1757-899X/87/1/012067.

[99] C. Guo, L. Zhou, J. Lv, Effects of expandable graphite and modified ammonium polyphosphate on the flame-retardant and mechanical properties of wood flour-polypropylene composites, Polym. Polym. Compos. 21 (2013) 449–456. doi:10.1002/app.

[100] C. Prapruddivongs, N. Sombatsompop, Roles and evidence of wood flour as an antibacterial promoter for triclosan-filled poly(lactic acid), Compos. Part B Eng. 43 (2012) 2730–2737. doi:10.1016/j.compositesb.2012.04.032.

[101] S.C. Brian., Fundamental of Fourier Transform Infrared Spectroscopy, Second, CRC press, Taylor & Francis Group, 2011. doi:10.1002/1521-3773(20010316)40:6<9823::AID-ANIE9823>3.3.CO;2-C.

[102] Nuclear Magnetic Resonance Spectroscopy, Reson. – J. Sci. Educ. 9 (2004) 34–49. https://www.ias.ac.in/article/fulltext/reso/009/01/0034-0049.

[103] A. Isao, Ando;Tetsuo, Solid State nmr of Polymers, Elsevier Science B.V, 1998.

[104] J.U. Izunobi, C.L. Higginbotham, Polymer molecular weight analysis by1H NMR spectroscopy, J. Chem. Educ. 88 (2011) 1098–1104. doi:10.1021/ed100461v.

[105] L.M. Harwood, T.D.W. Claridge, Introduction to Organic Spectroscopy, Oxford University Press, 1996. doi:10.1007/s11746-015-2722-4.

[106] I.P. Gerothanassis, A. Troganis, V. Exarchou, K. Barbarossou, Nuclear Magnetic Resonance (Nmr) Spectroscopy: Basic Principles and Phenomena, and Their Applications To Chemistry, Biology and Medicine, Chem. Educ. Res. Pr. 3 (2002) 229–252. doi:10.1039/B2RP90018A.

[107] M. Huang, S. Li, M. Vert, Synthesis and degradation of PLA – PCL – PLA triblock copolymer prepared by successive polymerization of 3 -caprolactone and DL -lactide, 45 (2004) 8675–8681. doi:10.1016/j.polymer.2004.10.054.

[108] J.L. Espartero, I. Rashkov, S.M. Li, N. Manolova, M. Vert, NMR Analysis of Low Molecular Weight Poly (lactic acid) s, 9297 (1996) 3535–3539.

[109] Y. Waseda, E. Matsubara, K. Shinoda, X-Ray Diffraction Crystallography;

Introduction, examples and solved problems, First, Springer-Verlag Berlin Heidelberg, 2011. doi:10.1007/978-3-642-16635-8.

[110] T. Huxford, X-Ray Crystallography, in: S.M.K. Hughes (Ed.), Brenner's Encycl. Genet., Second, Elsevier, Academic Press, 2013: pp. 366–368. doi:10.1016/B978-0-12-374984-0.01657-0.

[111] A.A. Bunaciu, E. gabriela Udriştioiu, H.Y. Aboul-Enein, X-Ray Diffraction: Instrumentation and Applications, Crit. Rev. Anal. Chem. 45 (2015) 289–299. doi:10.1080/10408347.2014.949616.

[112] M. Dunlap, J.E. Adaskaveg, Introduction to the Scanning Electron Microscope. Theory, Practice & Procedures, (1997). https://imf.ucmerced.edu/downloads/semmanual.pdf.

[113] B.J. Inkson, Scanning Electron Microscopy (SEM) and Transmission Electron Microscopy (TEM) for Materials Characterization, in: Mater. Charact. Using Nondestruct. Eval. Methods, First, Woodhead Publishing, 2016: pp. 17–43. doi:10.1016/B978-0-08-100040-3.00002-X.

[114] K. Fukushima, D. Tabuani, M. Dottori, I. Armentano, J.M. Kenny, G. Camino, Effect of temperature and nanoparticle type on hydrolytic degradation of poly(lactic acid) nanocomposites, Polym. Degrad. Stab. 96 (2011) 2120–2129. doi:10.1016/j.polymdegradstab.2011.09.018.

[115] H. Tsuji, Hydrolytic Degradation-Poly (lactic acid), in: Biopolym. Online, Wiley-VCH, Weinheim., 2010: pp. 343–381. doi:10.1002/3527600035.bpol4005.

[116] R. Pantani, F. De Santis, F. Auriemma, C. De Rosa, R. Di Girolamo, Effects of water sorption on poly(lactic acid), Polym. (United Kingdom). 99 (2016) 130–139. doi:10.1016/j.polymer.2016.07.008.

[117] I. Valentina, A. Haroutioun, L. Fabrice, V. Vincent, P. Roberto, Tuning the hydrolytic degradation rate of poly-lactic acid (PLA) to more durable applications, AIP Conf. Proc. 1914 (2017) 3–8. doi:10.1063/1.5016801.

[118] M. Karamanlioglu, R. Preziosi, G.D. Robson, Abiotic and biotic environmental degradation of the bioplastic polymer poly (lactic acid): A review, Polym. Degrad.

Stab. 137 (2017) 122–130. doi:10.1016/j.polymdegradstab.2017.01.009.

[119] S. Djellali, N. Haddaoui, T. Sadoun, A. Bergeret, Y. Grohens, Structural, morphological and mechanical characteristics of polyethylene, poly(lactic acid) and poly(ethylene-co-glycidyl methacrylate) blends, Iran. Polym. J. (English Ed. 22 (2013) 245–257. doi:10.1007/s13726-013-0126-6.

[120] J.-H. Wu, C.-P. Wu, M.C. Kuo, Y. Tsai, Characterization and Properties of Reactive Poly (Lactic Acid)/Ethylene–Vinyl Alcohol Copolymer Blends with Chain-Extender, J. Polym. Environ. 24 (2016) 129–138. doi:10.1007/s10924-016-0755-x.

[121] K. Hashima, S. Nishitsuji, T. Inoue, Structure-properties of super-tough PLA alloy with excellent heat resistance, Polymer (Guildf). 51 (2010) 3934–3939. doi:10.1016/j.polymer.2010.06.045.

[122] Y.-S. He, J.-B. Zeng, G.-C. Liu, Q.-T. Li, Y.-Z. Wang, Super-tough poly(l-lactide)/crosslinked polyurethane blends with tunable impact toughness, RSC Adv. 4 (2014) 12857. doi:10.1039/c4ra00718b.

[123] Y. Chen, D. Yuan, C. Xu, Dynamically vulcanized biobased polylactide/natural rubber blend material with continuous cross-linked rubber phase, ACS Appl. Mater. Interfaces. 6 (2014) 3811–3816. doi:10.1021/am5004766.

[124] Y. Huang, C. Zhang, Y. Pan, W. Wang, L. Jiang, Y. Dan, Study on the Effect of Dicumyl Peroxide on Structure and Properties of Poly(Lactic Acid)/Natural Rubber Blend, J. Polym. Environ. 21 (2013) 375–387. doi:10.1007/s10924-012-0544-0.

[125] M. Zhang, Development of Polyhydroxybutyrate Based Blends for Compostable Packaging, Loughborough University Institutional Repository, 2010.

[126] M.H. Espinosa, P.J.O. Toro, D.Z. Silva, Microstructural analysis of poly (glycidyl methacrylate) by 1 H and 13 C NMR spectroscopy, 42 (2001) 3393–3397.

[127] M.M. Haque, D. Puglia, E. Fortunati, M. Pracella, Effect of reactive functionalization on properties and degradability of poly (lactic acid)/ poly (vinyl acetate) nanocomposites with cellulose nanocrystals, REACT. 110 (2017) 1–9. doi:10.1016/j.reactfunctpolym.2016.11.003.

[128] A. V Reis, R. Fajardo, I.T.A. Schuquel, M.R. Guilherme, A.F. Rubira, E.C. Muniz,

Reaction of Glycidyl Methacrylate at the Hydroxyl and Carboxylic Groups of Poly (vinyl alcohol) and Poly (acrylic acid): Is This Reaction Mechanism Still Unclear ?, J. Org. Chem. 74 (2009) 3750–3757.

[129] C. Republic, thermochimica acta High-temperature behaviour of hexagonal boron nitride ', Science (80-.). 283 (1996) 359–367.

[130] A.J. Brandolini, D.D. Hills, NMR Spectra of Polymers and Polymer Additives, CRC press, (2000).

[131] S. Agarwal, N. Naumann, X. Xie, Synthesis and Microstructural Characterization of Ethylene Carbonate-?-Caprolactone/L-Lactide Copolymers Using One- and Two-Dimensional NMR Spectroscopy Seema, Macromolecules. 35 (2002) 7713–7717. doi:10.1021/ma020584k.

[132] G.C. Liu, Y.S. He, J.B. Zeng, Q.T. Li, Y.Z. Wang, Fully biobased and supertough polylactide-based thermoplastic vulcanizates fabricated by peroxide-induced dynamic vulcanization and interfacial compatibilization, Biomacromolecules. 15 (2014) 4260–4271. doi:10.1021/bm5012739.

[133] K. Suganuma, K. Horiuchi, H. Matsuda, H.N. Cheng, A. Aoki, T. Asakura, NMR analysis and chemical shift calculations of poly (lactic acid) dimer model compounds with different tacticities, Polym. J. 44 (2012) 838–844. doi:10.1038/pj.2012.106.

[134] N.E. Jacobsen, Nmr spectroscopy explained, First, John Wiley & Sons, Inc., 2007. doi:http://dx.doi.org/10.1002/9780470173350.

[135] J. Keeler, Understanding NMR Spectroscopy, Second, John Wiley & Sons, Inc., 2010.

[136] L. Suryanegara, A.N. Nakagaito, H. Yano, The effect of crystallization of PLA on the thermal and mechanical properties of microfibrillated cellulose-reinforced PLA composites, Compos. Sci. Technol. 69 (2009) 1187–1192. doi:10.1016/j.compscitech.2009.02.022.

[137] T. Kawai, N. Rahman, G. Matsuba, K. Nishida, T. Kanaya, M. Nakano, H. Okamoto, J. Kawada, A. Usuki, N. Honma, K. Nakajima, M. Matsuda, Crystallization and melting behavior of poly (L-lactic acid), Macromolecules. 40 (2007) 9463–9469. doi:10.1021/ma070082c.

[138] M. Murariu, A. Laure, L. Bonnaud, Y. Paint, A. Gallos, G. Fontaine, S. Bourbigot, P. Dubois, The production and properties of polylactide composites fi lled with expanded graphite, 95 (2010). doi:10.1016/j.polymdegradstab.2009.12.019.

[139] Y. Zhang, C. Wang, H. Du, X. Li, D. Mi, X. Zhang, T. Wang, J. Zhang, Promoting crystallization of polylactide by the formation of crosslinking bundles, Mater. Lett. 117 (2014) 171–174. doi:10.1016/j.matlet.2013.12.005.

[140] X. Shi, S. Wang, H. Yang, X. Duan, X. Dong, Fabrication and characterization of hexagonal boron nitride powder by spray drying and calcining-nitriding technology, J. Solid State Chem. 181 (2008) 2274–2278. doi:10.1016/j.jssc.2008.05.029.

[141] P.S.D.O. Patrício, F. V. Pereira, M.C. Dos Santos, P.P. De Souza, J.P.B. Roa, R.L. Orefice, Increasing the elongation at break of polyhydroxybutyrate biopolymer: Effect of cellulose nanowhiskers on mechanical and thermal properties, J. Appl. Polym. Sci. 127 (2013) 3613–3621. doi:10.1002/app.37811.

[142] S. Spinella, J. Cai, C. Samuel, J. Zhu, S.A. McCallum, Y. Habibi, J.M. Raquez, P. Dubois, R.A. Gross, Polylactide/poly(#-hydroxytetradecanoic acid) reactive blending: A green renewable approach to improving polylactide properties, Biomacromolecules. 16 (2015) 1818–1826. doi:10.1021/acs.biomac.5b00394.

[143] L. Lin, C. Deng, G.-P. Lin, Y.-Z. Wang, Super Toughened and High Heat-Resistant Poly(Lactic Acid) (PLA)-Based Blends by Enhancing Interfacial Bonding and PLA Phase Crystallization, Ind. Eng. Chem. Res. 54 (2015) 5643–5655. doi:10.1021/acs.iecr.5b01177.

[144] U. Riaz, A. Vashist, S.A. Ahmad, S. Ahmad, S.M. Ashraf, Compatibility and biodegradability studies of linseed oil epoxy and PVC blends, Biomass and Bioenergy. 34 (2010) 396–401. doi:10.1016/j.biombioe.2009.12.002.

[145] M.A. Huneault, H. Li, Morphology and properties of compatibilized polylactide/thermoplastic starch blends, Polymer (Guildf). 48 (2007) 270–280. doi:10.1016/j.polymer.2006.11.023.

[146] Q. Xing, X. Zhang, X. Dong, G. Liu, D. Wang, Low-molecular weight aliphatic amides as nucleating agents for poly (L-lactic acid): Conformation variation induced crystallization enhancement, Polymer (Guildf). 53 (2012) 2306–2314.

doi:10.1016/j.polymer.2012.03.034.

[147] P. Song, G. Chen, Z. Wei, Y. Chang, W. Zhang, J. Liang, Rapid crystallization of poly(l-lactic acid) induced by a nanoscaled zinc citrate complex as nucleating agent, Polym. (United Kingdom). 53 (2012) 4300–4309. doi:10.1016/j.polymer.2012.07.032.

[148] K. Hamad, M. Kaseem, H.W. Yang, F. Deri, Y.G. Ko, Properties and medical applications of polylactic acid: A review, Express Polym. Lett. 9 (2015) 435–455. doi:10.3144/expresspolymlett.2015.42.

[149] S. Chye Joachim Loo, C. Ping Ooi, Y. Chiang Freddy Boey, Influence of electron-beam radiation on the hydrolytic degradation behaviour of poly(lactide-co-glycolide) (PLGA), Biomaterials. 26 (2005) 3809–3817. doi:10.1016/j.biomaterials.2004.10.014.

[150] M.L. Cairns, G.R. Dickson, J.F. Orr, D. Farrar, K. Hawkins, F.J. Buchanan, Electron-beam treatment of poly(lactic acid) to control degradation profiles, Polym. Degrad. Stab. 96 (2011) 76–83. doi:10.1016/j.polymdegradstab.2010.10.016.

[151] D.J. Leonard, L.T. Pick, D.F. Farrar, G.R. Dickson, J.F. Orr, F.J. Buchanan, The modification of PLA and PLGA using electron-beam radiation, J. Biomed. Mater. Res. - Part A. 89 (2009) 567–574. doi:10.1002/jbm.a.31998.

[152] B.Y. Shin, D.H. Han, Compatibilization of immiscible poly(lactic acid)/poly(ε-caprolactone) blend through electron-beam irradiation with the addition of a compatibilizing agent, Radiat. Phys. Chem. 83 (2013) 98–104. doi:10.1016/j.radphyschem.2012.10.001.

[153] S. Lyu, D. Untereker, Degradability of polymers for implantable biomedical devices, Int. J. Mol. Sci. 10 (2009) 4033–4065. doi:10.3390/ijms10094033.

[154] Q. Zhou, M. Xanthos, Nanoclay and crystallinity effects on the hydrolytic degradation of polylactides, Polym. Degrad. Stab. 93 (2008) 1450–1459. doi:10.1016/j.polymdegradstab.2008.05.014.

[155] M. Shayan, H. Azizi, I. Ghasemi, M. Karrabi, Effect of modified starch and nanoclay particles on biodegradability and mechanical properties of cross-linked poly lactic acid, Carbohydr. Polym. 124 (2015) 237–244. doi:10.1016/j.carbpol.2015.02.001.

[156] Y. Kimura, T. Wakabayashi, K. Okada, T. Wada, H. Nishikawa, Boron nitride as a

lubricant additive, Wear. 232 (1999) 199–206. doi:10.1016/S0043-1648(99)00146-5.

[157] K. Lintinen, Y. Xiao, R. Bangalore Ashok, T. Leskinen, E. Sakarinen, M. Sipponen, F. Muhammad, P. Oinas, M. Österberg, M. Kostiainen, Closed cycle production of concentrated and dry redispersible colloidal lignin particles with a three solvent polarity exchange method, Green Chem. 20 (2018) 843–850. doi:10.1039/c7gc03465b.

[158] M. Culebras, A. Beaucamp, Y. Wang, M. Clauss, E. Frank, M.N. Collins, Bio-based structurally compatible polymer blends based on lignin and thermoplastic elastomer polyurethane as carbon fiber precursors, ACS Sustain. Chem. Eng. 6 (2018) 8816–8825. doi:10.1021/acssuschemeng.8b01170.

[159] M. Culebras, M.J. Sanchis, A. Beaucamp, M. Carsí, B.K. Kandola, A.R. Horrocks, G. Panzetti, C. Birkinshaw, M.N. Collins, Understanding the thermal and dielectric response of organosolv and modified kraft lignin as a carbon fibre precursor, Green Chem. 20 (2018) 4461–4472. doi:10.1039/C8GC01577E.

[160] J.F. Kadla, S. Kubo, Lignin-based polymer blends: Analysis of intermolecular interactions in lignin-synthetic polymer blends, Compos. Part A Appl. Sci. Manuf. 35 (2004) 395–400. doi:10.1016/j.compositesa.2003.09.019.

[161] C. Pouteau, P. Dole, B. Cathala, L. Averous, N. Boquillon, Antioxidant properties of lignin in polypropylene, 81 (2003) 9–18. doi:10.1016/S0141-3910(03)00057-0.

[162] G. Podstra, P. Alexy, B. Kos, The effect of blending lignin with polyethylene and polypropylene on physical properties, Polymer (Guildf). 41 (2000) 4901–4908.

[163] R. Liu, L. Dai, L.Q. Hu, W.Q. Zhou, C.L. Si, Fabrication of high-performance poly(L-lactic acid)/lignin-graft-poly(D-lactic acid) stereocomplex films, Mater. Sci. Eng. C. 80 (2017) 397–403. doi:10.1016/j.msec.2017.06.006.

[164] L. Dai, R. Liu, C. Si, A novel functional lignin-based filler for pyrolysis and feedstock recycling of poly(L-lactide), Green Chem. 20 (2018) 1777–1783. doi:10.1039/C7GC03863A.

[165] N. Rajeswara Rao, T. Venkatappa Rao, S.V.S. Ramana Reddy, B. Sanjeeva Rao, Effect of electron beam on thermal, morphological and antioxidant properties of kraft lignin, Adv. Mater. Lett. 6 (2015) 560–565. doi:10.5185/amlett.2015.SMS2.

[166] Q. Liu, S. Wang, Y. Zheng, Z. Luo, K. Cen, Mechanism study of wood lignin pyrolysis by using TG-FTIR analysis, J. Anal. Appl. Pyrolysis. 82 (2008) 170–177. doi:10.1016/j.jaap.2008.03.007.

[167] S.I. Kuzina, A.Y. Brezgunov, A.A. Dubinskii, A.I. Mikhailov, Free radicals in the photolysis and radiolysis of polymers: IV. Radicals in γ- and UV-irradiated wood and lignin, High Energy Chem. 38 (2004) 298–305. doi:10.1023/B:HIEC.0000041340.45217.bd.

[168] A. Kumar, T. Venkatappa Rao, S. Ray Chowdhury, S.V.S. Ramana Reddy, Compatibility confirmation and refinement of thermal and mechanical properties of poly (lactic acid)/poly (ethylene-co-glycidyl methacrylate) blend reinforced by hexagonal boron nitride, React. Funct. Polym. 117 (2017) 1–9. doi:10.1016/j.reactfunctpolym.2017.05.005.

[169] A.U. Rahman, M. Iqbal, F.U. Rahman, D. Fu, M. Yaseen, Y. Lv, M. Omer, M. Garver, L. Yang, T. Tan, Synthesis and characterization of reactive macroporous poly(glycidyl methacrylate-triallyl isocyanurate-ethylene glycol dimethacrylate) microspheres by suspension polymerization: Effect of synthesis variables on surface area and porosity, J. Appl. Polym. Sci. 124 (2012) 915–926. doi:10.1002/app.35026.

[170] M.A. Abdelwahab, S. Taylor, M. Misra, A.K. Mohanty, Thermo-mechanical characterization of bioblends from polylactide and poly(butylene adipate-co-terephthalate) and lignin, Macromol. Mater. Eng. 300 (2015) 299–311. doi:10.1002/mame.201400241.

[171] T. Dizhbite, J. Ponomarenko, A. Andersone, G. Dobele, M. Lauberts, J. Krasilnikova, N. Mironova-Ulmane, G. Telysheva, Role of paramagnetic polyconjugated clusters in lignin antioxidant activity (in vitro), IOP Conf. Ser. Mater. Sci. Eng. 38 (2012). doi:10.1088/1757-899X/38/1/012033.

[172] M.B. Coltelli, S. Bronco, C. Chinea, The effect of free radical reactions on structure and properties of poly(lactic acid) (PLA) based blends, Polym. Degrad. Stab. 95 (2010) 332–341. doi:10.1016/j.polymdegradstab.2009.11.015.

[173] M.C. Gupta, V.G. Deshmukh, Radiation effects on poly(lactic acid), Polymer (Guildf). 24 (1983) 827–830. doi:10.1016/0032-3861(83)90198-2.

[174] X. Lu, A. Weiss, Relationship between the Glass Transition Temperature and the Interaction Parameter of Miscible Binary Polymer Blends, Macromolecules. 25 (1992) 3242–3246. doi:10.1021/ma00038a033.

[175] A.T.R. Sugano-Segura, L.B. Tavares, J.G.F. Rizzi, D.S. Rosa, M.C. Salvadori, D.J. dos Santos, Mechanical and thermal properties of electron beam-irradiated polypropylene reinforced with Kraft lignin, Radiat. Phys. Chem. 139 (2017) 5–10. doi:10.1016/j.radphyschem.2017.05.016.

[176] S. Kubo, J.F. Kadla, Poly (Ethylene Oxide)/ Organosolv Lignin Blends : Relationship between Thermal Properties , Chemical Structure , and Blend Behavior, Macromolecules. 37 (2004) 6904–6911. doi:10.1021/MA0490552.

[177] T.K. Kwei, The Effect of Hydrogen Bonding on the Glass Transition of Polymer Mixtures, J. Polym. Sci. 22 (1984) 307–313. doi:10.1002/pol.1984.130220603.

[178] W. Ouyang, Y. Huang, H. Luo, D. Wang, Poly(Lactic Acid) Blended with Cellulolytic Enzyme Lignin: Mechanical and Thermal Properties and Morphology Evaluation, J. Polym. Environ. 20 (2012) 1–9. doi:10.1007/s10924-011-0359-4.

[179] S. Sahoo, M. Misra, A.K. Mohanty, Enhanced properties of lignin-based biodegradable polymer composites using injection moulding process, Compos. Part A Appl. Sci. Manuf. 42 (2011) 1710–1718. doi:10.1016/j.compositesa.2011.07.025.

[180] R. Kumar Singla, S.N. Maiti, A.K. Ghosh, Crystallization, Morphological, and Mechanical Response of Poly(Lactic Acid)/Lignin-Based Biodegradable Composites, Polym. - Plast. Technol. Eng. 55 (2016) 475–485. doi:10.1080/03602559.2015.1098688.

[181] H. Tsuji, Poly (Lactic Acid), in: S. Kabasci (Ed.), Bio-Based Plast. -Materials Appl., First, John Wiley & Sons, Ltd, 2014: pp. 171–239. doi:10.1002/9781118676646.ch8.

[182] A.P. Morales, A. Güemes, A. Fernandez-Lopez, V.C. Valero, S. de La Rosa Llano, Bamboo-polylactic acid (PLA) composite material for structural applications, Materials (Basel). 10 (2017) 1–22. doi:10.3390/ma10111286.

[183] M.R. Nurul Fazita, K. Jayaraman, D. Bhattacharyya, M.K. Mohamad Haafiz, C.K. Saurabh, M. Hazwan Hussin, H.P.S. Abdul Khalil, Green composites made of bamboo

fabric and poly (lactic) acid for packaging applications-a review, Materials (Basel). 9 (2016). doi:10.3390/ma9060435.

[184] H. Takagi, S. Kako, K. Kusano, A. Ousaka, Thermal conductivity of PLA-bamboo fiber composites, Adv. Compos. Mater. Off. J. Japan Soc. Compos. Mater. 16 (2007) 377–384. doi:10.1163/156855107782325186.

[185] J. Lin, Z. Yang, X. Hu, G. Hong, S. Zhang, W. Song, The effect of alkali treatment on properties of dopamine modification of bamboo fiber/polylactic acid composites, Polymers (Basel). 10 (2018). doi:10.3390/polym10040403.

[186] Y. Zuo, W. Li, P. Li, W. Liu, X. Li, Y. Wu, Preparation and characterization of polylactic acid-g-bamboo fiber based on in-situ solid phase polymerization, Ind. Crops Prod. 123 (2018) 646–653. doi:10.1016/j.indcrop.2018.07.024.

[187] S. Qian, K. Sheng, K. Yu, L. Xu, C.A. Fontanillo Lopez, Improved properties of PLA biocomposites toughened with bamboo cellulose nanowhiskers through silane modification, J. Mater. Sci. 53 (2018) 10920–10932. doi:10.1007/s10853-018-2377-2.

[188] S. Qian, K. Sheng, PLA toughened by bamboo cellulose nanowhiskers: Role of silane compatibilization on the PLA bionanocomposite properties, Compos. Sci. Technol. 148 (2017) 59–69. doi:10.1016/j.compscitech.2017.05.020.

[189] Y. Geng, X. Pei, X. He, P. Li, Y. Wu, Y. Zuo, Preparation and Characterization of Esterified Bamboo Flour by an in Situ Solid Phase Method, Polymers (Basel). 10 (2018) 920. doi:10.3390/polym10080920.

[190] T. Lu, S. Liu, M. Jiang, X. Xu, Y. Wang, Z. Wang, J. Gou, D. Hui, Z. Zhou, Effects of modifications of bamboo cellulose fibers on the improved mechanical properties of cellulose reinforced poly(lactic acid) composites, Compos. Part B Eng. 62 (2014) 191–197. doi:10.1016/j.compositesb.2014.02.030.

[191] L. Yao, Y. Wang, Y. Li, J. Duan, Thermal properties and crystallization behaviors of polylactide/redwood flour or bamboo fiber composites, Iran. Polym. J. 26 (2017) 161–168. doi:10.1007/s13726-017-0508-2.

[192] A. Kumar, V.R. Tumu, S. Ray Chowdhury, R.R. Ramana, A green physical approach to compatibilize a bio-based poly (lactic acid)/lignin blend for better mechanical,

thermal and degradation properties, Int. J. Biol. Macromol. 121 (2019) 588–600. doi:10.1016/j.ijbiomac.2018.10.057.

[193] G.W. Dietrich Fengel, W. de Gruyter, Wood-chemistry, ultrastructure, reactions, Walter de Gruyter& Co Berlin, 1984. doi:10.1007/BF02608943.

[194] L.L. Zhao, J.J. Su, J. Han, B. Zhang, L. Ou, Optimizing the balance between stiffness and flexibility by tuning the compatibility of a poly(lactic acid)/ethylene copolymer, RSC Adv. 7 (2017) 23065–23072. doi:10.1039/c6ra28843j.

[195] H.P.S. Abdul Khalil, I.U.H. Bhat, M. Jawaid, A. Zaidon, D. Hermawan, Y.S. Hadi, Bamboo fibre reinforced biocomposites: A review, Mater. Des. 42 (2012) 353–368. doi:10.1016/j.matdes.2012.06.015.

[196] F.H. Isikgor, C.R. Becer, Lignocellulosic biomass: a sustainable platform for the production of bio-based chemicals and polymers, Polym. Chem. 6 (2015) 4497–4559. doi:10.1039/c5py00263j.

[197] T. Afrin, T. Tsuzuki, R.K. Kanwar, X. Wang, The origin of the antibacterial property of bamboo, J. Text. Inst. 103 (2012) 844–849. doi:10.1080/00405000.2011.614742.

[198] N.K. Prosper, S. Zhang, H. Wu, S. Yang, S. Li, F. Sun, B. Goodell, Enzymatic biocatalysis of bamboo chemical constituents to impart antimold properties, Wood Sci. Technol. 52 (2018) 619–635. doi:10.1007/s00226-018-0987-0.

[199] A. Alberti, S. Bertini, G. Gastaldi, N. Iannaccone, D. MacCiantelli, G. Torri, E. Vismara, Electron beam irradiated textile cellulose fibres. ESR studies and derivatisation with glycidyl methacrylate (GMA), Eur. Polym. J. 41 (2005) 1787–1797. doi:10.1016/j.eurpolymj.2005.02.016.

[200] Y. Liu, J. Chen, X. Wu, K. Wang, X. Su, L. Chen, H. Zhou, X. Xiong, Insights into the effects of γ-irradiation on the microstructure, thermal stability and irradiation-derived degradation components of microcrystalline cellulose (MCC), RSC Adv. 5 (2015) 34353–34363. doi:10.1039/c5ra03300d.

[201] X. Ma, X. Zheng, M. Zhang, X. Yang, L. Chen, L. Huang, S. Cao, Electron beam irradiation of bamboo chips: degradation of cellulose and hemicelluloses, Cellulose. 21 (2014) 3865–3870. doi:10.1007/s10570-014-0402-4.

[202] U. Henniges, S. Okubayashi, T. Rosenau, A. Potthast, Irradiation of cellulosic pulps: Understanding its impact on cellulose oxidation, Biomacromolecules. 13 (2012) 4171–4178. doi:10.1021/bm3014457.

[203] H. Yang, R. Yan, H. Chen, D.H. Lee, C. Zheng, Characteristics of hemicellulose, cellulose and lignin pyrolysis, Fuel. 86 (2007) 1781–1788. doi:10.1016/j.fuel.2006.12.013.

[204] M.. Ramiah, Thermogravimetric and Differential Thermal Analysis of, J. Appl. Polym. Sci. 14 (1970) 1323–1337.

List of Publications

Science Citation Indexed (SCI) Journal Papers

1. Compatibility confirmation and refinement of thermal and mechanical properties of Poly (lactic acid)/Poly (ethylene-co-glycidyl methacrylate) blend reinforced by hexagonal boron nitride.
   Ashish Kumar, T.Venkatappa Rao, S. Ray Chowdhury, S.V.S Ramana Reddy
   Journal of Reactive and Functional Polymers 117 (2017) 1–9 (Impact Factor 3.151)
   https://doi.org/10.1016/j.ijbiomac.2018.10.057

2. Optimization of mechanical, thermal and hydrolytic degradation properties of Poly (lactic acid)/Poly (ethylene-co-glycidyl methacrylate)/Hexagonal boron nitride blend composites through electron-beam irradiation.
   Ashish Kumar, T.Venkatappa Rao, S. Ray Chowdhury, S.V.S Ramana Reddy
   Nuclear Inst. Methods in Physics Research B 428 (2018) 38-46
   (Impact Factor 1.323)
   https://doi.org/10.1016/j.nimb.2018.05.011

3. A green physical approach to compatibilize a bio-based poly (lactic acid)/lignin blend for better mechanical, thermal and degradation properties.
   Ashish Kumar, T.Venkatappa Rao, S. Ray Chowdhury, S.V.S Ramana Reddy
   International Journal of Biological Macromolecules 121, 588-600 (2019) (Impact Factor 3.929)
   http://dx.doi.org/10.1016/j.reactfunctpolym.2017.05.005

4. Physicochemical properties of fully bio-based and bio-degradable PLA/Bamboo powder composites.
   Ashish Kumar, T.Venkatappa Rao
   Composites Part B: Engineering 175 (107098), 1-9 (2019) (Impact Factor 6.864).
   https://doi.org/10.1016/j.compositesb.2019.107098

5. Effect of reinforcing particles on the thermal, mechanical and degradation properties of poly (lactic acid)/poly (ethylene-co-glycidyl methacrylate) blend **(Communicated).**
   Ashish Kumar, T.Venkatappa Rao

List of papers presented in national and international conferences

1. Effect of electron beam irradiation on thermal and mechanical properties of poly (lactic acid) / poly (ethylene-co-glycidyl methacrylate) blend" has been presented at an **International conference "Optics 17" held at NIT Calicut during 9-11 January 2017. Published in AIP Conference Proceedings 1849(1):020039 · June 2017 DOI: 10.1063/1.4984186**
   http://dx.doi.org/10.1063/1.4984186

2. Effect of reinforcing hexagonal boron nitride particles on the hydrolytic degradation properties of poly (lactic acid) / poly (ethylene-co-glycidyl methacrylate) blend" has been presented at **National conference "Recent Trends in Experiments and Theoretical Physics** held at SSU Palampur (H.P.) during 23-24 November 2017.

3. Impact of electron beam irradiation on degradation properties of poly (lactic acid)/poly (ethylene-co-glycidyl methacrylate) blend presented at **International Conference on Advanced Applications of Radiation Technology (NICSTAR-2018)** held at Hotel Courtyard by Marriott, Mumbai, India from 05-07 March 2018.

4. Effect of reinforcing particles on the thermal, mechanical and degradation properties of poly (lactic acid)/poly (ethylene-co-glycidyl methacrylate) blend presented at **International Conference on Advanced Functional Materials and Devices (ICAFMD-2019)** held at National Institute of Technology Warangal, India from 26-28 February 2019. (Best Oral Presentation)